

AD-A104 263

BOEING MILITARY AIRPLANE CO SEATTLE WA  
AIRCRAFT DIGITAL INPUT CONTROLLED HYDRAULIC ACTUATION AND CONTR--ETC(U)  
MAR 81 E T RAYMOND, C W ROBINSON F33615-77-C-2034

F/S 9/2

UNCLASSIFIED

AFWAL-TR-81-2012

NL

for 3  
A  
AD0263



2.

100

100



LEVEL II



AD A104263

AFWAL-TR-81-2012

AIRCRAFT DIGITAL INPUT CONTROLLED HYDRAULIC ACTUATION AND CONTROL SYSTEM

BOEING MILITARY AIRPLANE COMPANY  
P.O. BOX 3707  
SEATTLE, WASHINGTON 98124

MARCH 1981

TECHNICAL REPORT AFWAL-TR-81-2012

FINAL REPORT for PERIOD AUGUST 1977 - DECEMBER 1980

Approved for public release: distribution unlimited

AERO PROPULSION LABORATORY  
AIR FORCE WRIGHT AERONAUTICAL LABORATORIES  
AIR FORCE SYSTEMS COMMAND  
WRIGHT PATTERSON AIR FORCE BASE, OHIO 45433

DTIC  
ELECTE  
SEP 17 1981  
S D

DTIC FILE COPY

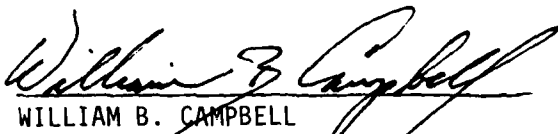
81 9 16 016


NOTICE

When Government drawings, specifications, or other data are used for any purpose other than in connection with a definitely related Government procurement operation, the United States Government thereby incurs no responsibility nor any obligation whatsoever; and the fact that the government may have formulated, furnished, or in any way supplied the said drawings, specifications, or other data, is not to be regarded by implication or otherwise as in any manner licensing the holder or any other person or corporation, or conveying any rights or permission to manufacture use, or sell any patented invention that may in any way be related thereto.


This report has been reviewed by the Office of Public Affairs (ASD/PA) and is releasable to the National Technical Information Service (NTIS). At NTIS, it will be available to the general public, including foreign nations.

This technical report has been reviewed and is approved for publication.

  
WILLIAM B. CAMPBELL  
Power Systems Branch  
Aerospace Power Division  
Aero Propulsion Laboratory

  
RICHARD D. FRANKLIN, Major, USAF  
Chief, Power Systems Branch  
Aerospace Power Division  
Aero Propulsion Laboratory

FOR THE COMMANDER

  
JAMES D. REAMS  
Chief, Aerospace Power Division  
Aero Propulsion Laboratory

"If your address has changed, if you wish to be removed from our mailing list, or if the addressee is no longer employed by your organization please notify AFWAL/POOS, W-PAFB, OH 45433 to help us maintain a current mailing list".

Copies of this report should not be returned unless return is required by security considerations, contractual obligations, or notice on a specific document.

REPORT DOCUMENTATION PAGE		READ INSTRUCTIONS BEFORE COMPLETING FORM
1. REPORT NUMBER AFWAL-TR-81-2012	2. GOVT ACCESSION NO. AD-A104263	3. RECIPIENT'S CATALOG NUMBER
4. TITLE (and Subtitle) AIRCRAFT DIGITAL INPUT CONTROLLED HYDRAULIC ACTUATION AND CONTROL SYSTEM		5. TYPE OF REPORT & PERIOD COVERED Final Report. August 1977-December 1980
7. AUTHOR(s) Eugene T./Raymond Curtiss W./Robinson		6. PERFORMING ORG. REPORT NUMBER
9. PERFORMING ORGANIZATION NAME AND ADDRESS Boeing Military Airplane Company P.O. Box 3707 Seattle, Washington 98124		8. CONTRACT OR GRANT NUMBER(s) F33615-77-C-2034
11. CONTROLLING OFFICE NAME AND ADDRESS Aero Propulsion Laboratory (AFWAL/POOS) Air Force Wright Aeronautical Laboratories (AFSC) Wright-Patterson AFB, Ohio 45433		10. PROGRAM ELEMENT, PROJECT, TASK AREA & WORK UNIT NUMBERS 62203F 14 31453025
14. MONITORING AGENCY NAME & ADDRESS (if different from Controlling Office)		12. REPORT DATE March 1981 (12) 214
		13. NUMBER OF PAGES 211
		15. SECURITY CLASS. (of this report) Unclassified
		15a. DECLASSIFICATION/DOWNGRADING SCHEDULE
16. DISTRIBUTION STATEMENT (of this Report) Approved for public release; distribution unlimited.		
17. DISTRIBUTION STATEMENT (of the abstract entered in Block 20, if different from Report)		
18. SUPPLEMENTARY NOTES		
19. KEY WORDS (Continue on reverse side if necessary and identify by block number) Digital Electrohydraulic Actuator (DEHA)      Monitor feedback Digital wordstream      Multistepper Dynavector actuator      Parallel-digital (absolute) control Harmonic drive      Power-adaptive control Incremental-digital control      Power-recoverable control		
20. ABSTRACT (Continue on reverse side if necessary and identify by block number) This document reports the development of an incremental digitally-controlled electrohydraulic actuation system (DEHA). An electronic digital controller and a prototype DEHA unit, with an electric-stepper-motor-driven rotary distributor valve, two hydraulic drive motors, and a torque-summing gearbox, were assembled. Significant reductions in the hydraulic power normally required with a conventional geared hydraulic motor system, and some degree of hydraulic power recovery were obtained.		

BLANK

SUMMARY

The use of digital computers in conjunction with electrically-controlled analog hydraulic actuators requires the use of intermediate digital-to-analog (D/A) signal conversion units. Since the use of on-board digital computers or individual microprocessors to provide command signals to hydraulic actuators are foreseen for future aircraft, a research and development program was undertaken to design, fabricate, and demonstrate an actuation system that can provide an output of a precise displacement or movement for each electrical input pulse transmitted from a digital computer.

The first task was to study potential aircraft applications for a digital electrohydraulic actuation (DEHA) system, and to select one in order to define the performance and physical size requirements for a demonstration unit. Since the Air Force F-16 Lightweight Fighter aircraft was just entering service and had a full fly-by-wire control system with actuator requirements readily available, it was decided that one of its actuation systems would make an excellent model. The F-16 rudder actuation system was selected as the basis for the DEHA design and performance requirements.

Tradeoff studies of various DEHA concepts were conducted with the intent of finding a satisfactory design and a qualified subcontractor for the fabrication of a demonstration unit. A survey letter was sent to twenty-four hydraulic equipment manufacturers; and, based on their replies and a number of plant visits, fourteen were invited to submit design proposals.

Two of the supplier companies, Bendix Electrodynamics Division and Sundstrand Aviation Mechanical, did submit proposals. However, in view of the shortcomings of the concepts proposed, a number of alternate designs were devised at Boeing. These were compared; and, in consideration of their relative advantages, complexity, and development risk, one of these was selected for development.

DTIC  
ELECTE  
S SEP 17 1981 D  
D

Accession For	
NTIS GRA&I	<input checked="" type="checkbox"/>
DTIC TAB	<input type="checkbox"/>
Unannounced	<input type="checkbox"/>
Justification	
By _____	
Distribution/	
Availability Codes	
Dist	Avail and/or Special
A	

Two hydraulic drive motors, controlled by a dual-channel rotary distributor valve driven by an electric stepper motor, were utilized in the selected design. Fixed-cylinder-block hydraulic motors with a rotating swash plate were used rather than conventional motors with a rotating cylinder block; and, the two motors were mounted on a torque-summing gearbox which could be used to drive an aerodynamic control surface through a series of linked torque tubes and hinge-line mounted planetary gearboxes. The use of the fixed-cylinder-block motors and the separate rotary valve which externally commutates flow to the motor pistons, rather than internally through valve-plate kidney slots as in conventional motors, were chosen in order to obtain a reduction in hydraulic flow required for slewing the control surface at high rates under low-load conditions. In addition, the rotary distributor valve offers the possibility of reducing the steady-state quiescent leakage flow associated with electrohydraulic servovalves.

A prototype DEHA unit was assembled with hydraulic drive motors, rotary distributor valve, and torque-summing gearbox designed and fabricated by suppliers selected by competitive bidding. An off-shelf electric stepper motor and a feedback shaft encoder were purchased; and, the gearbox was loaded with an existing conventional hydraulic motor which was used as a pump to supply resisting load torque and as a motor to supply an aiding load.

Significant reductions in the hydraulic power normally required, with a conventional geared hydraulic motor system controlled by proportional valves, were obtained. However, the measured power reductions were considerably lower than predicted reductions. The failure to achieve the predicted reductions, and also the predicted degree of power reversibility under following (aiding) loads, was attributed to unexpected motoring resistance in the combined motor, valve, and load pump assembly. It is believed that most of the resistance was due to flow restrictions in the distributor valve which could be relieved by the redesign suggested herein.

Frequency response of the hydromechanical portion of the DEHA system was virtually flat out to 5 Hz and it acted as a second-order system with a break frequency of about 10 Hz. However, the digital controller response was

deficient in that severe low pass filtering of the input signal was necessary to enable the stepping motor drive to follow that input signal.

Durability of the unit was less than desired due to unexpected stress cracking of the rotary distributor valve housing; and, the durability test was cut short of the planned number of actuation cycles required to demonstrate 1,000 hours of flight operation. The same design changes which could reduce motoring resistance would also serve to relieve the high cyclic stresses experienced with the current design, and would thereby increase unit durability.

The program was of value in that it provided a comprehensive comparison of digital actuation schemes for a specific application and an actual demonstration of the load-adaptive feature of the selected concept. However, since there is a concern about the possibility of a single failure jamming a motor-driven power-hinge system, other load-adaptive control schemes which can be applied to hydraulic ram type servoactuators may have better prospects of acceptance.

## FOREWORD

This report was prepared by the Boeing Military Airplane Company Advanced Airplane Branch in Seattle, Washington. It is the final report of research and development work funded by Air Force Contract F33615-77-C-2034, Aircraft Digital Input Controlled Hydraulic Actuation and Control System, which was accomplished under Project No. 3145-30-25 with AFWAL/PCOS between August 1977 and December 1980. The technical report was submitted by the authors in December 1980.

This research and development program was administered under the direction of the Aero Propulsion Laboratory, Air Force Wright Aeronautical Laboratories, Air Force Systems Command, Wright-Patterson Air Force Base, Ohio. The Air Force Project Manager was Mr. Kenneth E. Binns, and the Air Force Project Engineer was Mr. William E. Campbell. The Boeing Program Manager was Mr. Eugene T. Raymond and the Principal Investigator was Mr. Curtiss W. Robinson.

The authors wish to acknowledge the valuable technical contributions of the following individuals:

- a. From the Electronics Technology Organization in the Boeing Aerospace Company's Electronics Support Division: Messrs Paymond E. Pederson, Dale D. Henkes, and James E. Terry for the development of the digital controller unit.
- b. From the Aero Hydraulics, Inc. Company in Fort Lauderdale, Florida: Messrs. L.C. (Tom) Jennings, Robert E. Teeghman, and Rainer R. Elze for the design of the fixed-cylinder-block hydraulic drive motors.
- c. From the Bendix Electrodynamics Division in North Hollywood, California: Messrs. Ralph L. Vick, Robert K. Van Ausdal, and Abraham P. Horstin for the design of the rotary distributor valve.

- d. From the Smith-Williston, Inc. company in Seattle, Washington:  
Messrs. Frank G. Williston, Bernhard A. Pearson, and John Jacobs for the design of the torque-summing gearbox.
  
- e. From the Sigma Instruments, Inc. Motion Control Division in Braintree, Massachusetts:  
Messrs. Tom Beeling and John Morin for their consultation regarding electronic controls for their electric stepper motor.
  
- f. From the Boeing Military Airplane Company, Advanced Airplane Branch in Seattle, Washington:  
Messrs. H. Floyd Hillman and Armand Longchamps for their assistance in conducting laboratory tests of the digital electrohydraulic actuation system.

## TABLE OF CONTENTS

<u>Section</u>	<u>Page</u>
I INTRODUCTION	1
II APPLICATION SELECTION	3
III REQUIREMENTS AND OBJECTIVES	5
3.1 GENERAL DESIGN REQUIREMENTS	5
3.2 GENERAL PERFORMANCE REQUIREMENTS	6
3.2.1 Movement in Discrete Steps	7
3.2.2 Use of Multiple Step Sizes	7
3.2.3 Transient Excursions at Low Stepping Rates	8
3.2.4 Output Rate Saturation	8
3.2.5 Consequences of Partial Hydraulic Supply Failure	8
3.2.6 Consequences of Single Electrical or Electrohydraulic Valve Malfunction	9
3.3 SPECIFIC PERFORMANCE REQUIREMENTS	9
3.3.1 Output Rotation Capability	9
3.3.2 Output Rate Versus Resolution Capability	9
3.3.3 Static Torque Capacity	9
3.3.4 Output Stiffness	9
3.3.5 Dynamic Requirements	9
3.4 ADDITIONAL CHARACTERISTICS DESIRED	10
3.4.1 Absolute Positional Ten-Bit Response	10
3.4.2 Hardover Failure Immunity	10
3.4.3 Aircraft Envelope Compatible	11
3.4.4 Good Frequency Response	11
3.4.5 Low Steady-State Power Demand	11
3.4.6 Adaptable to Load and Rate	11
3.4.7 Adequate Load Stiffness	12
3.4.8 Dual Hydraulic System Redundancy	12
3.4.9 Low Sensitivity to Feedback Failure	12
3.4.10 High-Power-Level D/A conversion	13
3.4.11 Minimum Valving Complexity	13

## TABLE OF CONTENTS (Continued)

<u>Section</u>	<u>Page</u>
IV CONCEPT SELECTION	14
4.1 INDUSTRY SURVEY	14
4.2 EFFORTS AND TO OBTAIN A SUBCONTRACTOR	15
4.3 ACTUATION CONTROL CONCEPTS CONSIDERED	15
4.3.1 Parallel-Digital Actuation Control Concepts	15
4.3.1.1 Differential Position-Summing Arrangements	16
4.3.1.2 Cascaded Valve Arrangements	19
4.3.1.3 First-Stage Torque-Summing Arrangements	19
4.3.2 Incremental-Digital Actuation Control Concepts	23
4.3.2.1 Hydraulic-Amplified Stepping Motors with Net Position-Error Storage	23
4.3.2.2 Electrohydraulic Steppers With Stepwise Position-Error Storage	26
4.3.2.3 Stepper Motor With Hydraulic Incremental Torque Rebalance	32
4.4 CONCEPT EVALUATION AND SELECTION	39
4.4.1 Candidate Arrangements Selected for Final Evaluation	39
4.4.2 The Selected Concept	40
4.5 COMPONENT SELECTION AND ARRANGEMENT	41
4.5.1 Means of Generating, Combining, and Transmitting Torque	41
4.5.1.1 Torque Generation and Transmission Elements	41
4.5.1.2 Means of Combining Motor Torques and Overcoming Hydraulic Failures and Mechanical Jams	42
4.5.2 Major Component Decisions	45
4.5.2.1 Fixed-Cylinder-Block vs Rotary-Block Hydraulic Motors	45
4.5.2.2 Number of Hydraulic Motor Pistons	47
4.5.2.3 Valving schemes	50
4.5.2.4 Electric Stepper Motor Choice	51
4.5.3 Major Subassemblies and Component Arrangement	53
4.5.3.1 Digital Controller	53
4.5.3.2 Dual Electric Stepper Motor	55

TABLE OF CONTENTS (Continued)

<u>Section</u>	<u>Page</u>
4.5.3.3 Hydraulic Distributor Valve	55
4.5.3.4 Hydraulic Motors	56
4.5.3.5 Motor Clutches	56
4.5.3.6 Torque-Summing Gearbox	56
4.5.3.7 Harmonic Drive	57
4.5.3.8 Shaft Encoder	57
4.5.3.9 Jam Detection and Clutch Logic Circuit	57
4.5.3.10 Power-Hinge Torque Tubes and Gearboxes	57
4.6 DEMONSTRATION SYSTEMS	58
4.6.1 Suitcase Digital Controller	58
4.6.2 DEHA Prototype Demonstration System	60
4.6.2.1 Electric Stepper Motor	60
4.6.2.2 Hydraulic Distributor Valve	64
4.6.2.3 Hydraulic Motors	64
4.6.2.4 Motor Clutches	64
4.6.2.5 Torque-Summing Gearbox	64
4.6.2.6 Harmonic Drive	64
4.6.2.7 Shaft Encoder	64
4.6.2.8 Jam Detection and Clutch Logic Circuit	65
4.6.2.9 Power-Hinge Torque Tubes and Gearboxes	65
4.6.2.10 Hydraulic Load Pump	65
V DIGITAL CONTROLLER DEVELOPMENT	66
5.1 CONTROL FUNCTIONS	66
5.1.1 Command Signal Generation	66
5.1.2 Monitor Feedback	72
5.2 CONTROL CIRCUIT DESIGN	73
5.2.1 Low-Pass Filter	75
5.2.2 A/D Converter	75
5.2.3 Microprocessor Authority and Functions	75

TABLE OF CONTENTS (Continued)

<u>Section</u>	<u>Page</u>
5.2.4 Basic Open-Loop Operation	77
5.2.4.1 Error-Correction Command	77
5.2.4.2 Displays	77
5.2.4.3 Analog Output	78
5.3 CONTROLLER TESTING	78
VI DEHA DESIGN AND FABRICATION	80
6.1 GENERAL ARRANGEMENT	80
6.2 ROTARY DISTRIBUTOR VALVE	81
6.2.1 Valve Design	81
6.2.2 Valve Fabrication	89
6.3 HYDRAULIC MOTOR	92
6.3.1 Hydraulic Motor Design	92
6.3.2 Hydraulic Motor Fabrication	98
6.4 TORQUE-SUMMING GEARBOX	98
6.4.1 Gearbox Design	98
6.4.2 Gearbox Fabrication	100
6.5 DEHA UNIT ASSEMBLY	104
VII DEHA EVALUATION TESTING	111
7.1 COMPONENT TESTS	111
7.1.1 Rotary Distributor Valve Tests	111
7.1.1.1 Breakaway Torque Test	111
7.1.1.2 Break-in Run	111
7.1.1.3 Proof Pressure Tests	114
7.1.1.4 Leakage Tests	114
7.1.1.5 Distribution Pattern Check	118
7.1.1.6 Rated Flow Pressure Drop Test	119
7.1.2 Hydraulic Motor Tests	119
7.1.2.1 Hand Torque Test	119
7.1.2.2 Proof Pressure Test	125
7.1.2.3 Shaft Seal Leakage	125
7.1.2.4 Internal Leakage Test	125
7.1.2.5 Breakout Friction Test	125

## TABLE OF CONTENTS (Concluded)

<u>Section</u>	<u>Page</u>
7.1.2.6 Stall Torque Test	125
7.1.2.7 Dynamic Balance	126
7.1.3 Torque-Summing Gearbox Tests	126
7.2 DEHA PROTOTYPE UNIT TESTS	126
7.2.1 Break-in and Functional Checkout Tests	130
7.2.1.1 Tracking and Reversing Test	130
7.2.1.2 Slewing Test	134
7.2.2 Performance Tests	135
7.2.2.1 Flow-Demand Performance Tests	135
7.2.2.2 Additional Testing to Isolate Factors Increasing Demand Flow	138
7.2.2.3 Frequency Response Test	139
7.2.2.3.1 Test Procedure	141
7.2.2.3.2 Frequency Response Test Results	145
7.2.3 Durability Tests	159
7.2.3.1 Test Procedure	160
7.2.3.2 Durability Test Results	163
VIII POST-TEST EVALUATION	169
8.1 PERFORMANCE EVALUATION	169
8.2 DESIGN EVALUATION	175
8.2.1 General Design Considerations	175
8.2.2 Specific Design Details	176
IX CONCLUSIONS	179
REFERENCES	182
APPENDIX A POWER ADAPTABILITY AND POWER REVERSIBILITY FEATURES	183
APPENDIX B CONTROLLER ELECTRONIC CIRCUITS	188
GLOSSARY OF TERMS	192
LIST OF ABBREVIATIONS, ACRONYMS, AND SYMBOLS	194

## LIST OF ILLUSTRATIONS

<u>Figure</u>		<u>Page</u>
1	F-16 integrated servoactuator schematic diagram	4
2	Digital actuation control concepts considered	17
3	Differential position-summing actuation and control arrangements	18
3a	Cascaded piston actuator	18
3b	Cascaded array of three-input-terminal swash-plate differentials positioning hydraulic motor control valves	18
4	Cascaded valve arrangement (for a three-bit parallel digital actuator)	20
5	First-stage torque-summing arrangements	22
5a	Torque motor with staged coils	22
5b	High-level torque summing with spring position feedback	22
5c	High-level torque summing with encoder position feedback	22
6	Abex prototype electrohydraulic pulse motor	25
7	Electrohydraulic linear stepper actuator (ELSA)	27
8	Electrohydraulic rotary stepper actuator	29
9	Dual ELSA pilot stage proposed by Sundstrand	30
10	Overall hydraulic-motor-driven actuation system proposed by Sundstrand	31
11	Electrohydraulic stepper motor arrangements with external-commutating rotary valves	34
11a	System with fixed-cylinder-block hydraulic motors	34
11b	System with rotary-cylinder-block hydraulic motors	34
12	Electrohydraulic stepping motor arrangement with external-commutating electrohydraulic valves	36
13	Incremental Dynavector actuator proposed by Bendix Electrodynamics Division	38
14	Typical installation arrangements of a DEHA rudder actuation system	44
14a	Torque-summing arrangement	44
14b	Velocity-summing arrangement	44
15	Hydraulic motor cylinder block tradeoffs	46

LIST OF ILLUSTRATIONS (Continued)

<u>Figure</u>		<u>Page</u>
16	Rotary-cylinder-block electrohydraulic stepper	48
17	Three-state output-switching fluid valve	52
18	DEHA configured for aircraft installation	54
19	Suitcase digital controller	59
20	Dual-hydraulic-channel DEHA unit configured for the prototype system	61
21	Prototype DEHA viewed from drive-motor side	62
22	Prototype DEHA viewed from load-pump side	63
23	Suitcase controller panel layout	67
24	Sigma Instruments stepper logic unit circuit	68
25	Sigma Instruments stepper-motor driver card schematic	69
26	Signal input network	71
27	Digital controller schematic	74
28	First-order (times three) functional filter	76
29	Digital controller frequency response	79
30	Pneumatic stepper motor fabricated at Boeing in 1976	82
31	Rotary valve porting sequence	83
32	Rotary valve cross-section showing balanced porting	84
33	Spool-sleeve design using pressure and return ports in parallel rows.	86
34	Four-phase valve porting geometry with spool slots folded together	88
35	Six-phase spool and sleeve metering geometry	90
36	Hydraulic distributor valve with original two-piece spool	91
37	Bendix stepper-driven rotary distributor valve	93
38	Thirty-degree six-piston hydraulic motor with connecting-rod coupling of pistons	95
39	Thirty-degree six-piston hydraulic motor with extended pistons and guides	96
40	Thirty-five degree six-piston hydraulic motor with rotating piston shoes	97

LIST OF ILLUSTRATIONS (Continued)

<u>Figure</u>		<u>Page</u>
41	Hydraulic drive motor developed by Aero Hydraulics, Inc. for the DEHA program	99
42	Torque-summing gearbox developed by Smith-Williston, Inc. for the DEHA program	103
43	Mechanical components - DEHA prototype unit	105
44	Intended motor phasing	109
45	Corrected motor phasing	109
46	Test setup for motoring the rotary distributor valve	113
47	Test setup for hand turning the rotary distributor valve	115
48	Hydraulic motor single-port fluid adapter	123
49	Hydraulic motor stall torque test circuit	127
50	Gearbox lubrication pump	128
51	Hydraulic flow bench	129
52	Schematic diagram of the DEHA performance test setup	131
53	Electric pulse generator for single-step commands	132
54	Flow-demand performance curves	136
55	Solartron frequency analyzer and Hewlett-Packard mini-computer and digital plotter.	140
56	Frequency response test schematic	142
57	Static gain of digital controller	143
58	Overall system frequency response at low signal	146
59	Overall system frequency response	147
60	Digital controller frequency response	148
61	Frequency response of DEHA at .10 volts command	149
62	Frequency response of DEHA at .28 volts command	150
63	Frequency response of DEHA at .32 volts command	151
64	Frequency response of low pass filter	152
65	Frequency response of digital circuits & DEHA with filter capacitor	153
66	Frequency response of digital circuits & DEHA without filter capacitor	154

LIST OF ILLUSTRATIONS (Concluded)

<u>Figure</u>		<u>Page</u>
67	Frequency response with .28 volts command	155
68	Frequency response with one DEHA motor unpowered	156
69	Frequency response of digital circuitry	157
70	Digital circuitry linearity study	158
71	Schematic diagram of the DEHA durability test setup	162
72	John Fluke Manufacturing Co. Data Logger	164
73	Shuttle-relay valve with dual relief-valve function	172
74	Typical installation of check-relief valves	174

## LIST OF TABLES

<u>Table</u>		<u>Page</u>
1	F-16 Rudder Servoactuator Parameters	4
2	Gearbox Speed and Torque Ratios	101
3	DEHA Performance Parameters	102
4	Rotary Distributor Valve Breakaway Torque Test Data	112
5	Rotary Distributor Valve Internal Leakage Test Data	116
6	Rotary Distributor Valve Shaft Seal Leakage Test Data	118
7	Rotary Distributor Valve Distribution Pattern Data	120
8	Rotary Distributor Valve Rated Flow Pressure Drop Data	122
9	Hydraulic Drive Motor Test Results	124
10	Summary of Frequency Response Test Conditions	144
11	Durability Test Cycling Schedule	161
12	Test Parameter Limits for Automatic Shutdown of the Durability Test	165

BLANK PAGE

## I. INTRODUCTION

Present trends in aircraft actuation systems are toward electrically controlled hydraulic actuators. Centrally located on-board digital computers or individual microprocessors are foreseen to provide the command signals to these actuators.

Digital computers have been used for many years for inertial navigation and air data computing systems; and, they are now being developed for primary flight control systems and for the control of other aircraft functions such as engine variable geometry controls and radar antenna drives. Conventional hydraulic ram actuators and motors controlled by electrohydraulic servovalves are normally used for these tasks. Flight control surfaces are positioned either by conventional integrated hydraulic servoactuators, which can accept both mechanical input commands from the pilot and electrical commands from the autopilot and stability augmentation systems, or by all-electrical-command "fly-by-wire" actuators with electrohydraulic servovalves. In each case, the electrohydraulic valves are analog devices; and, digital-to-analog (D/A) signal conversion is required to adapt them to digital control systems.

The purpose of the research and development program reported herein was to examine hydraulic actuation and control techniques that can be directly controlled by digital computers. The concept desired was to provide an output of a precise displacement or movement for each electric pulse transmitted from a computer or microprocessor. Upon identification and analysis of candidate concepts, one was to be selected and a prototype unit designed and fabricated and its performance demonstrated in laboratory tests. The unit was to be called a digital electrohydraulic actuator (DEHA).

The program description/specifications specified that actuation concepts that do not require the conversion of digital command signals to analog form were to be investigated. It also specified that the concepts must be capable of performing continuous duty, high response, and high cycle rate type functions. In addition, a preference for concepts which provide direct rotary output was expressed.

In addition to eliminating the need for electronic D/A conversion provisions, it was deduced that a DEHA system might provide the following additional advantages over conventional fly-by-wire servactuators:

- a. A finer degree of repeatable position resolution without much of the hysteresis error associated with analog systems. This could improve aircraft tracking and weapon delivery.
- b. Elimination of hardover transients due to open-circuit failure of a feedback element. This would eliminate a worrisome failure effect of fly-by-wire servactuators and thereby improve flight safety.
- c. A reduction of the steady-state quiescent leakage flow associated with conventional electrohydraulic servovalves. This would reduce power drain and heat generation in the hydraulic supply system.

In addition, it was found that some of the candidate actuator arrangements could be configured to adapt to changes in load so as to require less fluid flow per unit of motion at low load than at high load, such as with a variable-displacement hydraulic motor. Aircraft hydraulic systems are often sized by maximum flight control actuation rates which occur at low loads such as in gusty air during landing. The reductions in peak hydraulic flow demands achieved through the use of power-adaptive actuators could allow attractive reductions in aircraft weight through the use of smaller pumps, hydraulic lines, reservoirs, and other components.

In this report, the candidate concepts which were considered, the power-adaptive hydraulic stepper motor actuation system which was selected, and its design and performance are described and discussed.

## II. APPLICATION SELECTION

The first task in this research and development program was to study potential aircraft applications for a DEFA system, and to select one in order to define the performance and physical size requirements for a prototype unit. It was apparent that many utility and secondary flight control actuation functions are viable candidates for control with microprocessors or digital computers. It was also clear that the requirements for continuous-duty modulating actuation systems, such as for primary flight control surfaces or engine inlet control devices, are more demanding, and that, if a concept could be developed to meet those more demanding requirements, it could also be adapted to meet lesser requirements.

Since the Air Force F-16 Lightweight Fighter Aircraft was just entering operational service and has a full fly-by-wire flight control system with actuator requirements readily available, it was decided that one of its actuation systems would make an excellent application for the desired actuator. The F-16 rudder actuation system was selected as the basis for the DEFA design, and the detailed design requirements were based on the parameters of the existing hydraulic servoactuator listed in Table 1. A schematic diagram of the actuator is shown in Figure 1.

TABLE 1 F-16 RUDDER SERVOACTUATOR PARAMETERS

1. Type	Tandem Fly-by-wire Hydraulic Acuator with Mechanical Feedback
2. Hydraulic Fluid	MIL-H-5606
3. Supply Pressure psi	3100 Nominal (2800 minimum)
4. Rated Output Stall Torque lb ft @ 3000 lb/in <sup>2</sup> (Both system Active)	4792
5. Maximum Surface Deflection Degrees	+30
6. No-Load Rate deg/s	120
7. Hysteresis Requirement	3.5% of Peak Input (Total Width)
8. Threshold Requirement	0.2% of Rated Input
9. Response Requirement at 24 rad/s frequency: at 140 rad/s frequency:	Amplitude ratio - 4db ± 0.5db Phase Shift less than 90 deg Amplitude ratio less than - 32db
10. Actuator Stiffness $\frac{\text{lb-in}}{\text{rad}}$	2,633,000
11. Rated Hydraulic Flow (per system)	4.97
12. Surface Inertia lb-in <sup>2</sup> gpm	2475

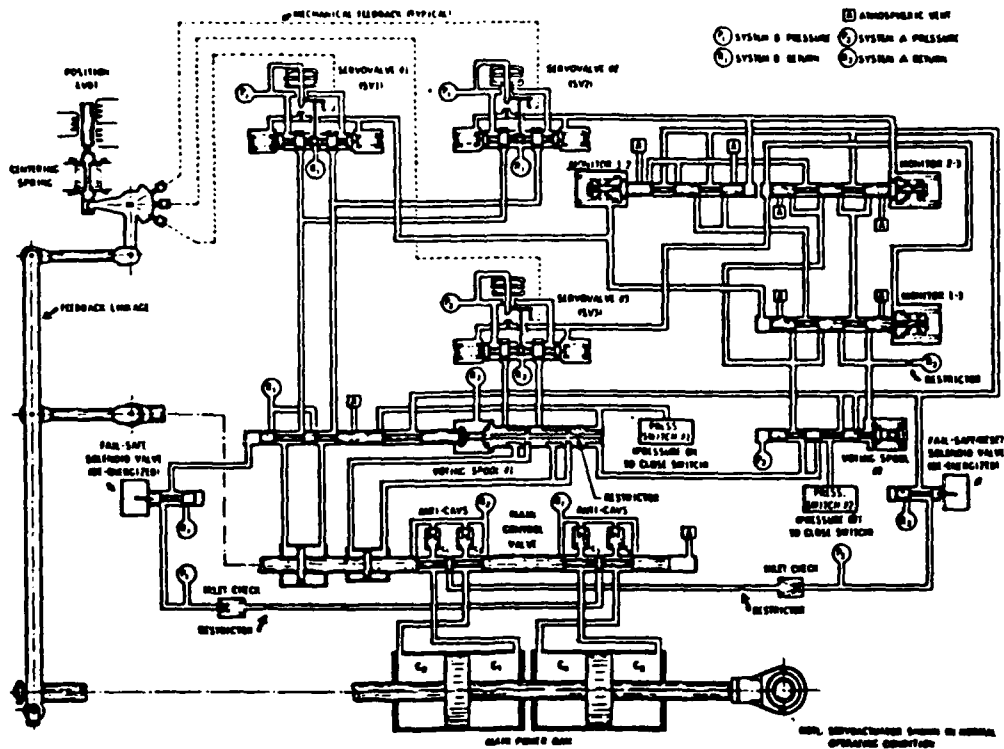


Figure 1 F-16 integrated servoactuator schematic diagram  
(From SAE Paper 760940, Reference No. 3)

### III. REQUIREMENTS AND OBJECTIVES

Following the selection of the F-16 rudder actuation system as an aircraft function representative of a potential application for a digital electrohydraulic actuator, performance and design criteria pertinent to the application of a DEHA for performing that function were established. A problem-statement specification was prepared for use in assessing candidate actuation control concepts and for use in soliciting design proposals from hydraulic servoactuator suppliers. It included the known pertinent performance requirements for the F-16 rudder actuation system and a prioritized listing of additional characteristics desired in a DEHA system.

#### 3.1 GENERAL DESIGN REQUIREMENTS

In order to obtain equivalence to the F-16 rudder servoactuator, including its dual hydraulic power source redundancy, it was decided that only those actuation unit arrangements which include two torque producing elements, which can be powered from two constant-pressure 3,000-psi hydraulic sources, would be considered. It was also proposed that concepts must be capable of being configured as an acceptable aircraft component which could be installed within the aft body and vertical fin envelope of the F-16 aircraft to replace the current fly-by-wire dual-tandem linear analog rudder servoactuator. Such an actuator would be required to meet all pertinent electric, hydraulic, and mechanical design requirements normally specified for aircraft flight control servoactuators.

In addition, it was specified that the control valving for the prototype unit must be capable of responding directly to digital binary-word input signals directly from a digital computer or microprocessor to command the actuator output member to move in step increments of several sizes. The requirement for capability to respond to binary-word input signals was for convenience. Although other codes may be considered in actual systems, binary codes are well known and the type most commonly used in computer data processing.

The requirement for control valving capable of commanding the output to move in step increments of several sizes was specified as a means of resolving the problem of output rate vs resolution which occurs whenever a stepping motor must be designed to move at a high output rate and also maintain a capability for small individual high-resolution steps. A second reason for specifying a multi-stepper type response was that almost any direct absolute electrical or hydraulic digital actuator not employing an A/D feedback was seen to require a response of this type.

The potential for reducing hydraulic power consumption by skipping the pressurization of one or more pistons when slewing the rudder at high rates under relatively low hinge-moment load conditions was also recognized. However, since there are other means of obtaining the potential power savings, piston skipping was not made a requirement.

In addition to hydraulic power savings, it was recognized that digitally-controlled actuators could provide improved actuator positioning accuracy giving finer control surface position resolution which could improve aircraft tracking capability and weapon delivery. It was also recognized that a digitally-controlled actuator could be designed to minimize the risk of *hardover failures* by using open-loop control with a monitoring encoder feedback used only for condition initializing and low-rate error correction.

On the F-16 servoactuators, mechanical feedback to the electrohydraulic servovalves is used to reduce the risk of *hardovers* which is inherent in units with electrical feedback to the control valve summing junction. However, with the mechanical feedback summed with the inputs to the servovalve torque motor at the jet pipe armature, as shown in Figure 1, the hysteresis error of the entire servoactuator can be no better than that obtained from the electrohydraulic valves because there is no place to insert electronic gain and phase compensation in the servoactuator forward loop.

## 3.2 GENERAL PERFORMANCE REQUIREMENTS

A basic and overriding requirement was that the DEHA be capable of meeting the specified performance requirements currently met by the F-16 dual-tandem linear servoactuator. The following general requirements were also specified.

### 3.2.1 Movement in Discrete Steps

The servo output shall move from one commanded position to another in a series of discrete steps.

In order to follow a binary word which can be assumed to change by least-bit increments during flight maneuvers, a DEHA servo must be capable of moving in steps corresponding approximately to the least variations of the input word.

### 3.2.2 Use of Multiple Step Sizes

The size of actuator output steps shall be governed by the rate of change of the magnitude of the net input digital word. These step amplitudes shall vary as a binary progression.

This feature was intended to allow relief of the switching rate vs. resolution problem. A DEHA system must move an output through a limited stroke at a defined rate by a switching process which produces discrete steps. Any decrease of this least step size will increase the required stepping rate. With multiple step sizes, the problem of producing an adequate stepping rate would be relieved.

The use of multiple step sizes was not a mandatory feature, but was allowed if needed to relieve stepping rate problems and as a potential method of reducing motor volumetric displacement at high output slew rates.

### 3.2.3 Transient Excursions at Low Stepping Rates

For slowly changing input word magnitudes, the servo output shall move in steps corresponding to the least-bit increment in the input word. No large (greater than one least-bit) transient output excursions will be permitted in transition between adjacent least-bit output values.

This stipulation limits the individual output steps to 100% overshoot of a least-bit step.

### 3.2.4 Output Rate Saturation

Large transient step commands shall cause the actuator output member to move toward the commanded position at a saturation limited rate.

Large step commands may occur as at startup of a system; and, such step commands should be answered by an output response at a pre-determined limited rate.

### 3.2.5 Consequences of Partial Hydraulic Supply Failure

Following the loss of either hydraulic supply system, the unit shall continue to operate but may suffer an approximately fifty percent reduction in output torque capability and a doubling of the least-bit step size seen at the output.

It is desirable for hydraulic supply failure to be reflected as a loss of torque or resolution and not as a loss of control surface stroke. Loss of surface rate capability could also be tolerated better than stroke loss. This preserves the ability of an aircraft to return to its base and land after a single hydraulic system power failure.

3.2.6 Consequences of Single Electrical or Electrohydraulic Valve Malfunction.

The unit shall continue to operate with only a loss of output resolution following malfunction of any single valve or electrical signal input in any possible valve or signal state.

This requires a functional continuity of the DEHA system following any conceivable single component failure.

3.3 SPECIFIC PERFORMANCE REQUIREMENTS

3.3.1 Output Rotation Capability

The output member which could be coupled directly to the F-16 rudder shall be capable of rotating  $\pm 30$  degrees.

3.3.2 Output Rate Versus Resolution Capability

The DEHA shall be capable of driving the rudder at a rate of 120 deg/s while maintaining a capability to step with a least-bit increment of 0.06 deg. This does not imply that the 120 deg/s rate must be made up of 0.06-deg steps.

3.3.3 Static Torque Capacity

The DEHA shall be able to produce a static torque of 4000 lb-ft. with a differential pressure of 2800 psi available to both torque producing elements.

3.3.4 Output Stiffness

With only one of the two torque producing elements pressurized, the blocked-port stiffness of the DEHA at the output member shall be at least 400,000 lb-in/rad.

### 3.3.5 Dynamic Requirements

- a. Load poles, defined as the dominant second-order response characteristic of the actuator response when driving a rudder mass load of  $2,475 \text{ lb-in}^2$ , must have a frequency  $> 40 \text{ Hz}$ .
- b. Load pole damping must be  $> 0.7$  either with or without encoder feedbacks connected.

### 3.4 ADDITIONAL CHARACTERISTICS DESIRED

The following additional characteristics, listed in their approximate order of importance, were included in the problem-statement specification to apprise the bidders of the target properties which would be used in evaluating proposed concepts. It was also stated that it was not expected that all of these desirable characteristics would be obtainable with any given design.

#### 3.4.1 Absolute Positional Ten-Bit Response

A DEHA servo should be one having an absolute positional response to a digital word of no less than 10 bits. The reference system made up of a hydraulic analog position servo with an electronic D/A input exhibits absolute positional response, hence the DEHA can do no less. A 10-bit resolution giving, 1024 parts of an input variable or output full stroke, was believed to be a minimum acceptable resolution for any specific flight condition. Surface force gain (sensitivity) at high flight dynamic pressures may require higher surface resolution equivalent to more bits in the input word.

#### 3.4.2 Hardover Failure Immunity

A DEHA servo should not be prone to hardover failure upon total loss of electronic feedback or upon loss of a specific electronic feedback component. All electrohydraulic servos using electronic feedback of output position, or spring feedback as in the F-16 servos, are vulnerable to hardover

surface transients upon loss of the feedback transducer signal, or spring breakage in the case of the F-16. This is a major area of potential improvement for a DEHA servo and this area must be exploited in order to achieve one potential advantage of a DEHA device.

#### 3.4.3 Aircraft Envelope Compatible

A DEHA servo should be adaptable to the minimum envelope requirements for actuation of a thin aerodynamic surface trailing edge control surface. One of the best means of meeting this requirement with a unit providing a direct rotary output, which was an expressed preference in the contract specifications, is with rotary gearboxes transmitting output torque to the control surface at its hinge line.

#### 3.4.4 Good Frequency Response

A DEHA servo should have frequency response to small-amplitude periodic inputs comparable to that of an analog type valved-ram servo.

#### 3.4.5 Low Steady-State Power Demand

A DEHA servo should have small hydraulic power demand when holding against a steady output load. The only significant hydraulic power demand of a valved ram servo under these conditions amounts to a few tenths of a gpm of open-center flow in the hydraulic first stage of each electrohydraulic servo valve used. Steady internal leakage flow in excess of the amount drawn by a conventional analog type valve actuator system would be considered a serious defect in a DEHA system.

#### 3.4.6 Adaptable to Load and Rate

A DEHA servo should be able to run at least two different power levels in order to adapt its servo power consumption to non-coincident maximum load and rate requirements. A hydraulic motor commutated by an independent free-cycling valve system will adjust its hydraulic power consumption to the load that is applied to its shaft. DEHA concepts which provide comparable

power savings as an inherent feature of their design were desired. The use of independent variable-ratio or variable-displacement mechanisms adapted for the sole purpose of improving efficiency, and which could also be adapted to analog units, were not considered acceptable means of satisfying this requirement.

#### 3.4.7 Adequate Load Stiffness

A DEHA servo should be one having load stiffness equivalent to that of an analog type valved ram servo in the same application. This requirement insists on output stiffness equivalence to a system consisting of an electronic D/A converter driving a valved-ram hydraulic servo with a high gain position feedback. Equivalent output stiffness for both systems should yield comparable second order load-pole frequencies for equal mass loading.

#### 3.4.8 Dual Hydraulic System Redundancy

A DEHA servo should have dual redundancy of power supply and valving inherent in the servo design without additional gross duplication of system components. This can be restated to say that the simplest acceptable system having no single-thread failure modes would be considered the best system.

#### 3.4.9 Low Sensitivity to Feedback Failure

A DEHA servo should not be fully dependent on an A/D encoder or similar instrument in a feedback path in order to achieve a conversion from a digital input to a rotational position output. Full dependence upon such a feedback would imply a high gain feedback from such a position sensing instrument. An open-circuit failure of such a sensor would cause an immediate hardover failure of the actuator system. This was not intended to imply that an A/D feedback could not be employed in a monitor capacity so long as proper safeguards against sudden hardover failures were employed.

#### 3.4.10 High-Power-Level D/A Conversion

A DEHA servo should have D/A conversion accomplished at the maximum possible (hydraulic) power level. Candidate DEHA systems could be formulated which would be nothing more than a revised or somewhat improved (electromechanical) D/A converter stage followed by a conventional hydraulic position-feedback servo. It is difficult to justify such a DEHA servo over a system which uses electronic D/A conversion unless an advantageous combination of component functions can be arranged between the input signal element and the motor output of the DEHA. This combination should justify itself by specific performance advantages such as power economy and immunity to specific failures.

#### 3.4.11 Minimum Valve Complexity

A DEHA servo should achieve a maximum bit level of resolution with a minimum number of discrete hydraulic valving elements and/or valve stages. This was required simply to make the resulting DEHA cost competitive with a conventional system using an electronic D/A conversion.

## IV. CONCEPT SELECTION

The next major task was to select a single concept with sufficient merit to warrant development of a prototype unit. This was accomplished by reviewing existing digital actuator types, deriving additional concepts as necessary, and evaluating those designs which had the potential for meeting the stated requirements and desired objectives.

### 4.1 INDUSTRY SURVEY

A survey letter requesting information about concepts which could be offered as candidates for consideration was sent to twenty-four hydraulic equipment manufacturers. It was found that a number of them have acquired considerable experience and were marketing digital-control actuation systems, including the microprocessors and encoders, for industrial uses such as flow control and for positioning machine tool workpieces. Some of these systems include electric stepper motors for controlling hydraulic or pneumatic valves, and others use multiple solenoid valves. A number of them had also investigated digital-control actuation schemes for aircraft applications and jet-engine fuel controls.

Although many of the schemes depended on electronic digital-to-analog conversion, they did contain one or more components which could be used in a DEHA system. At least three different hydraulic stepping motor schemes were outlined by various manufacturers. All full parallel digital actuators found in current use were of a type requiring cascaded spool valves, one valve per resolution bit, and were typically used for positioning in machine tools.

#### 4.2 EFFORTS TO OBTAIN A SUBCONTRACTOR

After reviewing the information obtained, it appeared that the requirement to provide a DEHA unit with performance equivalent to the existing F-16 electrohydraulic servoactuator would eliminate all but absolute or parallel digital servos which will reproduce the weighted value of the sum of all of the bits of a digital input word in the form of a proportional position output. Although none of the companies contacted had an existing concept for the flight control application, it was believed that several were capable of generating one. Therefore, the problem-statement specification noted in Section III, outlining the design and performance requirements, and noting the acceptable design approaches for the actuator type and the primary elements, was sent to the fourteen most promising suppliers. They were invited to submit proposals for the design and fabrication of a small-scale model and two full-scale prototype DEHA units.

Twelve of the selected suppliers declined to bid; however, the following two did submit bids, and their proposed concepts are described in subsections 4.3.2.2 and 4.3.2.3 respectively:

Sundstrand Aviation Mechanical  
Bendix Electrodynamics Division

#### 4.3 ACTUATION CONTROL CONCEPTS CONSIDERED

In the following subsections, each of the control concepts considered are identified. Because it is difficult to distinguish digital control mechanisms according to different designs and different system techniques, they have been categorized according to signal structure. That breakdown results in the use of the terms parallel-digital (absolute) control and incremental-digital (stepper) control.

##### 4.3.1 Parallel-Digital Actuation Control Concepts

The essential feature of a parallel digital wordstream is embodied in the simultaneous update of each of its bit states at equally spaced time intervals controlled by a computer clock. The output of a digital

electrohydraulic actuator responding to such a signal must be either a displacement, velocity, or force proportional to the sum of these timely coincident weighted bits of the reference input wordstream. The summing process can be done with any one of the three types of mechanization identified in Figure 2 which are discussed below.

#### 4.3.1.1 Differential Position-Summing Arrangements

A number of arrangements, where the output positions of several actuators which can be commanded to either their fully retracted or fully extended positions and are differentially summed, can be considered either as a final output stage or as a pilot stage to a mechanical-input servovalve used to position a linear piston servoactuator or a hydraulic motor.

One such type is a cascaded piston arrangement such as shown in Figure 3a, with rams having binary weighted strokes whose stroke lengths vary from each other as in a binary progression (1X, 2X, 4X, 8X, etc). Each piston is controlled by a two-position three-way valve. Supply pressure acting on the rod-end side of the pistons keeps each ram retracted until its head-end side is pressurized to move it full stroke against its stop. The number of output positions (N) is determined by the number of pistons as  $N=2^n$  eg:16 positions for the 4-piston unit shown. Therefore, it is seen that ten pistons would be required to obtain the 1,024 output positions necessary to meet the specified position resolution requirement of the F-16 rudder.

Another arrangement of this type uses a cascaded array of three-input-terminal swash-plate differential mechanisms as shown in Figure 3b. Each input terminal is positioned by a two-position piston controlled by a solenoid valve; and, the piston strokes vary as in a binary progression. To accomplish this binary weighting, both the stroke ratios of the pistons and the input-output ratio of the individual swash-plate devices may be used to relieve the apparent requirement for a 512:1 ratio between required piston strokes to obtain a ten-bit device.

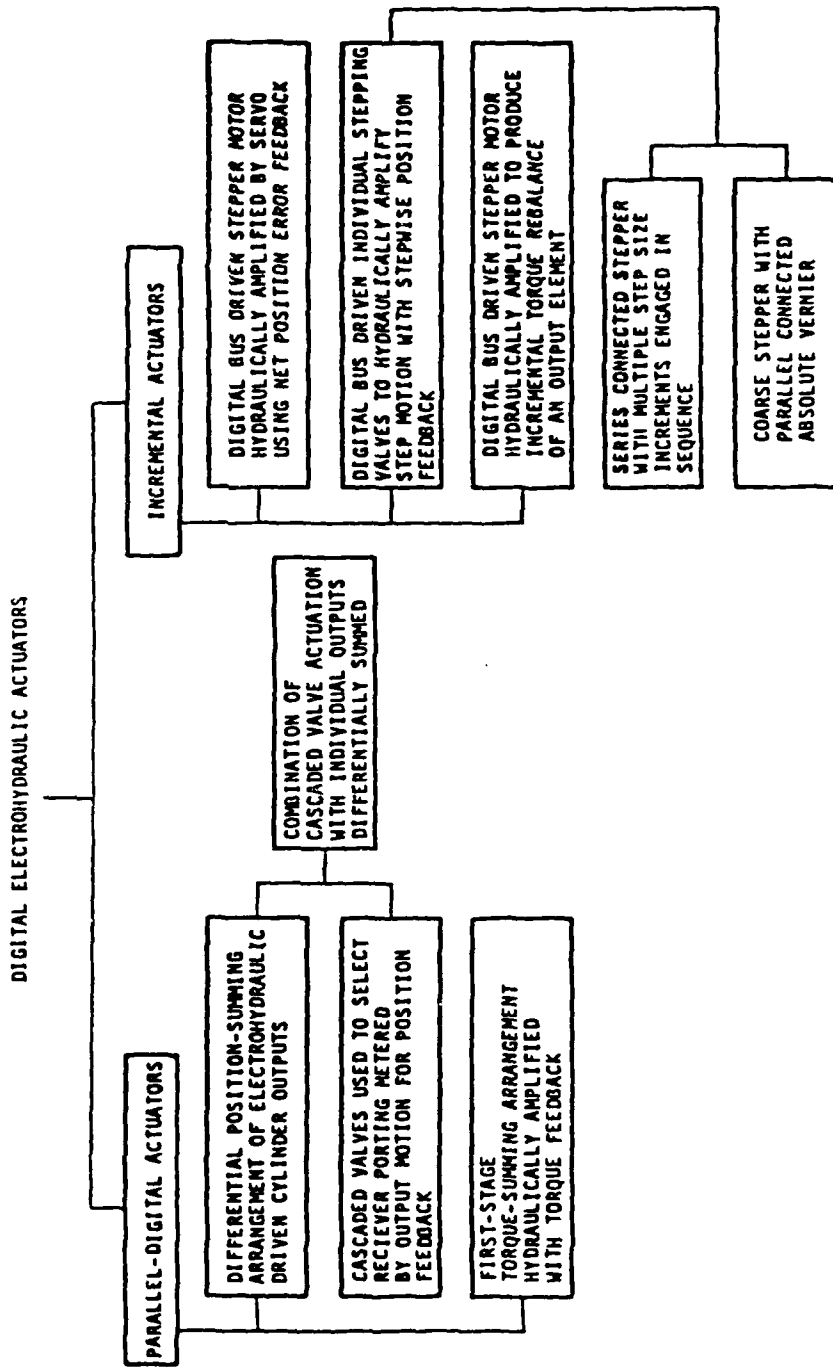


Figure 2 Digital actuation control concepts considered

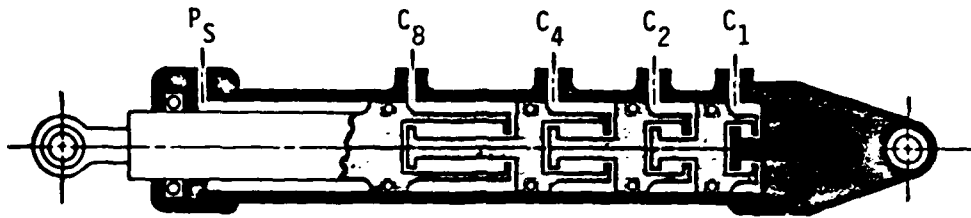


Figure 3a Cascaded piston actuator

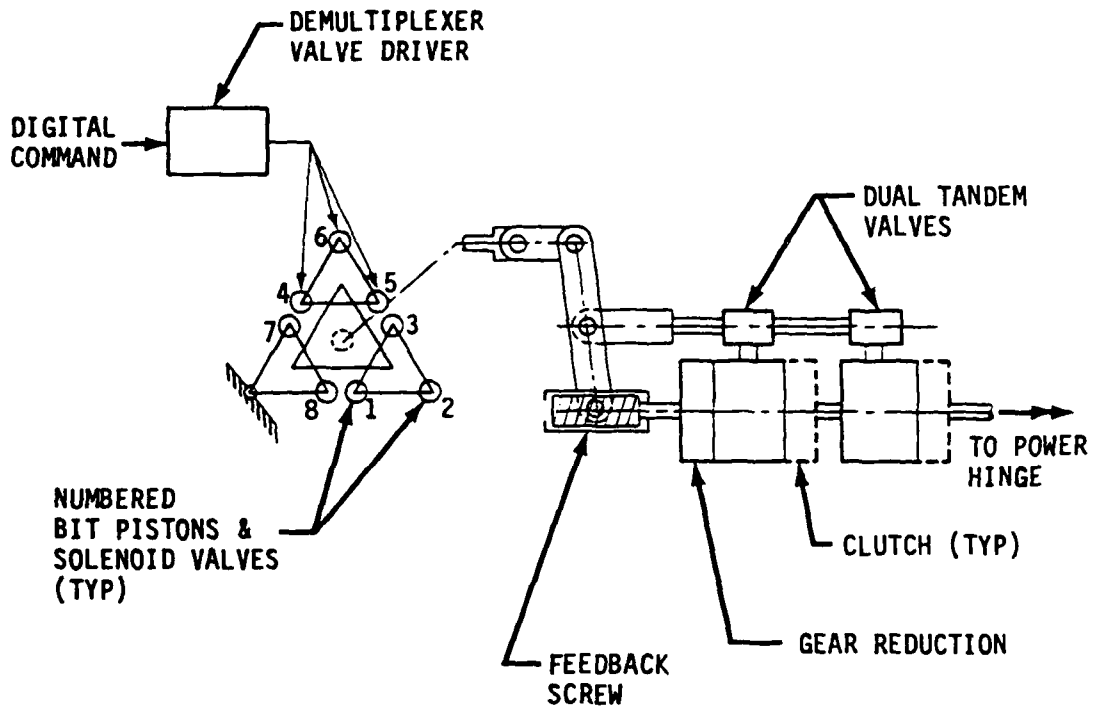


Figure 3b Cascaded array of three-input-terminal swash-plate differentials positioning hydraulic motor control valves

Figure 3 Differential position-summing actuation and control arrangements

Both of these arrangements require a large number of valves and dynamic seals to control and seal the multiplicity of actuator pistons. Aside from being relatively complex, the scheme yields unacceptable transient behavior when responding to a smoothly varying input signal. This transient disturbance originates in the nature of a binary sequence where, for example, counting from seven to eight implies the removal of seven unit bits and the addition of eight unit bits. To avoid transient output excursions, such significant adding processes must be accomplished simultaneously, since any time mismatch may result in an unacceptable transient disturbance of the output. This approach was eliminated both for its complexity and for its unsolved transient problem.

#### 4.3.1.2 Cascaded Valve Arrangements

A number of arrangements where valves are cascaded to generate an absolute positional output by encoding the input signal to least-bit spaced receiver ports controlled by the actuator output can be considered. One such type, shown in Figure 4, uses both supply and return ports for fixed-point control. The three-bit actuator shown has three sets of output piston metering lands acting as control elements. Chamber  $C_1$  and  $C_2$  are controlled by three two-position solenoid valves with multi-porting arrangements. Pressurizing the piston moves the actuator and load with the output stopping as soon as the piston lands balance the supply and return ports.

Since all such arrangements require a separate spool valve or equivalent for each bit count of the parallel digital input word, ten-bit units such as required for the F-16 rudder application would require ten valves. This approach was eliminated on the basis that a design with ten such valves and the necessary fluid passages and porting would be too complex for practicality.

#### 4.3.1.3 First-Stage Torque-Summing Arrangements

The third of the three parallel-digital control concepts considered operates in the first stage of an electrohydraulic actuation system through a summation of torques developed by the armature of an electrohydraulic

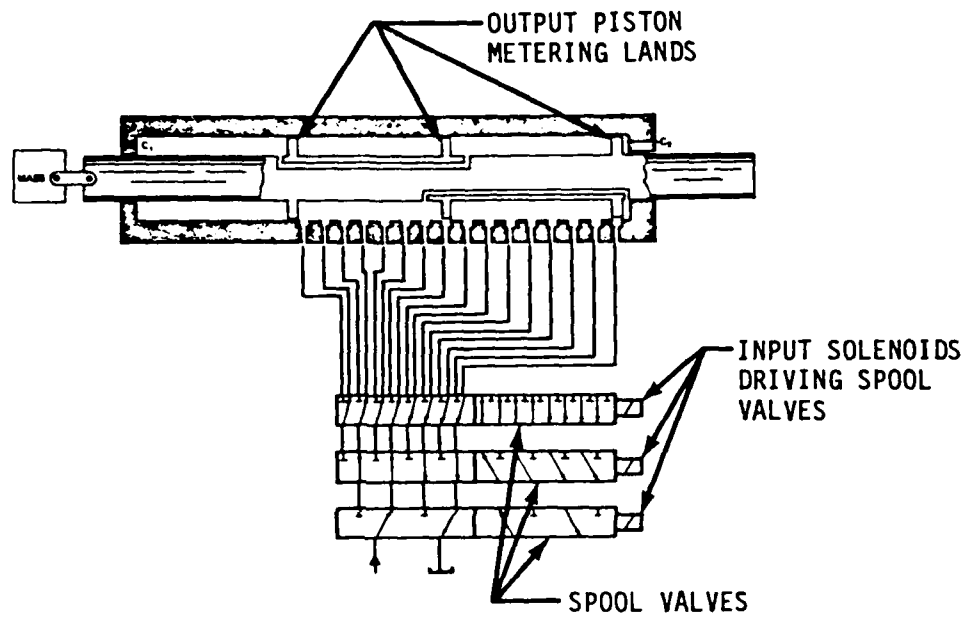


Figure 4 Cascaded valve arrangement  
 (for a three-bit parallel digital actuator)

servovalve torque motor or equivalent device. Such arrangements provide a number of individual torques or forces equal to their weighted bit count and those torques or forces are bit-weighted to be proportional to the elements of the digital binary word. A feedback torque proportional to the control surface output deflection is added to this summed torque and the resulting output torque is amplified to produce a hydraulic flow to an actuator ram or hydraulic motor. The resulting device is relatively simple and takes the general form of an electrohydraulic servovalve.

One such torque-summing arrangement is shown in Figure 5a which illustrates an electrohydraulic servovalve with several electrical coils. The total number of turns of all coils equals the number of turns of a single coil which normally is used in analog servovalves. Input signals, all with the same voltage, create different torques due to binary staging of the coil turns, and with a total number of torque combinations equal to  $2^n$ , where  $n$  equals the number of coils.

This approach was initially rejected for two reasons. It appeared that precise bit weighting would be very difficult to achieve at the low torque levels which would be produced by the incremental coils of a torque motor input; and, some initial reservations about this scheme came from its rather obvious similarity to the conventional form of an electronic D/A converter. In a later consideration of the possibilities of this approach, two methods of overcoming the initial objection involving the low-level torque summing in the servovalve torque motor were devised. They are presented here for the possible use of future innovators in this field. However, it should also be noted that, for fine output resolution requirements such as the ten-bit requirement for the F-16 rudder, an equivalent number of switching valves is required.

In the arrangement shown in Figure 5b, the bit-weighted torque summed on the armature element is produced by a system of rolling ball pistons in which both ball diameter and lever arm to the armature fulcrum are used to set bit weights. Three-way on-off solenoid valves are used to energize the bit pistons. The main advantage of this scheme is in the high level of torque which can be summed on the input armature element which makes for a system having very high precision and potentially very high response bandwidth.

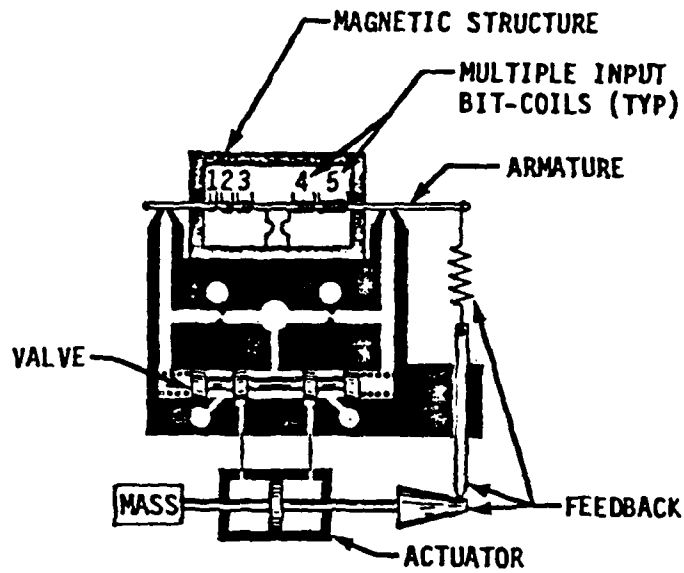


Figure 5a Torque motor with staged coils  
(from reference no. 2)

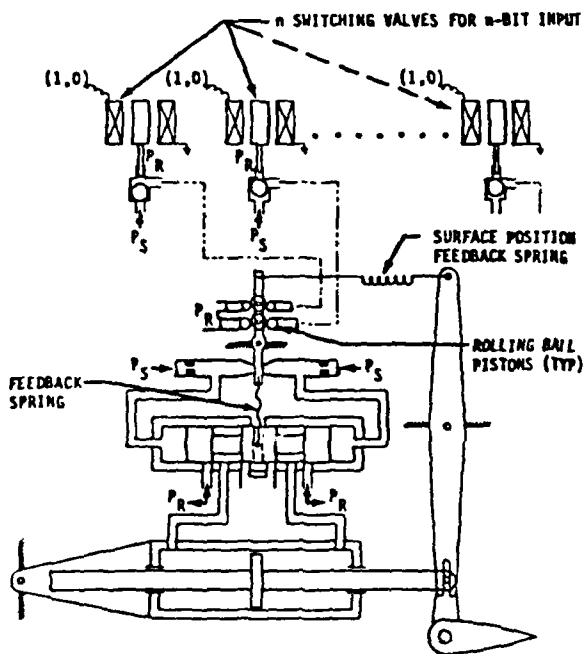


Figure 5b High-level torque summing  
with spring position feedback

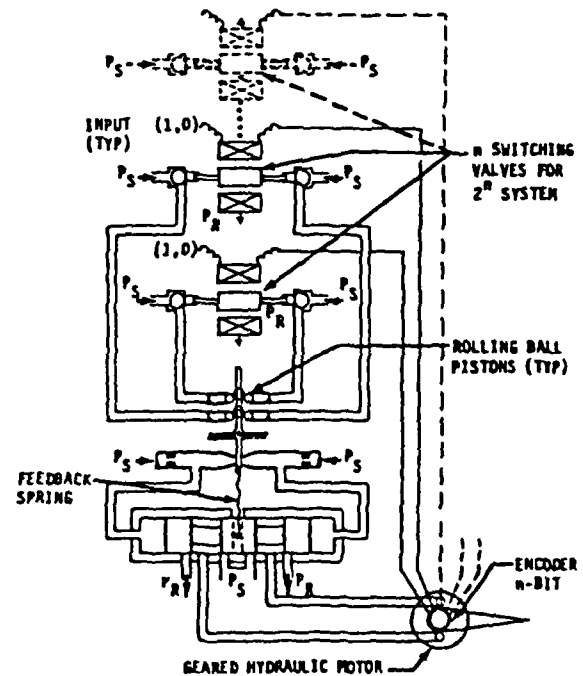


Figure 5c High-level torque summing  
with encoder position feedback

Figure 5 First-stage torque-summing arrangements

In the arrangement shown in Figure 5c, the torque summing is accomplished with the same ball piston scheme illustrated in Figure 5b; however, output position feedback is obtained from an output shaft encoder instead of from a spring feedback to the armature element. The individual bit outputs of the output encoder are each used to drive one terminal of one of the input solenoid coils where the opposite terminal of that center-tapped coil is connected to the same appropriate bit of the input command signal.

Another possible configuration, which should be mentioned, has the form of Figure 5b but omits the spring feedback of output position by simply grounding the right end of the feedback spring shown. An output encoder is used in this case to feed surface output position to the central control computer which generates the error signal to drive the input solenoid coils of the input valves.

#### 4.3.2 Incremental-Digital Actuation Control Concepts

Incremental or stepping actuators respond to signals which reflect only a change of switching state in the lowest order two bits of a parallel binary signal. Electrohydraulic steppers are devices that transform a stream of low-power electrical pulses into high-power mechanical motion. To reach a given position or velocity, a chronological sequence of single pulses in the form of a pulse train is required. The total output travel is proportional to the number of pulses, and velocity is proportional to the switching pulse rate. Three types of mechanization are identified in Figure 2 and are discussed below.

##### 4.3.2.1 Hydraulic-Amplified Stepping Motors with Net Position-Error Storage

These are conventional hydraulic positional servos amplifying the power level of the positional output of an electric stepping motor. An electrohydraulic stepping motor (EHSF) is a combination of an electric stepping motor and a hydraulic motor.

EHSM's are used as high-torque high-speed machine tool drives whose output motion is so precise and repeatable that position feedback may not be needed in the machine's positioning system. That is, the positioning system operates open loop rather than closed loop as most hydraulic servomechanisms. For machine tool applications, EHSM's can help solve such problems as: accurately repeated positioning; precise, variable-speed control; and accurate acceleration and deceleration.

Starting in 1970, Hydraulics & Pneumatics magazine has published a number of articles on the subject; and in 1972, two articles regarding the performance and specifications of EHSM's. The first, Reference 3, defined the terms usually used to describe the specifications and performance of electrohydraulic stepping motors with special emphasis on electric stepping. The second, Reference 4, presented specification charts and performance curves for the six EHSM's available in the United States.

In a Wright Aeronautical Laboratories' development program conducted by the Lockheed-Georgia Company in 1975 and 1976, and documented in Reference 5, an EHSM using an aircraft hydraulic motor was constructed by the Abex Corporation Aerospace Division and evaluated for use in actuating aircraft utility functions. That design, shown in Figure 6, was called an electrohydraulic pulse motor. It has a conventional mechanical-input servovalve driven by an electric stepper motor through a screw differential which sums the valve input with the high-gain feedback of hydraulic motor output position. In addition, an output encoder feedback circuit around the electrical stepper motor was provided.

Although it has been concluded that such systems lack sufficient bandpass to be considered acceptable for flight control applications, there is

- no inherent reason that adequate response cannot be obtained. However, it became very clear during the course of this program that further work is required on stepping motor ramping control to improve the response of this element to a level comparable to that of the contemporary hydraulic analog type position servo.

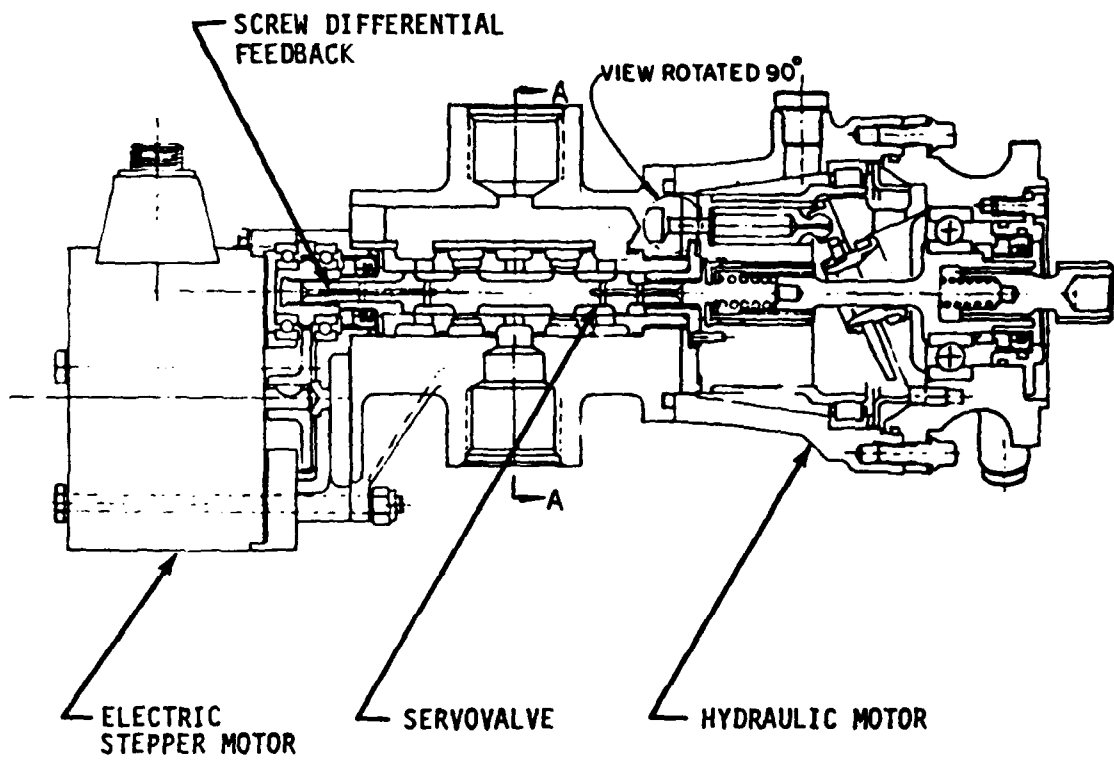


Figure 6 Abex prototype electrohydraulic pulse motor

#### 4.3.2.2 Electrohydraulic Steppers with Stepwise Position-Error Storage

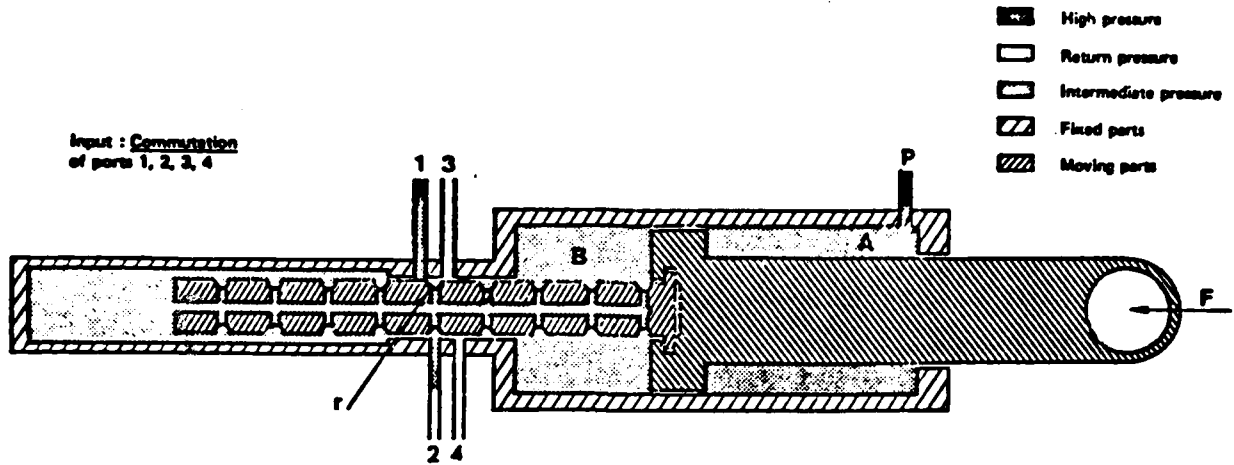
Linear-output ram actuators of this type known as electrohydraulic linear stepper actuators (ELSA) have been developed and demonstrated by the Air Equipement Division of the D.B.A. (Ducillier, Bendix, Air Equipement) corporation in France. A typical ELSA design, shown in Figure 7, generates step outputs by a hydraulic bridge action in which upstream orifices are controlled in an on-off mode while downstream feedback orifices are formed by fixed transmitter-receiver ports modulated by grooves in the piston tail rod.

A separate system of solenoid-operated selector valves, or combination of valves, alternately connects one of the four fixed transmitter ports to system pressure, its adjacent port to return, and closes the two opposite ports. This connects one of the receiver-port grooves to either pressure or return so that the head-end side of the actuator piston is either pressurized to allow one stepwise move to the right, or is vented to return to allow one stepwise move to the left. Thus, the four transmitter ports will provide four output positions for each receiver groove.

Individual steps are made directly at a very high power level with damping of transient step response comparable to that of a conventional hydraulic valved ram or motor servo. The basic problem of all stepping motor type devices, which limits their dynamic response, is their tendency to lose phase lock with the input pulse train when subject to sudden and repeated high acceleration demands. The ELSA tends to alleviate this phase-lock problem by simply raising the accelerating force or torque capability of the stepper to more-or-less overpower the problem.

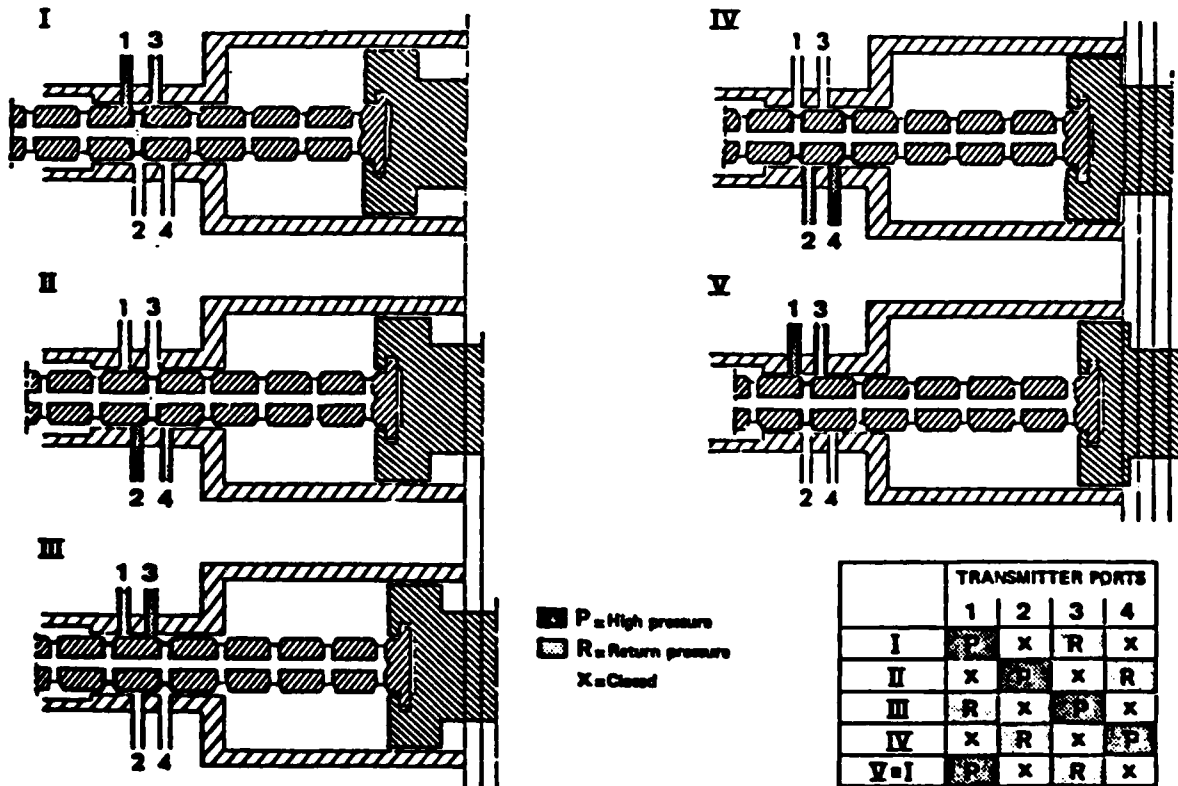
The following variations of the basic ELSA design have also been demonstrated by Air Equipement:

- a. A coarse-step ELSA series coupled to a vernier ELSA.  
This allows faster slewing of the initial motion followed by stepping in fine increments to the final position.



ELECTROHYDRAULIC LINEAR STEPPER ACTUATOR (E.L.S.A.)<sup>\*</sup>

<sup>\*</sup>Air Equipment, DBA, France, Proprietary Item



E.L.S.A. - OPERATING PRINCIPLE

Figure 7 Electrohydraulic linear stepper actuator (ELSA)

- b. An ELSA combined differentially with an absolute vernier.  
The vernier unit, with three binary-weighted two-position pistons acting on a swash plate, can be commanded simultaneously with the ELSA inputs to resolve out least bits while the course-step ELSA follows the input signal.
- c. A rotary valve which serves the ELSA equivalent function of transmitter-receiver porting can be coupled to and commanded to control either a hydraulic motor or ram.  
A schematic of one such unit is shown in Figure 8.

In the DEHA arrangement submitted by the Sundstrand Aviation Mechanical Division, in response to the problem-statement specification noted in Sections III and 4.2. they proposed a system utilizing a dual-linear hydraulic-stepper pilot stage. This could be used to drive the main power control valves of a conventional analog linear servoactuator or the mechanically-controlled servovalves in a hydraulic-motor-driven rotary actuation system such as the system they designed for actuating the intermediate and upper rudders on the B-1 bomber. The proposed system included two major subassemblies as follows.

- a. Dual Linear Hydraulic Stepper Pilot Stage

This unit was made up of two ELSA's each controlled by two 2-position 3-way solenoid valves; and the two ELSA's were mechanically linked as shown in Figure 9 to sum their outputs. Each ELSA had an additional solenoid bypass valve and position sensor, and a third sensor monitored the position of their output summing link. These are shown in Figure 10 which shows the dual ELSA pilot stage connected to the power drive unit of the B-1 rudder control system.

- b. Digital Actuator Controller

This is an electronic control circuit which accepts the digital input words for controlling the ELSA stepping solenoid valves. It provides a continuous monitoring error correction capability plus the capability for

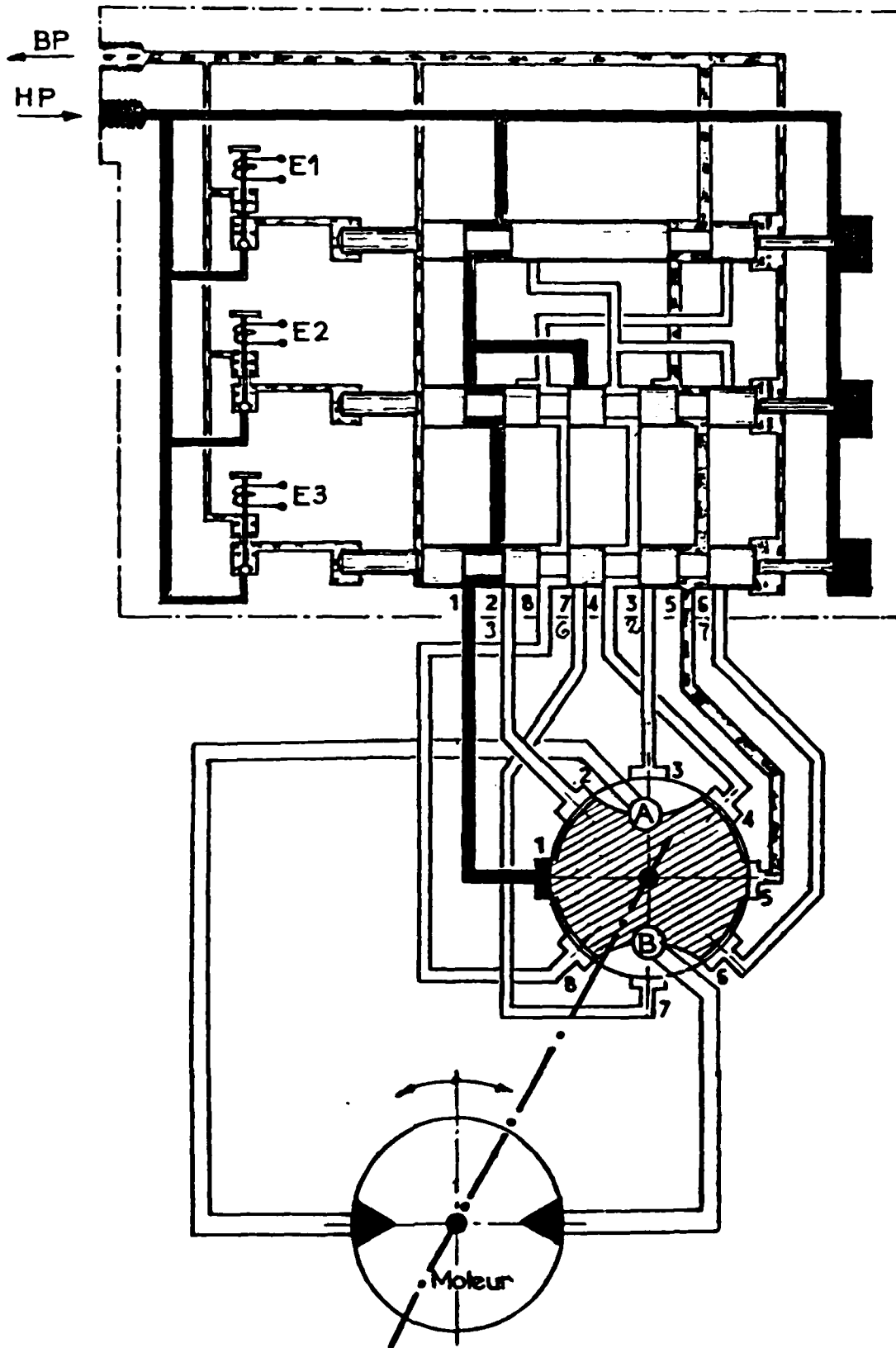


Figure 8 Electrohydraulic rotary stepper actuator

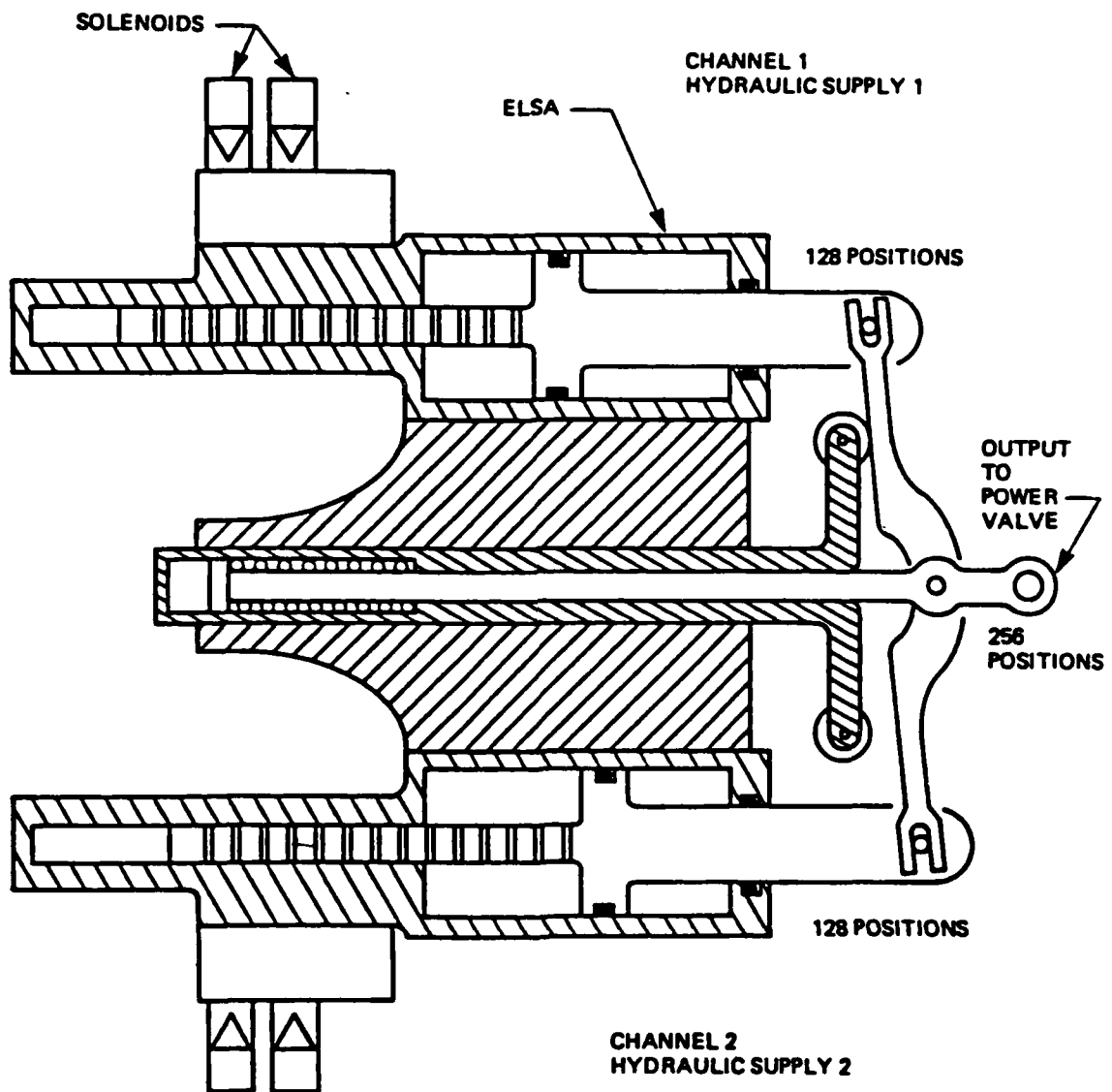


Figure 9 Dual ELSA pilot stage proposed by Sundstrand

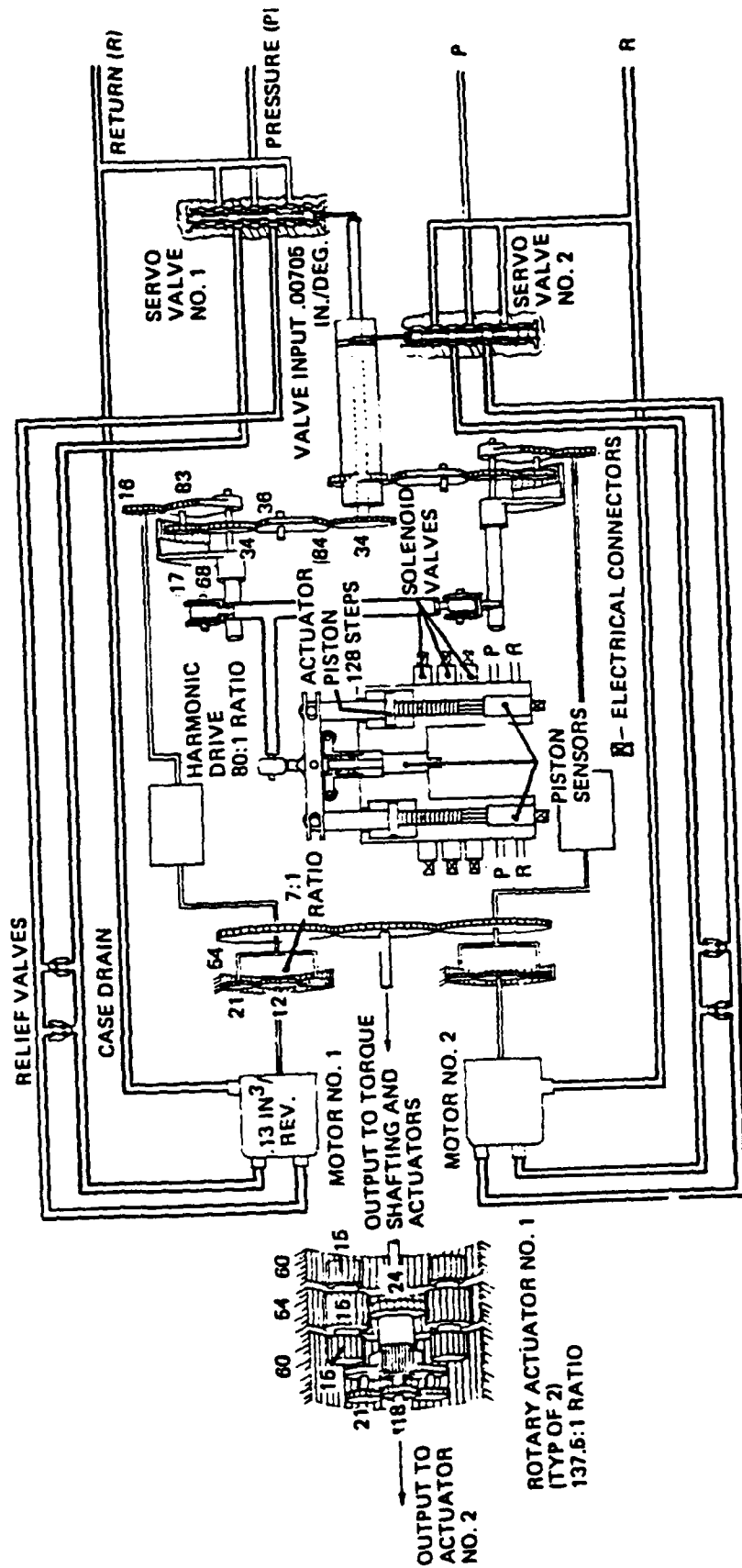


Figure 10 Overall hydraulic-motor-driven actuation system proposed by Sundstrand

initialization, to bring the output in agreement with the input command upon startup, and error correction following a major failure of either ELSA unit.

The proposed ELSA actuators are the type developed by the Air Equipement Division of DBA in France which has a licensing agreement with Sundstrand. They have a source-pressure-biased unbalanced-area piston and a grooved tail rod which slides in a close fitting sleeve containing four fluid transmitter ports alternately controlled to pressure and return by the two solenoid control valves. The grooves in the tail rod act as receiver ports, and four incremental positions are obtained for each groove.

The digital actuator controller would provide step commands to each ELSA unit in an alternating cycle to move one ELSA unit at a time. Loss of hydraulic pressure or any other detected malfunction of an ELSA unit would cause that ELSA cylinder to be bypassed. Such bypassing causes the combined stepper package to double its output step size and to continue operation with no loss of output stroke. The LVDT's and A/D converters act as digital feedback monitor encoders to sense the output position of each ELSA unit and compare this output with the input command word.

One problem with the ELSA approach, as shown in Figures 7 and 9, in relation to the F-16 rudder application, is the large number (256 total) of receiver grooves which would be required in the two piston tail rods to obtain the 1,024 steps required to give the required (10-bit) degree of resolution. Even with two units, as proposed by Sundstrand, the required 128 grooves seems impractical.

#### 4.3.2.2 Stepper Motors With Hydraulic Incremental Torque Rebalance

In viewing the shortcomings of the foregoing concepts, an attempt was made to derive alternate approaches; and, from that effort, a number of additional digitally-controlled actuation concepts were formulated. The most promising were those utilizing hydraulic motors with external commutating distributor valves to port fluid sequentially to individual motor pistons in response to incremental input commands. Such arrangements have the properties

of a stepping motor while, at the same time, allowing the gross phase error between input and output to float as a function of output torque so as to achieve a degree of power adaptability in order to make the hydraulic power consumption responsive to output loading. It was postulated that a significant reduction of the hydraulic flow normally required for slewing at high rates under low-load conditions could be achieved due a torque-adaptive power turndown which reduces the effective displacement of the motor pistons. This phenomenon is described in Appendix A.

This approach also shares an advantage with all of the other incremental actuator forms previously mentioned in that it is less vulnerable to sudden catastrophic hardover failure induced by loss of position feedback continuity than are the more conventional forms of analog electrohydraulic position servos. This advantage results from the elimination of the need for a high-gain position feedback to give a high-frequency response. Only a low-gain monitor feedback of output position is required by any of the foregoing incremental servo devices.

A number of configurations of this type were derived. The two shown in Figure 11 each utilize electric-stepper-motor-driven rotary distributor valves to control two hydraulic motors constructed without the normal kidney-slot internal-commutating valve plate. The arrangement shown in Figure 11a has two fixed-cylinder-block hydraulic motors, and rotary valves which port fluid to the individual pistons in each motor which act against its rotating swash plate to drive its output shaft. The arrangement shown in Figure 11b has two rotary-cylinder-block motors, and rotary valves which port fluid to the pistons in each motor which react against its fixed swash plate to drive its cylinder block and output shaft.

In each configuration, the hydraulic motors operate essentially open loop with no correctional position feedback to the rotary valves. However, shaft encoders are used to close a low-gain monitor position loop around the stepper motor.

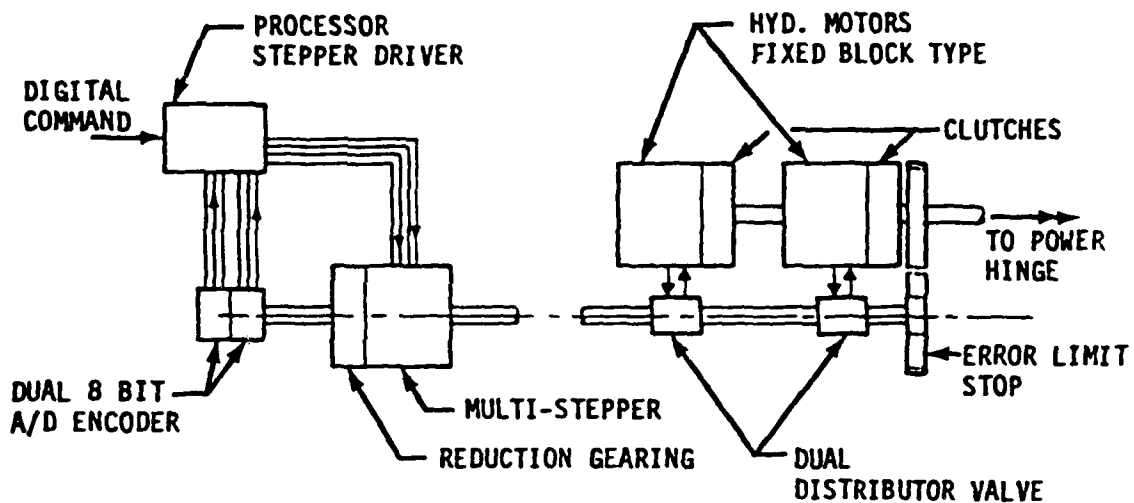


Figure 11a System with fixed-cylinder-block hydraulic motors

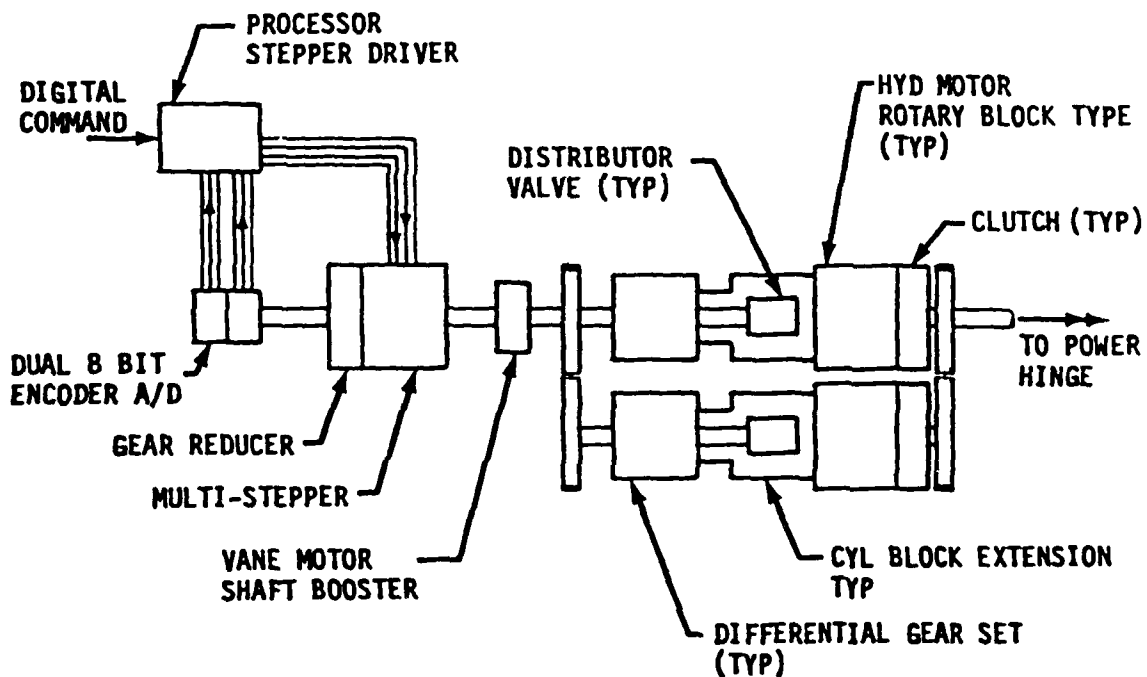


Figure 11b System with rotary-cylinder-block hydraulic motors

Figure 11 Electrohydraulic stepping motor arrangements with external-commutating rotary valves

Other arrangements similar to the configuration with two fixed-cylinder-block hydraulic motors shown in Figure 11a, except with the individual pistons of each motor ported to supply or return pressure by electrohydraulic switching valves rather than stepper-motor-driven rotary valves, were also considered. With three-state four-port valves, which can alternately port one cylinder port to supply and the other to return or both to return, one valve can be used for each pair of motor pistons. As shown in Figure 12, three valves can be used for each of two six-piston fixed-cylinder-block motors.

As in the arrangement shown in Figure 11a, the hydraulic motors operate open loop, and shaft encoders are used to close a monitor position loop around the digital controller. This arrangement also offers the power saving advantages common to all externally commutated motors.

In the DEHA arrangement submitted by the Bendix Electroynamics Division in response to the problem-statement specifications, they proposed a stepper motor controlled version of their Dynavector-type rotary hydraulic actuator which included the following five major subassemblies:

a. Hydraulic Digital Dynavector

Two rotary output actuators, each comprised of an integral captive-vane hydraulic orbital motor and epicyclic gear transmission based on the Bendix Dynavector principle, mounted back to back to a hydraulic manifold and attached to an output torque tube by means of an internal spline in the output shaft of each unit.

b. Potary Valve

A dual-tandem valve, driven by an electrical stepper motor, mounted on the hydraulic manifold to alternately port system supply and return pressure to the chambers of the Dynavector motors.

c. Electrical Stepper Motor

A Sigma Instruments Series 20-2235-D200 stepping motor mechanically coupled to the rotary valve.

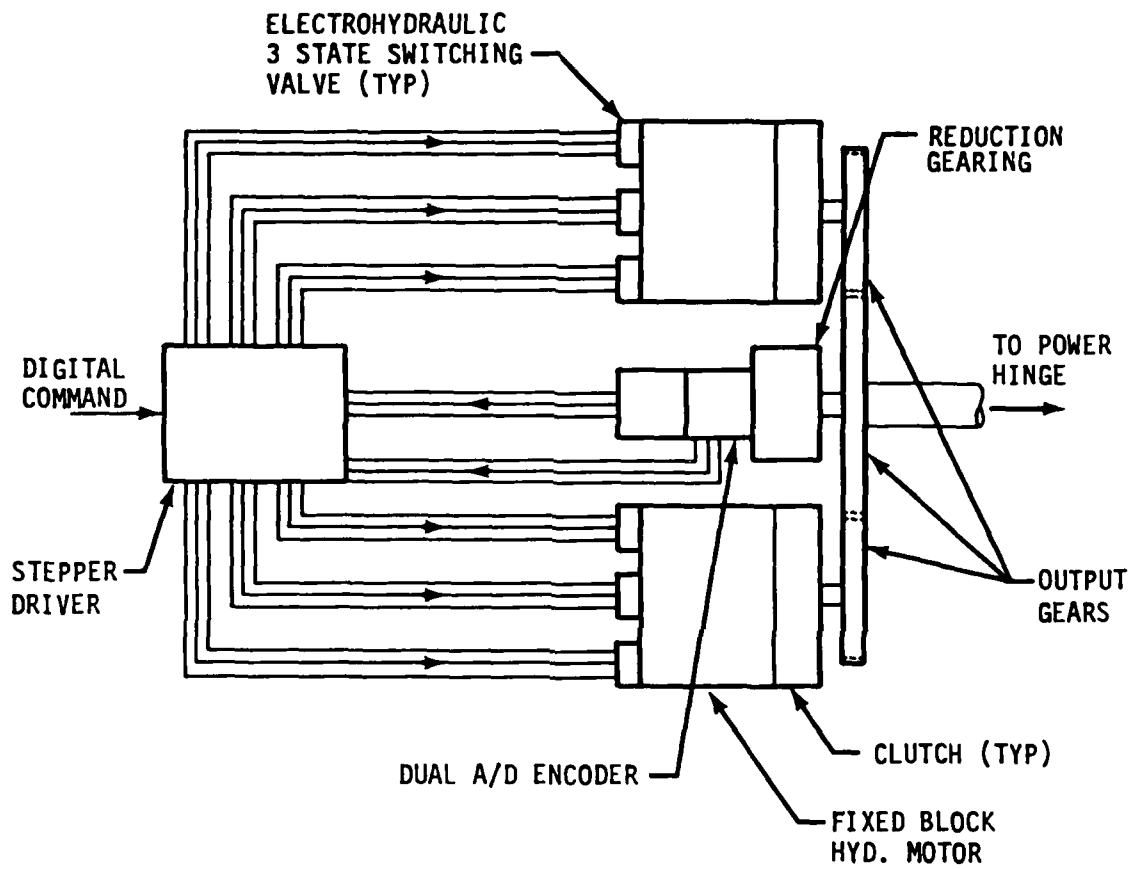


Figure 12 Electrohydraulic stepping motor arrangement with external-commutating electrohydraulic valves

d. Controller

A modified Sigma DMC-10 programmable stepping motor controller Model 29D02-1.

e. Electronic Drive System

A Sigma Bipolar chopper drive, power supply and chassis unit, Model 29B13-XXX.

The proposed Dynavector rotary actuator shown in Figure 13, was a special version of their analog type with control of the chamber pressures accomplished by use of the external rotary valve rather than by internal commutation as normally used. The high-speed low-torque output of the motor was converted to high-torque at low-speed in one step by the 45:1 transmission ratio of the epicyclic gearing. The motor would respond to the discrete command positions of the rotary valve to produce discrete output shaft positions without direct position feedback.

The tandem rotary valve, driven by the stepper motor, would port fluid from two separate hydraulic systems to the two Dynavector motors. The valve porting which is arranged to ensure pressure balance on the rotating spool, provides a transmission ratio of 2:1 between the valve and Dynavector motors which serves to decrease the required stepping rate and dynamic torque required from the stepper motor.

Three unloading pistons, located 120° apart as shown in the endwise cross-section view of Figure 13, serve to decouple one or the other Dynavector actuators upon loss of its supply pressure. Pressure from the active system displaces the pistons on the depressurized unit inward disengaging the two gears of the epicyclic transmission.

In the assessment of their proposed arrangement, it was concluded that if it were modified with an absolute output encoder and error correcting circuitry in the electronic controller, it would fulfill many of the specified requirements and objectives. With the encoder used in a low-gain error correcting circuit, the system would operate as an incremental digital

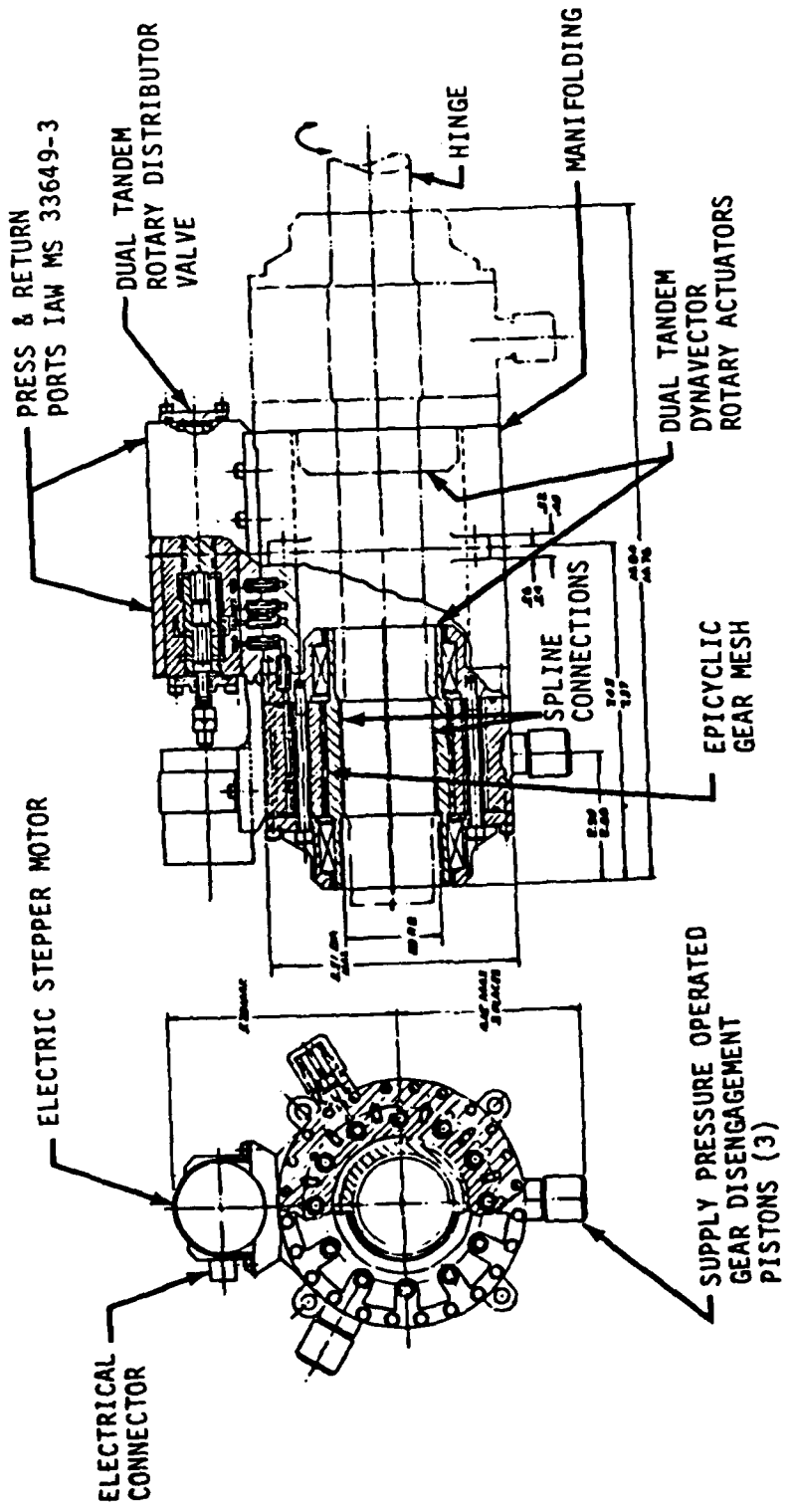


Figure 13 Incremental Dynavector actuator proposed by Bendix Electrodynamics Division

actuator with performance equivalent to that of the reference system but without the certain probability of a hardover transient upon open-circuit failure of the feedback element. Another attractive feature was that, with its externally-commutated rotary valve, the motor unit had the potential of effectively adapting its displacement volume to demand only that amount of hydraulic flow necessary to meet the imposed power demand. However, such power saving would be partially negated by the relatively high internal leakage rate across the Dynavector vane elements.

More importantly, there is a serious question about the use of a Dynavector unit as a primary flight control actuator. It is not easily adapted to the minimum space envelopes available for installation in thin aerodynamic surfaces, and its stiffness may be inadequate for some applications.

#### 4.4 CONCEPT EVALUATION AND SELECTION

The selection of one system arrangement for further development, was made by evaluating the candidate designs in regard to their potential for providing the following desired advantages which are above those originally anticipated:

- a. Elimination of hardover transients due to open-circuit failure of a feedback element.
- b. A significant reduction of the hydraulic flow required for slewing at high rates under low-load conditions.
- c. A reduction of the steady-state quiescent leakage flow associated with electrohydraulic servovalves.

##### 4.4.1 Candidate Arrangements Selected for Final Evaluation

None of the concepts considered exhibited an obvious clear-cut superiority over the others. Therefore, they were all examined to determine

which could provide all or most of the desired advantages noted above. The following components are considered the major elements which provide those advantages:

- a. The use of an output encoder to close an error-correcting monitor loop with a limited rate of error correction, when used in conjunction with a stepping motor drive, eliminates the possibility of sudden hardover transients due to open-circuit failure of a feedback element that exists with analog servoactuators.
- b. The use of a hydraulic motor with an external-commutating control valve system in an open-loop circuit allows a fixed-displacement motor to adjust its hydraulic flow demand to accommodate variable applied loads and provide significant reductions in peak flow demands for slewing at high rates under low-load conditions.
- c. The use of closed-center control valves eliminates the constant quiescent leakage flow associated with conventional electrohydraulic servovalves; and, the use of piston-type hydraulic motors avoids the high internal leakage associated with other motor types.

None of the parallel-digital actuation control concepts discussed in Section 4.3.1 embody those elements. In addition, they were all considered somewhat complex due to the large number of valves necessary to obtain the required ten-bit equivalent output resolution. Therefore, they were dropped from further consideration; and, the final evaluations were confined to the incremental-digital concepts.

#### 4.4.2 The Selected Concept

All of the incremental-digital concepts discussed in Section 4.3.2 can be arranged to provide two of the desired advantages noted above; ie: elimination of hardover transients due to feedback failures and a reduction in quiescent leakage flow. However, only the stepper motors with hydraulic incremental torque rebalance through the use of closed-center valving to

externally commutate hydraulic motors had the capability of adapting to the load torque in a manner which would reduce hydraulic power and flow demands under low loads, and the potential for returning power and flow to the hydraulic supply system under aiding loads. These characteristics, although not specifically tied to digital control, had not been demonstrated before and appeared to be worthy of pursuit.

In addition, such arrangements with rotary distributor valves driven by electric stepper motors appeared to be reasonably simple in comparison with most of the other equivalent types, and they required fewer parts. Therefore, in view of its power-adaptive capability and relative simplicity, this concept was selected as the most promising and with sufficient merit to warrant the development of a prototype unit. The next step was to determine the best design arrangement of individual components of such a system which could best meet the design and performance requirements and objectives.

#### 4.5 COMPONENT SELECTION AND ARRANGEMENT

In adapting the selected approach to an aircraft rudder actuation system, it was necessary to consider a number of important factors before the detailed selections of component types and their arrangement could be made. Those factors included the following:

- a. Means of transmitting torque to the rudder surface.
- b. Means of combining the outputs of two hydraulic motors.
- c. Means of overcoming hydraulic failures and jams.

Following the selection of those means, the major subassemblies and component choices were made.

##### 4.5.1 Means of Generating, Combining, and Transmitting Torque

##### 4.5.1.1 Torque Generation and Transmission Elements

The following means of generating and transmitting torque to the control surface were considered:

- a. Hydraulic motors driving hinge-line rotary gear actuators through a high-speed torque shaft.
- b. Hydraulic motors driving a low-speed torque shaft through a close-coupled gearbox.
- c. Direct rotary actuators such as vane types.
- d. Linear actuators driving helical spline couplings.

The latter was rejected as not meeting the desired intent of the contract specifications since there are a number of other actuation services, such as secondary flight controls, antenna drives, and gun drives, which are good applications for digitally controlled hydraulic actuation with hydraulic motors but are not adaptable to the limited rotation provided by helical splines. Direct rotary vane actuators have the same shortcomings in addition to high internal leakage which has limited their use for other aircraft actuation applications.

Of the two arrangements for using hydraulic motors, systems which transmit the motor output through low-torque high-speed shafts to rotary gearboxes mounted on the surface hinge line, such as in the E-1 rudder system, are considered superior. They provide an efficient structural tie and distribution of torque from the control surface to its supporting fin. More importantly, with the major speed reduction gearing at the hinge line, the torsional stiffness of the torque transmitting elements benefit from the relative irreversibility of the hinge-line gear units. Systems using hydraulic motors close coupled to a gearbox to drive directly into a control surface torque box may not meet system stiffness requirements without a severe weight penalty required to obtain adequate surface torque-box stiffness.

#### 4.5.1.2 Means of Combining Motor Torques and of Overcoming Hydraulic Failures and Mechanical Jams

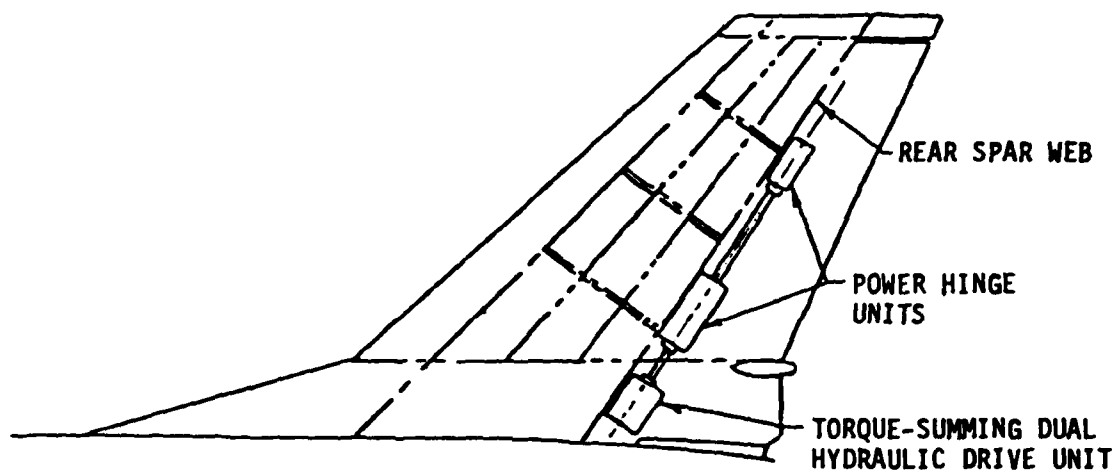
Both the use of two motors driving the high-speed torque shaft through a torque-summing gearbox, and two motors coupled in a velocity-summing

arrangement with differential gearing were considered. Examples of these arrangements, as applied to the F-16 rudder system, are shown in Figure 14. There are a number of arguments, pro and con, for each.

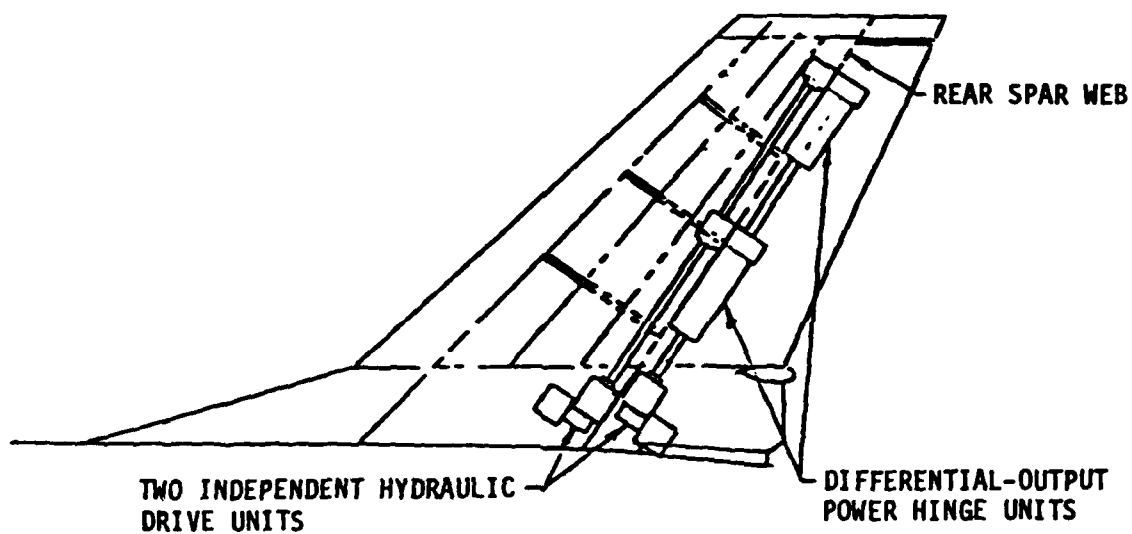
The torque-summing arrangements will generally be easier to install since the hydraulic motors and torque-summing gearbox would be mounted at the base of the fin, behind the fin rear spar and the one output shaft aligned with the rudder hinge axis as shown in Figure 14a. Whereas, with the velocity-summing arrangement, the hydraulic motors would be mounted, one ahead and one behind the rear spar, with two separate motor output shafts running parallel to the rudder hinge as shown in Figure 14b. Thus, it is seen that this velocity-summing approach has the obvious weakness that it leaves little room for either aerodynamic balance area or counterweights ahead of the surface hinge and causes a structural weight penalty by introducing cutouts in the rear-spar web. With the exception of the rear-spar structural problem, these factors do not apply to the F-16 rudder which has neither counterweights nor forward aerodynamic balance area. However, these features may be used on other aircraft which would make the application of velocity-summing power hinges difficult.

Another problem, common to all multiple-drive rotary-output actuation systems, is how best to ensure continued operation in the event of power supply failures or jams. In a dual hydraulic drive system, continued operation must be ensured following failure of the hydraulic supply to either of the two drive units. With two hydraulic motors coupled in a torque-summing arrangement, it is necessary that the inactive drive motor be made to either free wheel or be declutched so that it does not prevent the active motor from transmitting power to the output shaft.

None of the torque-summed systems provides a means for continued operation following a jam in the output gearing, however. This is a general problem with such systems, including the B-1 rudder system, and all parts must be designed as well as possible to minimize the possibility of jamming. An alternative which can be considered for some aircraft is the use of redundant control surfaces each driven by a separate actuation system.



14a Torque-summing arrangement



14b Velocity-summing arrangement

Figure 14 Typical installation arrangements of a DEHA rudder actuation system

A velocity-summing system would use two independent hydraulic motors with outputs mixed on a final differential gear set at the surface hinge output. The motors would each require a pressure-released brake to provide a reaction point in the event of a hydraulic system pressure failure. Such a system protects itself automatically against seizure of either motor or main gear reduction unit since, with the differential gearing, the active motor will continue to supply output torque to the surface.

For the prototype demonstration unit, a torque-summing arrangement was selected, partially because a precedent has already been established for torque summing on the B-1 rudder system, but primarily because it would be less complex and would be assembled at lower cost than a velocity-summing arrangement.

#### 4.5.2 Major Component Decisions

##### 4.5.2.1 Fixed-Cylinder-Block Vs Rotary-Block Hydraulic Motors

An electrohydraulic stepper motor could be built around either a fixed-cylinder-block or a rotary-cylinder-block hydraulic motor. Each type of motor had a number of basic advantages and drawbacks which are diagrammed in Figure 15. A decision was made to develop a fixed-cylinder-block "barrel-engine-type" hydraulic drive motor with a high cam angle, especially for this program, to reduce starting friction. The reasons for this choice were as follows:

- a. An existing high-torque small-step-angle electric stepper motor could be adapted to either a six or nine-piston hydraulic motor by the use of a multi-phased rotary valve, whereas only a single-phase valve, could be used with a rotary block design. With a single-phase valve, stepper rotation and hydraulic motor rotation would be identical. This would have required the use of a large angle stepping motor; 15 deg/step for a six-piston motor pair or 10 deg/step for a nine-piston motor pair. The rotary-block design would have dictated a special design for a stepping motor having its permanent magnet structure in its outer element or field

CHOICE OF FIXED-CYLINDER-BLOCK MOTOR  
VERSUS A ROTARY-BLOCK MOTOR

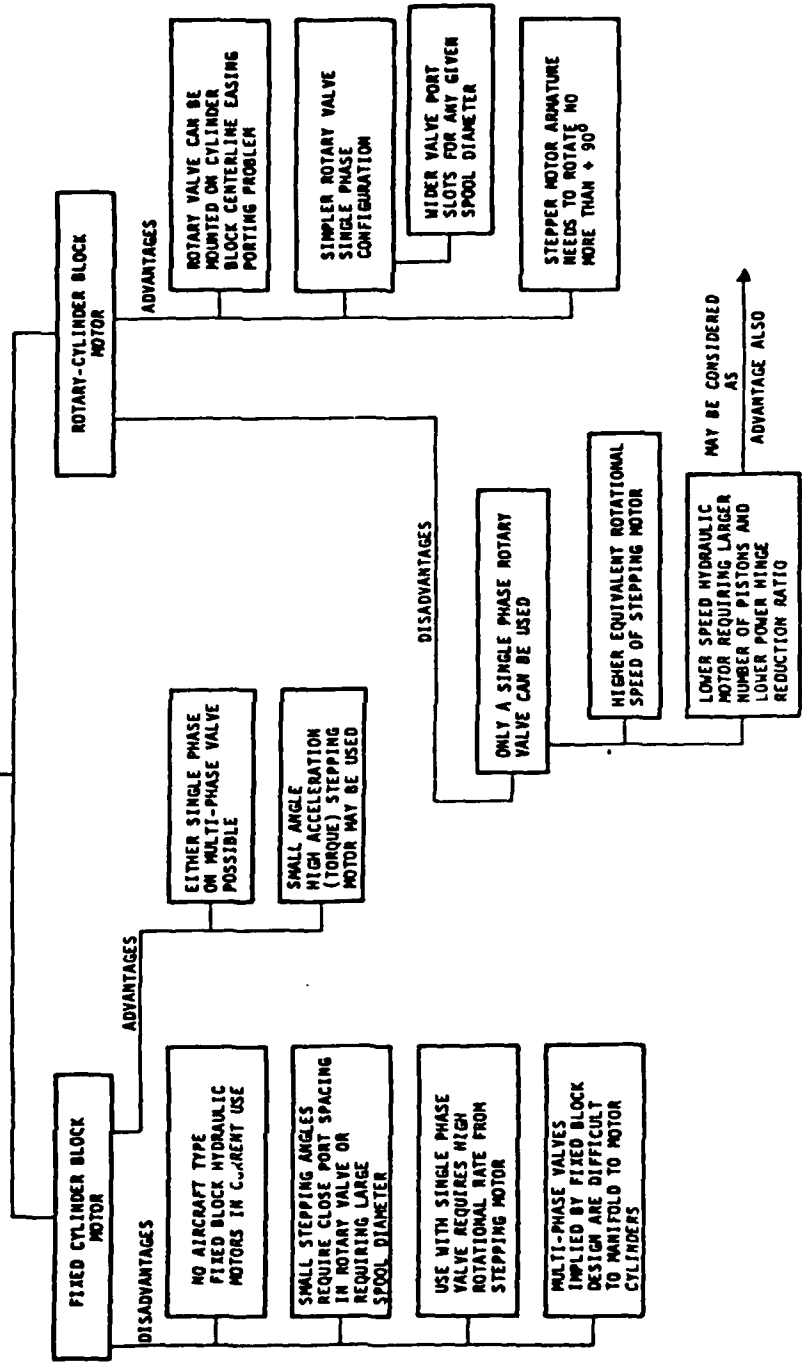


Figure 15 Hydraulic motor cylinder block tradeoffs

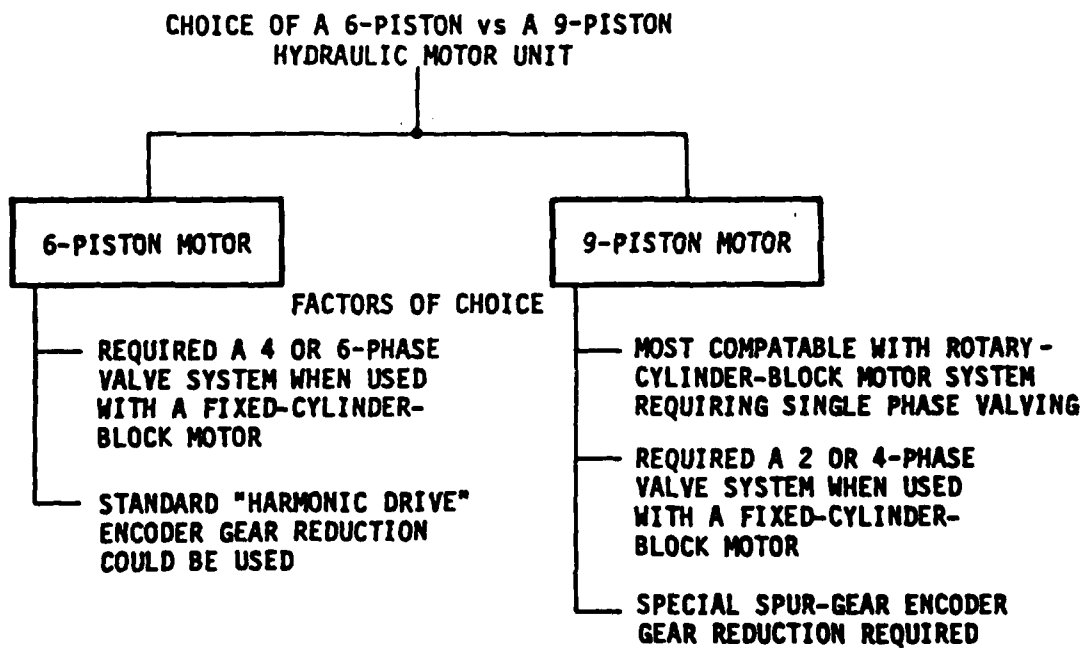
ring assembly, while the wound poles would have been placed in the central armature. No such stepping motor was readily available in a high-torque 10 or 15-degree step angle version. On the other hand, the fixed-block motor was compatible with the use of an available stepping motor.

- b. The required steps to modify an existing rotary-block hydraulic motor to incorporate a spool-type rotary valve within the motor cylinder block appeared to be as costly as the design of a complete fixed-block motor.

The decision to undertake the design of a fixed-block motor was made before a practical method of configuring a free-commutating rotary valve with a rotary-block motor had been discovered. Such a practical method of coupling a valve and rotary-block motor was devised later and is included for reference as Figure 16.

#### 4.5.2.2 Number of Hydraulic Motor Pistons

Either a six-piston or a nine-piston hydraulic motor could be adapted to run with a step sequence set by an existing electrical stepping motor. The factors governing this choice are as follows:



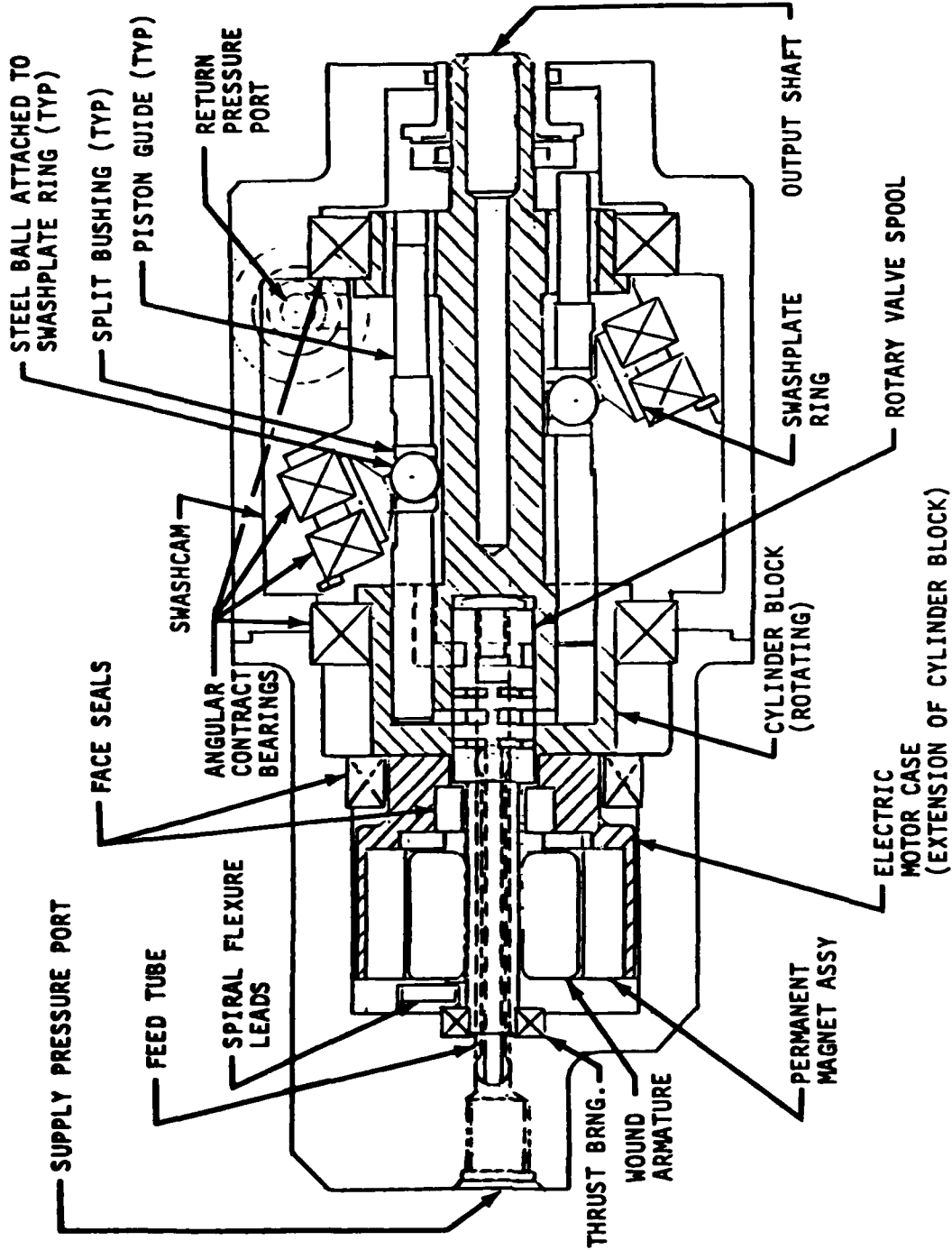


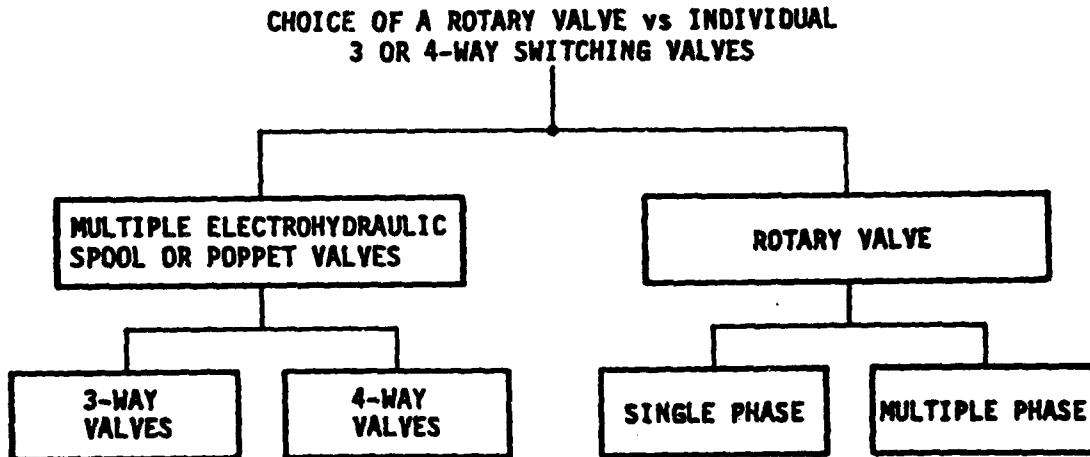
Figure 16 Rotary-cylinder-block electrohydraulic stepper

A decision was made to use a six-piston motor after a fixed-cylinder-block motor design had been selected. The reasons for this decision were as follows:

- a. Valve porting for a four-phase, nine-piston-motor valve would be somewhat less practical due to the resulting close circumferential spacing of valve sleeve ports unless valve spool diameter were increased above the diameter required for an equivalent six-piston-motor valve.
- b. A two-phase nine-piston-motor valve required a stepping rate higher than that guaranteed by the stepping motor manufacturer, tentatively chosen to be Sigma Instruments Inc, assuming that motor size and output gear ratio were fixed.
- c. Motor-to-encoder gear reduction for a six-piston motor could use an available 80/1 harmonic drive gear reduction unit. The use of a nine-piston motor required a spur gear reduction set in addition to the high power gears mixing torque from the hydraulic motors.

#### 4.5.2.3 Valving Schemes

Several types of valving schemes could be used to drive a multi-piston or many-chambered vane type hydraulic or pneumatic motor. The following potential choices were considered:



A decision was made to develop a system around a rotary spool valve driven by an electrical stepping motor. The reasons for this decision are as follows:

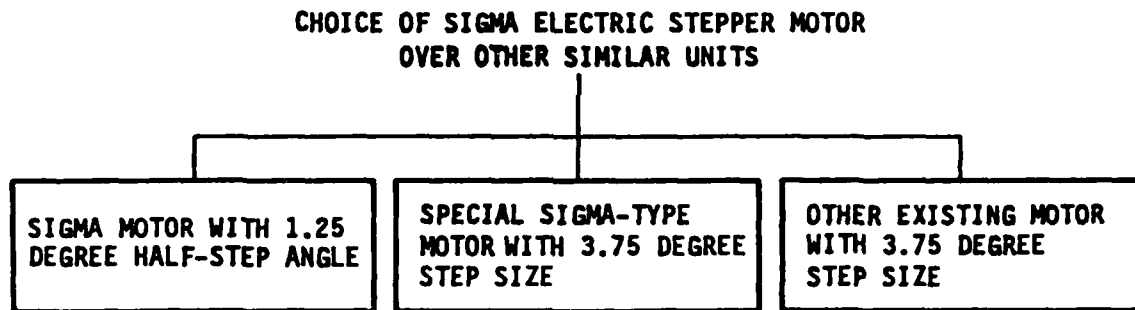
- a. A system consisting of two six-piston hydraulic motors and using a total of six four-way electrohydraulic valves would require twice the power-hinge gear reduction ratio required of a rotary valve system having the same number of pistons in order to give comparable resolution and slew rate. Such a high reduction ratio was believed to negate the potential advantage of motor power reversibility which was theoretically available from either system.
- b. Doubling the number of electrohydraulic valves to twelve would have allowed equal output gear ratios for either multiple-valve or rotary-valve systems. This doubling of the number of individual valves was judged to

be impractical because of cost, space required for valves, and because of probable valve reliability problems.

A type of hydraulic pressure switching valve having three output states on its two load ports (these states are 1-0, 0-1, and 0-0) could have been developed. Use of such valves would have reduced the number of valves required back to six. Development of such electrohydraulic valves was judged to be beyond the scope and financial resources of this program. A possible design for such a switching valve is illustrated in Figure 17.

#### 4.5.2.4 Electric Stepper Motor Choice

The selection of an electric stepping motor to drive the rotary hydraulic valve was made in conjunction with the choice of motor piston count. Once the piston count had been selected, the least-bit input stepping motor rotation was set at 3.75 degrees. Factors in this choice are outlined below.



A Sigma Instruments Inc. stepping motor, having a half-step slew rate of 6,000 steps per second at 200 oz-in of torque, was chosen for the prototype system. The least-step angle of the motor was a 1.25-deg half step, and this required three half steps to produce the required 3.75-deg motion equivalent to the desired least-bit rotation. The following reasoning lead to this choice.

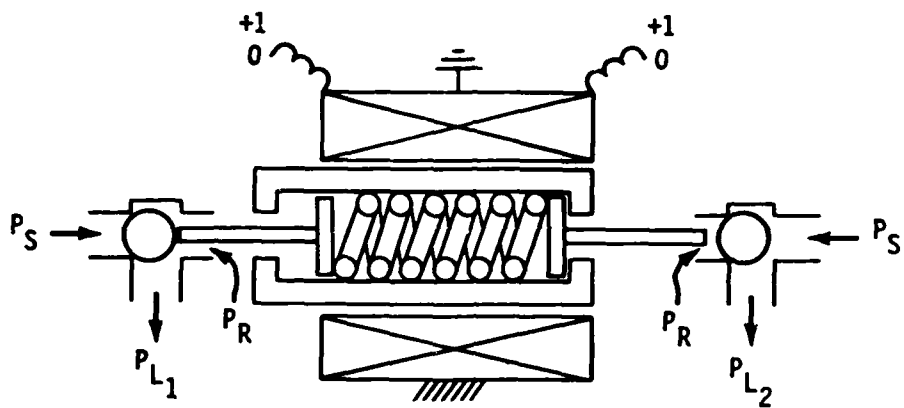


Figure 17 Three-state output-switching fluid valve

- a. The time delay required to produce a special motor of the Sigma type with a basic 3.75-deg step angle was thought to be excessive. Costs involved in such a development would have adversely impacted the DEHA program.
- b. Some torque overdesign of the stepper unit was thought to be desirable to allow for over-specification friction from the rotary valve unit which was not yet fabricated.
- c. No large stepping motor (with output greater than 200 oz-in at design speed) which produced a 3.75-deg step angle directly as a single step could be found.

However, in retrospect, this was an unwise decision. See Sections 5.1.1, 6.2.1.c, and 8.1.

#### 4.5.3 Major Subassemblies and Component Arrangement

Figure 18 is a schematic of the selected system as it would be configured for an aircraft installation. This system should not be confused with the somewhat abbreviated prototype system described in Section 4.6.2. which was used for demonstrating the concept in the laboratory. The major subassemblies and components for an aircraft system include the following:

##### 4.5.3.1 Digital Controller

A multi-channel electronic control circuit designed to perform the following functions:

- a. Receive the integrated digital wordstream of commands from pilot, autopilot, and stability augmentation system.
- b. Align output with initial condition input in response to a shaft encoder feedback unit.
- c. Convert the digital error commands to a series of coded electrical pulses.

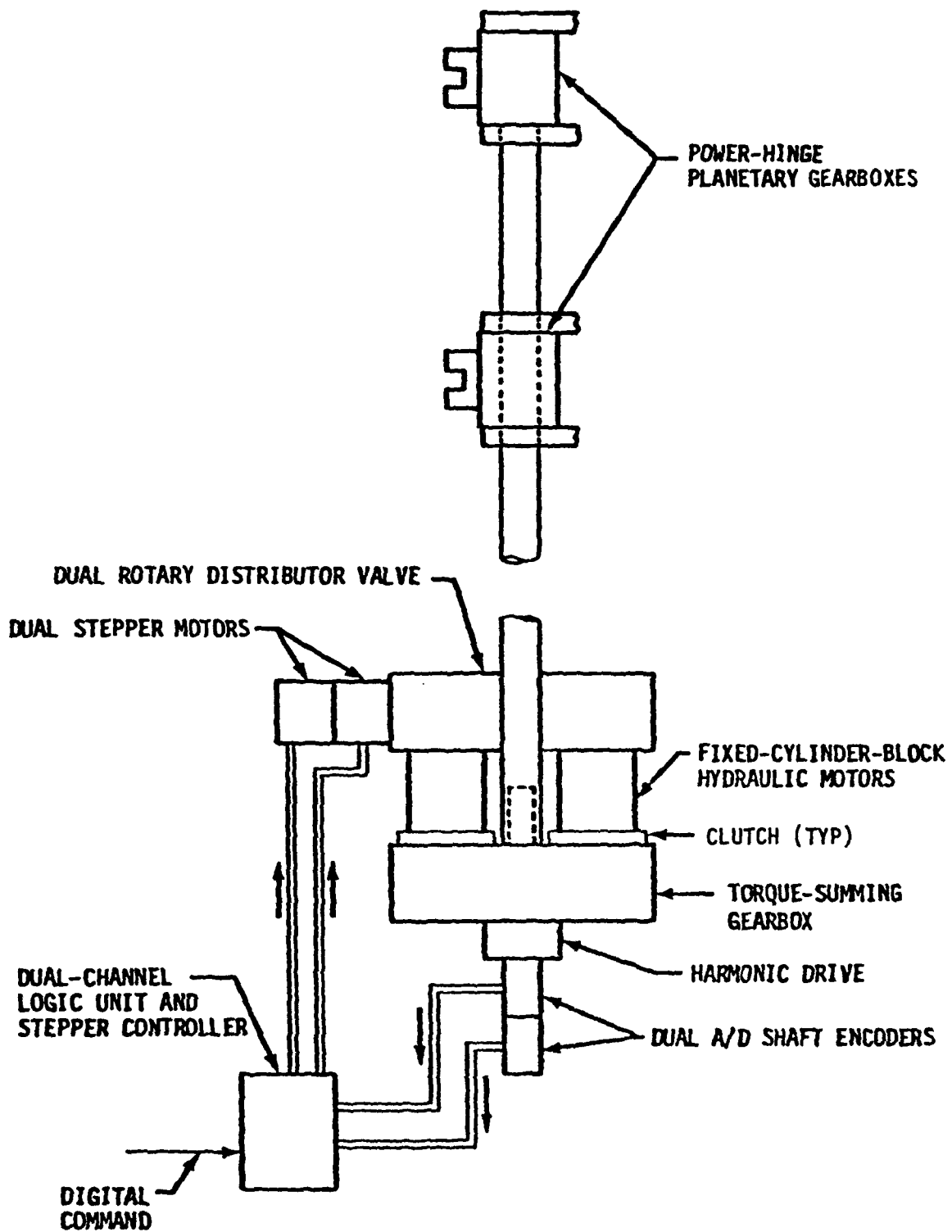


Figure 18 DEHA configured for aircraft installation

d. Amplify and translate the electrical pulses to the dual electrical stepper motors.

e. Execute the following logic.

Assuming that the input is in the form of a 10-bit binary wordstream, and the encoder provides an 8-bit feedback signal, the controller would function as follows. When the sensed error exceeds four least bits, a corrective input of four least bits of appropriate sign would be inserted into the stepper command at a limited rate. When the measured error reaches eight least bits, the monitor feedback function would be shifted from one element of the dual encoder to the other (standby) element. When the measured error reaches sixteen least bits, the error correcting function would be disabled allowing the system to respond as an open-loop stepping motor.

A microprocessor-based controller utilizing a mature 8-bit fixed-instruction-set microprocessor is envisioned at this time.

#### 4.5.3.2 Dual Electric Stepper Motor

Two input stepper motors output on a common shaft to provide dual redundancy.

#### 4.5.3.3 Hydraulic Distributor Valve

A dual rotary-spool valve with the metering lands machined on a common spool.

The valve sleeve would include a series of annular-ring manifolds to port fluid alternately to each of the six individual pistons in each hydraulic motor. Either a 2-cycle, 4-cycle, or a 6-cycle valve rotating at one-half, one-quarter or one sixth of the hydraulic motor speed could be used. The actual selection would depend on the capability of the selected stepper motor to meet the applicable step size, torque, and rate requirements.

#### 4.5.3.4 Hydraulic Motors

Two externally-commutated fixed-displacement hydraulic motors.

Two units would provide the dual hydraulic redundancy currently provided to the F-16 rudder. The external commutation would allow the fixed displacement motor to adjust its hydraulic flow demand to accommodate variable applied loads and demand less hydraulic flow, than an internally-commutated motor, for slewing at high rates under low-load conditions. Fixed-cylinder-block motors with rotating swash plates were used on the prototype unit; however, with a thorough packaging design effort, a better design may be possible using modified rotating-cylinder-block motors similar to the design shown in Figure 16.

#### 4.5.3.5 Motor Clutches

An electrically-operated clutch for each hydraulic motor.

These would be used to prevent a system jam in the event of seizure of either motor.

#### 4.5.3.6 Torque-Summing Gearbox

A gearbox containing two drive pinions, one driven gear with an output shaft extending through each side, and three mounting pads.

Two mounting pads would be used for the hydraulic motor clutches whose output shafts would be connected to the drive pinions through spline couplings. The third-pad would be for a harmonic drive gear reducer which would be connected to one end (the detection end) of the output shaft. The other (power output) end of the output shaft would be connected to an output torque tube leading to power-hinge gearboxes mounted on the flight control surface hinge line.

#### 4.5.3.7 Harmonic Drive

A high-reduction harmonic drive for driving a single-turn shaft encoder.

The gear reduction would be selected to produce one output revolution for the full range of output motion at the output shaft. Note: A half-revolution, 180-deg 10-bit encoder was used successfully on the prototype unit.

#### 4.5.3.8 Shaft Encoder

A dual single-turn absolute binary analog-to-digital shaft encoder.

The encoder would provide monitoring feedback to the digital controller, and input to the jam detection and clutch logic circuit.

#### 4.5.3.9 Jam Detection and Clutch Logic Circuit

This circuit would be designed to utilize the shaft encoder for detecting the error angle of the torque-summed output shaft with respect to the commanded input. The circuit would be programmed to momentarily declutch one motor output clutch and then the other when an error angle persists, indicating that one of the motors had seized. The circuit would discriminate between the motor which follows the input and the one which doesn't, and operate to permanently declutch the latter.

#### 4.5.3.10 Power-Hinge Torque Tubes and Gearboxes

A series of planetary gearboxes mounted along the rudder hinge line and connected with power transmitting torque tubes driven by the torque-summing gearbox.

#### 4.6 DEMONSTRATION SYSTEMS

It was originally planned that, before a full-scale prototype DEHA unit was fabricated, a small-scale model of the selected concept would be designed, fabricated, and tested to evaluate its feasibility. However, it was soon recognized that, because of the need to create new hydraulic motor and rotary valve designs, the development of a small-scale model would be nearly as expensive as a full-scale dual-channel prototype. Therefore, it was decided to forego the small-scale model and to demonstrate the digital controller and monitor feedback system independently of the total hydromechanical DEHA system.

It was also recognized that the demonstration of a full-up rudder actuation system, with the complete mechanical gear train, would require more funds than were available for the program. Therefore, a simple means of loading the full-scale DEHA prototype unit was devised. These two demonstration systems are briefly described as follows. More detailed explanations are provided in following sections.

##### 4.6.1 Suitcase Digital Controller

A portable electronic control unit packaged in an aluminum carrying case, as shown in Figure 19, was designed and fabricated to demonstrate the operation of the selected electric stepper motor and shaft encoder arranged with a low-gain monitor feedback circuit. This unit included a stepping motor identical to the one used to drive the rotary valve of the DEHA, all electronic logic necessary for input to the Sigma stepper motor drive electronics, circuits to implement the monitor feedback principle, and also a reduction gear train coupling the stepping motor to a digital shaft encoder identical to the encoder used in the DEHA unit. This gear reduction ratio duplicated the total reduction from the stepper motor shaft to the encoder in the final DEHA unit which allowed the demonstration unit to be operated without any of the hydraulic components. Suitable connections were provided so that the same electronics set built into that unit could be shifted to drive the DEHA stepper and to receive positional signals from its encoder.

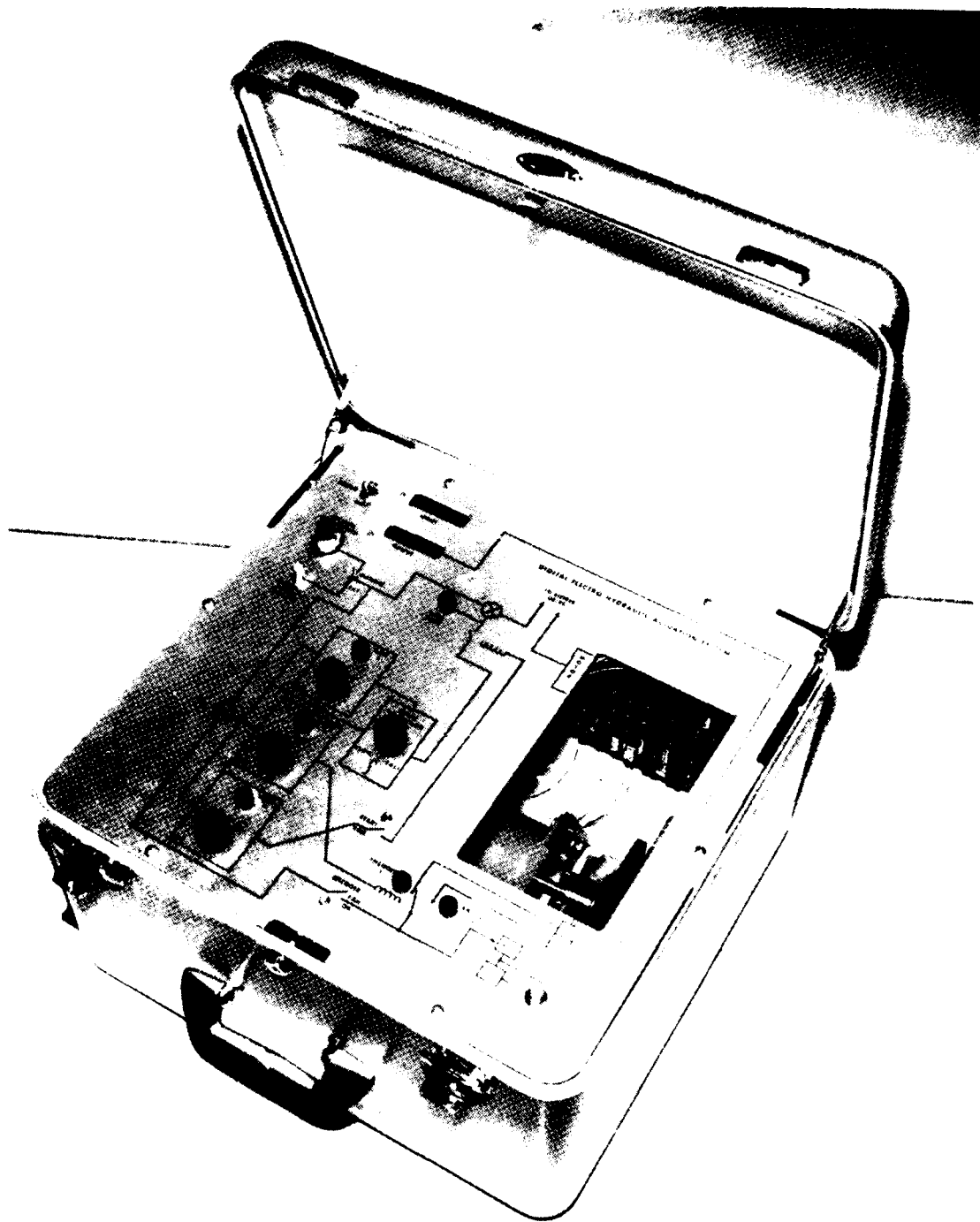


Figure 19 Suitcase digital controller

A single-channel microprocessor-based logic unit designed and fabricated for use in conjunction with the available stepping-motor power controller, Sigma Instruments, Inc. Model DMC-10, was used to amplify and transfer signals from the microprocessor logic unit to the electrical stepper motor. The controller was designed to operate in a laboratory rather than an aircraft environment, and to be capable of performing all of the primary functions of an aircraft unit except redundancy management. It included a software routine which, when invoked, operated to modify the digital word from the shaft encoder to simulate an encoder malfunction. As the microprocessor detected an error, its test software energized a light to simulate a switch to a standby encoder.

For stand-alone demonstrations, means of manually generating 10-bit input commands were included. This was a potentiometer feeding a 10-bit A/D converter which, in turn, was connected to the microprocessor logic. An alternate analog input to the A/D converter allowed frequency response testing of the total DEHA system.

#### 4.6.2 DEHA Prototype Demonstration System

The system used for laboratory demonstrations of the recommended DEHA concept is shown in Figures 20, 21, and 22. It included many of the major subassemblies and components visualized for an all-up aircraft system, as described in Section 4.5.3, except for the following revisions, deletions, and substitutions. More detailed descriptions are provided in Section VI.

##### 4.6.2.1 Electric Stepper Motor

An available single stepper motor, Sigma Model 21-3450D144-B015-K, was used in order to avoid the cost for design, development, and fabrication of two aircraft-quality motors on a single shaft. It is a two-phase type with a permanent magnet rotor which provides 288 (1.25-deg) half steps at a maximum stepping speed of 6,144 steps/s. Its running torque is 600 oz-in at 50 steps/s, and its maximum holding torque is 738 oz-in at 50 steps/s.

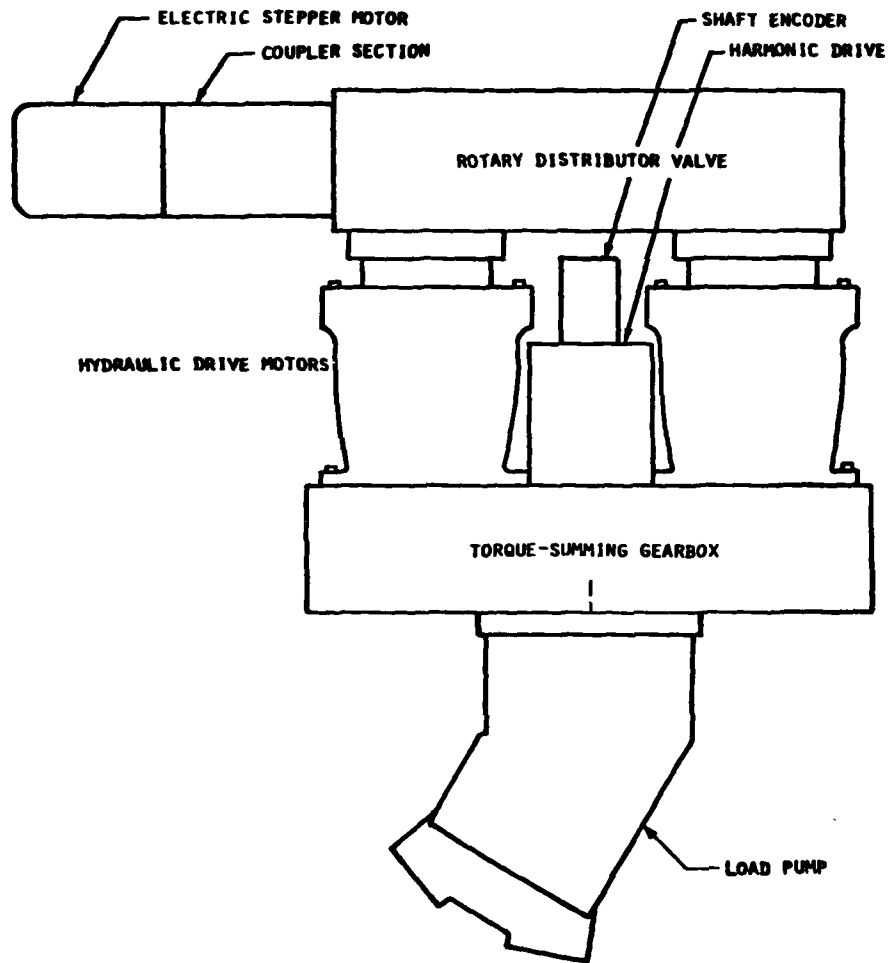


Figure 20 Dual hydraulic channel DEHA unit configured for the prototype system



Figure 21 Prototype DEHA viewed from drive-motor side



Figure 22 Prototype DEHA viewed from load-pump side

#### 4.6.2.2 Hydraulic Distributor Valve

A dual rotary-spool valve such as visualized for an aircraft system, and as described in Section 6.2., was used.

#### 4.6.2.3 Hydraulic Motors

Two externally-commutated fixed-displacement aircraft-type hydraulic motors, such as described for the recommended DEHA concept in Sections 4.5.2.1, 4.5.2.2, and 6.3, were used.

#### 4.6.2.4 Motor Clutches

No motor clutches were used in the laboratory demonstration system. No plans for demonstrating means for preventing a complete system jam in the event of hydraulic motor seizure were included in this program.

#### 4.6.2.5 Torque-Summing Gearbox

A gearbox similar to that visualized for an aircraft system was used. However, rather than drive a torque tube to a power-hinge gearbox, a fourth pad for mounting a hydraulic load pump was provided. The detail design is described in Section 6.4.

#### 4.6.2.6 Harmonic Drive

A harmonic drive, such as visualized for an aircraft system, was used to reduce the gearbox output speed to a speed compatible with the shaft encoder. The harmonic drive is also described in Section 6.4.

#### 4.6.2.7 Shaft Encoder

An available single shaft encoder, Astrosystems, Inc. Model EC1011S-2, rather than a dual unit, was used. It is an electromagnetic resolving absolute digital type with 11-bit absolute natural binary (2,048 steps) output for 360-deg input rotation and with a 0.0025-sec data refresh rate.

#### 4.6.2.8 Jam Detection and Clutch Logic Circuit

No such circuit was used for the laboratory demonstration system. As noted in 4.6.2.5 above, the program contained no plans for demonstrating means for preventing system jams.

#### 4.6.2.9 Power-Hinge Torque Tubes and Gearboxes

As previously noted, these items were not provided for the laboratory demonstration system.

#### 4.6.2.10 Hydraulic Load Pump

A Sperry-Vickers bent-axis hydraulic motor, Model MF3913-30, was used in a hydraulic loading circuit so that it could act as a fixed-displacement pump to provide resisting loads of various magnitudes, and alternatively, as a fixed-displacement motor to provide aiding loads.

## V. DIGITAL CONTROLLER DEVELOPMENT

### 5.1 CONTROL FUNCTIONS

The digital controller unit was required to perform two basic functions; ie: to generate signal commands to the electrical stepper motor in response to input commands, and to provide a monitor feedback. The monitor feedback allows position initialization (to bring the output into agreement with the input command upon system startup) and updating of the output (by replacing commanded steps which may have been missed for any reason).

#### 5.1.1 Command Signal Generation

The arrangement of the input command and monitor control functions are shown in Figure 23 and were repeated on the control panel of the suitcase demonstrator unit which was also the electronics set used to drive the DEHA prototype unit. An input command could be introduced as a ten-bit digital wordstream from an external source or be derived from a ten-bit encoder system built into the demonstrator unit with access from an input dial on the control panel. The unit output signal came from an effective ten-bit encoder whose decimal equivalent readout is displayed alongside of the decimal equivalent of the input dial setting. The error between input and output was computed continuously and converted to the form of a directional pulse train having three pulses for each least bit of system error. This pulse train was used to command the stepper logic unit shown in Figure 24, which sequenced the bipolar chopper electronic drive ensemble of Figure 25 to switch current across appropriate windings in the stepper motor to advance its rotor in steps.

The three-for-one multiplication of command bits to stepper-command pulses resulted from an unfortunate choice of the number of rotary valve phases per revolution which was locked into the valve design before the difficulty of the three-for-one pulse conversion was fully appreciated. As shown in Section 6.4.2, the four-phase valve requires 3.75 degrees input rotation for each least-bit output step of the DEHA torque-summing gearbox. This is obtained with three consecutive 1.25-degree half steps from the

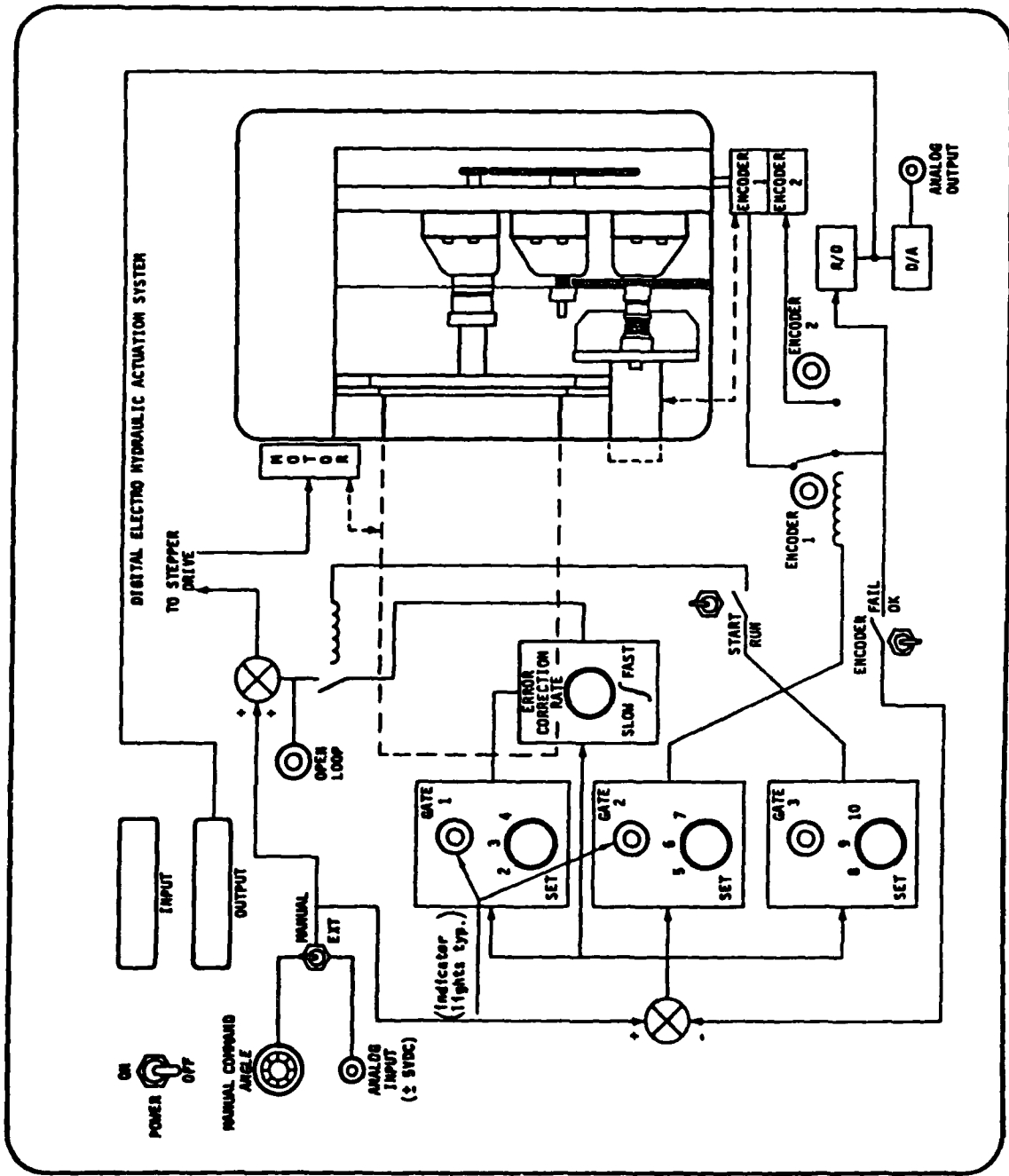
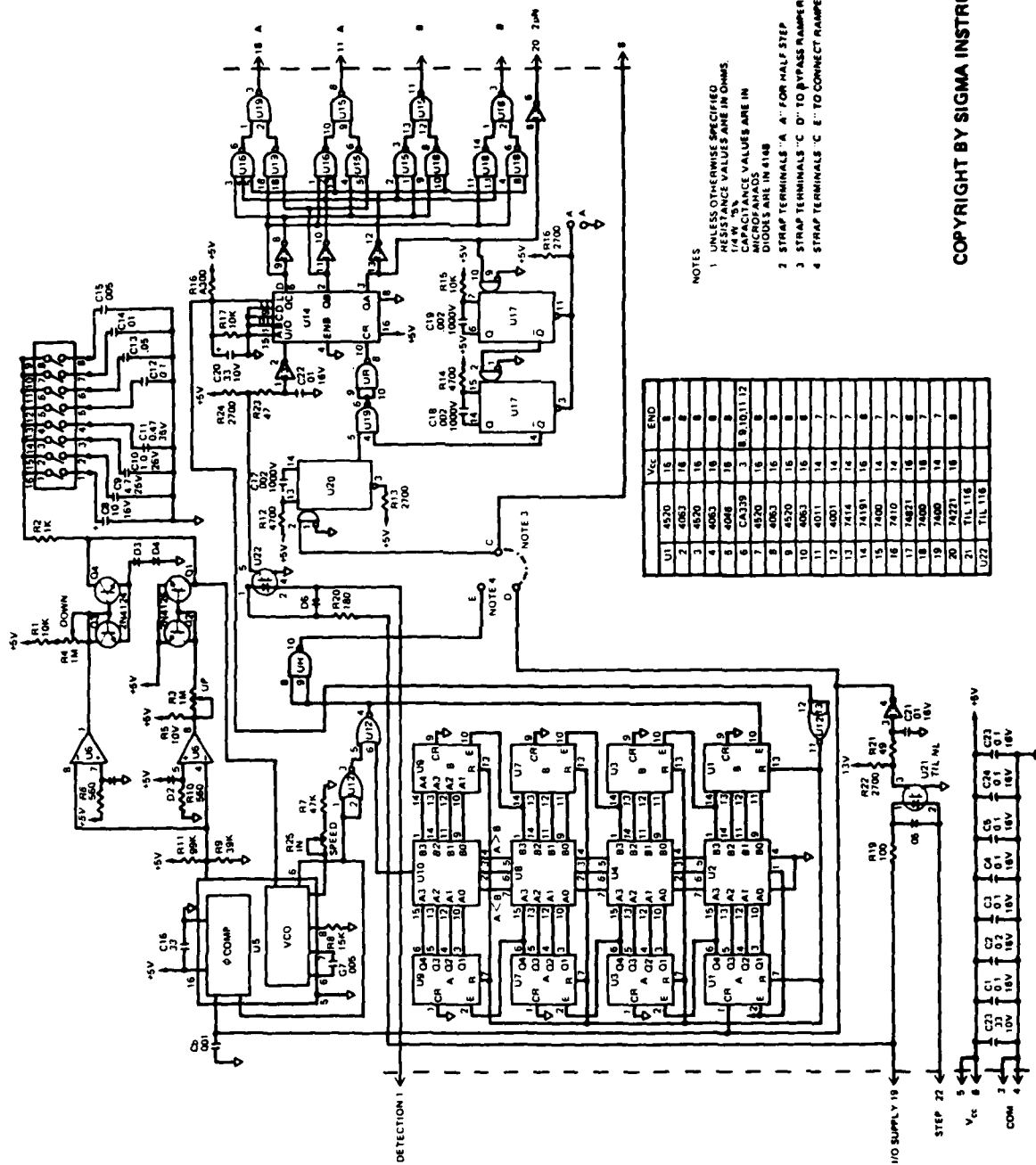


Figure 23 Software controller panel layout

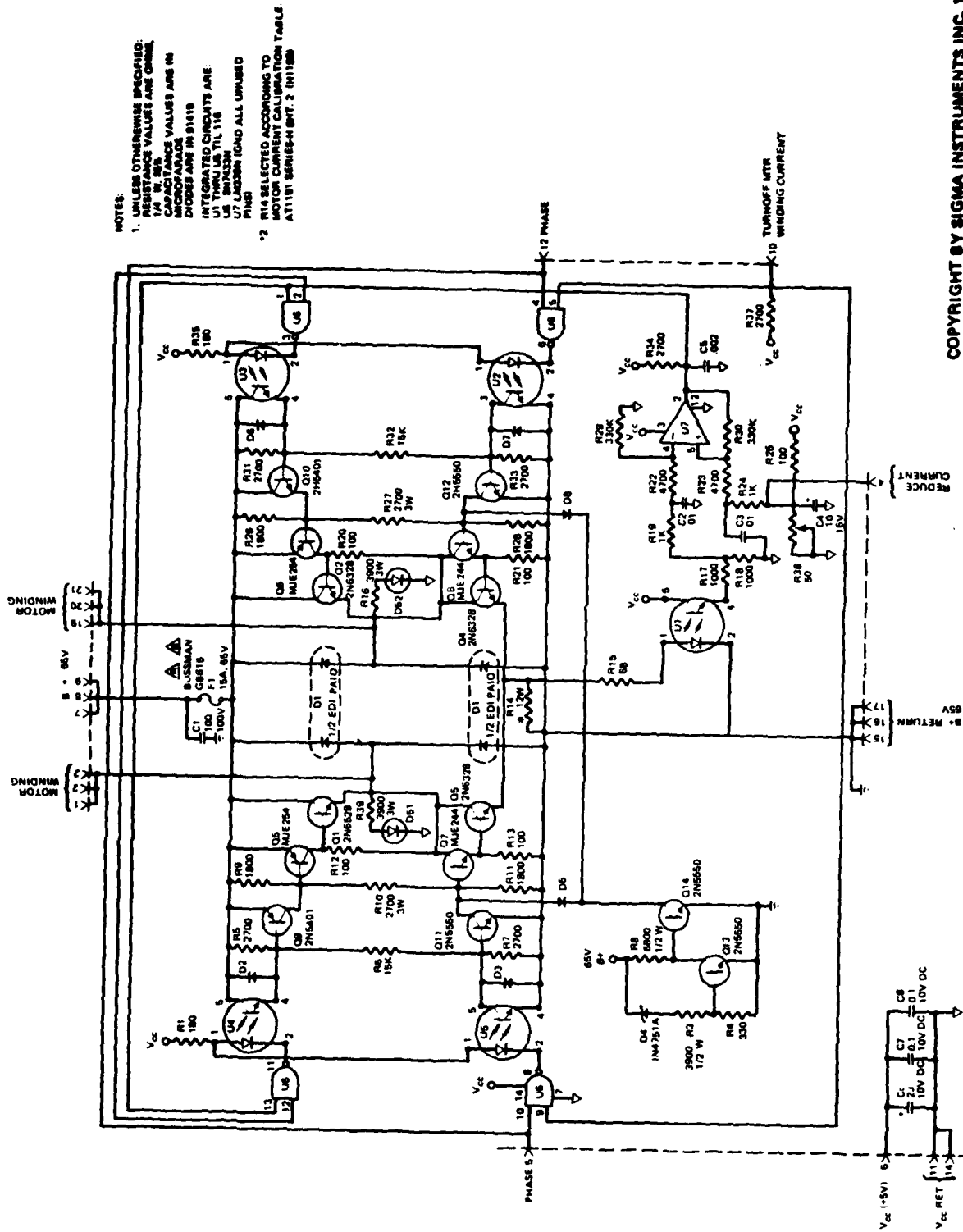


UIC	END
U1	4520 16 8
U2	4520 16 8
U3	4520 16 8
U4	4520 16 8
U5	4520 16 8
U6	4520 16 8
U7	4520 16 8
U8	4520 16 8
U9	4520 16 8
U10	4520 16 8
U11	4520 16 8
U12	4520 16 8
U13	4520 16 8
U14	4520 16 8
U15	4520 16 8
U16	4520 16 8
U17	4520 16 8
U18	4520 16 8
U19	4520 16 8
U20	4520 16 8
U21	4520 16 8
U22	4520 16 8
U23	4520 16 8
U24	4520 16 8
U25	4520 16 8
U26	4520 16 8
U27	4520 16 8
U28	4520 16 8
U29	4520 16 8
U30	4520 16 8

- NOTES
- 1 UNLESS OTHERWISE SPECIFIED RESISTANCE VALUES ARE IN OHMS. CAPACITANCE VALUES ARE IN MICROFARADS. DIODES ARE IN 1N48
  - 2 STRAP TERMINALS "A" "A'" FOR HALF STEP
  - 3 STRAP TERMINALS "C" "D" TO BYPASS RAMPER
  - 4 STRAP TERMINALS "C" "E'" TO CONNECT RAMPER

COPYRIGHT BY SIGMA INSTRUMENTS INC. 1978

Figure 24. Sigma Instruments stepper logic unit circuit.



COPYRIGHT BY SIGMA INSTRUMENTS INC. 1978

Figure 25. Sigma Instruments stepper-motor driver card schematic

selected Sigma stepper motor. However, initial attempts to drive the stepper motor by bursts of three pulses applied near the maximum-rate performance limit of the motor were totally unsuccessful. The ramping function initially provided with the Sigma bipolar chopper drive unit was not usable as a smoothing function for sinusoidal inputs.

The electronics loop shown in Figure 26 was devised as a way of circumventing this three-for-one pulse conversion problem. It includes an Intel 8748 microprocessor as a summing junction of a digital integrator and feedback loop. The analog-converted error signal of this loop is used to drive a voltage-to-frequency converter which then is counted up or down as the sign of the loop error changes. The three-for-one pulse conversion is made at the microprocessor input. However, it should be recognized that this loop and its three-for-one pulse conversion would be unnecessary, except perhaps as a forward-loop noise filter, if a proper match of step size and least-bit equivalent output rotation had been designed into the unit. For instance, with a six-phase valve, 2.5 degrees input rotation is required for each least-bit output step. That corresponds exactly with the 2.5-degree full-step size of the selected stepper motor.

When the Sigma ramper function was eliminated, A/D input noise became a major problem. Least-bit jitter in the A/D output word caused stepping motor pulses to be output erratically. Shielding and noise reduction techniques applied to the A/D converter failed to reduce the noise below the least-bit level. The failure of these noise reduction measures made it necessary to operate the three-for-one conversion loop as a low-pass first-order filter to suppress the A/D noise to an acceptable level that would not adversely effect the stepping motor least-bit response.

The setting of this input-signal first-order filter at approximately 0.4 Hz became the dominant factor in all frequency response measurements. An 8-Hz second-order filter placed in the input-signal channel upstream of the A/D had no noticeable effect in allowing the first-order characteristic filter frequency to be raised to a significantly higher level.

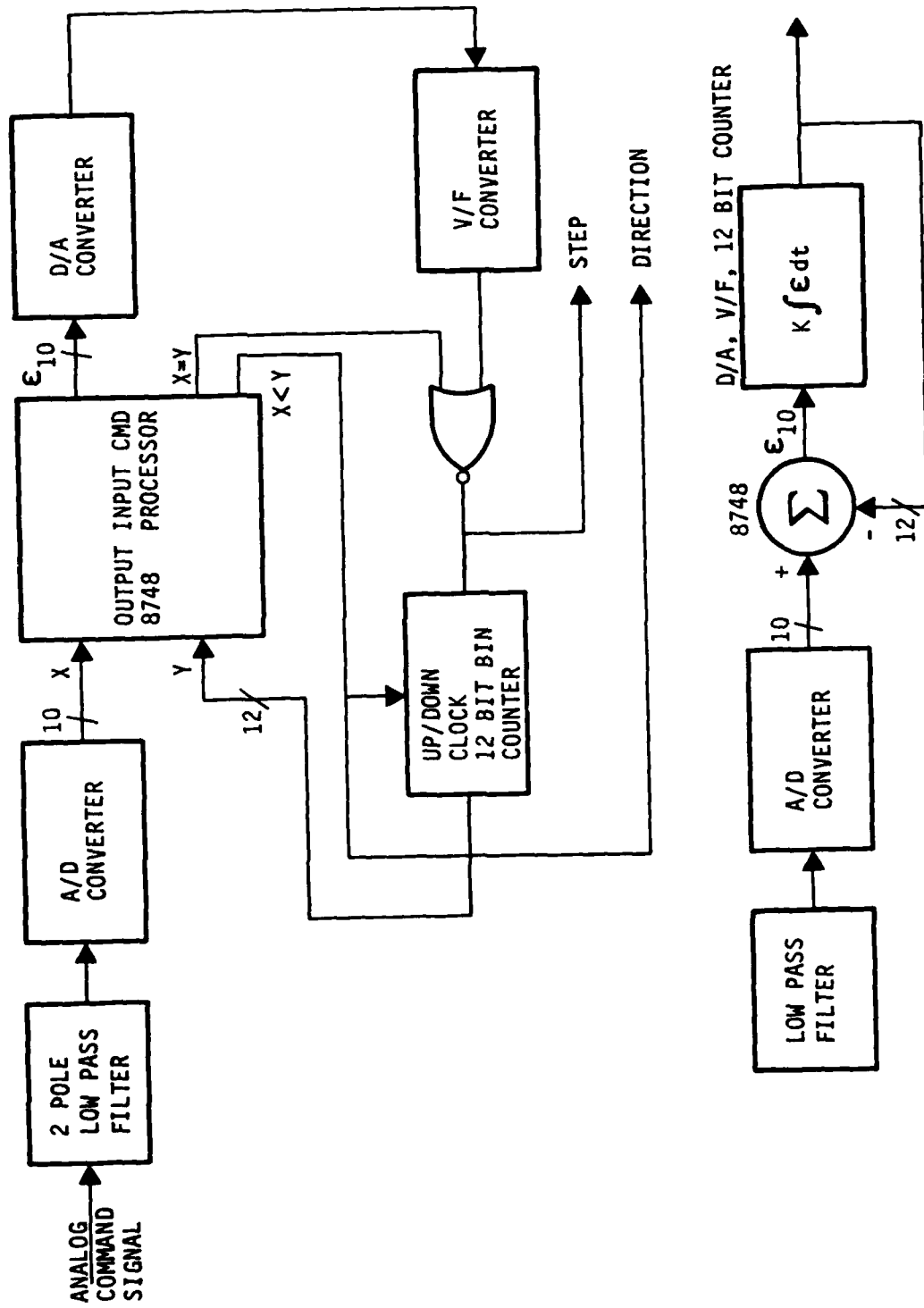


Figure 26 Signal input network

The overall performance of the stepper motor drive electronics was thus disappointing in that limitations of the electronics, necessitated by the need to provide pulse-train smoothing for the stepper motor, became the limiting factor in the frequency-response performance of the overall DEHA system. The final data indicates that the frequency response of the stepper motor through to the unit encoder output was essentially flat to ten Hz. The dominant attenuation in the overall system was from the first-order lag characteristic produced by the steered up-down counter loop at the stepper input. Attempts to draw this loop tighter to raise its first-order response characteristic frequency to match the performance of the electromechanical system resulted in erratic performance of the stepper motor.

The use of a first-order filter to smooth the stepper input pulse train to an acceptable degree is not suggested as a practical expedient. Its use here serves to illustrate one of the problems which is associated with the use of microprocessor electronics to drive free-commutated electrical stepping motor units. It is evident that more work is needed to perfect electronic drivers for stepping motors before such motors can be freely substituted for analog type servos of either electrical or electrohydraulic types.

#### 5.1.2 Monitor Feedback

The error between input and output, which is computed continuously, is compared with each of three successive gate threshold values. As the sensed error exceeds each threshold value, a signal light is illuminated on the panel section representing that gate. When the first gate threshold is reached, a stepwise integrator is started and its output is summed with the input command to form a correction error signal. This integrator is latched at zero output when its input variable (the system error signal) reaches zero. If the action of the integrator does not prevent the system error from increasing, the second gate threshold will be exceeded. At this point, an indicator light signals that, in a real system, a standby feedback encoder circuit had replaced the primary feedback encoder which is assumed to have malfunctioned.

If the system error should continue to increase up to the third gate setting, the entire feedback loop would be disabled causing the circuit to revert to an open-loop stepping motor type of response. A start switch is provided to inhibit this open-loop disable function with an indicator light to show when the third gate function is locked out. This feature allows the system to be started with a large initial error.

## 5.2 CONTROL CIRCUIT DESIGN

The digital controller was designed to provide a means by which the stepping motor, and ultimately the hydraulic valve, could be actuated according to an input command signal. The driving signal can be selected from one of the sources. A switch on the front panel selects either manual or external modes.

In the manual mode, a front panel control drives a potentiometer between -5 and +5 volts DC generating the controller input command voltage. In the external mode, the input command voltage (between -5 and +5 volts DC) is generated externally and input via a connector on the front panel labeled "analog input". In either case, the resulting input command voltage is fed through a low-pass filter, to an A/D converter for conversion into a digital command word of 10-bit resolution. The 10-bit digital command word thus becomes the basis for system control and stepping motor positioning.

The remaining functions of the digital controller can be divided into three main categories; motor control, monitor feedback and front panel display.

At the onset of the controller design, a microprocessor was chosen as the main ingredient for accomplishing these functions. From a systems point of view, this approach appeared to be most consistent with the overall DEHA design philosophy of digital position control with incremental motion control. Referring to Figure 27, a signal flow description follows:

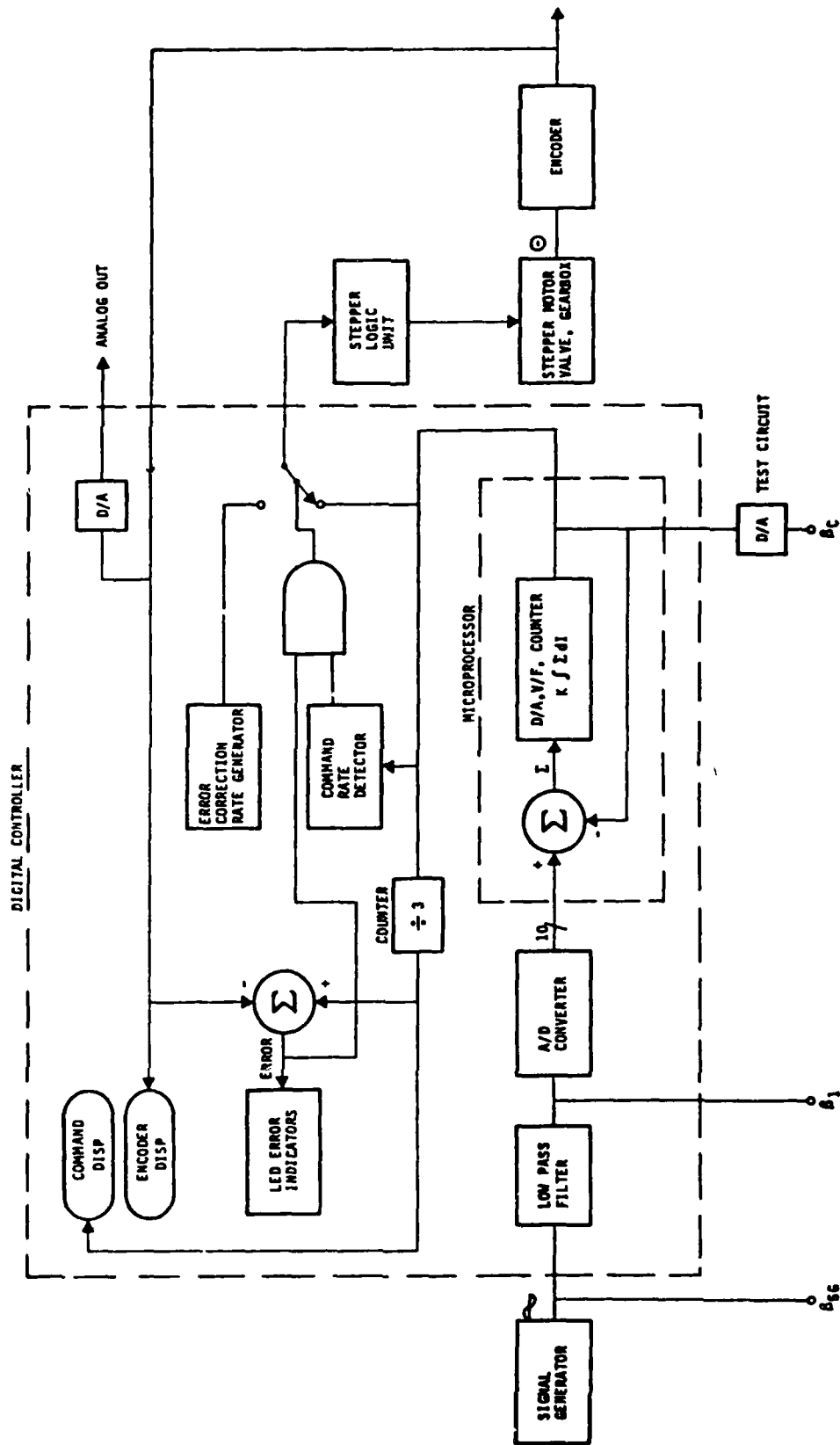


Figure 27 Digital controller schematic

### 5.2.1 Low-Pass Filter

The input command voltage is filtered for high-frequency noise rejection and to integrate out any large discontinuities that might exist in the command voltage.

### 5.2.2 A/D Converter

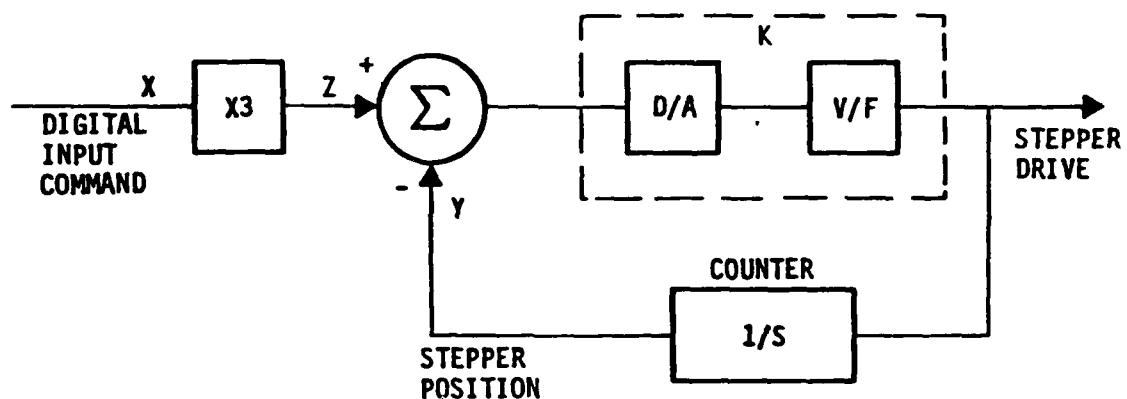
The filtered command voltage is then digitized by a 10-bit resolution A/D converter. The result is a 10-bit command word placed on a digital data bus in a form that the microprocessor can understand and utilize. The concept of digital data bus control could at this point be expanded to include control words to be input via an external digital bus tying the DEHA digital controller unit into a central command computer or control system.

### 5.2.3 Microprocessor Authority and Functions

During the initial stages of development of the digital controller, it was found that the demands placed on system throughput rate (2,000 bits/sec in and 6,000 pulses per sec (PPS) out) could not be accommodated by a single microprocessor. At this point, a second microprocessor was added and the controller tasks were divided into two groups: motor control, handled by an Intel 8748 microprocessor, and monitor-feedback and front-panel displays and switches handled by an Intel 8085 microprocessor. Detailed monitor and display circuits are shown in Appendix B, in Figures B2 and B3.

The digitized command signal noted in Section 5.2.2 is input to the 8748 microprocessor and multiplied by a factor of three in the 8748 program software. This new (3x) command signal then becomes the driving signal for a digital integrator loop placed around the 8748 microprocessor, with the loop output being the stepper drive signal. Referring to Figure 28 and to Figure B1, this can be described as follows:

The 8748 microprocessor functions as the summing junction for a digital integrator and feedback loop. The digital command word is multiplied by three at the X input to the 8748. The result is a new digital input command word  $Z = 3X$ . From this value the microprocessor subtracts the digital stepper motor position signal  $Y$  to generate an error signal  $E = Z - Y$ . This digital error signal passes through a digital-to-frequency converter before becoming the stepper drive signal. The stepper drive signal is the output of a voltage/frequency (V/F) converter which generates the motor step rate proportional to the error signal. The stepper drive signal or step rate is converted back to digital form and integrated by a counter in the feedback loop to the Y-input of the 8748. The counter/integrator output is also the stepper motor commanded position since the integration of rate is position. The foregoing is described mathematically as follows:



$$E = Z - Y, Y = \frac{KE}{S}$$

$$Y = \frac{K(Z - Y)}{S}$$

$$\frac{Y}{Z} = \frac{K}{K + S}$$

Where  $K$  is the integrator gain, and  $S$  is the complex frequency variable

Figure 28 First-order (times three) functional filter

AD-A104 263

BOEING MILITARY AIRPLANE CO SEATTLE WA F/G 9/2  
AIRCRAFT DIGITAL INPUT CONTROLLED HYDRAULIC ACTUATION AND CONTR--ETC(U)  
MAR 81 E T RAYMOND, C W ROBINSON F33615-77-C-2034

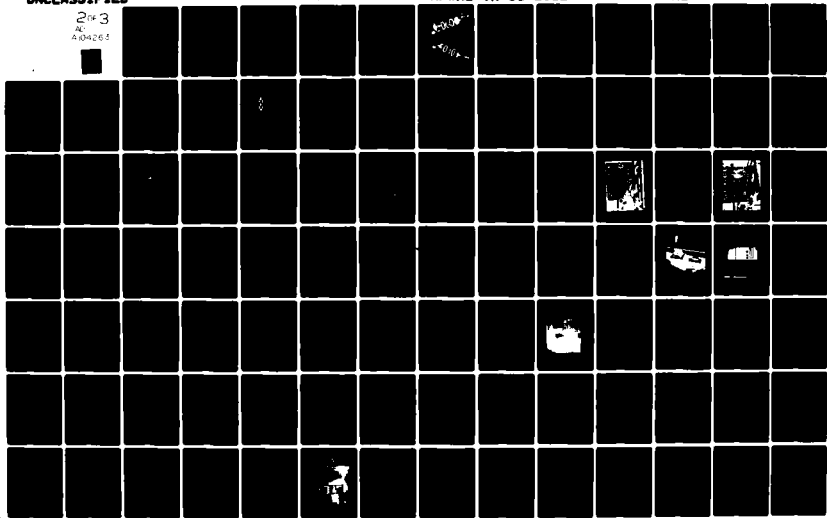
UNCLASSIFIED

AFWAL-YR-81-2012

ML

2 of 3  
AC  
A04263

3-8-81  
4-15-81



## 5.2.4 Basic Open-Loop Operation

It was intended that the digital controller operate primarily in an open-loop mode using a monitor feedback function for occasional update or error correction without relying heavily on feedback for motor control. In addition, the controller was designed to operate without significant effect or loss of performance after a total loss of feedback. Thus, the remaining controller functions have very little effect on gross stepper motor control except at low speeds (below stepper start-stop speeds) or during system power-up and initialization.

### 5.2.4.1 Error-Correction Command

The Sigma stepper motor drive electronics receives the stepper drive rate signals noted in Section 5.2.3 or error-correction-rate signals depending on the status of the command rate detector and the monitor feedback error. The command-rate detector senses when the stepper drive (command) rate falls below stepper stop-start speeds and switches the error correction rate generator to the Sigma driver electronics if an error exists. This function allows the stepper motor to be stepped by error correction pulses at times when it is not being controlled by command pulses. The speed of the error-correction-rate generator can be adjusted by a front panel control.

### 5.2.4.2 Displays

The stepper drive-rate signal noted in Section 5.2.3 is input to a divide-by-three counter in the 8085 microprocessor. The current count is displayed on a four-digit LED numerical display on the front panel of the digital controller. Likewise the digital encoder signal or monitor feedback is displayed on a four-digit LED encoder display positioned just below the command display on the front panel. The difference between these two displays represents the error signal used as a part of the monitor feedback function as follows:

a. Gate 1 Set for Detection of Errors Between 1 and 5 Least Bits

Gate 1 LED will light when the Gate 1 threshold level is exceeded, indicating that a correction-signal pulse train is being inserted into the command pulse train by the error-correction-rate generator.

b. Gate 2 Set for 5, 6 or 7 Least Bits

When the system error is equal to or larger than this setting, Gate 2 LED will light and a switch from Encoder 1 to Encoder 2 will be made. An LED by each encoder will light to indicate the operational one.

c. Gate 3 set for 8, 9 or 10 Least Bits

As above, an LED will light with the system responding now by running in the open-loop mode. An open loop LED indicator will light and all monitor feedback functions and encoders will be disabled.

5.2.4.3 Analog Output

A D/A converter reads the encoder signal and outputs a voltage between -5 and +5 volts DC proportional to the angle of the absolute encoder. This signal is continuously supplied to a connector on the front panel.

5.3 CONTROLLER TESTING

Refer to Fig (29) and (69) for digital controller frequency response.

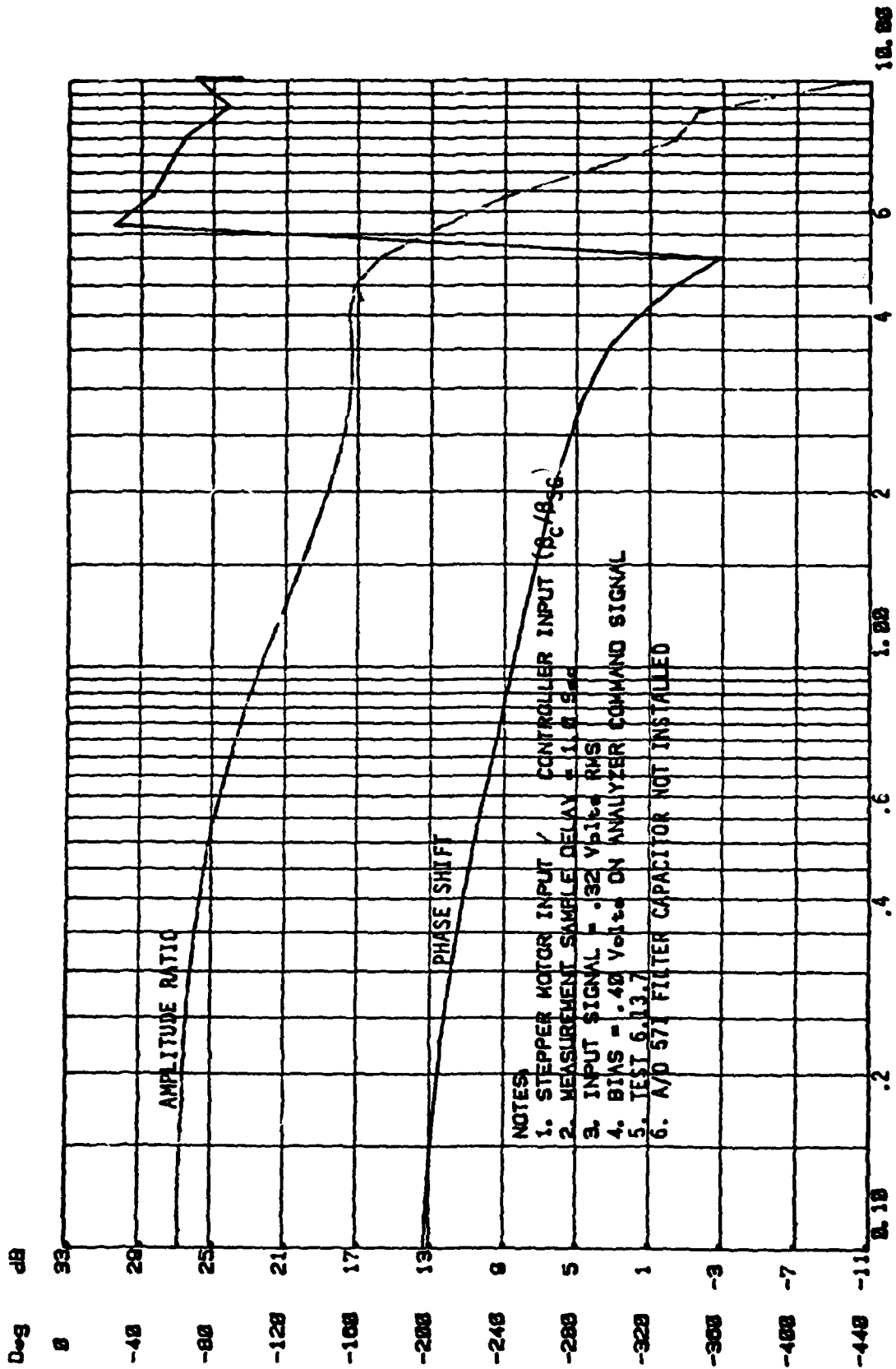


Figure 29 Digital controller frequency response

## VI. DEHA DESIGN AND FABRICATION

### 6.1 GENERAL ARRANGEMENT

The basic arrangement of a DEHA unit suitable for an application to the F-16 rudder is illustrated in Figure 18. In the prototype unit, the following design parameters were adjusted for reasons of part availability and thus economy. Spacing between centerlines of hydraulic motors was set by the availability of torque summing gears having adequate torque capacity at a 15/16 reduction ratio. The rotary valve axis was located at right angles to the motor axes to minimize cylinder head-space clearance volume under compression between the valve rotor and the cylinders. This placement of the stepping motor was compatible with the space available for the current F-16 rudder actuator. In the prototype DEHA unit, the positions of encoder and output shaft were reversed from the position shown in Figure 18 to allow the use of a hydraulic motor as a load pump mounted directly on the torque summing gearbox as shown in Figure 20. Only one channel of electronics was used with a single stepper motor and a single output encoder. This was justified on the basis that development of redundant electronics was outside the scope of this program.

The general arrangement of the DEHA mechanism evolved in an effort to fit the necessary motor gearbox and valve components into an existing cavity in the F-16 structure. This basic cavity is bounded on the top by the rudder surface, on the bottom by the engine tailpipe and on the front by the rear spar web of the aircraft fin. The DEHA configuration chosen placed the hydraulic motors fore and aft in a parallel arrangement with their output shafts parallel to the rudder hinge axis. A single spool dual-channel rotary valve was mounted at right angles to the motor output axes in order to minimize the length of connecting tubes between valve rotor and the individual motor cylinders. This valve location was the only one possible in the present F-16 actuator mounting space available if a single-piece dual system valve was to be used. From a functional point of view, either a single dual-system valve mounted with its axis parallel to the motor output shafts or a pair of

individual valves geared together would have been preferable. Such valve placement would have allowed a valve error limiter to be placed as a simple stop between relative rotation of the valve and motor or valve and gearbox output shafts. However, with a single-piece dual valve in this position, the vertical length along the rudder hinge line was insufficient to allow the valve and its stepper motor to fit between the engine tailpipe and the rudder surface.

## 6.2. ROTARY DISTRIBUTOR VALVE

### 6.2.1 Valve Design

Of the three major mechanical component developments involved in the DEHA program, the rotary valve element required the greatest amount of innovation. This type of porting sequence was demonstrated at the Boeing Company in 1976 as part of a research program using a small six-piston radial pneumatic motor sized to the requirements of a fin actuator for a HOBOS (homing bomb system) glide bomb. Three three-way on-off pneumatic valves manufactured by the Chandler Evans Control Systems Division were borrowed from the HOBOS bomb system to drive the pistons of this motor. Stepping-motor-type drive electronics were used to drive the valves of this demonstration system. The basic principle of this type of porting sequence had been used in the design of electric stepping motors before, but had not been applied previously to a fluid motor. Figure 30 shows a parts breakdown of this earlier fluid stepping motor type fabricated at Boeing.

The desired porting sequence for the DEHA rotary valve was supplied to prospective subcontractors as part of a valve procurement specification written by Boeing. Following the award of a subcontract to the Bendix Electroynamics Division, a proposed method of subdividing a 360-degree valve circumference to generate the appropriate sequence for a six-piston fluid motor was transmitted to them separately in the form of Figure 31. A suitable method of fabricating a multiple-port rotary valve sleeve and spool which produced a balanced pressure distribution on the spool element had been proposed earlier by Bendix. A cross section of that type of valve is illustrated in a two-phase version in Figure 32.

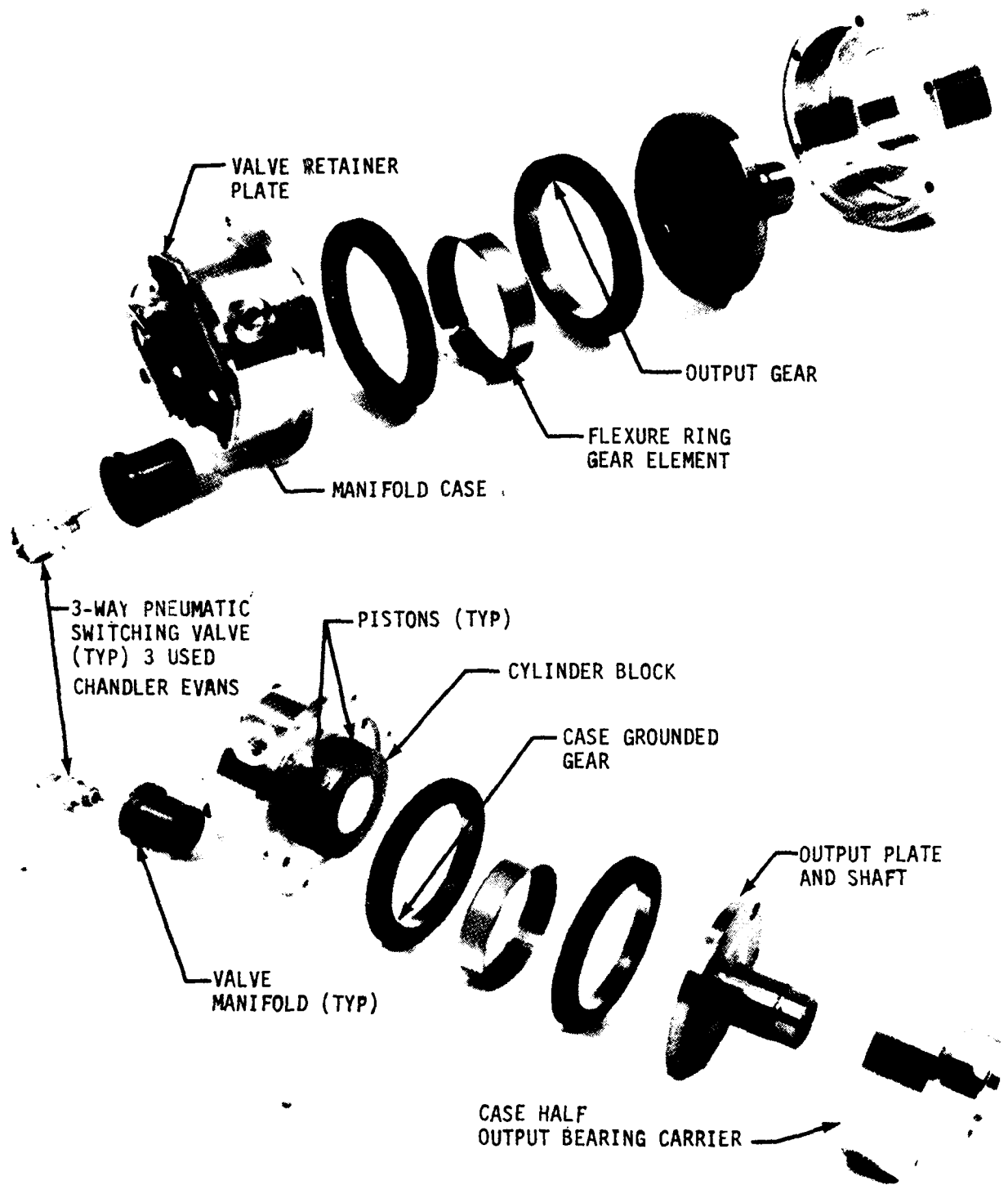
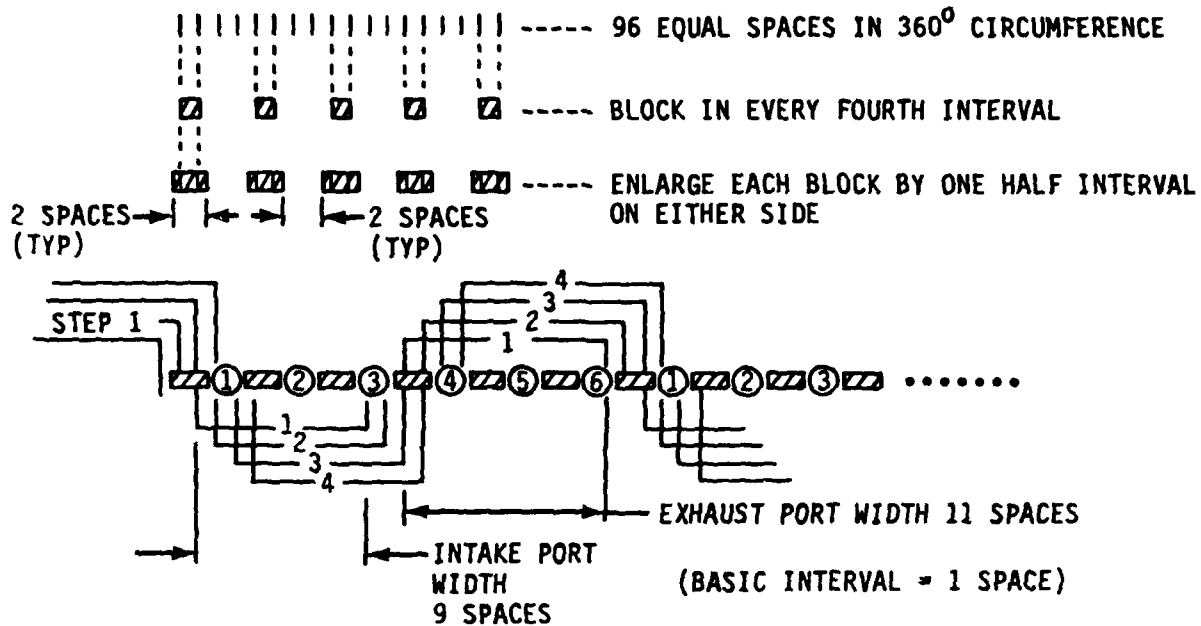


Figure 30 Pneumatic stepper motor fabricated at Boeing in 1976

**SUGGESTED VALVE SEQUENCE**

**DEVELOPMENT OF SPOOL PORTING GEOMETRY**

**START WITH:**



ABOVE PORT GEOMETRY GENERATES THE SEQUENCE LISTED IN SECTION 3.3.2.1 SHEET 11 OF VALVE SPEC. ALSO LISTED BELOW

TO PRESSURE	TO RETURN
123	456
123	456
123	456
23	4561
234	561
234	561
234	561
34	5612
345	612
345	612
345	612
45	6123
⋮	⋮
⋮	⋮
⋮	⋮
ETC	ETC

Figure 31 Rotary valve porting sequence

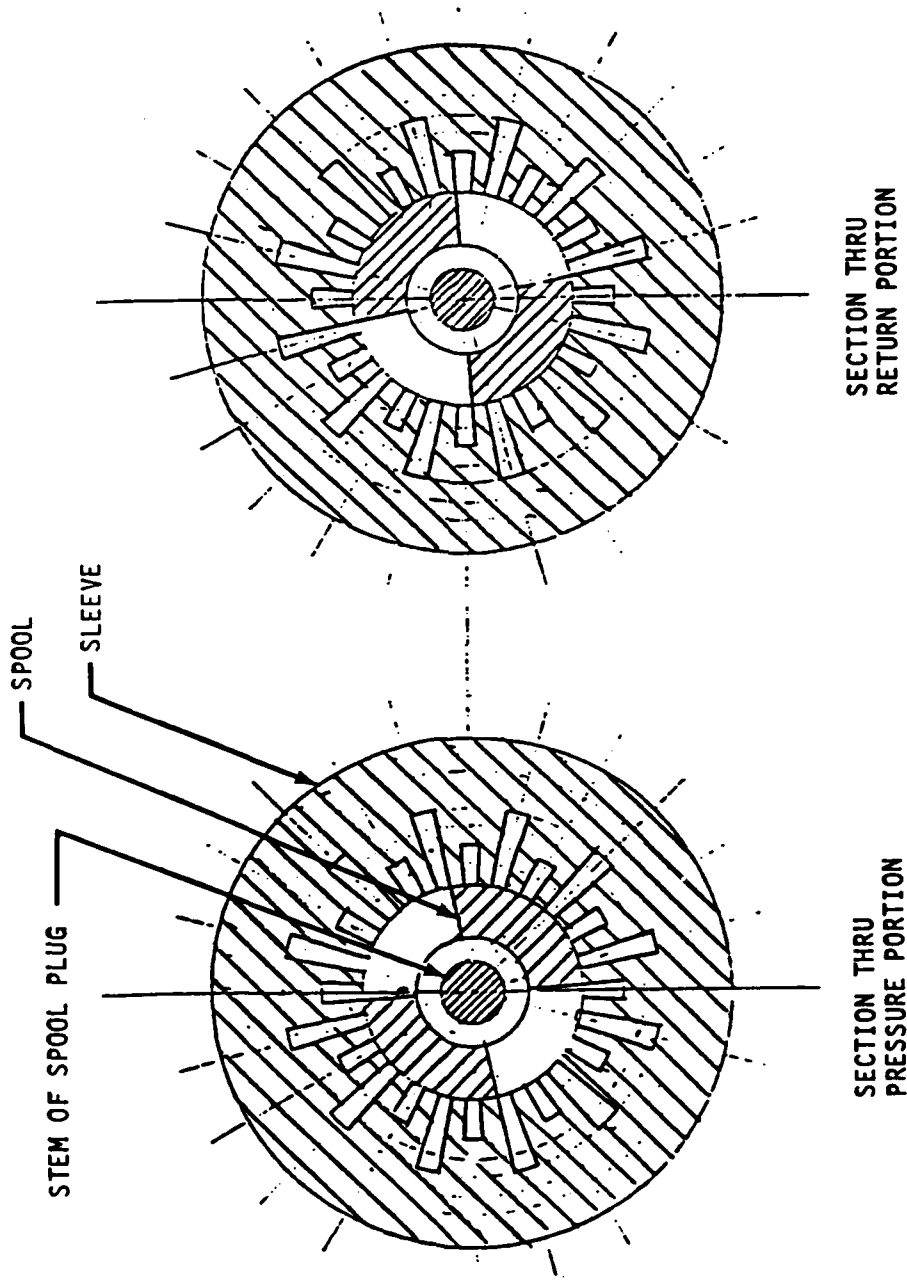


Figure 32 Rotary valve cross-section showing balanced porting

The major design problems of the valve sleeve evolved to be one of decreasing sleeve internal pressure drop by shortening connecting passageways and by increasing these passage cross-sectional areas without unreasonably increasing the cylinder clearance volume between valve metering edge and motor cylinder ports. A less critical problem was simply to prevent unreasonable growth of the valve sleeve outer diameter to accommodate the large number of apparently necessary passages.

The basic design problem was broken down in the following way in an attempt to isolate a near optimum solution.

a. Problem 1 Location of Annular Passages

If a pressure-balanced spool design were to be used, some system of annular cylinder feed passages was required in either the sleeve or the manifold block to interconnect the valve metering slot ports on opposite sides of the valve sleeve. The ideal location for such passages would be internal within the sleeve wall. This location would give maximum passage cross section with absolute minimum passage volume. With these passages internal to the sleeve, a lapped or slip fit could be used between sleeve and housing.

The next best alternative placement of annular sleeve passages was on the external sleeve surface which required a heavy press or shrink fit of sleeve to housing to prevent cross-port leakage.

b. Problem 2 Need for Longitudinal Passages

Longitudinal sleeve passages were required if cylinder feed slots in the inner sleeve wall were arranged in two parallel annular rows. This two-row arrangement of ports, illustrated in Figure 33, allowed the leakage across pressurized lands of the spool to be minimized. This design requires longitudinal feed passages in the spool or housing to connect the two parallel rows of cylinder feed slots to the circular port pattern of the hydraulic motor.

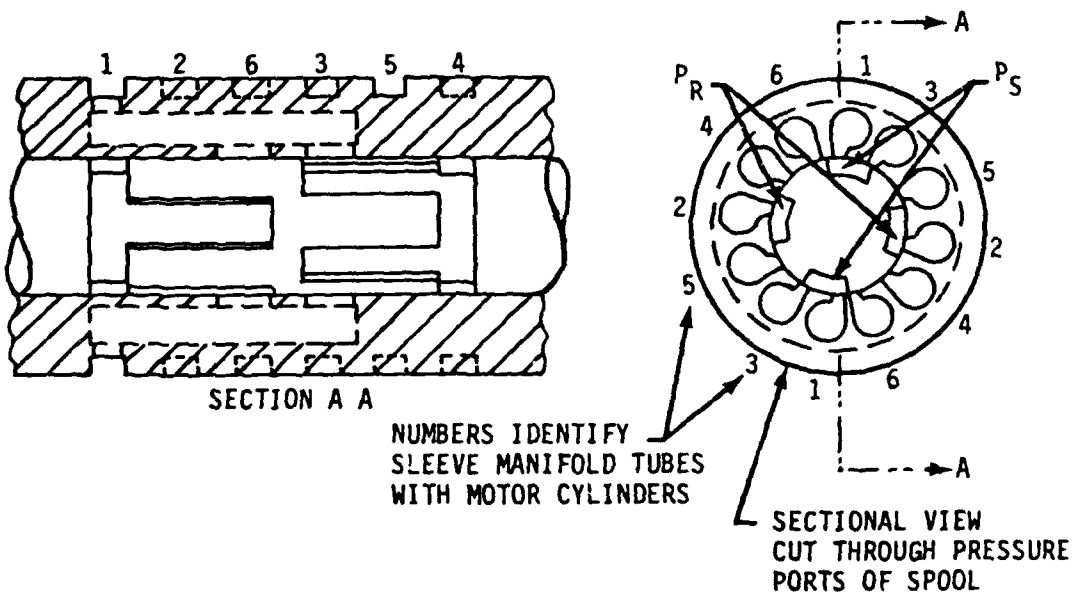
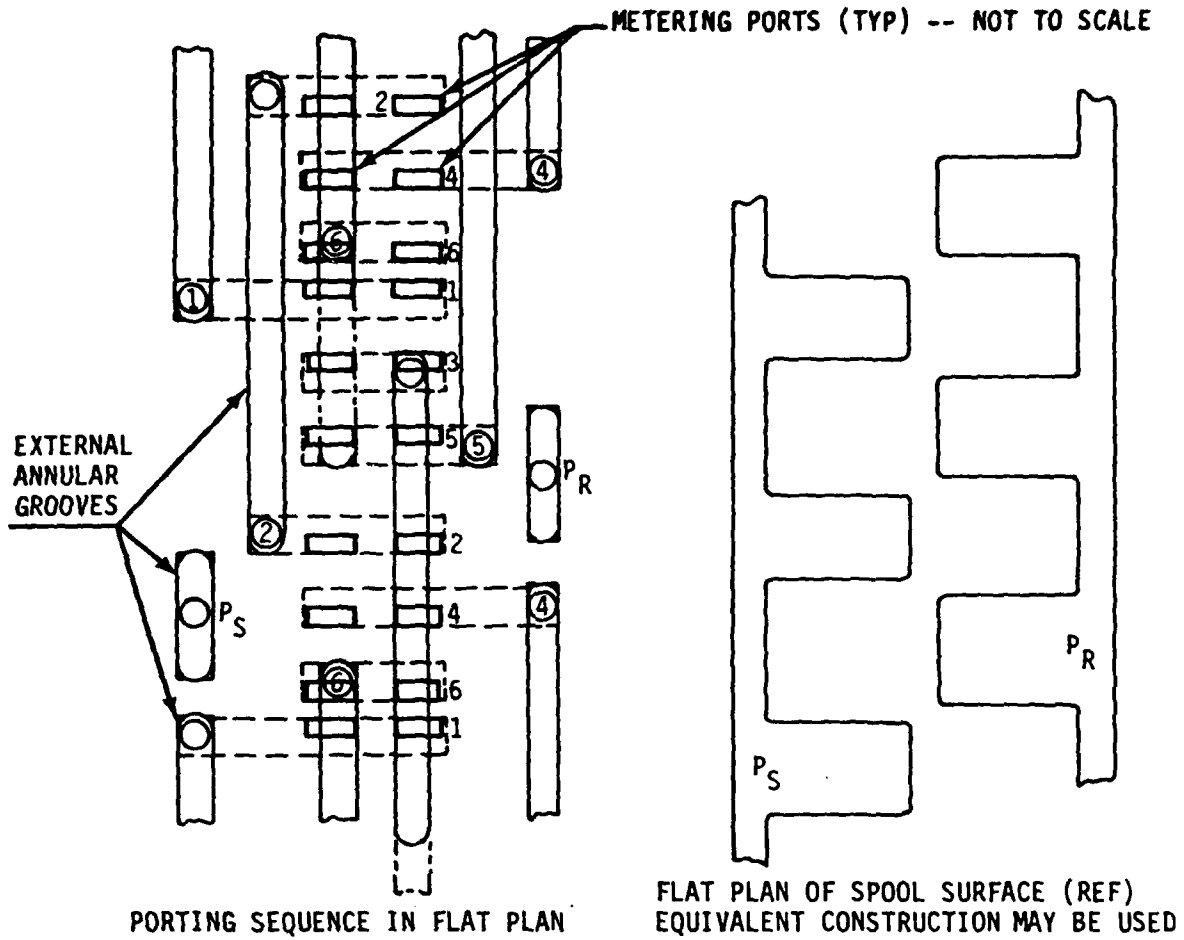


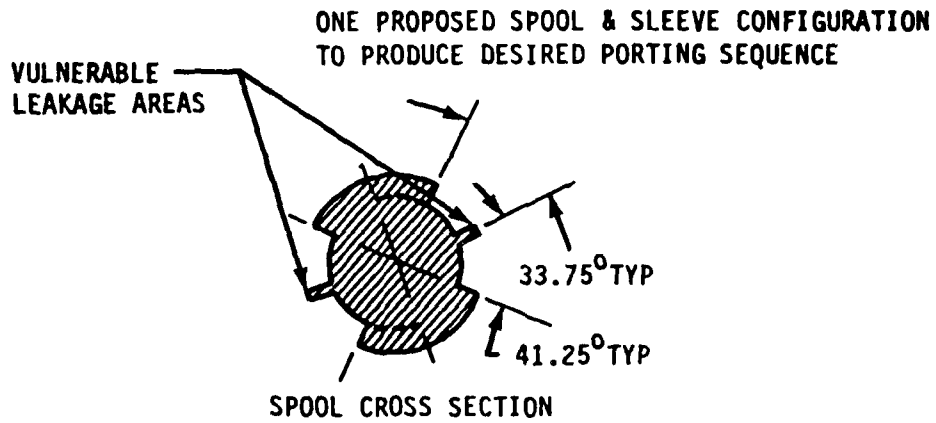
Figure 33 Spool-sleeve design using pressure and return ports in parallel rows

If the spool surface feed slots were folded together as shown in Figure 34, then the cylinder feed slots could be spread in a longitudinal pattern to align with appropriate motor cylinders. Such an arrangement needs no longitudinal passage connections, since this function is served by the elongated surface slots in the valve spool. Without the need to provide space for longitudinal passages, much more sleeve internal volume could be devoted to annular passages. This configuration was clearly superior to the one of Figure 33 in terms of both decreased valve pressure drop and minimum added cylinder clearance volume. The difficulty of sealing between passages traversing the outer surface envelope of the sleeve cylinder was also reduced with this configuration. The only disadvantage of this second configuration appeared to be the high potential for pressure-to-return leakage across the relatively narrow elongated surface land areas of the valve spool. (Note: This spool land leakage problem can be solved by using a six-phase valve in place of a four-phase valve. See Figure 35).

c. Problem 3 Reduction of Metering Slot Complexity

The number of spool metering slots and longitudinal feed passages (for the basic configuration of Figure 33) required to implement a four-phase valve using the original concept proposed by Bendix appeared to be excessive as it required that all six cylinder feed slots be included in each 90-degree sector of the sleeve inner cylinder. A method of reducing this required number of metering slots and longitudinal passages (if used) was devised which alternated cylinder metering slots between the first and second 90-degree quadrant of the sleeve inner surface. This scheme is illustrated in the lower right hand view of Figure 33. The required number of internal passages in the sleeve is cut in half by this arrangement.

The basic metering scheme of Figure 33 was selected for the DEHA prototype valve using full annular feed and distribution passages on the outside of the sleeve body. The sleeve was shrink fitted to the manifold block and the alternate quadrant metering scheme described above was used to reduce the number of required longitudinal passages. This decision was influenced strongly by the apparent need to reduce leakage across the spool lands separating pressure and return areas.



BELOW THE SPOOL-SLEEVE INTERFACE AREA IS DEVELOPED IN A FLAT PATTERN

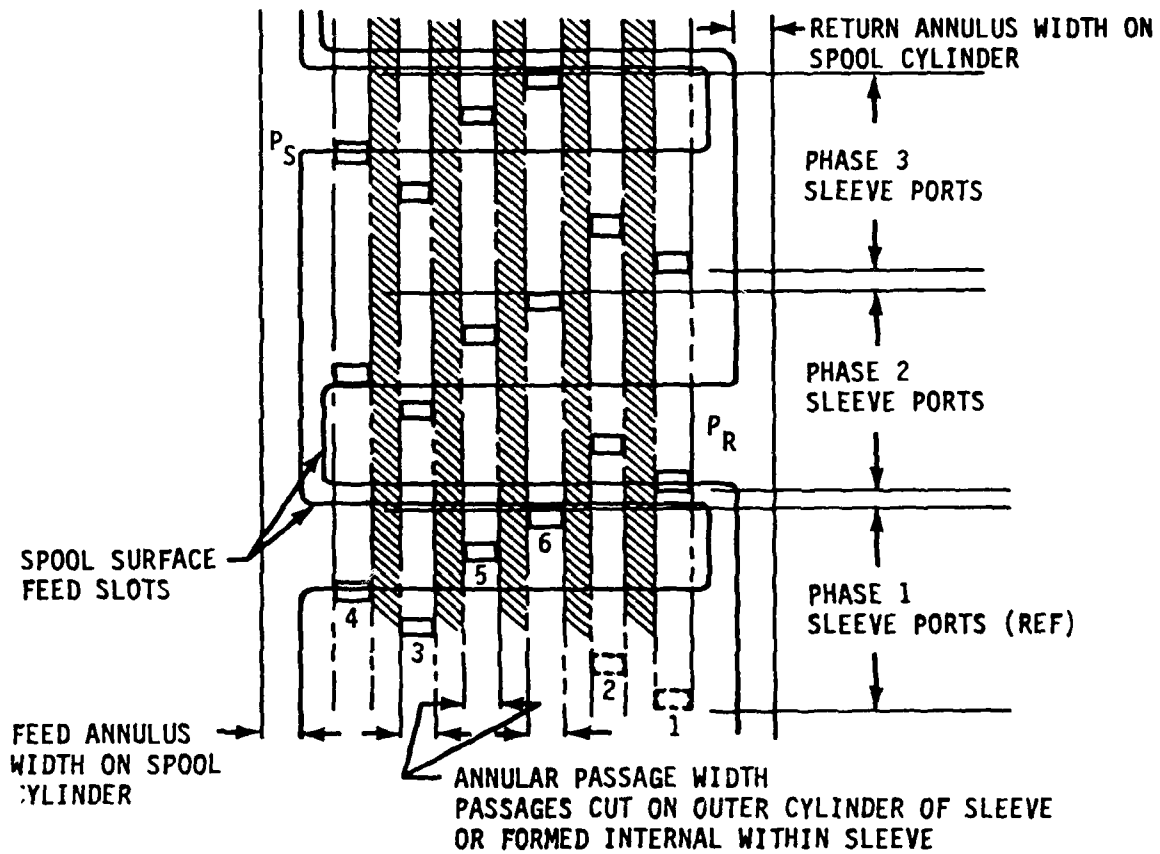


Figure 34 Four-phase valve porting geometry  
with spool slots folded together

However, the heavy shrink fit between sleeve and housing contributed to the external cracking in the housing which occurred during the test phase of the program. A better design solution would have used the alternative metering scheme shown in Figure 34 with annular passages internal to the sleeve envelope. This would have allowed a slip fit to be employed between sleeve and housing, with housing and sleeve keyed together, and housing passages drilled from the housing quill tube recesses directly to the mating sleeve ports drilled in the sleeve normal to the sleeve centerline. The original Bendix sequential metering port arrangement could have been used with only two longitudinal feed and two return slots in the spool surface to minimize leakage area on the spool-to-sleeve interface. The leakage problem between the longitudinal surface slots in the valve rotor could have been solved by going from a four-phase to a six-phase valve. Figure 35 illustrates how this design separates the pressure and return feed slots on the spool surface. The six-phase design also solves the problem of the 3.75-deg least-bit valve rotation mentioned in Section 5.1.1 which requires an odd number of three electric stepper motor pulses to move the valve for a least-bit equivalent rotation. With a six-phase valve, the least-bit rotation would be 2.5 deg which corresponds to the natural step size of the available Sigma stepper motor presently used to drive the valve.

#### 6.2.2 Valve Fabrication

The first major difficulty in the valve fabrication occurred when the original two-piece spool was assembled. The external lands of the spool mandrel (central element of the two-piece spool shown in Figure 36) were damaged during the process of pressing the mandrel into the outer sleeve of the spool element. This damage was indicated by excessive leakage between supply and return ports which occurred at all valve positions during initial testing at Bendix. An attempt was made to repair this damage by electron beam welding; but, although the leakage was reduced, it was still well outside of the specification requirement. The source of this leakage was isolated to the inward deflection of the spool tubular outer element between the slots feeding pressure to the cylinder ports. At this point, the two-piece spool design

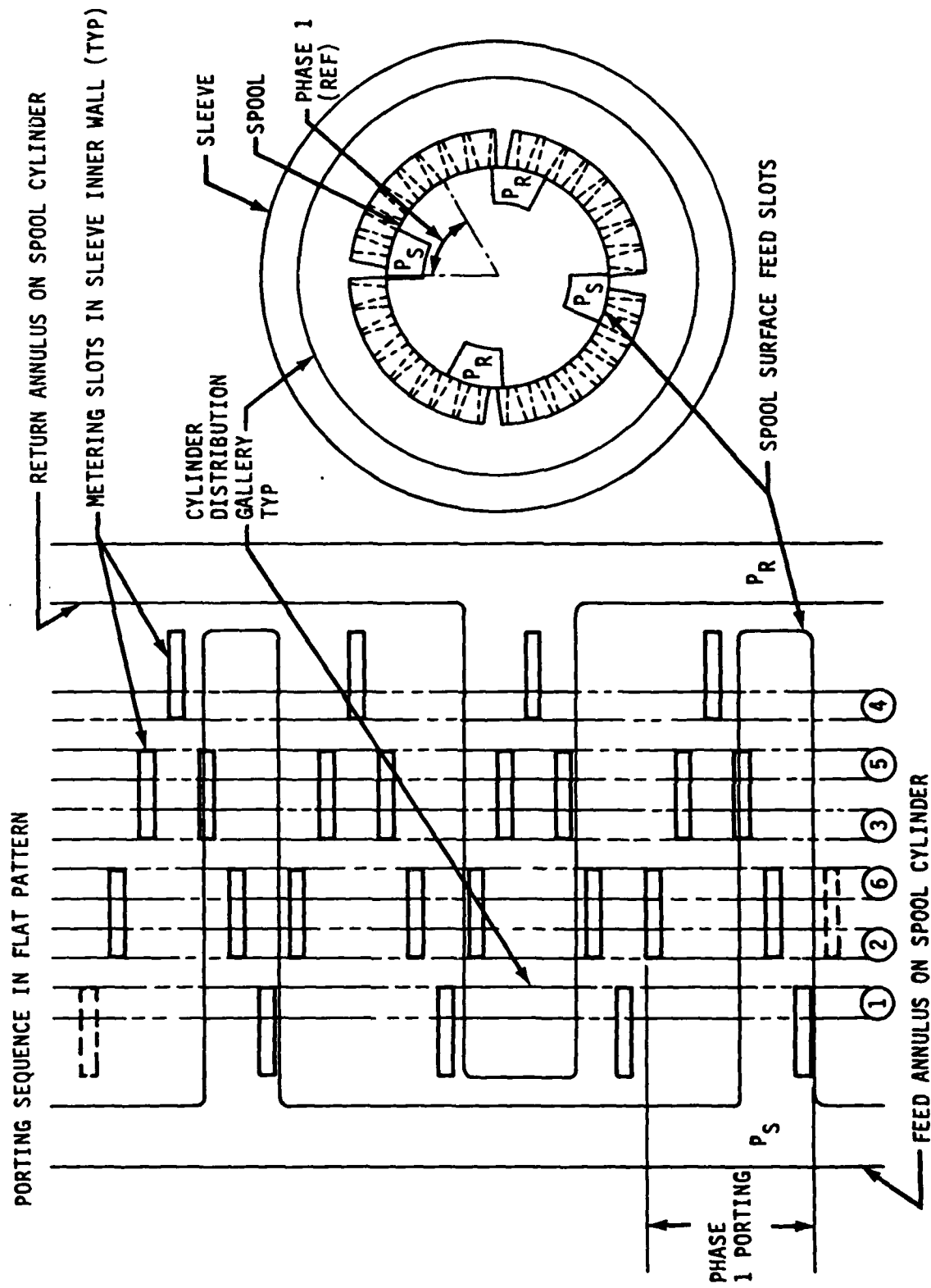


Figure 35 Six-phase spool and sleeve metering geometry

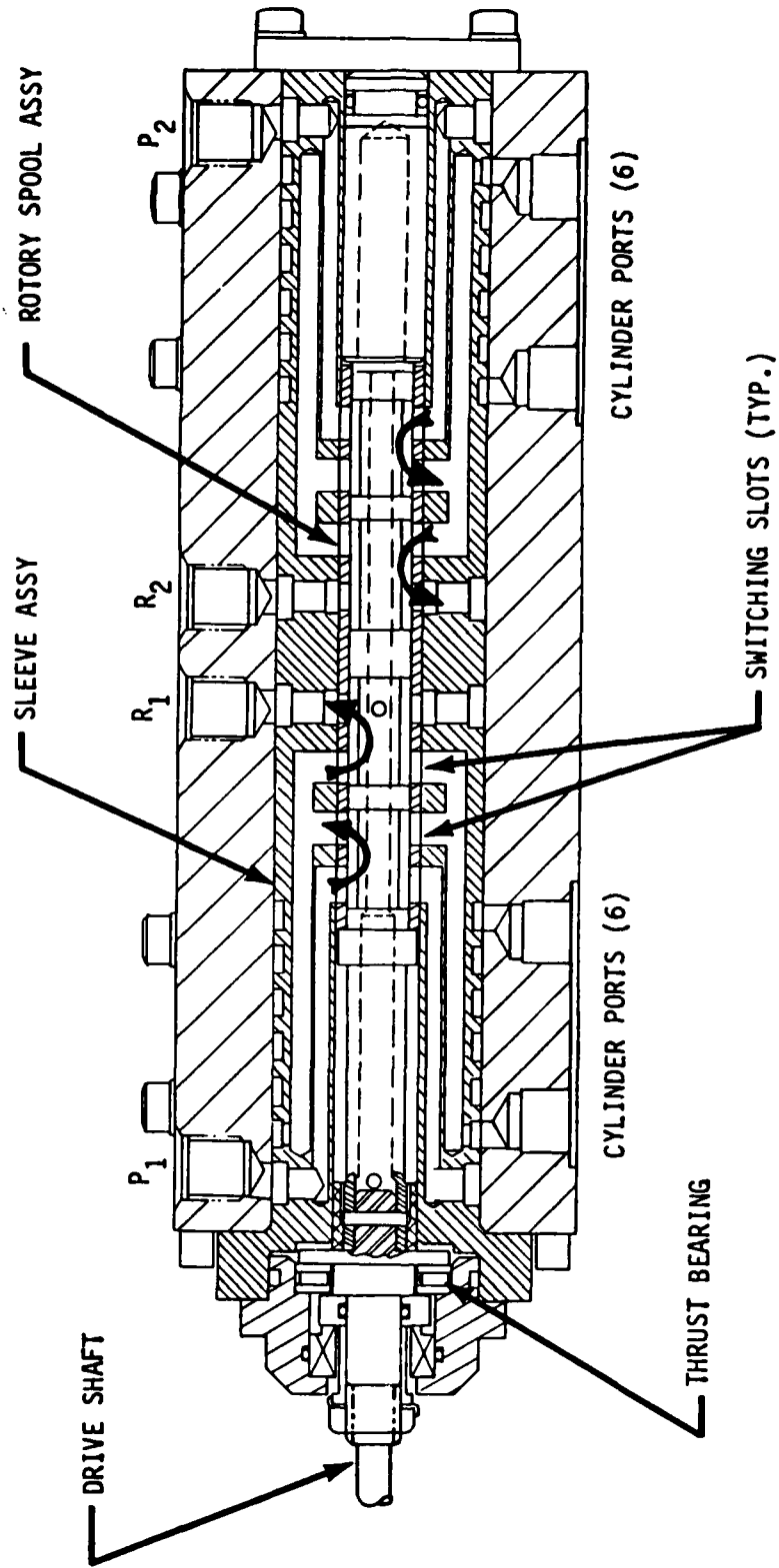


Figure 36 Hydraulic distributor valve with original two-piece spool

abandoned and a single-piece spool was machined with milled metering slots on the general plan of Figure 33 illustrated in Section 6.2.1. This valve spool was lapped to the previously lapped sleeve bore; and, the resulting leakage, although much improved, was significantly over the specified value. Average leakage was approximately 250 cc/min vs the specified value of 200 cc/min. Figure 37 illustrates some of the details of this final valve design.

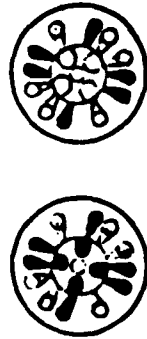
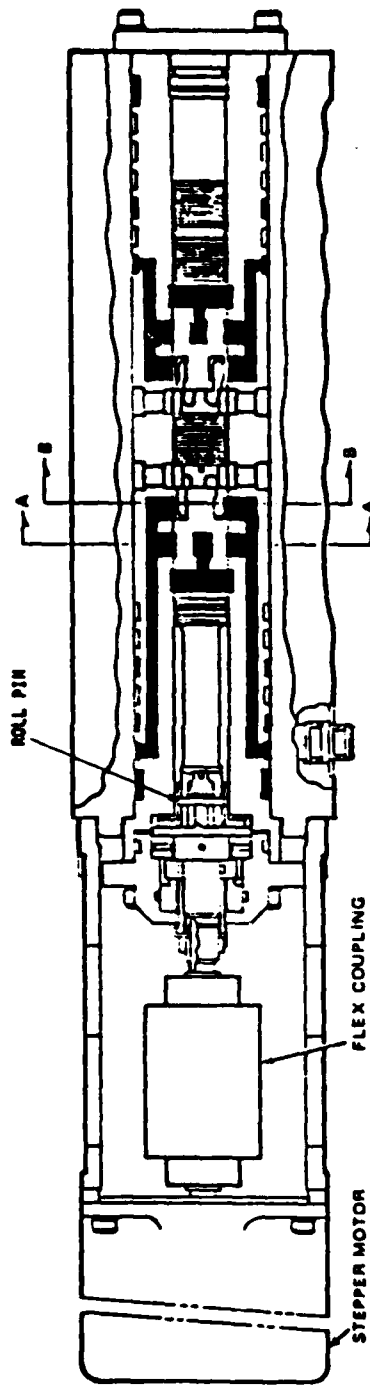
A second problem occurred which was not evident at the time of valve acceptance by Boeing for assembly into the DEHA system. A heavy shrink fit had been used to fit the valve sleeve into its manifold block. This was later verified by the existence of an approximate 0.006-in diametral bulge of the manifold block across the centerline of the sleeve. Surface stresses evidenced by this bulge are believed to have been a factor in producing a number of planar delamination cracks that formed in the area of the manifold test ports during durability and performance testing. These cracks started in the heavily stressed area of the block surface bulge and propagated more or less in a plane parallel to the block surface without penetrating to within 0.6 in of the sleeve outer wall. These cracks did penetrate into the test ports internal boss areas and made it necessary to plug five of the cylinder test ports in the valve housing during the test program to stop leakage from the cracked area between these test ports.

Early in the test program, the roll pin coupling the valve input shaft to the rotary valve spool sheared. See Figure 37. Disassembly indicated that an undersized roll pin had been placed in the pilot holes prepared for the line-ream operation of the final hole which was planned to take the larger roll pin which was intended to join the two parts. The line-ream operation was then accomplished, the larger roll pin inserted, and the unit reassembled and realigned.

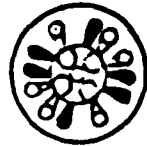
### 6.3 HYDRAULIC MOTOR

#### 6.3.1 Hydraulic Motor Design

Some difficulty was anticipated in developing a fixed-cylinder-block hydraulic motor (without the normal shaft commutated valving) which was



SECTION A-A



SECTION B-B

VALVE POSITION DEGREES	ACTUAL PORTING SEQUENCE					
	SYSTEM 1			SYSTEM 2		
	PRESSURIZED	TO RETURN	PRESSURIZED	TO RETURN	PRESSURIZED	TO RETURN
0	123	456	12	3456		
3.75	123	456	123	456		
7.5	23	4561	123	456		
11.25	234	561	123	4561		
15	234	561	23	4561		
18.75	234	561	234	561		
22.5	34	5612	234	561		
26.25	345	612	34	5612		
30	345	612	345	612		
33.75	45	6123	345	612		
37.5	456	123	345	612		
41.25	456	123	45	6123		
45	456	123	456	6123		
48.75	56	1234	456	6123		
52.5	561	234	456	6123		
56.25	561	234	456	6123		
60	561	234	56	6123		
63.75	561	234	561	6123		
67.5	61	2345	561	6123		
71.25	612	345	561	6123		
75	612	345	561	6123		
78.75	612	345	61	6123		
82.5	12	3456	612	6123		
86.25	123	456	612	6123		
90	123	456	12	3456		

- BOEING SPECIFICATION S190-99188
- BENDIX ELECTRODYNAMICS DIVISION P/N 3321109
- TYPE: ROTARY SPOOL, TWO SYSTEM, FOUR PHASE
- 12 CYLINDER PORTS ARE PRESSURIZED 4 TIMES PER REV. IN THE SEQUENCE SHOWN AT LEFT

Figure 37 Bendix stepper-driven rotary distributor valve

required by specification to have a break-out operating friction lower than any known motor of that type. In addition, it was specified that the motors be capable of surviving a 750-hour endurance test under a load and speed cycling schedule similar to that outlined in Table IV of MIL-M-7997B.

Boeing in-house studies identified the types of motors which would yield low starting friction, a compact small diameter envelope, and exhibit adequate durability. These designs fell into three general types.

a. Type I Motor

This motor is a close mechanical equivalent of a Sperry Vickers bent-axis rotary-block motor. An antifriction bearing supports the non-rotating element of the swash cam which is anchored to the case by a universal joint. Individual universal-ball-jointed piston rods connect the pistons to this swash-cam non-rotating member as shown in Figure 38.

b. Type II Motor

This type of low-friction axial-piston motor has long pistons supported in bores on either side of the non-rotating swash-cam element which is supported from the rotating cam by a system of antifriction bearings. Pistons are attached to radial pins in the non-rotating cam element by individual universal joint devices as shown in Figure 39.

c. Type III Motor

This third type of motor has long pistons supported in bores on either side of the swash cam which in this case is a rotating element. Flat-faced rotary piston shoes are trapped between the two sides of a piston slot and the swash-cam disc. This type of motor fits into a much smaller diameter cylindrical envelope than the designs of the other two types. See Figure 40.

These three preliminary motor designs were used as reference devices around which a single motor procurement specification was written. Proposed motor designs were received from four motor manufacturers. One design closely

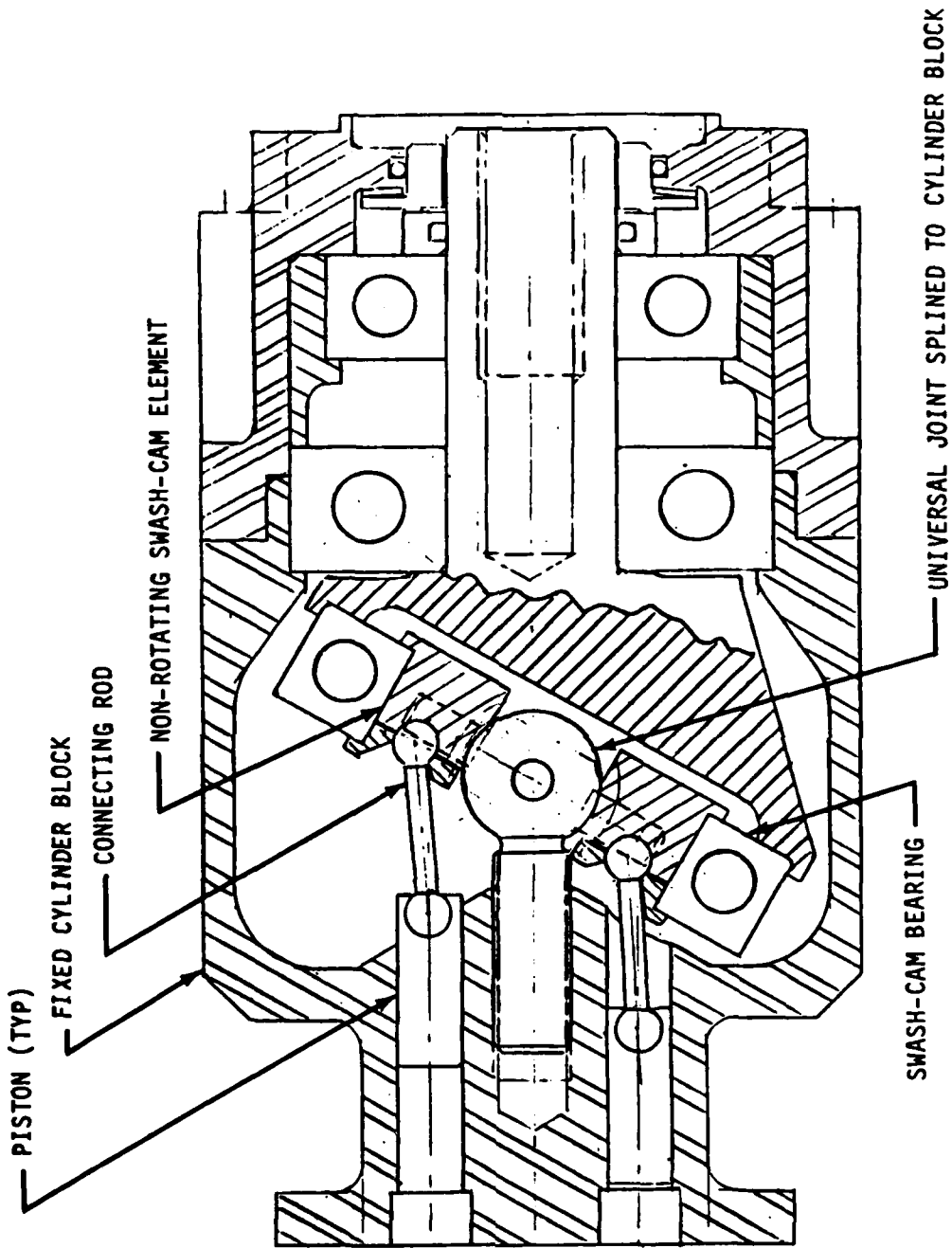


Figure 38 Thirty-degree six-piston hydraulic motor with connecting-rod coupling of pistons

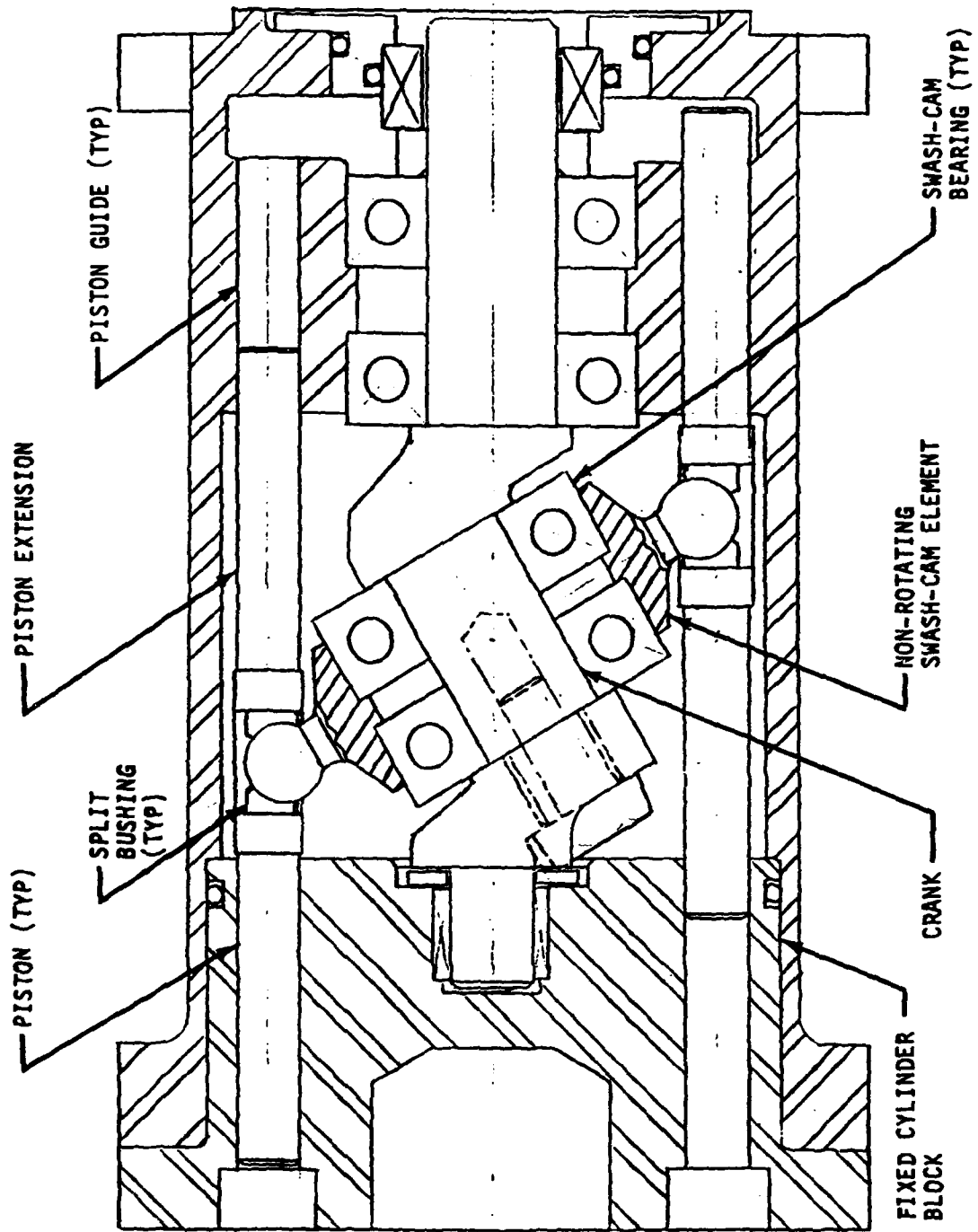


Figure 39 Thirty-degree six-piston hydraulic motor with extended pistons and guides

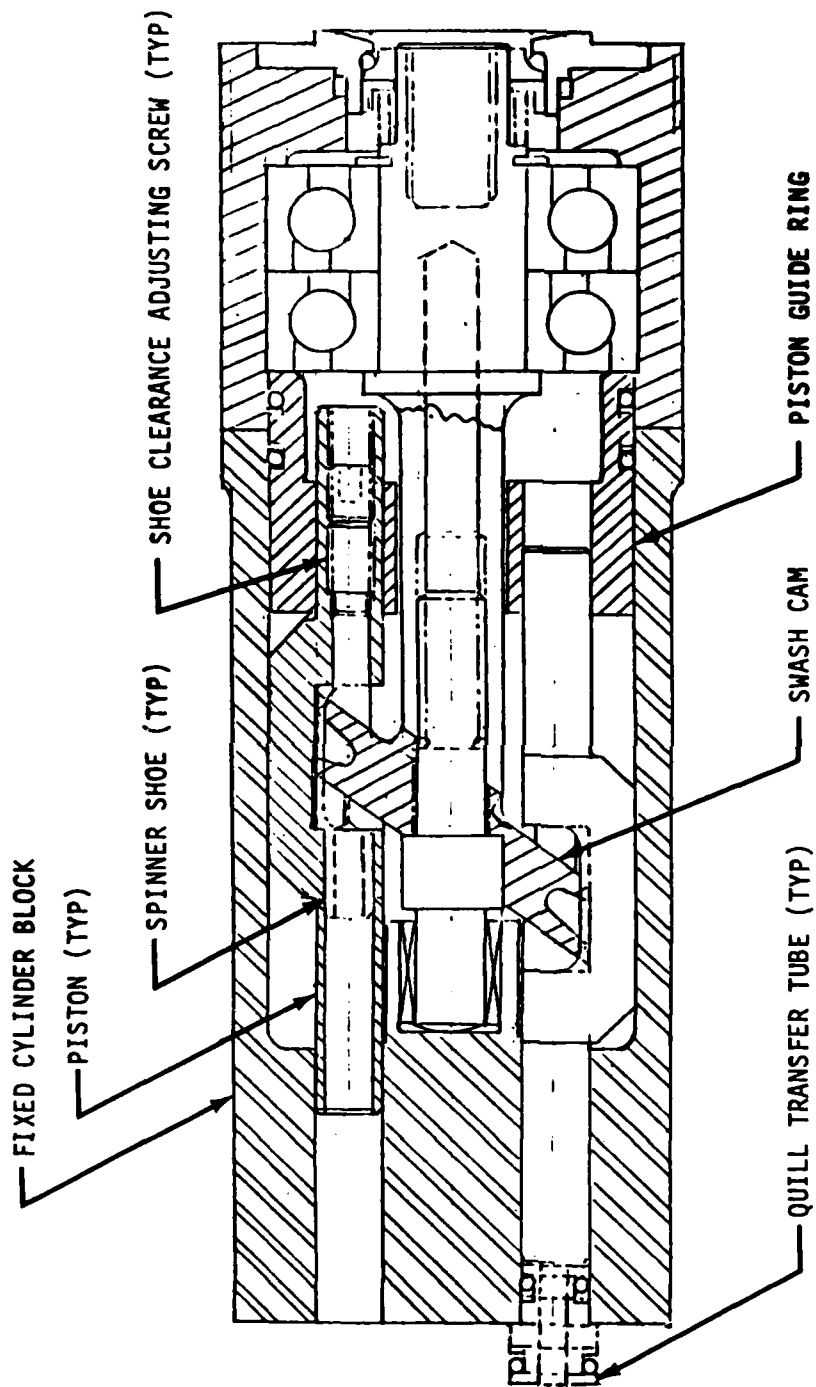


Figure 40 Thirty-five degree six-piston hydraulic motor with rotating piston shoes

approximated the Type I motor discussed in subparagraph a. This design was rated technically superior but was priced somewhat beyond the means of the DEHA program. A second basic design which was proposed with minor variation by two potential subcontractors did not use either a guided piston design or an antifriction-bearing-supported non-rotating element of the swash cam assembly. These designs were rated unsatisfactory on the basis of probable non-compliance with the specified break-away friction specification.

The third proposed motor design did not fit any of the reference types exactly. It did incorporate an antifriction-bearing-supported non-rotating cam element. Pistons were unsupported and cantilevered from the cylinder working bores. The pistons contacted the cam element on a line generated by the intersection of a conical piston end surface and the inclined plane of the swash cam element. The durability of this swash cam piston mechanism was recommended by the fact that these same parts were in current use on a production rotary-cylinder-block motor-pump. This design of the Aero Hydraulics Division of the Garrett Corporation was accepted with some lingering doubts as to the durability of the cam piston interface design. This design, shown in Figure 41, proved to be very durable; and, its break-out starting friction was well below the specified limit.

#### 6.3.2 Hydraulic Motor Fabrication

Fabrication of three new prototype flight-weight hydraulic motor units was accomplished. They met or exceeded every acceptance test requirement, and were delivered on time. Even considering the fact that many current production parts were used in their design, the performance of the contractor, Aero Hydraulics of Fort Lauderdale, Florida, was commendable.

### 6.4 TORQUE-SUMMING GEARBOX

#### 6.4.1 Gearbox Design

Once the other DEHA system variables, such as the number of motor pistons and bit count of the monitor feedback encoder, had been established,

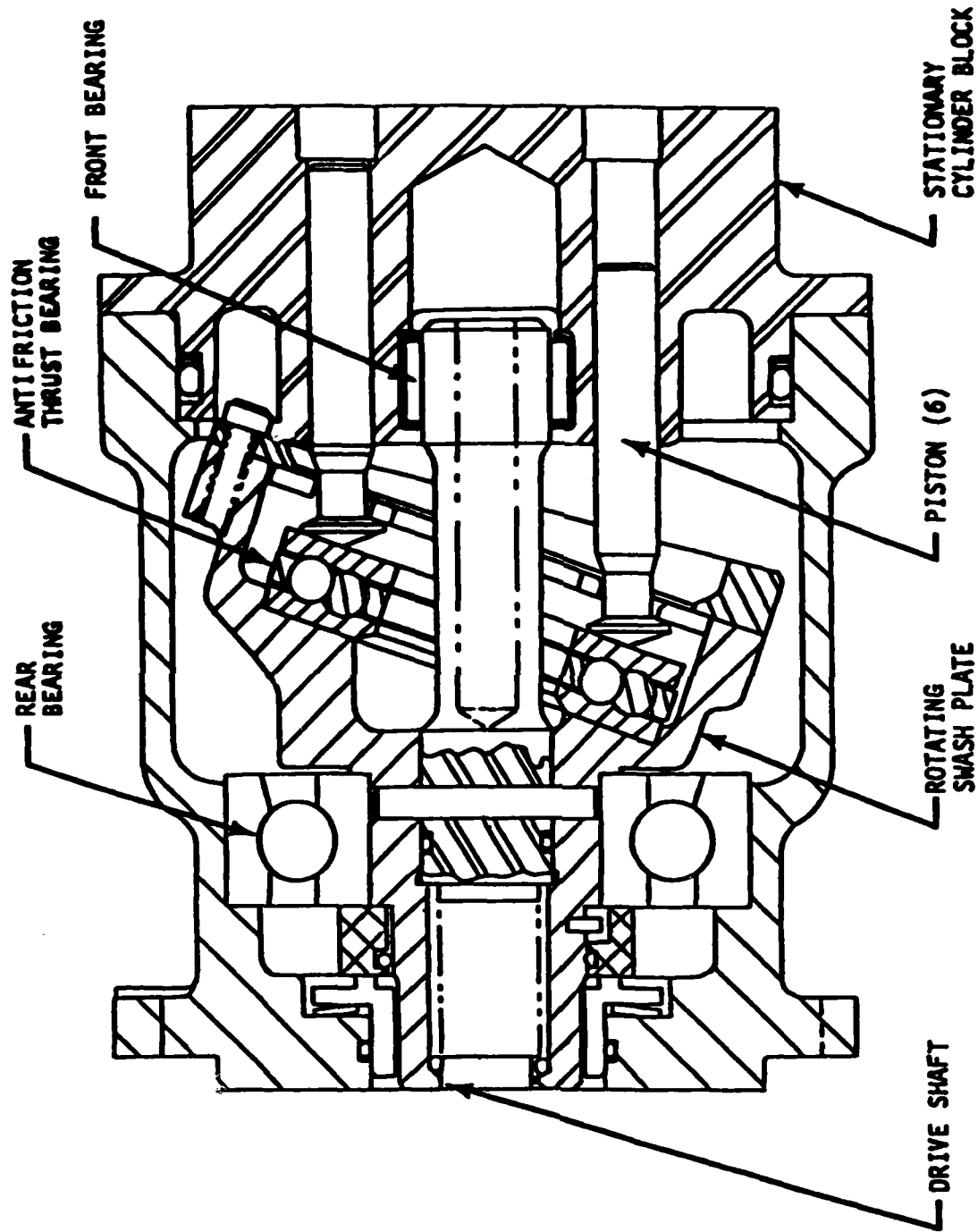


Figure 41 Hydraulic drive motor developed by Aero Hydraulics, Inc.  
for the DEHA Program

the design of the torque-summing gearbox became a routine design problem. It was necessary that a least-step of 15 degrees generated by a switch of the motor porting sequence should produce a least-bit rotation at the encoder on a ten-bit scale. With the six-piston motors which were developed under the program, the desired reduction ratio could be obtained by a 15/16 reduction ratio in the high-power output gears followed by an 1/80 reduction to the shaft input of the encoder. An available eleven-bit encoder was used to generate the desired ten-bit range in 180 degrees of rotation in order to allow the use of a standard 1/80 harmonic-drive reduction unit at the encoder drive terminal.

Helical gears of 12 diametrical pitch having 45 and 48 teeth were chosen for the torque-summing gear train connecting the hydraulic motors to the high speed output shaft which, in the F-16 installation, would drive the torque tubes linked to the power-hinge gearing. A mounting pad for a Sperry-Vickers MF 3913-30 hydraulic motor was provided in place of the output shaft coupling pad which would be used in an aircraft installation. This Vickers motor-pump unit was used as a load pump for measurement of output power transfer of the DEHA unit under load. No gearbox shaft seals were provided at either of the two hydraulic drive motor mounting pads or at the load pump mounting pad. The pad interface serves to retain the gearbox lubricant in each case.

#### 6.4.2 Gearbox Fabrication

A gearbox specification was prepared specifying the requirements summarized in Table 2 which provide the DEHA component speeds and rates shown in Table 3. Smith Williston Inc. of Seattle was selected to design and build one unit as shown in Figure 42, complete with a separately mounted lubrication unit.

The only difficulties associated with this unit resulted from design oversight in the writing of the specification and did not involve deficiencies of the performance or function of the unit.

TABLE 2 GEARBOX SPEED AND TORQUE RATIOS

	At motor-driven input shaft	At high-speed output shaft	At low-speed encoder shaft
<b>Gear Ratios</b>	$\times 15/16 =$		$\times 1/80 =$
<b>Rated Speed - rpm</b>	5120	4800	60
<b>Stall Torque lb-in</b>	188	400	
<b>Running Torque lb-in</b>	169	360	

TABLE 3 DEHA PERFORMANCE PARAMETERS

FOR DRIVING THE F-16 RUDDER  
THROUGH A 240:1 POWER HINGE SYSTEMS

PARAMETER	STEPPER MOTOR	DRIVE MOTORS	OUTPUT SHAFT	RUDDER	ENCODER
ONE OUTPUT STEP	(3) 1.25-DEG STEPS	15 DEG	14.06 DEG	0.059 DEG	0.176 DEG
TOTAL EXCURSION (1024 OUTPUT STEPS)	3,072 STEPS	42.67 REV	40 REVS	60 DEG	180 DEG
MAX. SLEW RATE	6,144 STEPS/SEC	5,120 RPM	4,800 RPM	120 $\frac{\text{DEG}}{\text{SEC}}$	60 RPM
MAX. LOAD TORQUE		*188 LB-IN	*400 LB-IN	4,000 LB-FT	

\*ASSUMING POWER HINGE EFFICIENCY = 50%

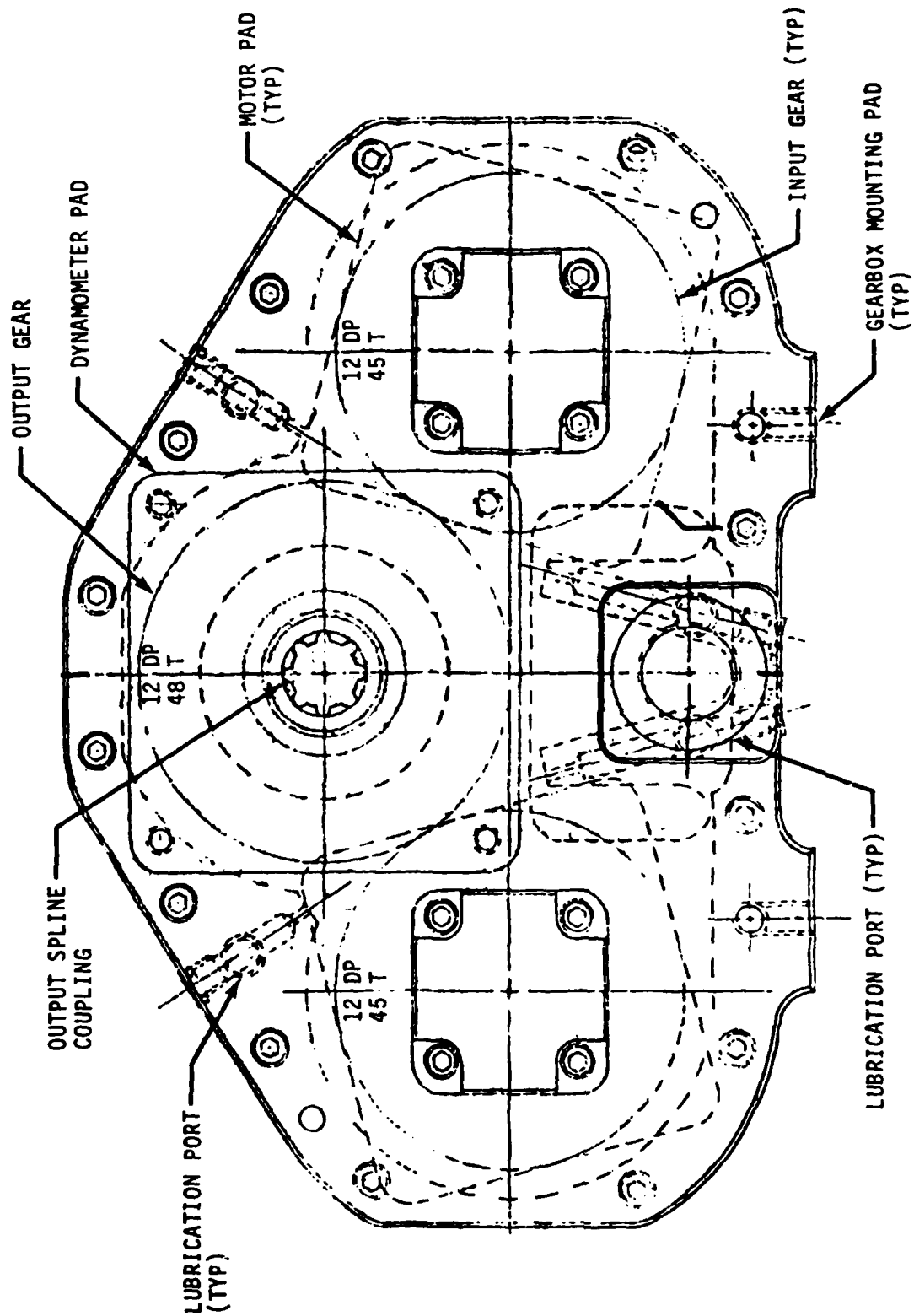


Figure 42 Torque-summing gearbox developed by Smith-Williston, Inc. for the DEHA program

One problem was caused by the lack of a phase-adjustment device between the two motor input splines. To obtain the proper phase setting, the two motors are set to the desired angles with one motor spline engaged to its gearbox input. Then, the back plate of the gearbox must be removed to allow the other motor input gear to be shifted one tooth at a time on the output gear until the second motor spline can be engaged.

A second problem of specification oversight was caused by the lack of an output shaft seal on the gear box. This requires that a special plate be provided to seal this output pad on the gearbox if it is necessary to run the DEHA unit unloaded without the load pump in place. However, by merely removing the splined quill shaft between the gearbox output shaft and the motor, with the motor left mounted on the pad, the motor acts as a coverplate to trap gearbox lubricant leakage.

#### 6.5 DEHA UNIT ASSEMBLY

An assembly drawing of the mechanical components of the DEHA prototype unit is illustrated in Figure 43. The shaft coupler which connects the stepper motor to the valve input shaft is made with collet type clamping ends. Clamping screws on these collet ends are reached through access holes in the stepper motor mounting sleeve in order to adjust valve and stepper relative alignment. Small angle adjustments of the rotary valve spool may be made with the system pressurized after the valve housing end cap, Bendix part number 3314793, has been removed and replaced with the special adjusting end cap provided by Bendix for this purpose. This special end cap incorporates an adjusting wrench which can be engaged in a slot in the end of the rotary spool and which can be used to turn the spool for angular adjustment with the No.1, and No. 2 systems pressurized.

The valve sleeve has been assembled in the valve housing manifold block with a heavy shrink fit and cannot be removed without probable damage to the sleeve and loss of proper fit between valve sleeve and spool. The valve spool may be removed for inspection by removing the stepper motor and motor mounting sleeve from the assembly. The left end-cap assembly, Bendix part

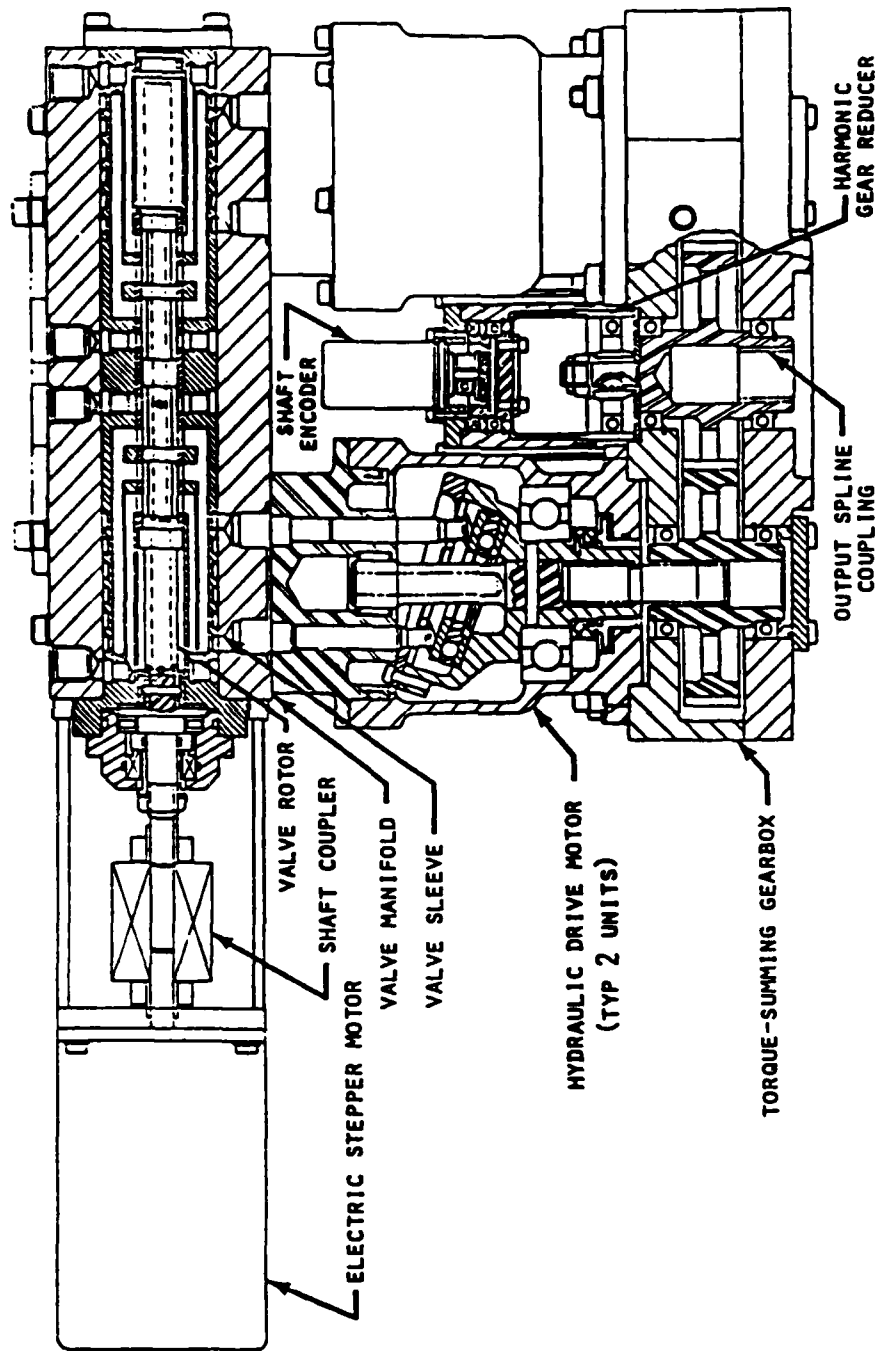


Figure 43 Mechanical components - DEHA prototype unit

number 3314788, containing the shaft seal and thrust bearing may then be removed as a unit with the valve spool by removing the four screws retaining the end cap to the valve-sleeve flange.

The valve housing manifold block may be removed from the hydraulic motor heads by removing eight 5/16" bolts which clamp the manifold to the motor heads. Quill tubes connecting the two motors to the manifold block should be kept with the individual motors. This is necessary because of the special configuration of the quill tubes used on the No. 2 motor. Quill-tube O-rings should be replaced whenever the manifold block is removed from the motors.

If hydraulic motors are to be removed from their gearbox pads for disassembly or replacement, care should be taken to note the exact installed phase angle between the two motors by noting the relative position of the pistons of each motor prior to removal of either motor from the torque-summing gearbox. The following procedure for removal and replacement of a motor is recommended to avoid loss of the phase-angle setting between motors.

- a. Remove only one motor at a time from the gearbox.
- b. Index one piston of the motor which is not to be removed to top dead center by rotating the gearbox output shaft and using a depth gage to place the two adjacent pistons at equal displacement from the motor head plane.
- c. Note the relative position of pistons in the motor to be removed so that this position may be reset before the motor is remounted on the gearcase.
- d. Remove the motor from the gearcase pad taking care not to damage the pad O-ring.
- e. Take care not to rotate the gearbox output shaft while the motor is uncoupled from the gearbox.
- f. If both hydraulic motors must be removed from the gearbox at the same time, use the method of establishing the proper motor phasing described later in this section to assemble the motors to their gearbox pads.

The hydraulic load pump unit is sealed to the gearbox pad by only a flat gasket. The load pump may be removed from the gearbox in order to remove or replace its quill shaft coupler but the load pump must be bolted in place on its gearbox pad whenever the DEHA unit is operated to prevent loss of gearbox lubricant from the load pump pad area which is not otherwise sealed off from the gearbox interior.

A number of problems which occurred during the initial assembly of the DEHA unit are described below.

A machining error was discovered in the valve manifold block when the hydraulic motor units were mated to the manifold using the original quill-tube port coupler design. The motor pilot flange recess in the manifold face was found to be eccentric with respect to the quill-tube hole pattern on the No. 2 system side of the manifold. To correct this mismatch, Bendix furnished a special set of quill tubes for the No. 2 motor coupling, with an eccentricity built into the individual quill tubes to correct for the eccentricity error in the motor indexing flange recess.

A second error was discovered when the controller electronic stepper driver was first run with the DEHA hydraulic components. The directional sense of the two identical monitor feedback encoders, one built into the controller assembly and the other on the torque-summing gearbox, were found to be of opposite sign. In order to run the monitor feedback loop of the controller on either encoder signal, it was necessary to provide for a sign change in the encoder readout when the hydraulic components were substituted for the suitcase demonstrator internal components.

A more serious error in the DEHA assembly was discovered only after the system efficiency, flow recovery and frequency response phases of the test plan had been completed. The fixed phase between the two hydraulic motor elements mounted on the torque-summing gearbox, was found to have been incorrectly adjusted during the installation of the motors to their gearbox input. The effect of this error on the test data is difficult to assess except by comparisons of system power demands; since the net combined motor

force vector rotates in a manner 15 degrees/per least-bit step, identical to that of the correctly phased system. The difference in system performance stems from the behavior of the individual motor force vectors during the stepping sequence. Operating with correct motor phasing, the two motors exhibit a separation between their motor force vectors which follows a sequence illustrated in Figure 44.

The major effect of the foregoing incorrect vector spacing would be an increase in motor net friction relative to net output torque. The motors were effectively fighting each other for part of their stepping cycle.

The following check will indicate that the motors are installed with the proper phase angle between their swash cam assemblies.

With the valve manifold removed so that motor pistons can be observed, and motors connected to their gearbox output, when viewing the motors from their shaft end in an orientation which would place the electric stepper motor to the right hand, when assembled, the right-hand hydraulic motor should be phased 60 deg ahead of the left-hand motor in a clockwise rotational sense as indicated on Figure 45. This phasing should be visible as evidenced by pistons on adjacent cylinders of the right hand motor appearing to be equidistant from top dead center at the same time when the designated No. 1 piston of the left hand motor is at top dead center.

PRESSURIZATION SEQUENCE			ANGULAR SEPARATION OF FORCE VECTORS 1 & 2
MOTOR #2	MOTOR #1		
12	123	-----	0
123	123	-----	30°
123	23	-----	0
123	234	-----	30°
	ETC.		ETC.

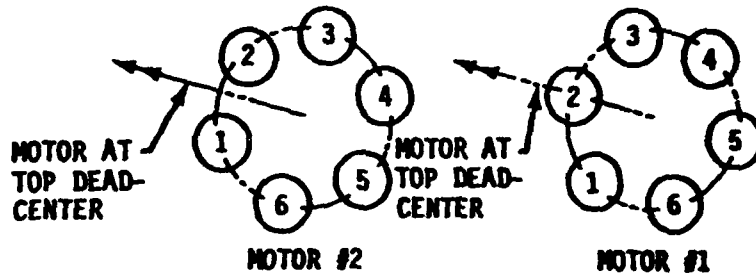


Figure 44 Intended motor phasing

The correct motor phasing was originally intended to be generated by the geometry above as seen looking into the manifold block port pattern with the stepping motor mounted on the right. However, due to a misunderstanding between Boeing and Bendix, the valve-to-manifold porting fabricated delivered the pressurization sequence illustrated below.

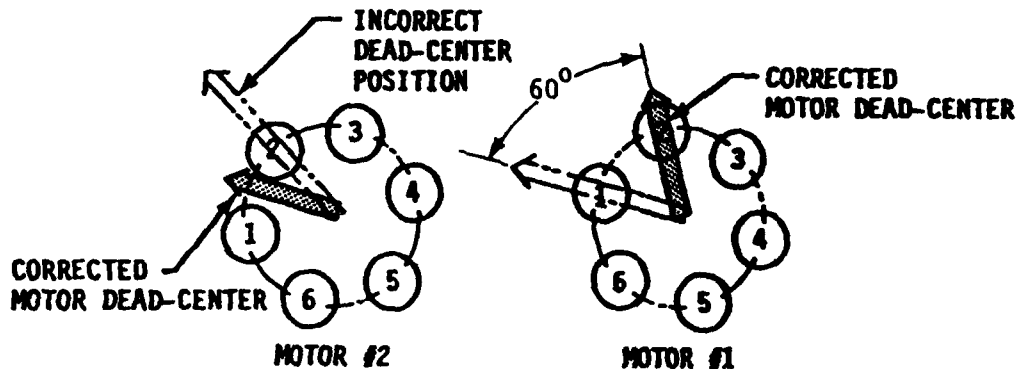


Figure 45 Corrected motor phasing

The two hydraulic motors were phased incorrectly during the initial performance tests with the motor force vectors oriented as indicated by the phantom arrows above. This phasing yielded the following sequence of relative angles between the force vectors of the number 1 and 2 motors.

PRESSURIZATION SEQUENCE

ANGULAR SEPARATION  
OF FORCE VECTORS 1 & 2

MOTOR #2		MOTOR #1	
12	----	123	60°
123	----	123	30°
123	----	23	60°
123	----	234	90°
23	----	234	60°
234	----	234	30°
234	----	34	60°
234	----	345	90°
		ETC.	ETC.

With the motor phasing corrected as described, the position of the force vectors is illustrated by the short solid arrows in Figure 45.

## VII. DEHA EVALUATION TESTING

### 7.1 COMPONENT TESTS

The following component tests were run by the three respective subcontractors prior to delivery of those units.

#### 7.1.1. Rotary Distributor Valve Tests

The following tests of the rotary distributor valve assembly, P/N 3321180, were conducted by the Bendix Electroynamics Division at their plant in North Hollywood, California.

##### 7.1.1.1 Breakaway Torque Test

With the valve filled with hydraulic fluid per MIL-H-5606, vented, and oriented with the spool stem in a horizontal position, a 3-inch diameter pulley and clamp were attached to the valve spool stem. Calibrated weights, in approximate 2-oz increments were applied to a Nylon line (wrapped on the pulley) until the spool rotated. The total weight required to initiate rotation in both directions, both immediately after pressurization to 3,000 psi and after 10 minutes high and low pressurization to 3,000 psi and 500 psi respectively, was recorded. The resulting data, taken just prior to and just after the break-in run, are shown in Table 4.

##### 7.1.1.2 Break-in Run

The valve mounted in the test setup shown in Figure 46, was run-in at 100 rpm for 40 min both in the clockwise and counterclockwise direction with the inlet ports pressurized to 500 psi and the cylinder ports and return ports blocked. The 40-min runs were made in 10-min segments alternating between the CW and CCW direction; and, the driving torque measured in those directions was 6 oz-in and 8 oz-in respectively. The runs were then repeated with the inlet ports pressurized to 3,000 psi; and, the driving torques measured in the CW and CCW directions were 6.5 oz-in and 13 oz-in respectively.

TABLE 4 ROTARY DISTRIBUTOR VALVE BREAKAWAY TORQUE TEST DATA

Breakaway Torque (oz-in) Taken Before Break-in Run

Direction	Immediate at zero pressure	Immediate at 500 psi	After 10 min at pressure of 500 psi	Immediate at pressure of 3,000 psi	After 10 min at pressure of 3,000 psi
Clockwise Rotation		28.8 26.4	28.8 26.4	21.6 21.6	21.6 21.6
Counter clockwise Rotation	33.6	28.8 28.8	28.8 28.8	21.6 19.2	21.6 21.6

Breakaway Torque (oz-in) Taken After Break-in Run

Direction	Immediate at zero pressure	Immediate at 500 psi	After 10 min at pressure of 500 psi	Immediate at pressure of 3,000 psi	After 10 min at pressure of 3,000 psi
Clockwise Rotation		28.8 28.8	28.8 28.8	21.6 21.6	21.6 21.6
Counter clockwise Rotation	28.8	28.8 28.8	28.8 28.8	21.6 21.6	21.6 21.6

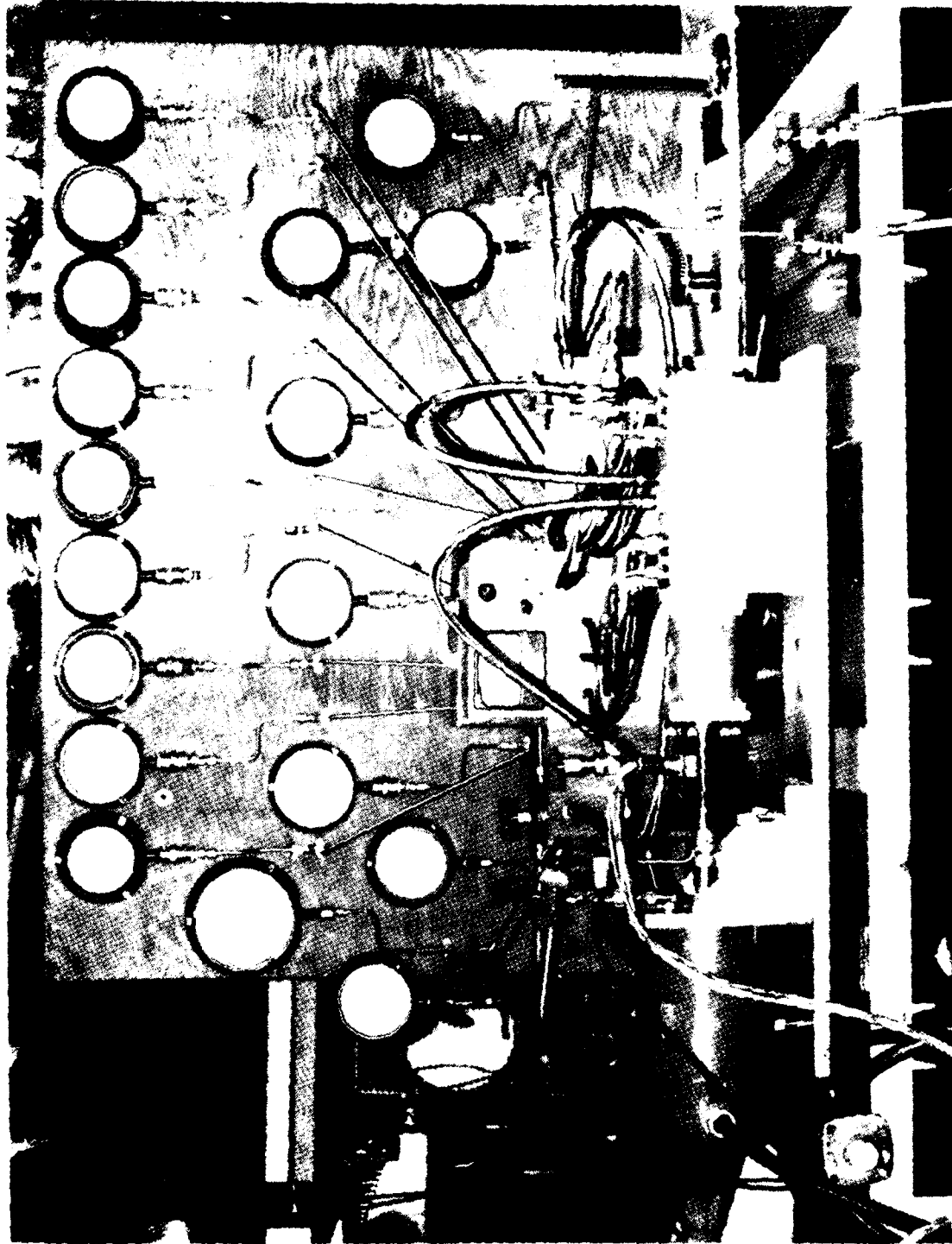


Figure 46 Test setup for motoring the rotary distributor valve

#### 7.1.1.3 Proof Pressure Tests

With the valve mounted in the test setup shown in Figure 47, the following proof pressure tests were run at the conditions noted below. The valve was then examined and found to be free of fluid leakage, except as noted in a and b below (and from the return ports in the supply pressure test). There was no evidence of failure or permanent distortion, either visually or as determined by a recheck of the breakaway torque.

##### a. Supply-Side Proof Pressure

A pressure of 4,500 psi was applied to both pressure ports with both return port open to atmosphere and all cylinder ports blocked. Then, the spool was periodically rotated in 7.5 degree increments until each of the six cylinder ports in each system had been pressurized for a minimum of one minute. The only leakage observed was a slight weepage of fluid from the end cap.

##### b. Return-Side Proof Pressure

With the pressure on the pressure ports reduced to 2,250 psi and the return ports blocked, the 2,250-psi supply pressure was held for two minutes. Some leakage was observed from the valve stem.

#### 7.1.1.4 Leakage Tests

The following leakage tests were run, and the data taken is summarized as noted.

##### a. Internal Leakage Test

With 3,000 psi supply pressure applied to both pressure ports, the valve spool was rotated until a pressure of 1,500 psi was attained at the System No. 1: Cylinder No. 1 port (S1:C1). The spool was then rotated 5.625 deg (1-1/2 steps) CCW; and, starting from that "zero" position, leakage flow

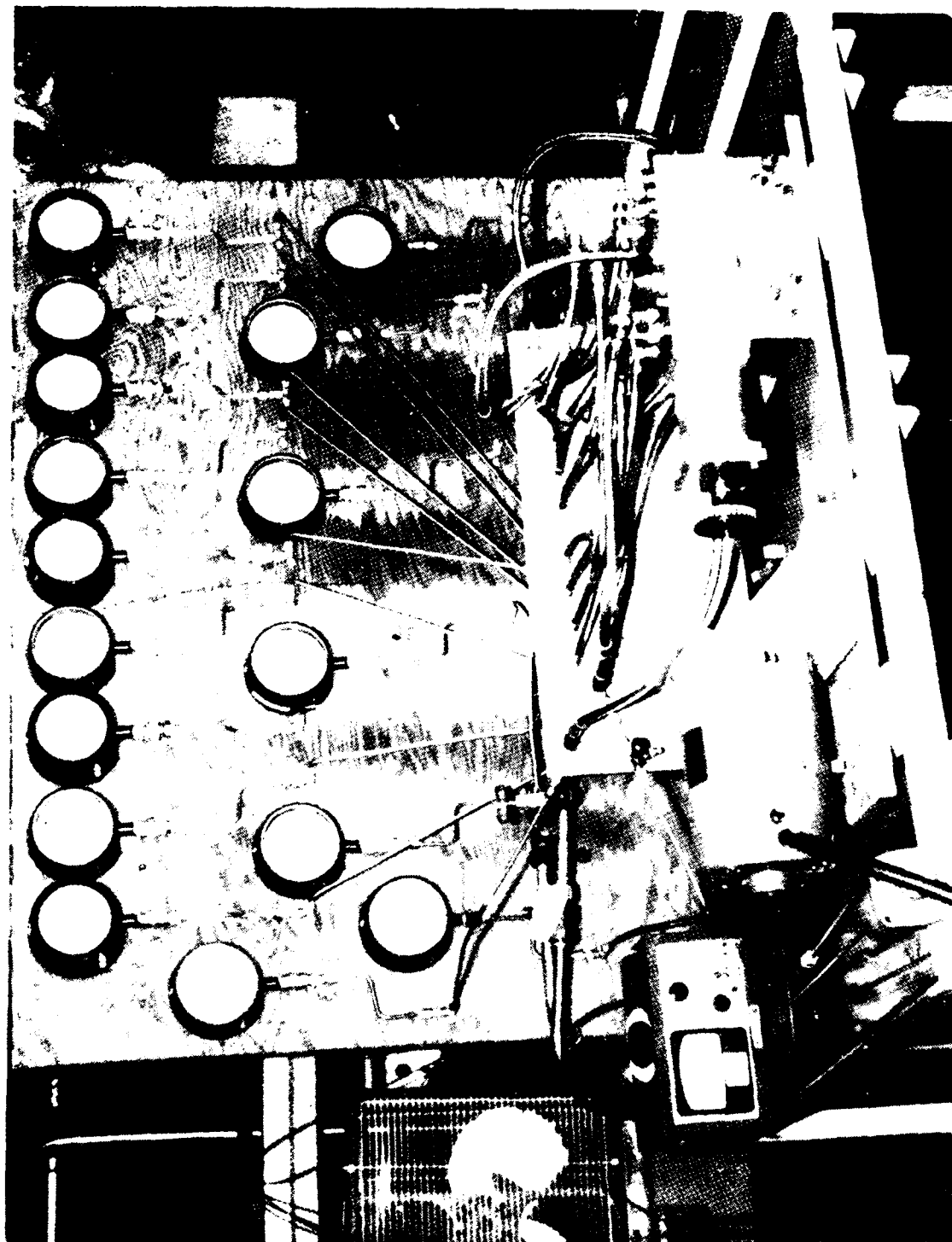


Figure 47 Test setup for hand turning the rotary distributor valve

was measured from both return ports. The spool was then rotated in 3.75-deg increments, for a total of 180 deg, and the next two high leakage points were also measured. The measured values are shown in Table 5.

TABLE 5 ROTARY DISTRIBUTOR VALVE INTERNAL LEAKAGE TEST DATA

Leakage from both return ports with 3,000 psi applied to both pressure ports at three valve spool positions as noted in Paragraph 7.1.1.4.a.

<u>System No. 1</u>		<u>System No. 2</u>	
Spool Position (Deg)	Leakage (cc/min)	Spool Position (deg)	Leakage (cc/min)

TEST WITH TWO-PIECE VALVE SPOOL

"zero"	960	"zero"	2,000
7.5	340	7.5	3,060
150	636	30	1,900

TEST WITH ONE-PIECE VALVE SPOOL

"zero"	180	"zero"	316
116.25	450	120	462
161.25	450	168.75	570

As noted in Section 6.2.2, the two-piece valve spool was abandoned after efforts to weld the leak path (caused by damage incurred while pressing the two pieces together) were unsuccessful (as seen by the excessive leakage values noted above). Although the internal leakage with the one-piece spool was considerably lower, the maximums noted above were considerably higher than the maximum allowable of 100 cc/min per system specified in the Boeing procurement specification. Nevertheless, in view of the time expended in obtaining the one-piece spool, it was decided that it would have to do; and, testing was continued.

b. Intersystem Leakage Test

With the P1 port pressurized to 3,000 psig, the R1 port pressurized to 50 psig, and the P2 and R2 ports open to atmosphere, the sum of the leakage from both ports was measured and recorded at the same "zero" position noted in 7.1.1.4.a. Then a 1/2-minute leakage sample from the P2 and R2 ports at each step (3.75-deg) position through 180 degrees was taken. After sampling, the spool was returned to the step position with the greatest leakage, and leakage was collected for 15 minutes. The recorded rate was 0.4 cc/min which was well under the 1.0 cc/min allowed.

c. Shaft Seal Leakage Test

The valve spool was driven at 650 rpm and at 1,300 rpm for one-half hour runs with 100 psi and with 600 psi applied to the System No. 1 return port. The leakage values are shown in Table 6; and, they are all below the 2.0 cc/hr maximum allowed.

TABLE 6 ROTARY DISTRIBUTOR VALVE SHAFT SEAL LEAKAGE TEST DATA

Motor Speed (rpm)	Leakage With 100 psi at R1 (cc/30 min)	Leakage With 600 psi at R1 (cc/30 min)
650	0.163	0.488
1300	0.326	0.242

7.1.1.5 Distribution Pattern Check

This test was run as a check on the angular positional accuracy with which the valve ports fluid from the two hydraulic supply lines to the six cylinder ports leading to each of the two hydraulic drive motors.

With 3,000-psi supply pressure applied to both pressure ports, the valve spool was rotated until a pressure of 1,500 psi was attained at the S1:C1 port. This was the "zero" position for this test. Then, the spool was rotated counterclockwise until the S1:C1 pressure read 2,800 psi, and the angle was recorded. The drum was then rotated clockwise, and the angles at which the S1:C1 pressure read 2,500, 2,000, 1,000, 500 and 200 psig respectively were recorded. Following that, the drum was rotated clockwise to the next step position (5.75 degrees nominal); and, the actual angle at which the pressure System No. 1 Cylinder No. 4 (S1:C4) port read  $1,500 \pm 25$  psig was recorded.

Then the spool was rotated CW for the next step position (7.5 deg), and the angle at which the pressure at the S2:C1 port read  $1,500 \pm 25$  psig was recorded. The spool was then rotated to the next step position (11.25 deg), and the angles at which the pressure at the S2:C4 port read 200, 500, 1,000, 1,500, 2,000, 2,500, and 2,800 psig respectively were recorded.

This procedure was continued for a full 180 degrees. The recorded data, plus the incremental angular errors at the 1,500-psi points, are shown in Table 7.

#### 7.1.1.6 Rated Flow Pressure Drop Test

With the cylinder ports of System No. 1 interconnected and the cylinder ports of System No. 2 interconnected, pressure was applied to the two pressure ports in amounts just sufficient to attain the specified rated flow of 9.3 gpm in each system with approximately 25-75 psig pressure at the two return ports. Those inlet pressures were measured and recorded at the spool "zero" position and at each 3.75-deg increment up to a total of 90 degrees. The resulting pressure loss data are shown in Table 8.

#### 7.1.2 Hydraulic Motor Tests

Acceptance tests of the fixed-cylinder-block hydraulic drive motors, P/N 4100363-1, were conducted by Aero Hydraulics, Inc. at their plant in Fort Lauderdale, Florida. Three motors were made, and the following tests were run with hydraulic fluid per MIL-H-5606 applied to the cylinders through a single-port fluid inlet adapter shown in Figure 48, bolted to the motor fluid end. The adapter was designed so that three adjacent pistons, of the total six, were pressurized at any one time. The test results are discussed below and the data presented in Table 9.

##### 7.1.2.1 Hand Torque Test

With the motor unpressurized, the torque required to rotate the shaft by hand with a 0-15 lb-in torque wrench was measured and the unit observed for freedom of rotation. All units were within the maximum allowance of 10 lb-in.

TABLE 7 ROTARY DISTRIBUTOR VALVE DISTRIBUTION PATTERN DATA

Vernier Angle deg	Switching System Port No. No.		Vernier Angular Position - deg For These Cylinder Port Pressures							Error Angle deg
			200	500	1000	1500	2000	2500	2800	
67.5	1	1	7.20	70.0	69.2	67.5	66.5	65.0	63.7	0
112.5	1	4				119.7				
157.5	2	1				163.5				
202.5	2	4	208.0	209.5	210.0	210.7	211.2	212.0	213.0	+8.2
247.5	1	2				249.5				
292.5	1	5				249.5				
337.5	2	2	341.5	340.0	339.0	338.2	337.5	336.7	335.7	+0.7
22.5	2	5				26.5				
67.5	1	3				67.5				
112.5	1	6	116.5	118.2	119.5	120.7	122.0	123.5	125.2	+8.2
157.5	2	3				164.0				
202.5	2	6				213.5				
247.5	1	4	253.0	251.5	250.5	250.0	249.0	248.0	246.5	+2.5
292.5	1	1				302.5				
337.5	2	4				339.5				
22.5	2	1	3.10	32.5	33.0	33.5	34.2	35.2	36.2	+11
67.5	1	5				69.0				
112.5	1	2				117.0				
157.5	2	5	171.2	168.7	167.0	165.0	163.5	161.7	160.0	+7.5
202.5	2	2				209.5				
247.5	1	6				255.7				
292.5	1	3	298.5	300.0	301.5	303.2	304.5	306.0	307.5	+10.7
337.5	2	6				342.2				
22.5	2	3				35.5				
67.5	1	1	79.0	77.5	76.5	76.0	75.2	74.2	72.5	+8.5

(Note: Ratio of Vernier Angle to Actual Valve Angle = 12:1)

TABLE 7 (Continued)

Vernier Angle deg	Switching System Port		Vernier Angular Position - deg For These Cylinder Port Pressure							Error Angle deg	
	No.	No.	200	500	1000	1500	2000	2500	2800		
112.5	1	4				115.2					+2.7
157.5	2	1				165.0					
202.5	2	4	204.5	206.2	207.5	208.2	209.0	210.0	211.2		+5.7
247.5	1	2				250.0					
292.5	1	5				303.5					
337.5	2	2	352.5	349.5	347.5	346.0	343.5	341.7	339.5		+8.5
22.5	2	5				34.5					
67.5	1	3				76.0					
112.5	2	3	115.0	116.2	117.0	117.5	118.5	119.2	120.0		+5.0
157.5	2	3				164.7					
202.5	2	6				209.0					
247.5	1	4	253.2	252.0	251.0	250.2	249.7	249.0	248.0		+2.7
292.5	1	1				298.2					
337.5	2	4				344.5					
22.5	2	1	27.5	28.2	29.2	30.0	30.5	31.2	32.5		+7.5
67.5	1	5				77.0					
112.5	1	2				124.5					
157.5	2	5	170.2	169.0	168.0	167.5	167.0	166.0	165.0		+10.0
202.5	2	2				218.0					
247.5	1	6				252.0					
292.5	1	3	297.2	298.0	298.7	299.2	300.0	300.7	301.7		+6.7
337.5	2	6				347.7					
22.5	2	3				29.5					
67.5	1	1	77.2	75.5	74.5	73.0	72.5	72.0	71.0		+5.5
Zero check	1	1				68.0					
									Avg Error	+6.2	

TABLE 8 ROTARY DISTRIBUTOR VALVE RATED FLOW PRESSURE DROP DATA

Valve Position - deg		Measured Δpressure - psi						Flow - gpm	
Drum Dial angle	Valve angle	System 1			System 2			System 1	System 2
		P <sub>1</sub>	R <sub>1</sub>	ΔP	P <sub>2</sub>	R <sub>2</sub>	ΔP		
0	0	403	212	191	510	238	272	9.0	9.0
45	3.75	442	212	230	515	238	277	9.0	9.0
90	7.5	482	212	270	488	238	250	9.0	9.0
135	11.25	478	213	265	500	238	262	9.0	9.0
180	1.5	460	213	247	512	238	274	9.0	9.0
225	18.75	475	213	262	468	239	229	9.0	9.0
270	2.25	480	212	268	435	239	196	9.0	9.0
315	26.25	427	212	215	445	239	206	9.0	9.0
360	3.0	400	212	188	466	238	228	9.0	9.0
45	3.75	483	212	271	463	239	224	9.0	9.0
90	7.5	491	212	279	430	239	191	9.0	9.0
135	11.25	440	212	228	445	238	207	9.0	9.0
180	1.5	401	211	190	481	238	243	9.0	9.0
225	18.75	413	212	201	463	238	225	9.0	9.0
270	2.25	430	212	218	435	239	196	9.0	9.0
315	26.25	410	211	199	460	238	222	9.0	9.0
360	3.0	404	212	192	505	238	267	9.0	9.0

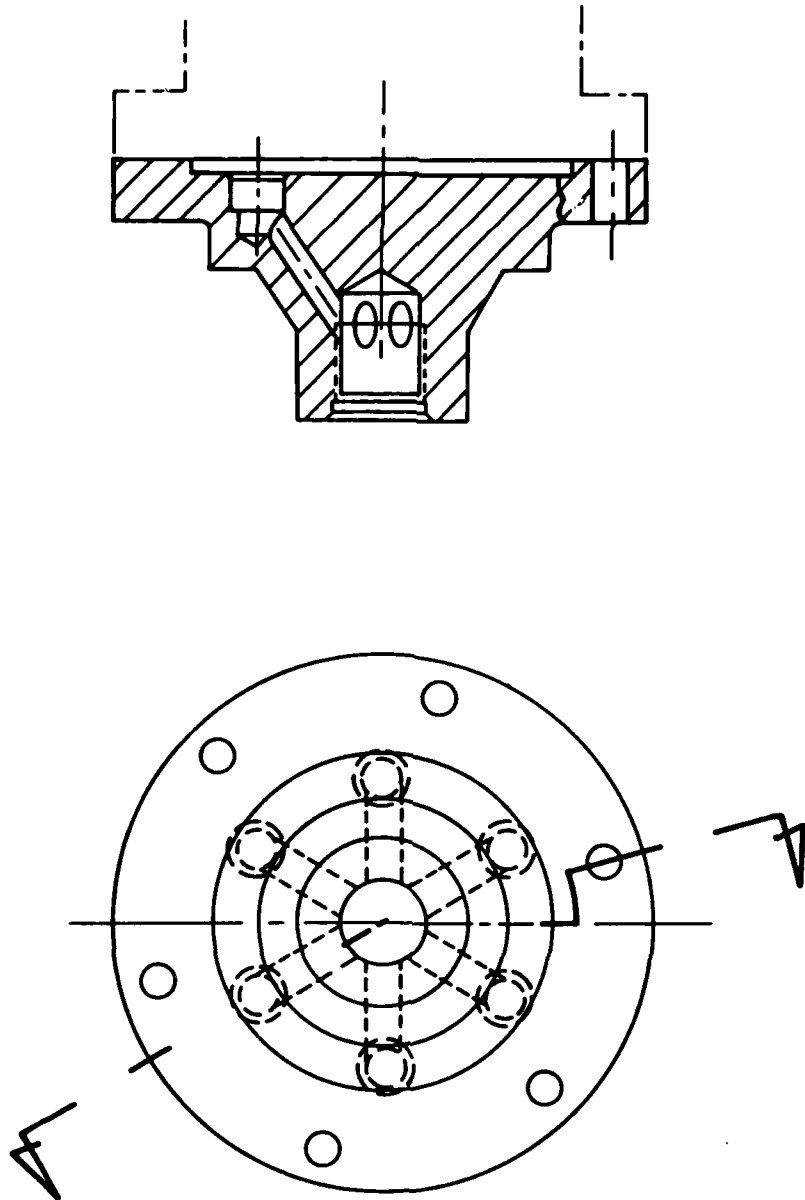


Figure 48 Hydraulic motor single-port fluid adapter

TABLE 9 HYDRAULIC DRIVE MOTOR TEST RESULTS

Motor Serial No. Test Phase	001	002	003
4.1 Hand Torque lb-in	5	7	4
4.2 Proof Pressure	Acceptable	Acceptable	Acceptable
4.3 Shaft Seal Leakage	Acceptable	Acceptable	Acceptable
4.4 Internal Leakage in <sup>3</sup> /min	1.95	1.52	6.35
4.5 Breakout Pressure psi	200	150	150
4.6 Stall torque lb-in	228	223	221
4.7 Balance	Acceptable	Acceptable	Acceptable

#### 7.1.2.2 Proof Pressure Test

A pressure of 4,500 psi was applied to the test adapter port while 900 psi was applied simultaneously to the case drain port. These pressures were held for two minutes and the motor observed for leakage. All units met the requirement of no observable leakage or weepage, except from open cylinders, and no more than one drop from the shaft seal in the two minutes.

#### 7.1.2.3 Shaft Seal Leakage

During all subsequent testing, the shaft seal area was continually monitored for leakage, and all units were within the maximum allowable leakage rate of 2 cc/hr.

#### 7.1.2.4 Internal Leakage Test

A pressure of 3,000 psi was applied to the test adapter port with the case drain port open, and leakage flow from the case port measured. The test adapter was reinstalled so that the opposite three pistons would be pressurized and the test was repeated. All units were well within the allowed internal leakage rate of 50in<sup>3</sup>/min.

#### 7.1.2.5 Breakout Friction Test

With one cylinder-port transfer tube blocked, the fluid inlet adapter was located so that only two adjacent pistons could be pressurized. Then, the motor output shaft was rotated 15 deg from the null-torque (bottom-dead-center) position, and inlet pressure gradually increased until rotation was observed. All units broke out at pressures well below the 600-psi limit.

#### 7.1.2.6 Stall Torque Test

With the fluid inlet adapter again mounted so that three adjacent pistons could be pressurized, the motor output shaft was rotated 90 deg from

the null-torque position. A torque sensor and reaction point were connected to the shaft as shown in Figure 49. Then, the inlet adapter port was pressurized to 3,000 psi and torque measured. All units provided torques well above the 188 lb-in specified minimum.

#### 7.1.2.7 Dynamic Balance

With all cylinders pressurized to 1,500 psi, the motor was mounted on a variable speed drive and driven in both directions at speeds up to the specified rated speed of 5,120 rpm. None of the motors exhibited objectionable vibration under any of the test conditions.

#### 7.1.3 Torque-Summing Gearbox Tests

The torque-summing gearbox, P/N 180-59203-1 was visually checked for leakage, backlash, and free rotation of the gear meshes by Smith-Williston, Inc. at their plant in Seattle, Washington. The assembly included the United Shoe Machinery Corporation Harmonic Drive speed reducer, P/N HDC 3C; and the Parker Hannifin, Hydra-Flex Division, lubrication pump, P/N PT7-VS2-T40-M3-1500-101, and associated accessory equipment, ie: pump motor, lubricant reservoir, flow control valves, relief valve, flow meters, and clear plastic hose lines as shown in Figure 50. The lubricant was Texaco's Rando HD-32 spindle oil with antiwear and anticorrosion additives.

### 7.2 DEHA PROTOTYPE UNIT TESTS

The following tests were run in the Mechanical Systems Laboratory at the Boeing Developmental Center, Seattle, Washington. Hydraulic power was supplied by a dedicated hydraulic power supply, which included a Denison Model 46A pump, a pressurized reservoir, and a hydraulic flow bench (shown in Figure 51) with control valves, pressure gages, and flow meters for supplying MIL-H-5606 fluid at pressures up to 3,000 psi to the test unit. A Sperry-Vickers MF 3913-30 fixed-displacement hydraulic motor was mounted on the output drive shaft pad of the torque-summing gearbox where it was operated as a load pump.

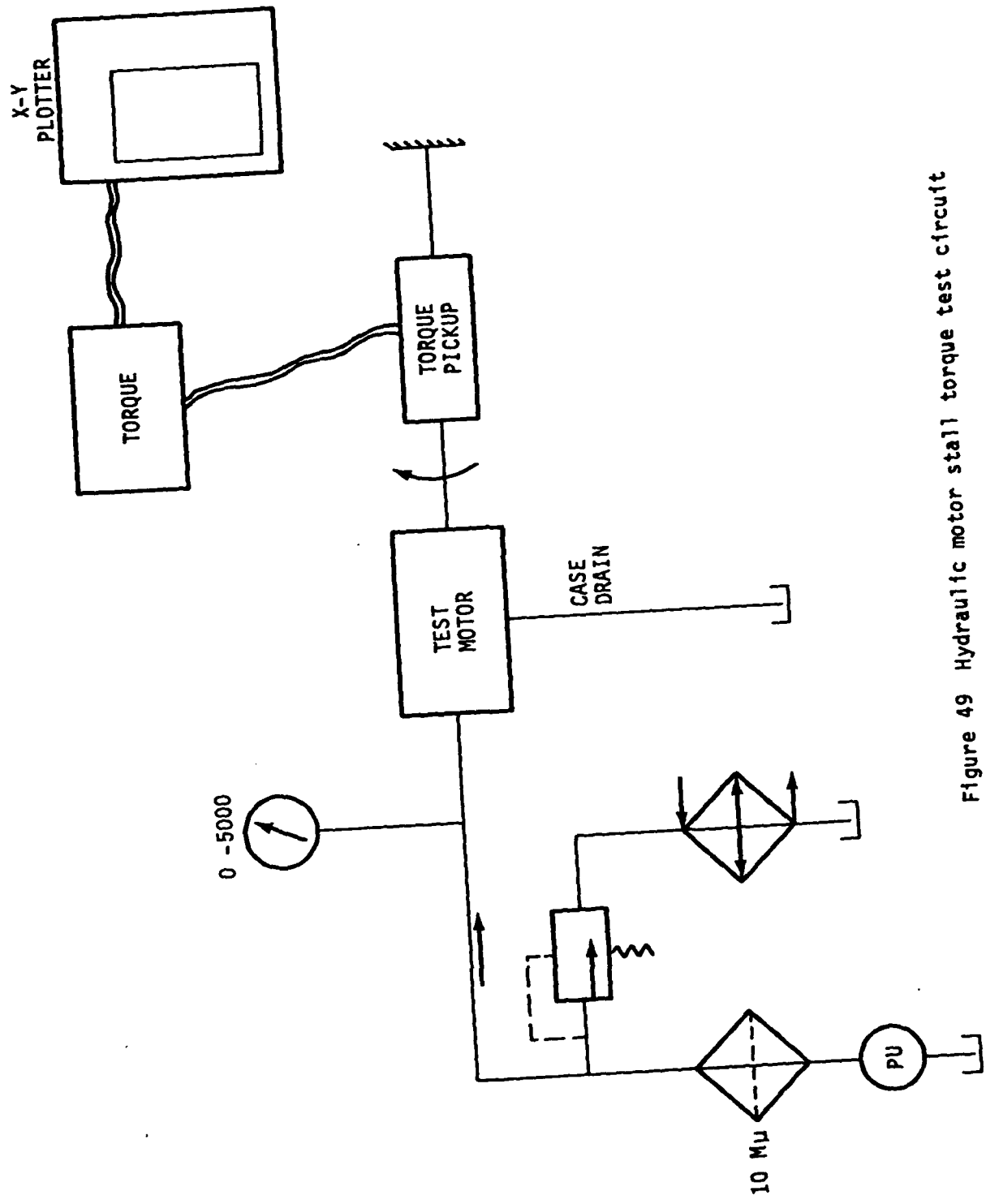


Figure 49 Hydraulic motor stall torque test circuit

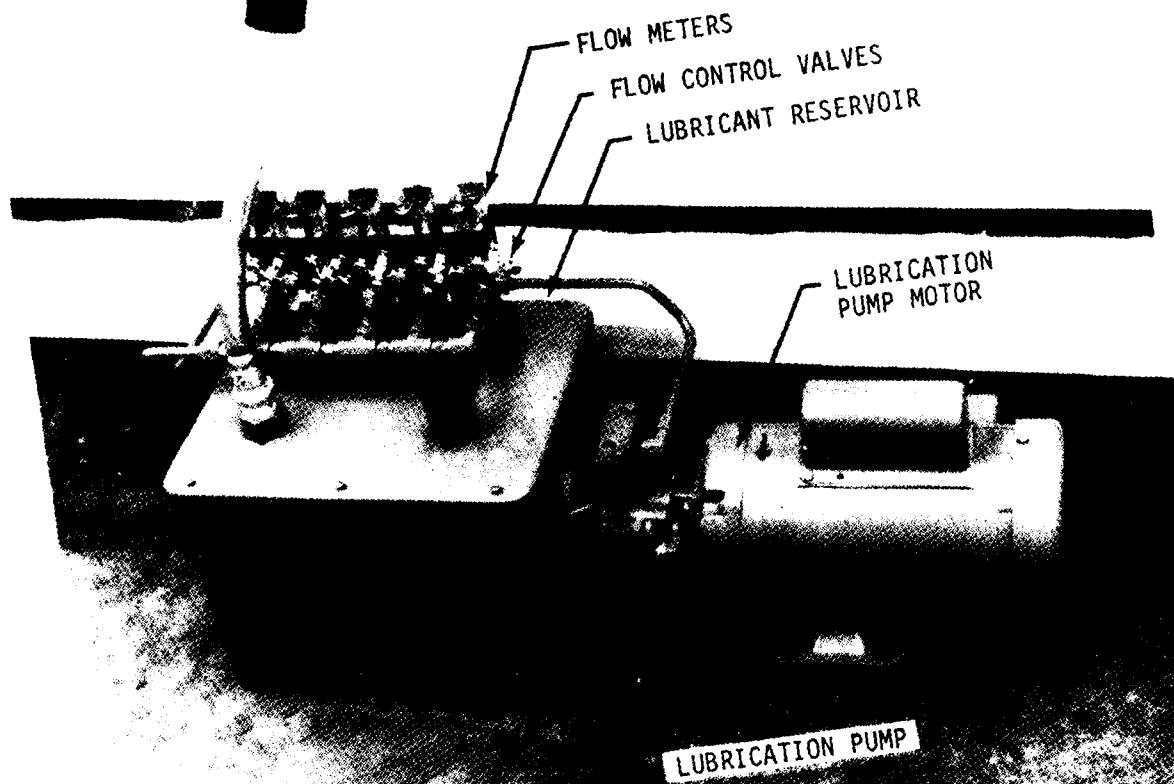


Figure 50 Gearbox lubrication pump

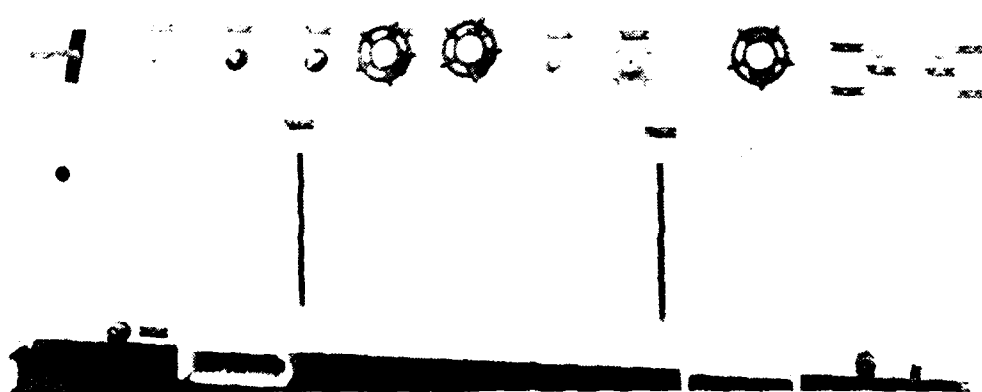
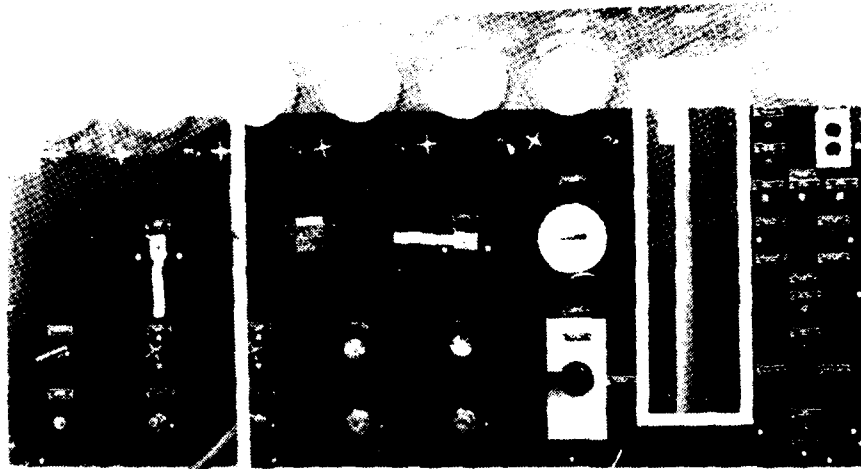


Figure 51 Hydraulic flow bench

### 7.2.1 Break-in and Functional Checkout Tests

For the following tests, the DEHA prototype unit and the load pump were connected to the hydraulic test circuit shown in Figure 52. Prior to running these tests, the encoder was aligned with the stepper motor per the following procedure.

The inlet control valves CV-1 and CV-2 were positioned to connect both pressure inlet ports of the distributor valve to the flow-bench pressure manifold, the load-pressure shutoff valves LPSOV-1 and LPSOV-2 were kept closed, and the load pressure regulators LPR-1 and LPR-2 were opened to their minimum pressure settings. Electrical input commands were supplied by a pulse generator as shown in Figure 53, which was capable of driving the stepper motor in single 1.25-degree steps in either direction upon command.

The hydraulic power supply was energized and a regulated pressure of 3,000 psi supplied to the two pressure ports of the distributor valve with the supply shutoff valve open and the alignment needle valve closed. Starting from the zero position, a series of 1.25-degree clockwise steps were made. The encoder clamp screws on the DEHA gearbox were loosened until the encoder body could be rotated, and the angular position of the encoder was adjusted until the least-bit change of the encoder occurred on the second clockwise step of the system beyond the zero mark and on every third clockwise step thereafter. Several adjustments were necessary to insure that each state change occurred on the third succeeding step. The encoder was then locked in position with the three external clamping screws.

#### 7.2.1.1 Tracking and Reversing Test

The purpose of this test was to determine if the unit would follow input commands smoothly without faltering in both the clockwise and counterclockwise directions up to its full load capability with both drive motors pressurized and with each of the two drive motors individually pressurized.

For this test, the supply shutoff valve was kept open, and the alignment needle valve kept closed. The inlet control valves CV-1 and CV-2

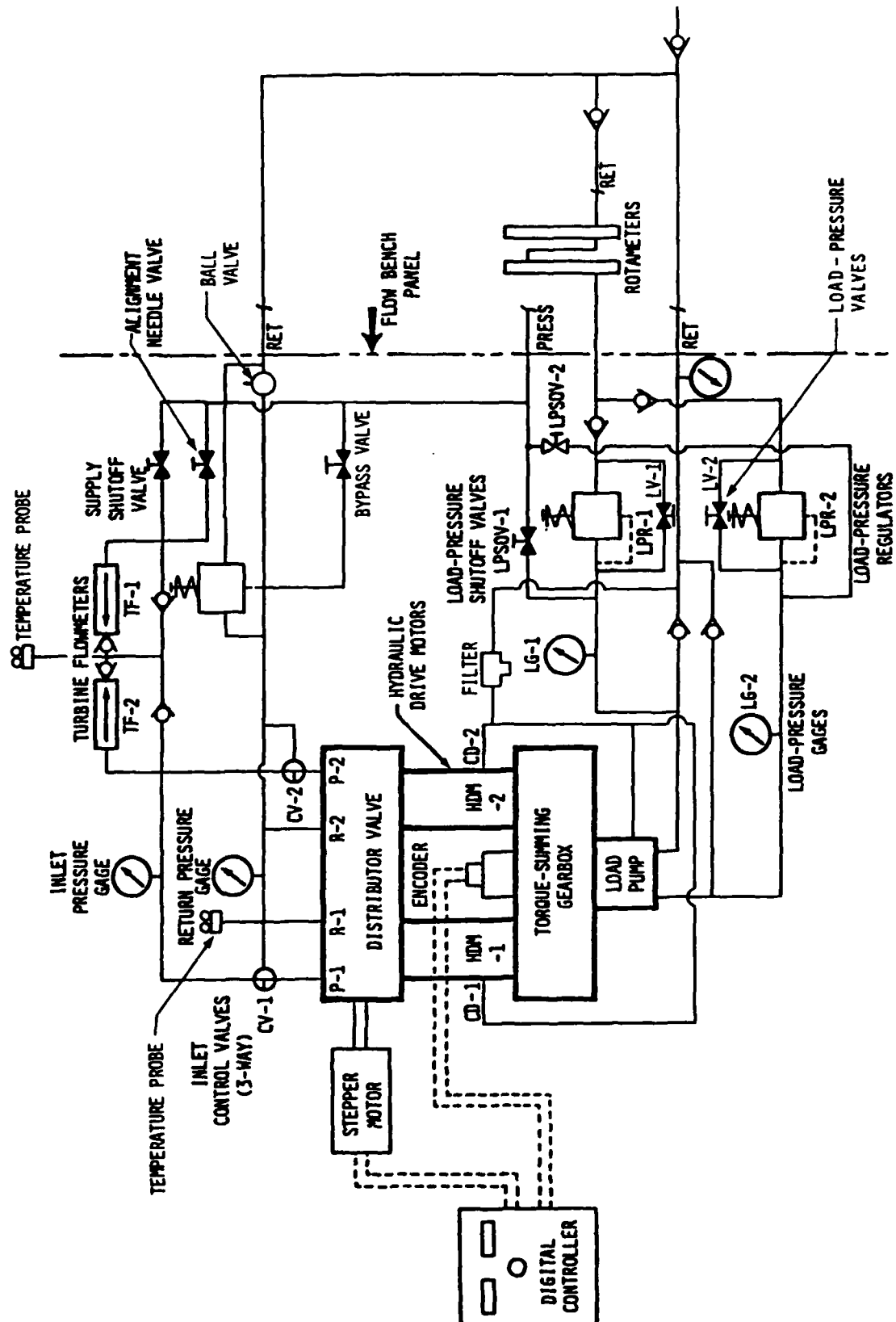


Figure 52 Schematic diagram of the DEHA performance test setup

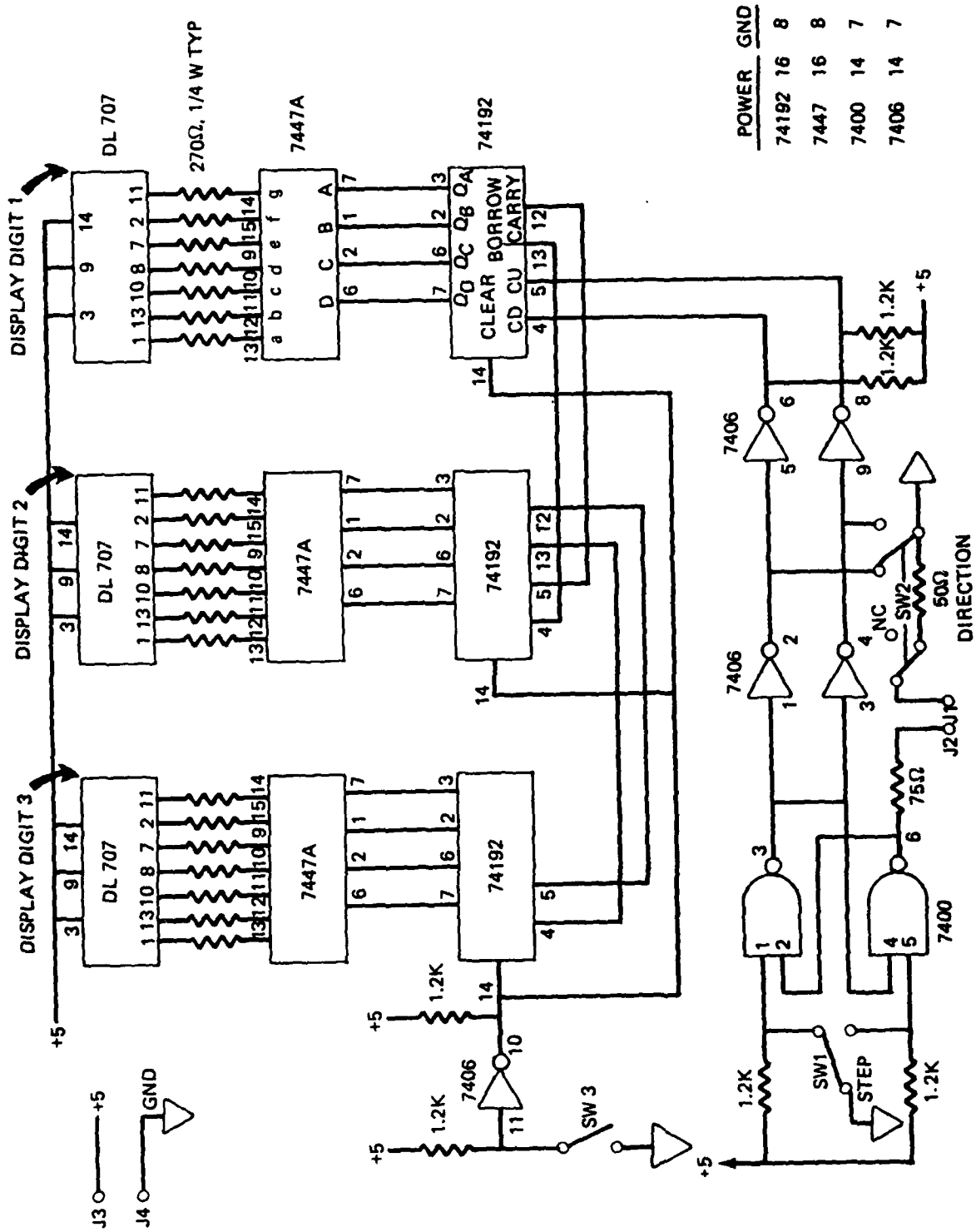


Figure 53. Electric pulse generator for single-step commands

and the load-pressure regulators LPR-1 and LPR-2 were adjusted as noted below. Electrical input commands were supplied through the digital controller by manually rotating the input potentiometer on the control panel.

The following detail procedure was used:

- a. The hydraulic power supply was energized; and, with a regulated pressure of 3,000 psi available from the pump, the inlet control valves were set to pressurize both inlet ports of the distributor valve with the load-pressure shutoff valves closed and the load-pressure regulators open to their minimum-pressure settings.
- b. Input commands were slowly applied in both the CW and CCW directions of rotation, and the encoder readout counter observed to see how well the output shaft followed the input commands. Flow readings at the flow bench rotameter and the two turbine flow meters were also observed.
- c. Load-pressure shutoff valve LPSOV-1 was then opened and adjusted along with load-pressure regulator LPR-1 to gradually increase the load pressure read on load gage LG-1. Input commands were slowly applied both CW and CCW and the encoder readout counter observed to see how well the output shaft followed at various increments of increasing load pressure. Flow readings at the flow bench rotameters and the two turbine flowmeters were also observed. The load was then increased until the stall point was reached (at approximately 2,850 psi load pump pressure).
- d. Load-pressure shutoff valve LPSOV-1 was then closed, and LPSOV-2 opened and adjusted along with load-pressure regulator LPR-2 to gradually increase the load pressure read on load gage LG-2; and, the test noted in Step c was repeated.
- e. Inlet control valve CV-2 was then set to shut off pressure to distributor valve port P-2 and connect it to the flow bench return manifold, thereby depressurizing hydraulic drive motor HDM-2; and, the tests noted in Steps c and d were repeated except that the stall-load pressure was approximately 1,400 psi.

- f. Inlet control valve CV-2 was then reset to pressurize distributor valve port P-2. Inlet control valve CV-1 was set to shut off pressure to distributor valve port P-1 and connect it to the flow bench return manifold, thereby depressurizing hydraulic drive motor HDM-1; and, the tests noted in Steps c and d were repeated again noting the stall-load pressure (approximately 1,400 psi).

#### 7.2.1.2 Slewing Test

The purpose of this test was to determine if the unit would follow input commands up to approximately one-half the maximum specified slewing rate with both one system and two systems pressurized.

For this test, the supply shutoff valve was kept open, and the alignment needle valve kept closed. The load-pressure shutoff valves were kept closed, and the load-pressure regulators open to their minimum-pressure settings. The inlet control valves were set as noted. Electrical input commands were supplied by a pulse generator capable of driving the stepper motor at speeds up to 3,000 1.25-degree steps per second (625 rpm).

The following procedure was used:

- a. The hydraulic power supply was energized; and, with a regulated pressure of 3,000 psi available from the pump, the inlet control valves were set to pressurize both inlet ports of the distributor valve. The stepper motor was then driven both clockwise and counterclockwise at each of the following speeds:

1,000 1.25-degree steps per second (208.3 rpm)

2,000 1.25-degree steps per second (416.7 rpm)

3,000 1.25-degree steps per second (625.0 rpm)

Stepper motor speed was controlled with the input pulse generator; and, the output speed compared to the input commands by measuring load pump flow with the flow bench rotameter. The DEHA output speeds and load pump flow rates corresponding to the foregoing input speeds were as follows:

Stepper Motor Step Rate	Drive-Motor Speed	Output-Shaft Speed	Load-Pump Flow-rate
1,000 sps	833 rpm	781 rpm	3.2 gpm
2,000 sps	1,667 rpm	1,562 rpm	6.4 gpm
3,000 sps	2,500 rpm	2,344 rpm	9.6 gpm

- b. The foregoing tests were repeated with inlet control valve CV-1 open to pressure and CV-2 vented to return.
- c. The foregoing tests were also repeated with inlet control valve CV-2 open to pressure and CV-1 vented to return.

#### 7.2.2 Performance Tests

Performance tests to determine the flow demand under both resisting and aiding loads, and the no-load frequency response were also run with the test setup shown in Figure 52.

##### 7.2.2.1 Flow-Demand Performance Tests

The purpose of these tests was to determine DEHA demand flow under various loads and speeds to verify the expected power saving features under low-load conditions, and to determine the rate of flow recovery when reversing with an aiding (following) load. Power efficiency and flow recovery phases of the performance test sequence were combined to produce the flow demand curves of Figure 54. These show the interaction between load in terms of load-pump pressure and speed in terms of pulse rate where each pulse represents a 1.25-degree rotation of the electrical stepper motor.

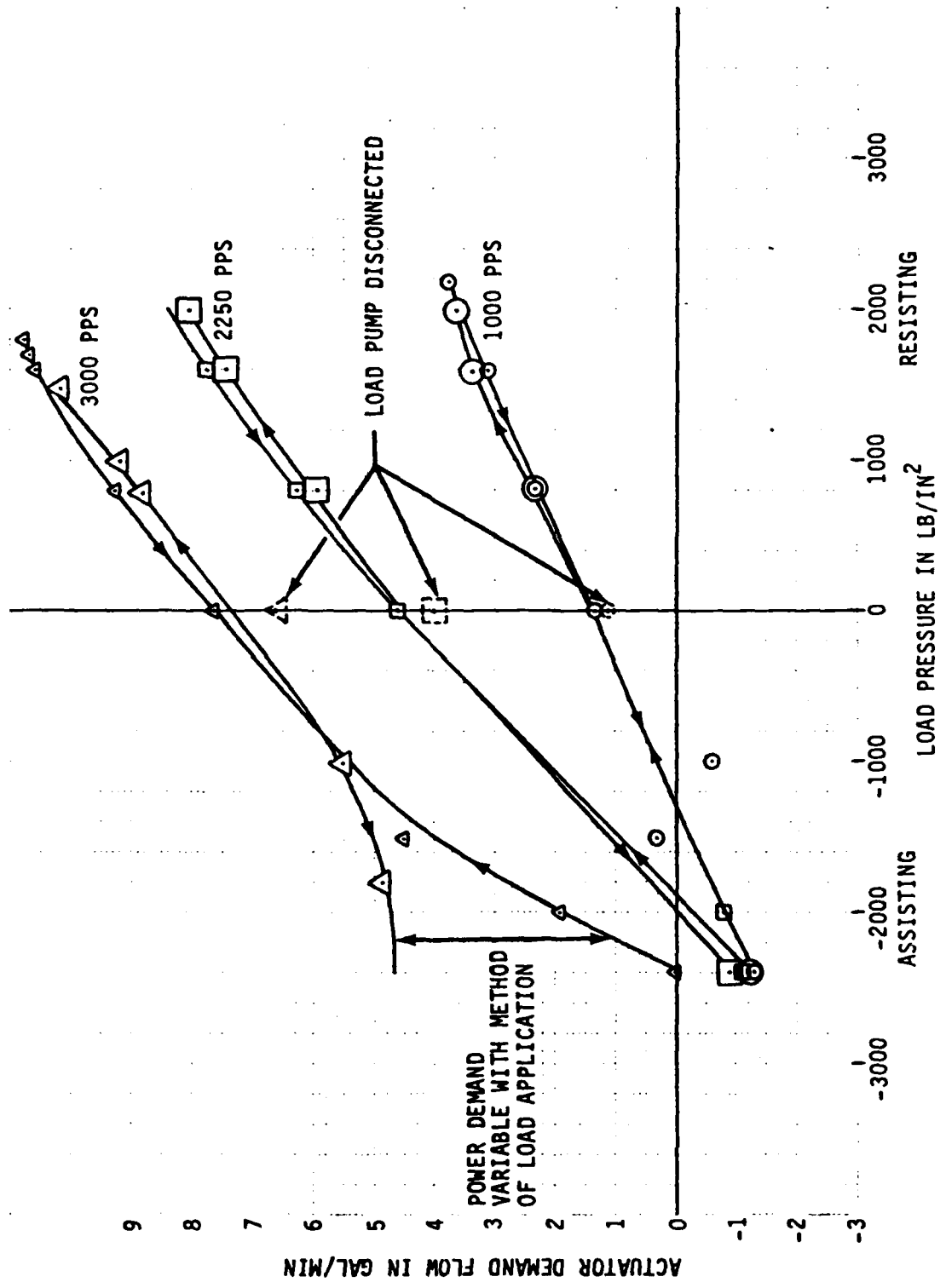


Figure 54 Flow demand performance curves

The general test procedure first set a steady output speed and then regulated the load-pressure at the load pump by manipulating the appropriate load-pressure relief valve setting. For overriding load cases, one load-pressure shutoff valve was used to supply motoring drive flow to the load pump with the pressure load-pressure relief valve used as a bleed-off regulator to control the load pump driving pressure. During overriding load runs, it was necessary to bypass the opposite regulator which was passing the load pump outflow to avoid small but significant pressure differentials which were produced by maximum flow across these load-pressure relief valves even when the valves were set to their minimum relief pressure setting.

A regulated back pressure of 200 psig was supplied to the return ports of the DEHA distributor valve to minimize the extent of motor cavitation. (Note: Some cavitation of motor cylinders is still believed to occur at the instant of cylinder pressure switching).

The test cases planned at an input rate of 2,000 pulse/s were modified to 2,250 pulse/s rate to avoid a test bench resonance which made accurate reading of gages very difficult at the 2,000 pulse/s frequency.

Early actuator demand flow tests experienced sagging inlet pressure at the DEHA distribution valve pressure ports during high-speed stepping particularly under overriding load conditions. Line flow capacity from the remotely located pressure-compensated pump supply to the DEHA test circuit was inadequate to handle the resulting high flows without unacceptable pressure drop. Increases of line capacity made by doubling line areas between the flow bench unit and the test circuit assembly were not very effective in preventing pressure loss at the DEHA inlet pressure ports. Final demand flow data was taken with the pressure-compensated supply pump set to 3,500 psig and a manual bypass used to regulate the pressure at the DEHA inlet to 3,000 psig. This single step removed most of the curvature from the demand flow curves taken earlier so that these curves approximate a family of straight lines.

### 7.2.2.2 Additional Testing to Isolate Factors Increasing Demand Flow

All flow demand data exhibited a dependence on system speed in a way which was independent of load. This dependence of flow demand on speed indicated the presence of a speed related drag torque on the drive motors or of a viscous drag associated with pressure drop in either or both of the hydraulic line systems feeding those motors or the load pump. The possibility of a viscous drag torque from the load pump or its associated line losses was eliminated by checking the zero-load points of the flow demand curves with the load pump disconnected by removing its quill shaft coupling element. The three reference points obtained in this way are shown on the zero-load axis of Figure 54. These points indicate the extent to which each flow demand curve can be moved downward to compensate for viscous type losses in the load pump. A further source of higher order drag is still indicated after this correction has been made by the fact that the curve intercepts on the zero-load axis are not located with magnitudes proportional to input speed or pulse rate.

A series of motoring tests were run to show the relative importance of distributor valve flow impedance versus drag included by friction in the DEHA motors. The total motoring drag of the unit was measured first by driving the system at various speeds (indicated by dynamometer flow rate) and measuring the load pump pressure. The DEHA rotary distributor valve was manually rotated to a position to give maximum motoring resistance from the DEHA motors during this motoring test. This test was then repeated with the motor cylinder test ports of the manifold block interconnected to effectively bypass the flow impedance of the rotary valve.

The difference between the two above sets of motoring friction data indicated that the valve impedance effect on only one of the DEHA motors contributed approximately 150 psig to the load pump pressure at a speed equivalent to 3,000 pulses/s. With both sides of the rotary valve bypassed at the motor test ports, the net motoring resistance measured by the load pump pressure was approximately 700 psig at the same 3,000 pulse/s equivalent system rate. About 400 psig of this 700 psig total could be explained by load pump total friction loss measured at the same speed.

The above results point strongly to the valve impedance flow losses as the major source of the velocity dependence of the flow demand curves. The motoring tests, being taken with the rotary valve held stationary, are not a true indicator of operating friction (velocity related) drag losses. However they do tend, by a process of elimination, to place the blame for the demand-flow velocity dependence on the flow resistance of the rotary valve which is generated during the process of switching pressure either from supply to return or from return to supply pressure.

#### 7.2.2.3 Frequency Response Test

The purpose of this test was to determine if the unit could meet the requirement specified for the F-16 rudder servoactuator, ie:

- a. With an amplitude of 2% input (peak to peak) (equivalent to a half amplitude of 0.6 degree or 10 least-bit steps of the DEFA output or 30 1.25-degree input steps by the stepper motor),
- b. and a frequency of 24 radians per second (3.82 Hz).
- c. the normalized amplitude ratio of the output to the input shall be less than 4.5 db, and
- d. the phase shift less than  $-90^\circ$ .

This test was also run in the test setup shown in Figure 51, with electrical input commands supplied by a Solartron EMR 1172 frequency analyzer. This analyzer is combined with a Hewlett-packard 9825 mini-computer, digital plotter, and associated software to generate the command signal, perform frequency sweeps, acquire data, and plot processed data. Additional features of the Solartron EMR 1172 are input signal bias reject, variable sample time, set sample delay time, adjustable command signal bias, and variable frequency step ratio. Figure 55 shows the frequency analyzer set up with the DEFA test system.

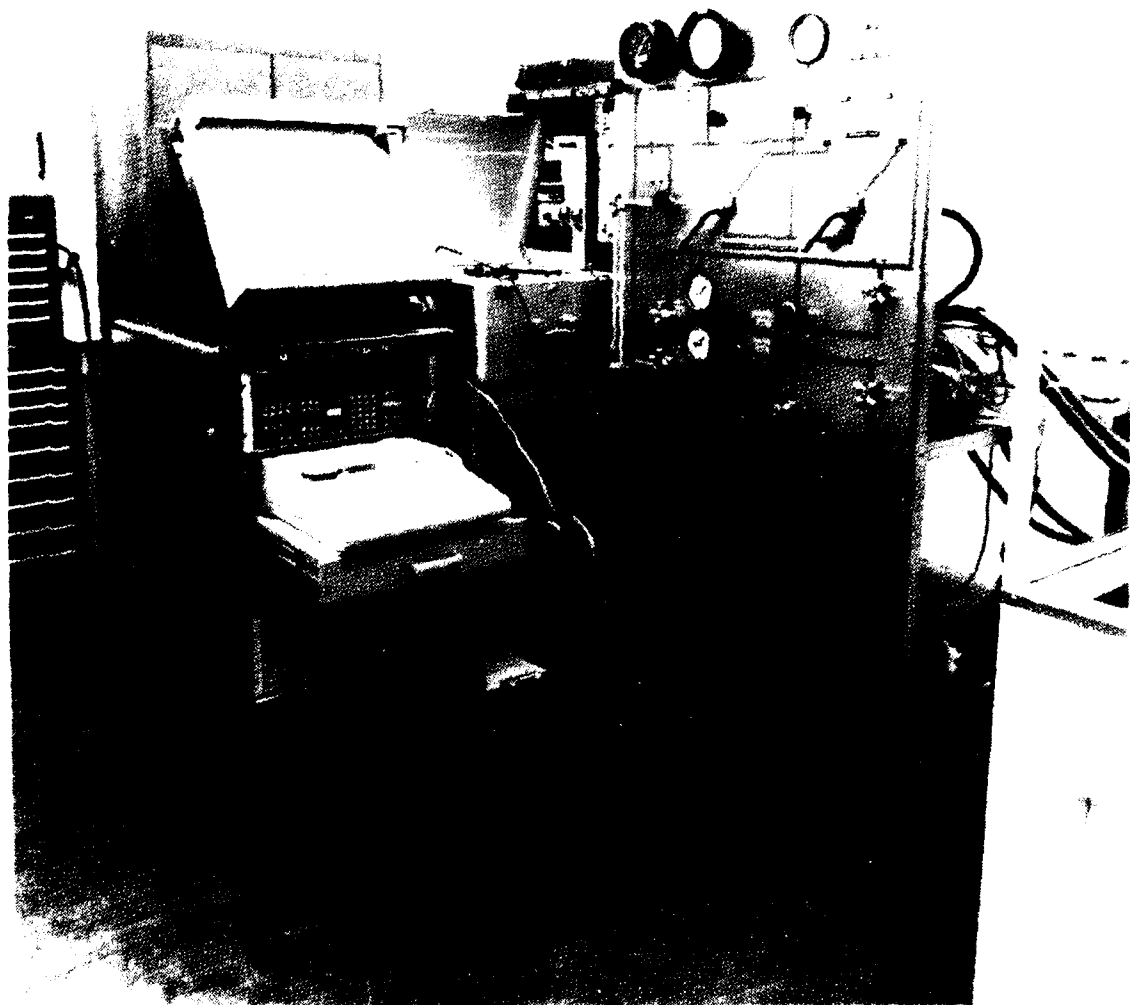


Figure 55 Solartron frequency analyzer and Hewlett-Packard mini-computer and digital plotter

#### 7.2.2.3.1 Test Procedure

The DEHA test system was set up as follows:

The supply shutoff valve was open, the alignment needle valve was closed, both input control valves, CV-1 and CV-2, were open to the pressure supply, both load-pressure shutoff valves were closed, and both load-pressure regulators were open to their minimum-pressure settings.

The frequency analyzer equipment was connected to the digital controller as shown schematically in Figure 56. Terminals on the digital controller panel were used to input the analog command signal ( $\beta_{SG}$ ) and obtain the analog encoder signal ( $\beta_{out}$ ). The other signals shown in Figure 56 were tapped at the appropriate locations in the digital controller, fed through a D/A converter if required, and connected to the frequency analyzer to obtain the transfer functions desired.

The digital controller was calibrated to determine the relation between command signal amplitude (volts rms) and the number of stepper motor command steps. The results, shown in Figure 57, indicate that 0.1 volt will give 57 command steps to the stepper motor at static (low frequency) conditions.

The specific test runs conducted and the frequency analyzer function(s) selected for each run are summarized on Table 10. Test runs beyond the basic test requirements were conducted to determine the frequency response of the several portions of the digital controller, the DEHA, and the total system. Other runs were accomplished to determine the linearity characteristics of the system.

The static gain for each transfer function obtained was checked at .05 Hz and 0.1 Hz. For all cases the value obtained at 0.1 Hz was identical with that obtained at .05 Hz within the resolution of the plotter equipment.

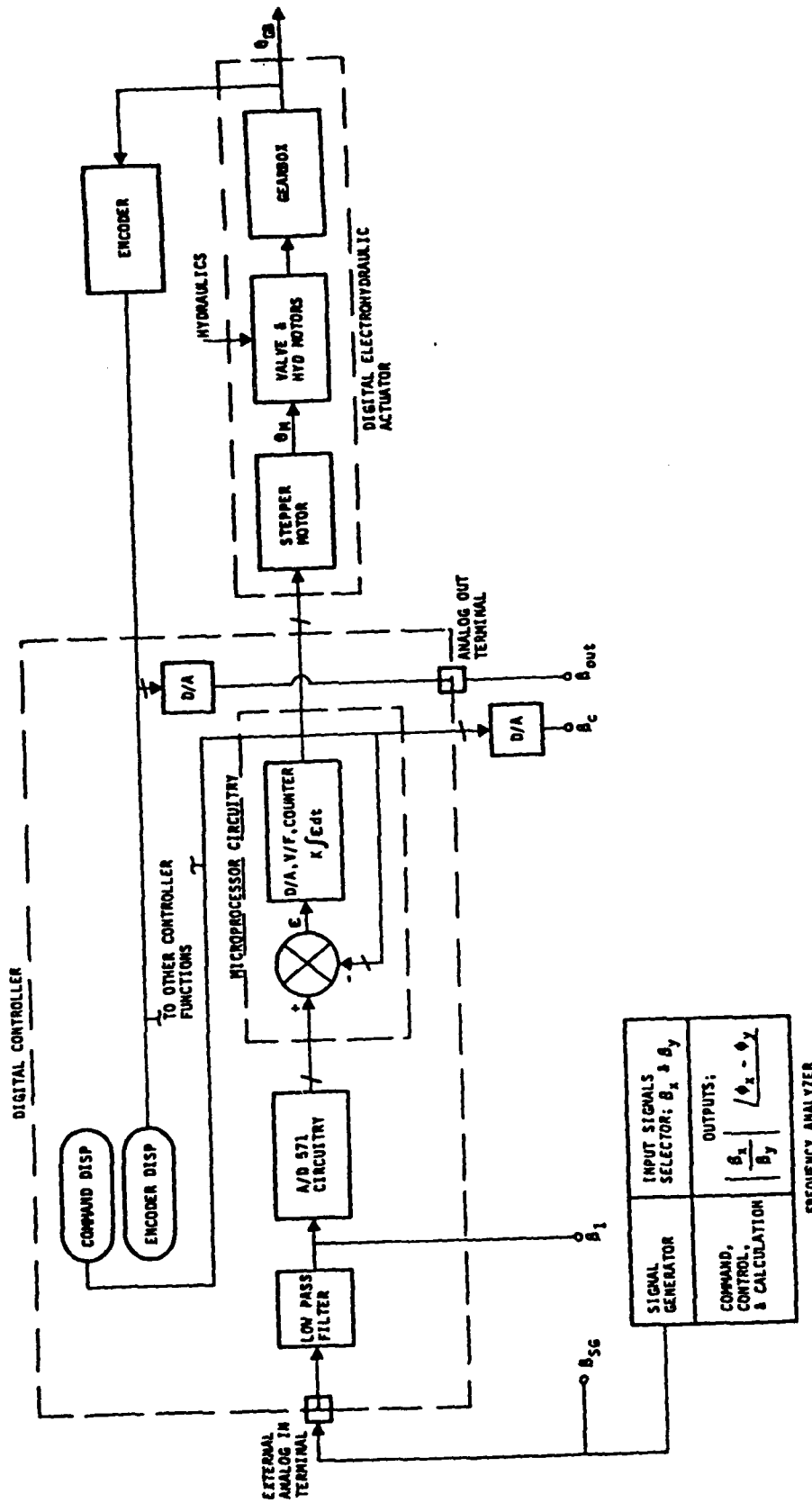


Figure 56 Frequency response test schematic

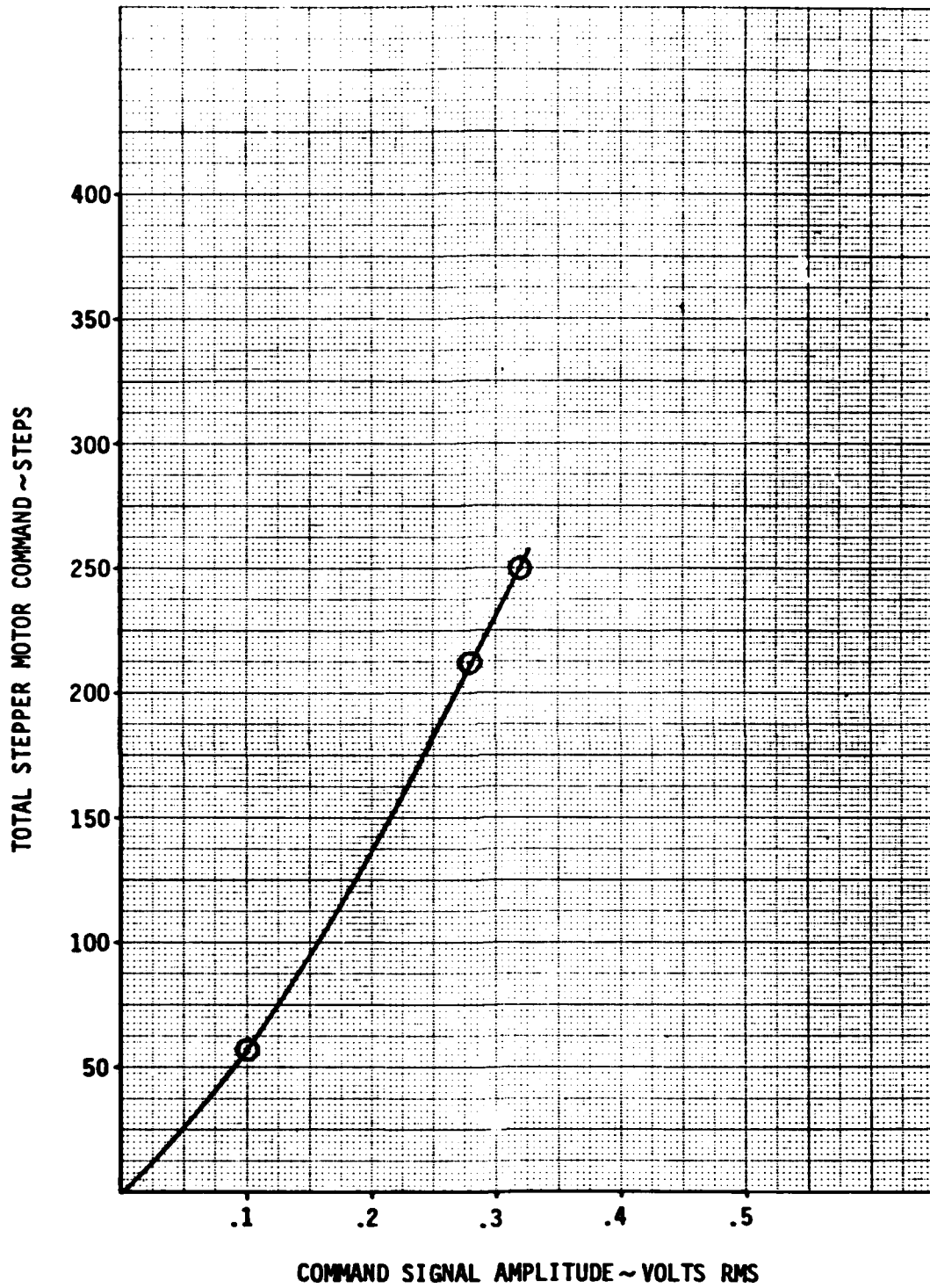


Figure 57 Static gain of digital controller

TABLE 10  
SUMMARY OF FREQUENCY RESPONSE  
TEST CONDITIONS

Test Number (Mo.Day.#)	Command Signal, $B_{SG}$ Volts RMS	Sample Delay, Sec	Command Signal Bias, Volts	Input- Reject Bias ON	Figure No.	Remarks
<u>Encoder Output/Digital Controller Input (<math>B_o/B_{SG}</math>)</u>						
5.30.1	.11	0.1	—	—	58	No filter capacitor
5.30.2	.11	1.0	—	—	58	
6.13.11	.32	1.0	—	Encoder	59	
<u>Stepper Motor Input/Digital Controller Input (<math>B_c/B_{SG}</math>)</u>						
6.13.7	.32	1.0	.40		60	No filter capacitor
<u>Encoder Output/Stepper Motor Input (<math>B_o/B_c</math>)</u>						
6.13.3	.10	1.0	.4	Encoder	61	
6.13.1	.28	1.0	.4	Encoder	62	
6.13.2	.32	1.0	.4	Encoder	63	
<u>L.P. Filter Output/Digital Controller Input (<math>B_1/B_{SG}</math>)</u>						
5.30.7	.33	0.1	—		64	
<u>Encoder Output/A/D571 Input (<math>B_o/B_1</math>)</u>						
5.30.3	.11	1.0		—	65	Filter capacitor installed
5.30.4	.33	1.0		—	65	Filter capacitor installed
5.30.5	.33	1.0		—	66	No filter capacitor
5.30.6	.33	1.0		Encoder	66	No filter capacitor
6.12.5	.28	1.0		Encoder	67	No filter capacitor
6.13.10	.28	1.0		Encoder	68	No filter capacitor One hyd motor not Line
<u>Stepper Motor Input/A/D571 Input (<math>B_c/B_1</math>)</u>						
6.12.3	.28	1.0	.40		69	No filter capacitor
6.13.4	.10	1.0	.40		70	No filter capacitor
6.13.5	.20	1.0	.40		70	No filter capacitor
6.13.6	.32	1.0	.40		70	No filter capacitor

#### 7.2.2.3.2 Frequency Response Test Results

A summary of the test runs is shown on Table 10 and the Bode plots for these runs are shown on Figures 58 through 70.

The frequency sweeps were generally from 0.1 to 8.0 Hz so that the maximum frequency would be greater than one octave above the specification performance frequency of 3.8 Hz.

The Input-Reject Bias function was used on the encoder analog signal for all runs, except the initial four, to remove the DC bias on that signal following the conversion from digital to analog mode.

A bias voltage was applied to the command signal to center the digital output signal from the microprocessor ( $\beta_c$ ) or encoder ( $\beta_o$ ) on the voltage range of the D/A converters. This was done to prevent generation of a discontinuous sinusoidal signal by the D/A converter.

After several test runs, the Sample Delay function was set at 1.0 second. This allowed the transient response of the test system, imposed by the step change from one command frequency to another, to decay prior to taking data.

Figures 58 and 59 show the overall transfer function ( $\beta_o/\beta_{SC}$ ) of the digital controller and DEHA for two command signal levels. The results on Figure 59 were obtained after removing a filter capacitor on the A/D571 circuit board while the result on Figure 58 were taken before removal. Removing the capacitor had the affect of shifting a first order lag break frequency from approximately 3.5 Hz to 7.0 Hz. This difference is observable in the roll-off and phase shift characteristics of Figures 58 and 59.

The frequency response of the digital controller ( $\beta_c/\beta_{SG}$ ) is shown on Figure 60.



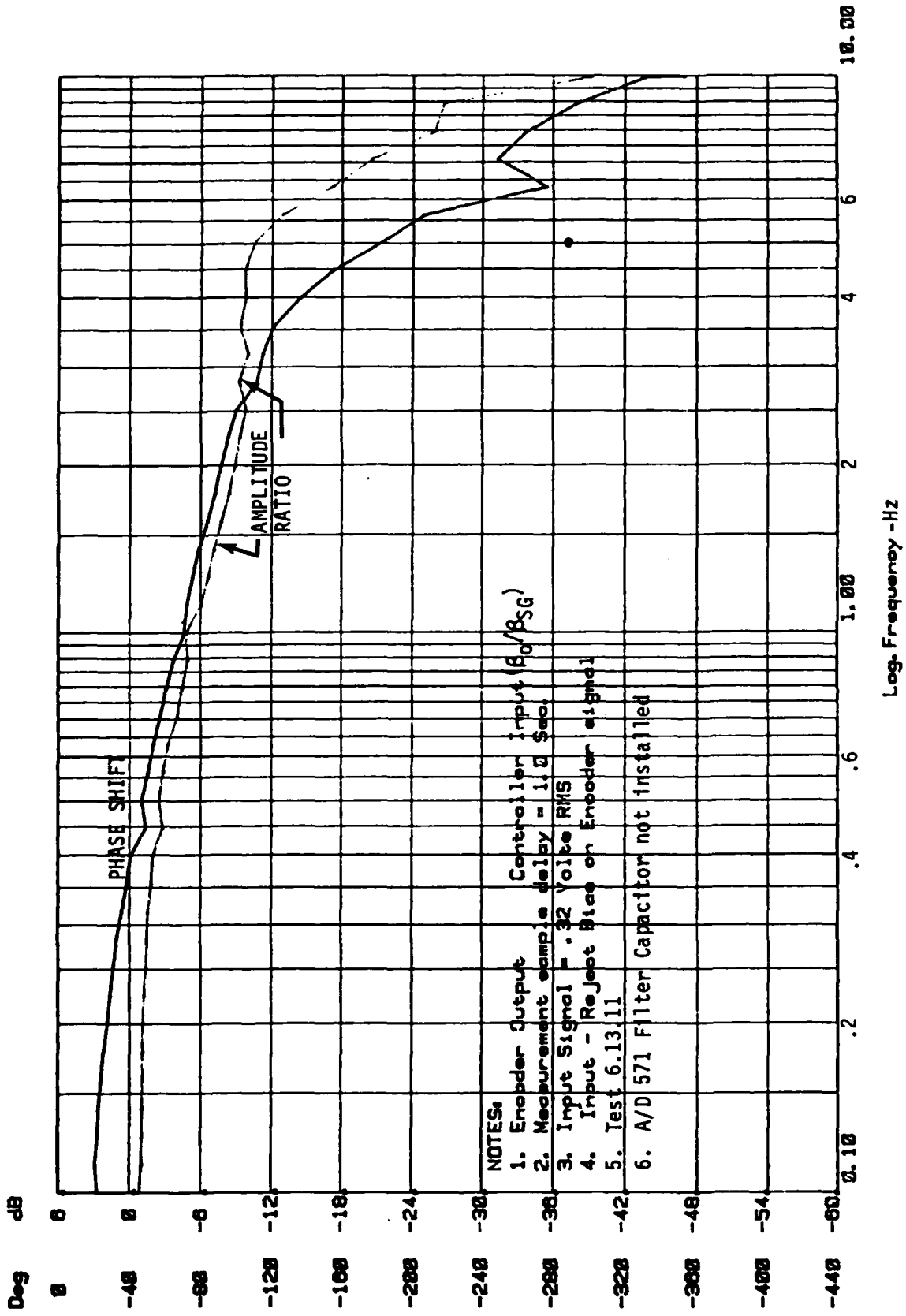


Figure 59 Overall system frequency response

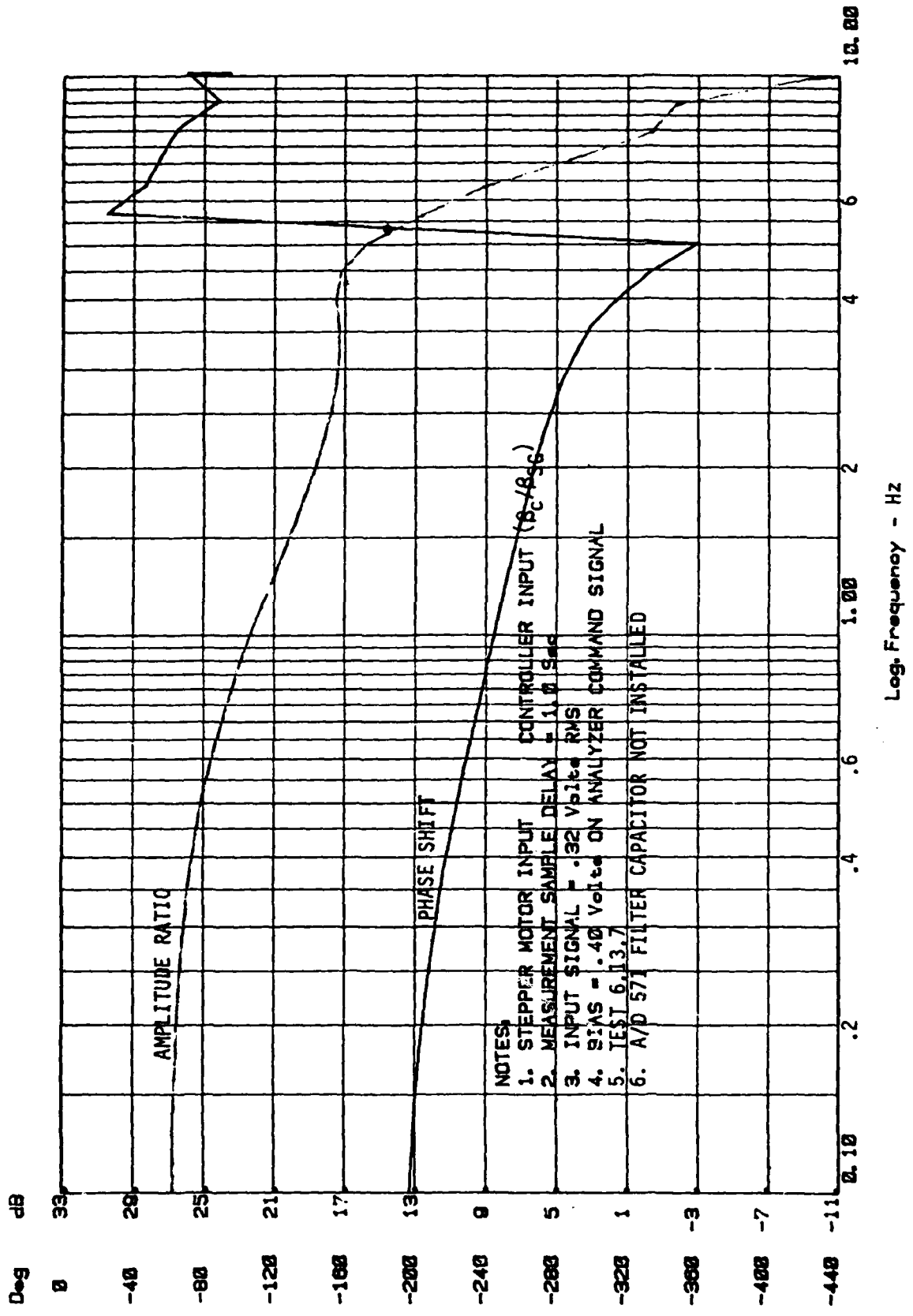


Figure 60 Digital controller frequency response

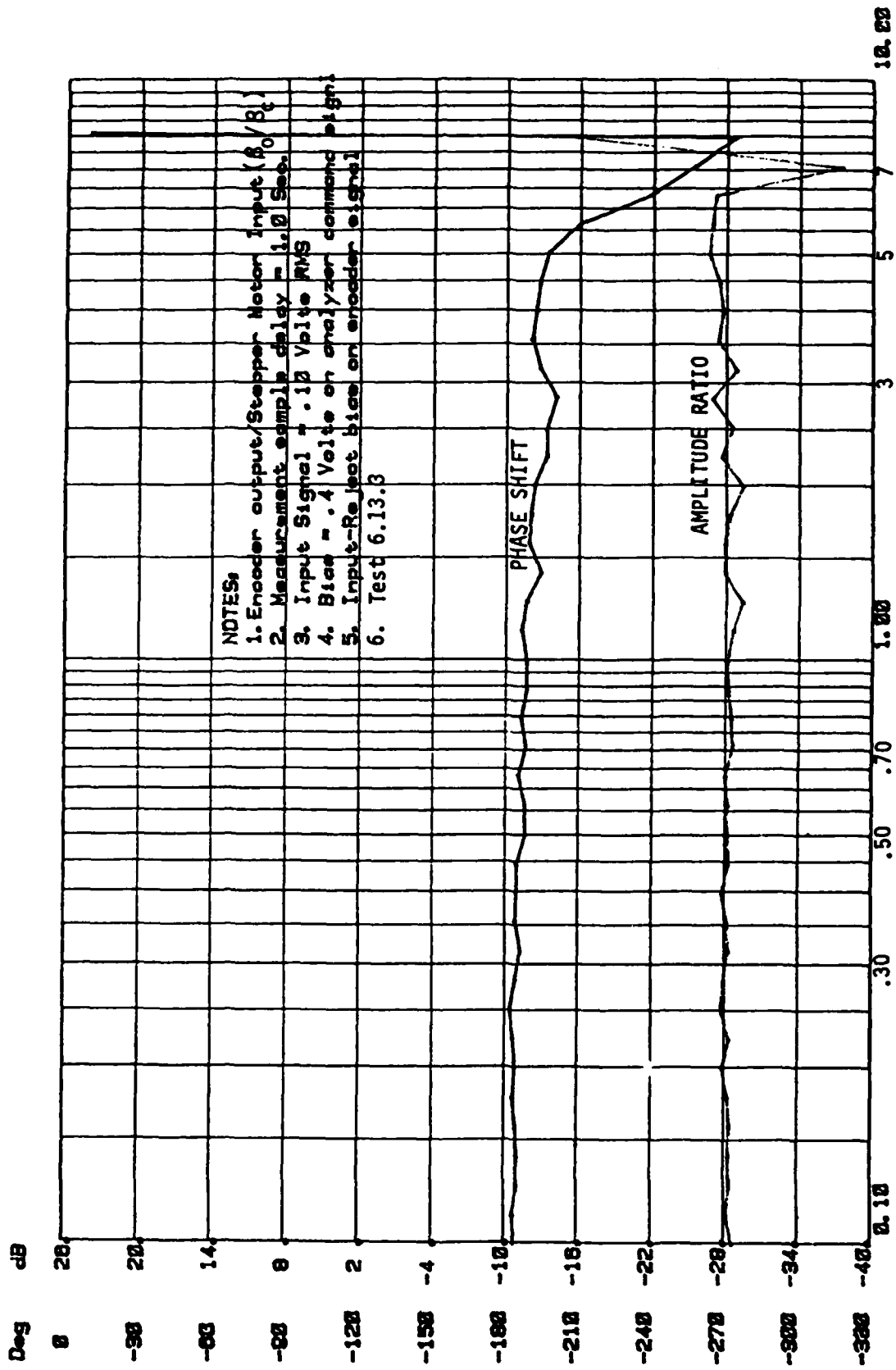


Figure 61 Frequency response of DEHA at .10 volts command

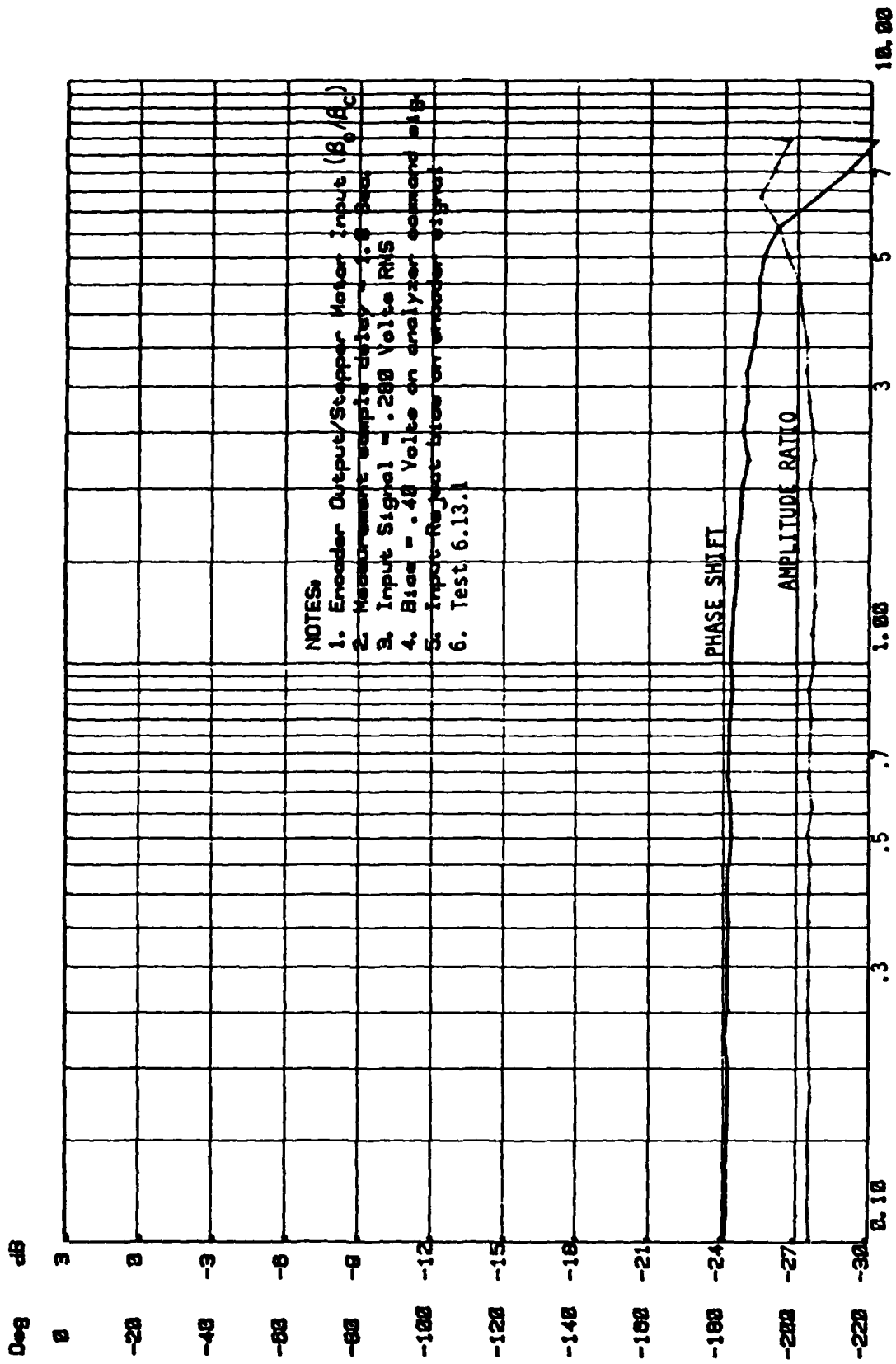
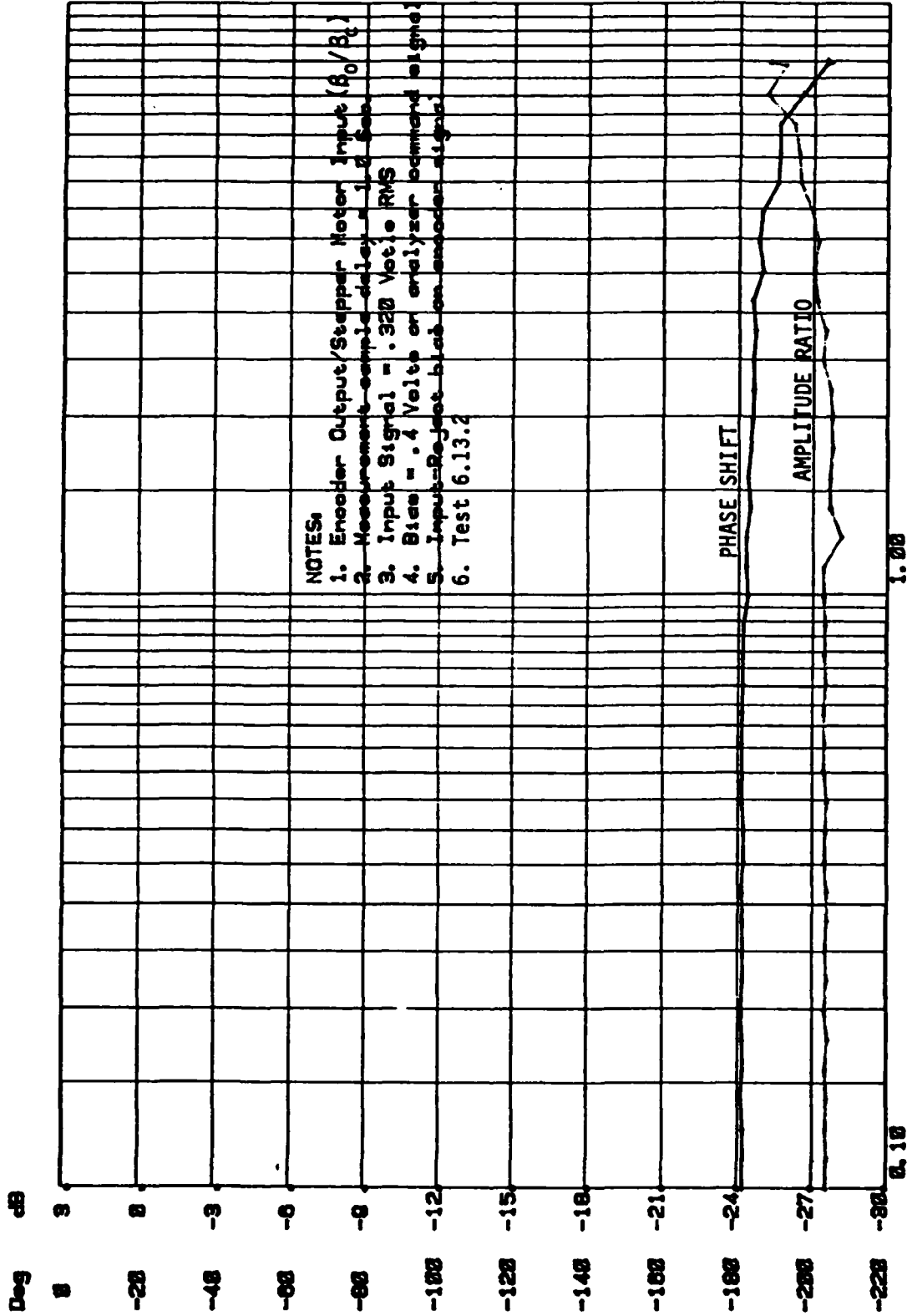


Figure 62 Frequency response of DEHA at .28 volts command



Log Frequency - Hz

Figure 63 Frequency response of DEHA at .32 volts command

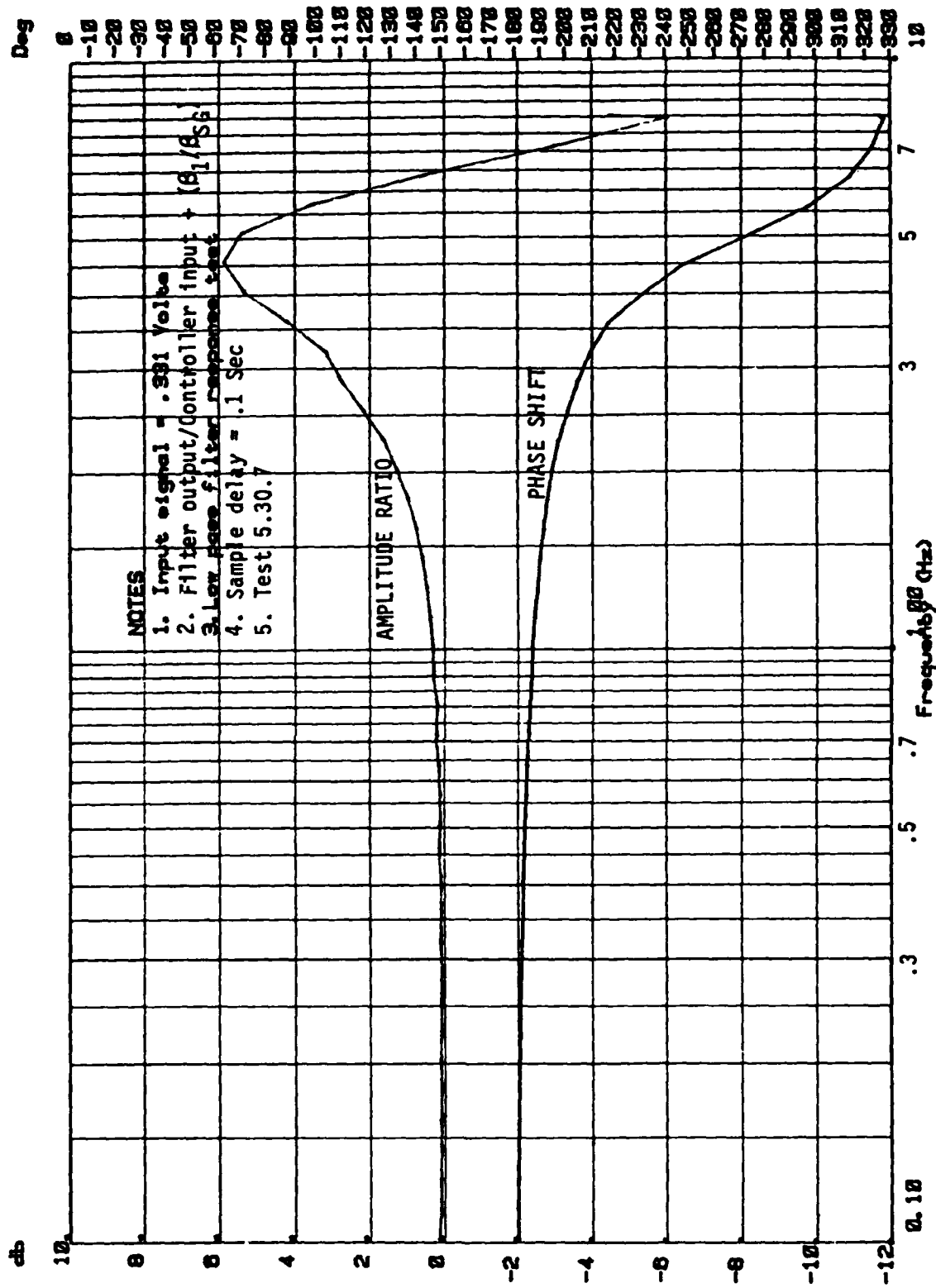
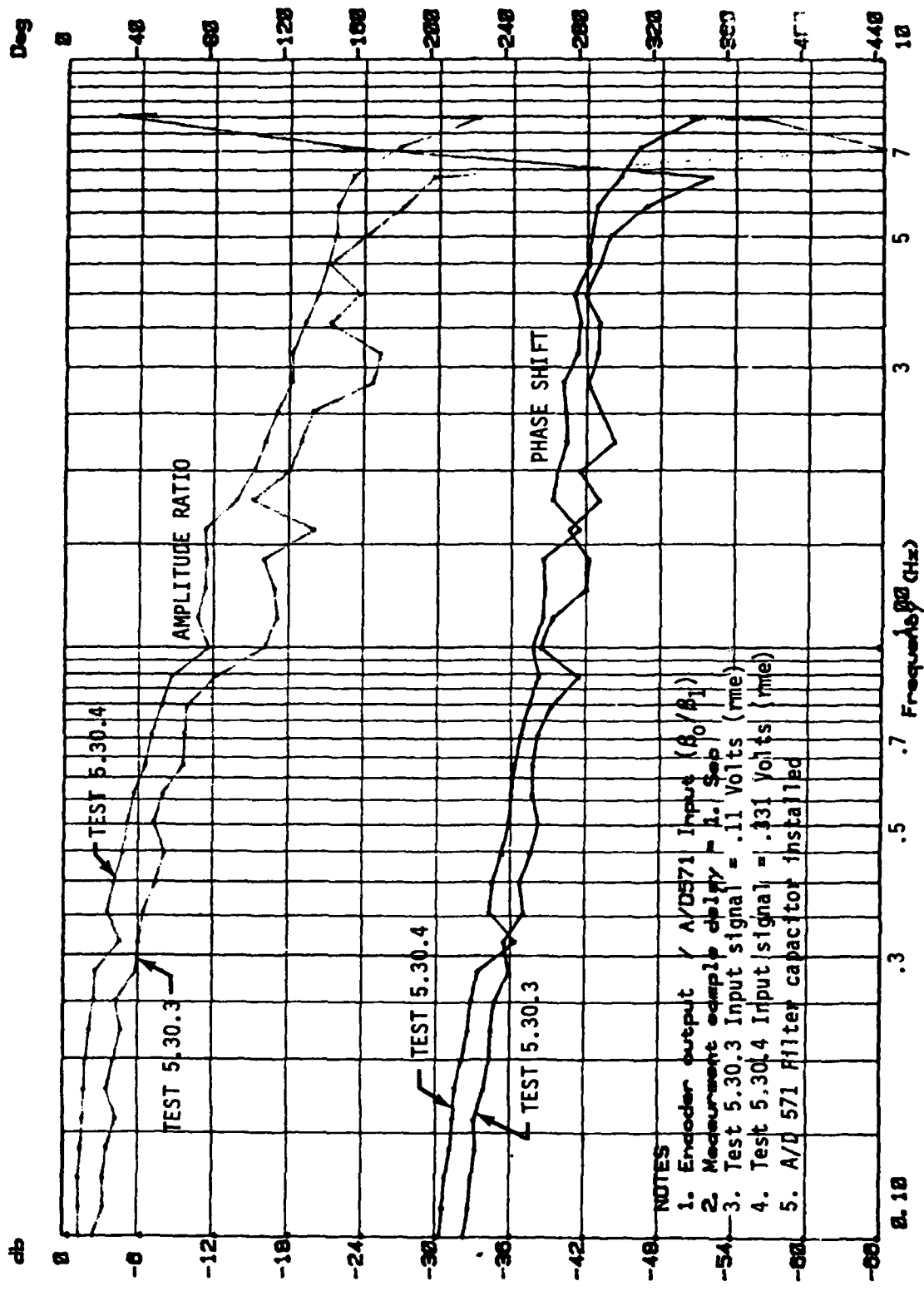
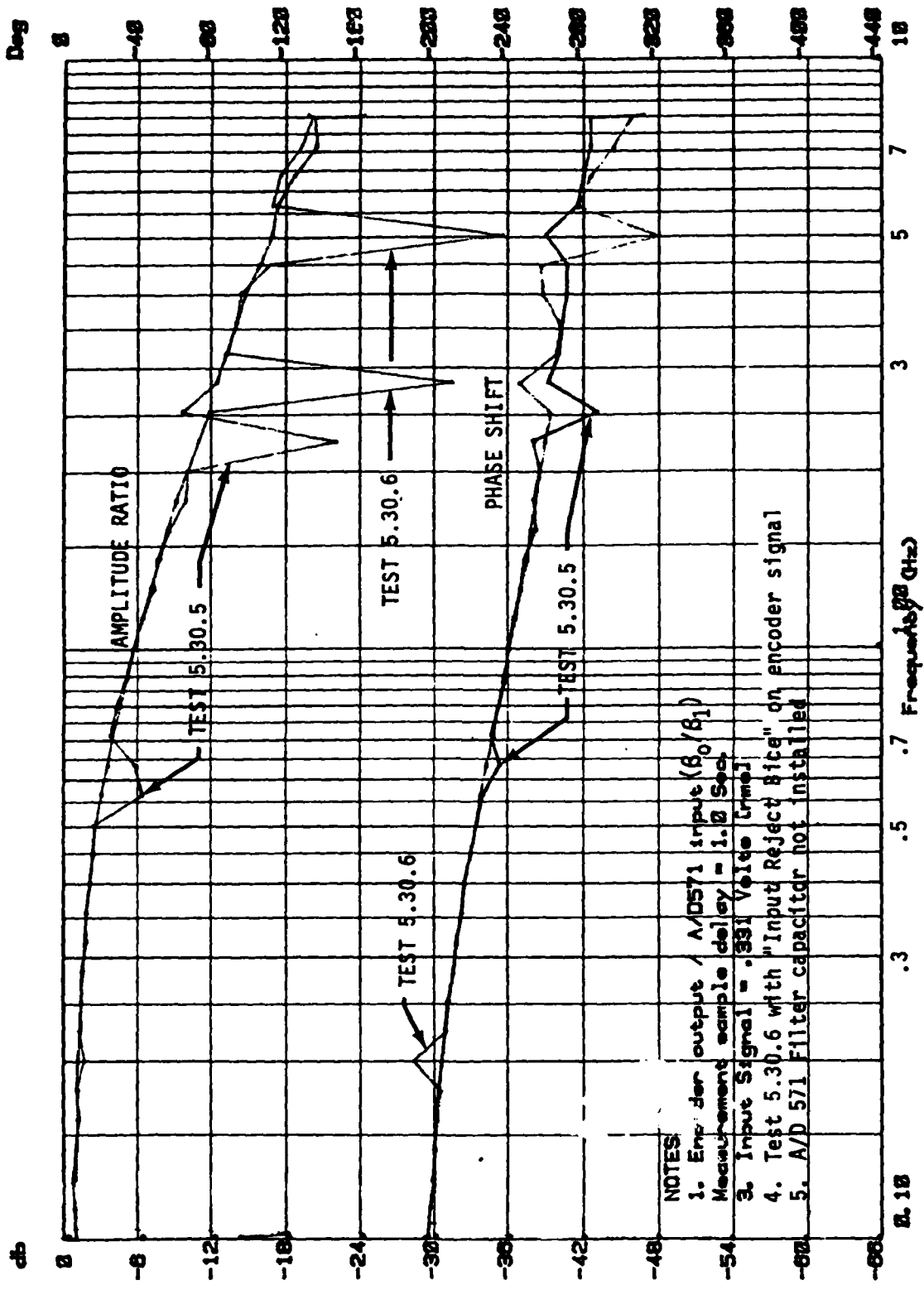


Figure 64 Frequency response of low pass filter



- NOTES
1. Encoder output / A/D 571 Input ( $\beta_0 / \beta_1$ )
  2. Measurements empty delay = 1.1 Sec
  3. Test 5.30.3 Input signal = .11 Volts (rms)
  4. Test 5.30.4 Input signal = .131 Volts (rms)
  5. A/D 571 Filter capacitor installed

Figure 65 Frequency response of digital circuits & DEHA with filter capacitor



NOTES  
 1. Encoder output / A/D571 input (60/81)  
 Measurement sample delay = 1.0 Sec  
 3. Input Signal = .331 Volts (rms)  
 4. Test 5.30.6 with "Input Reject Pipe" on encoder signal  
 5. A/D 571 Filter capacitor not installed

Figure 66 Frequency response of digital circuits & DEHA without filter capacitor

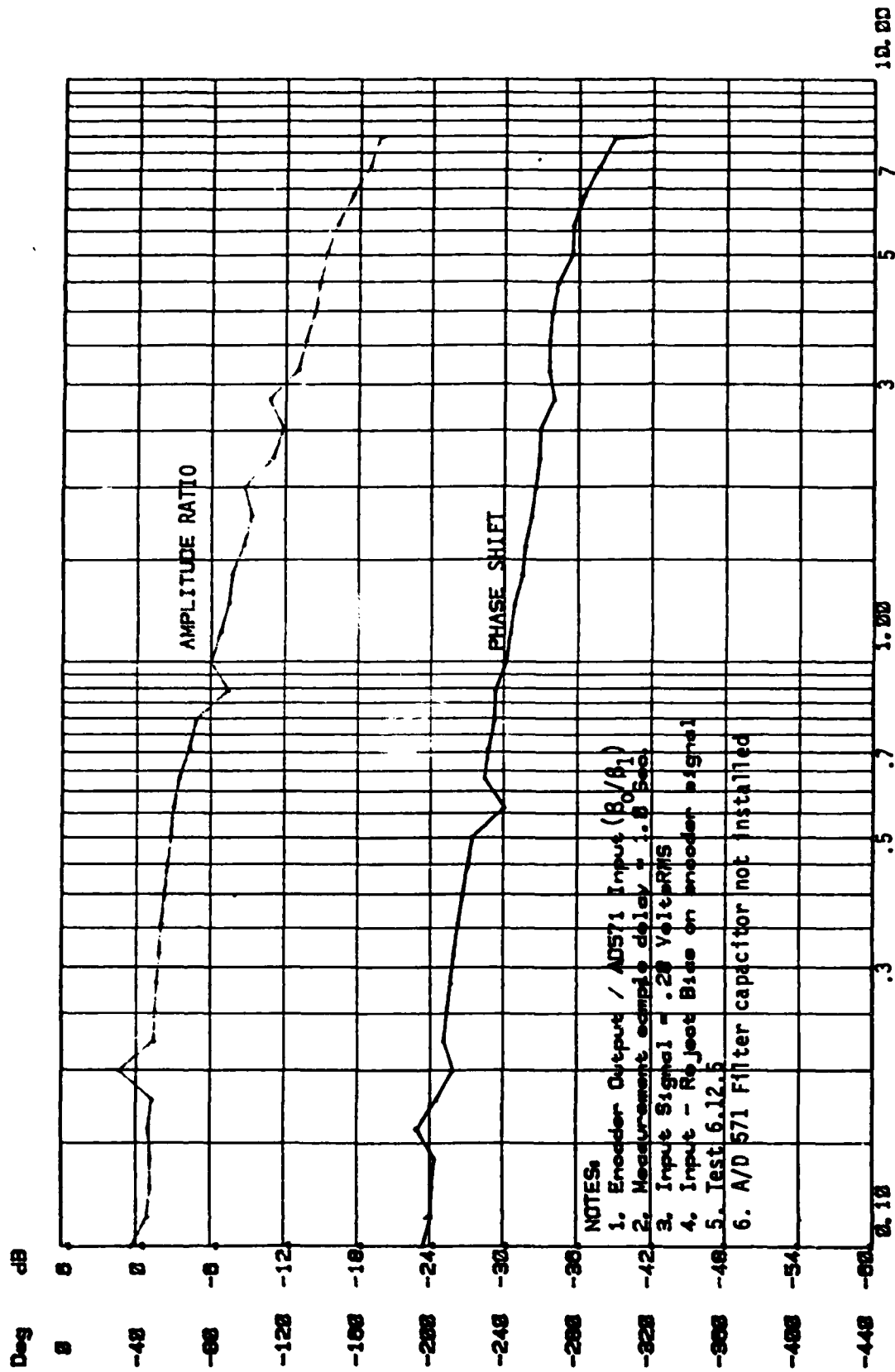


Figure 67 Frequency response with .28 volts command

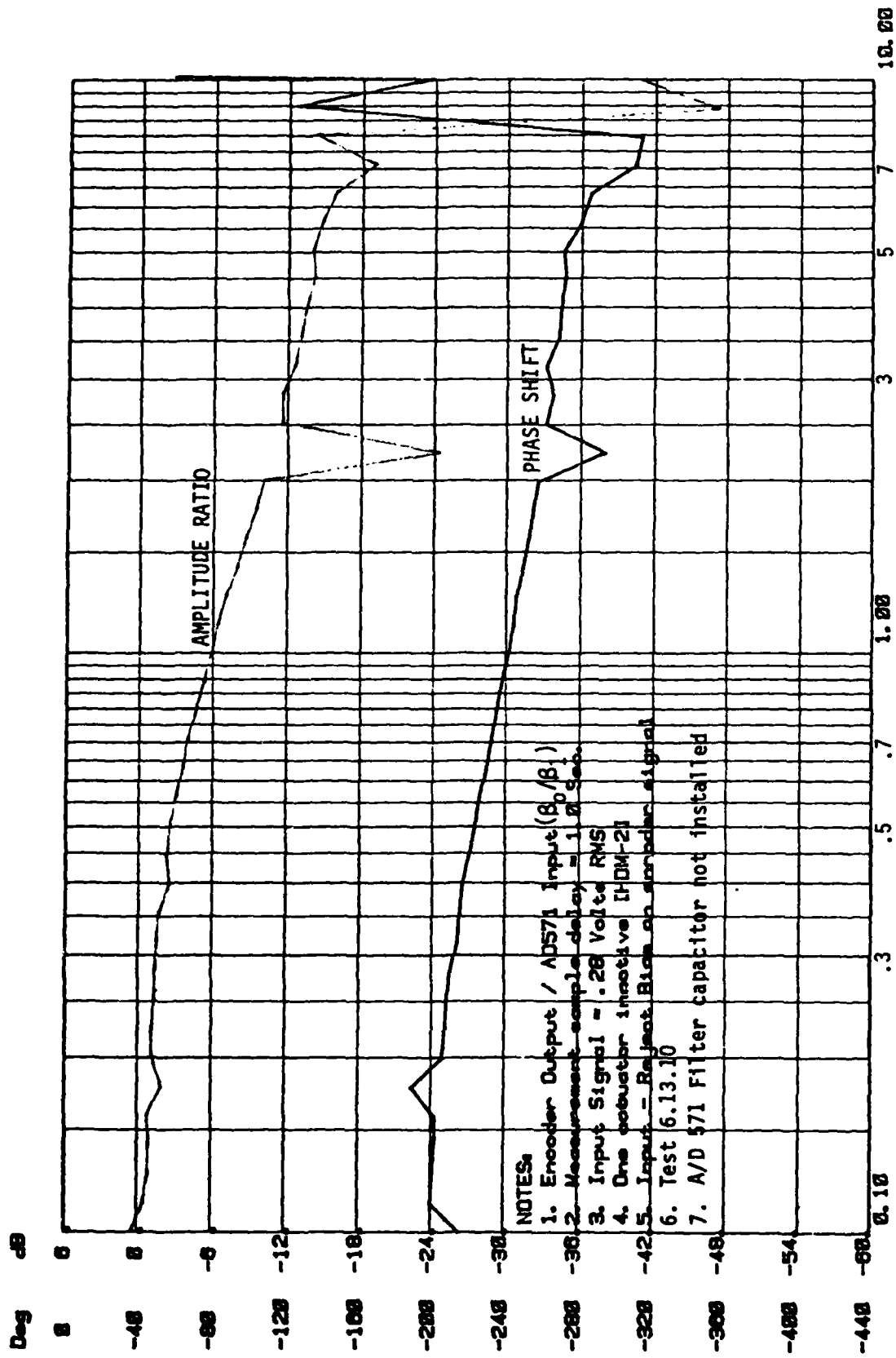


Figure 68 Frequency response with one DEHA motor unpowered

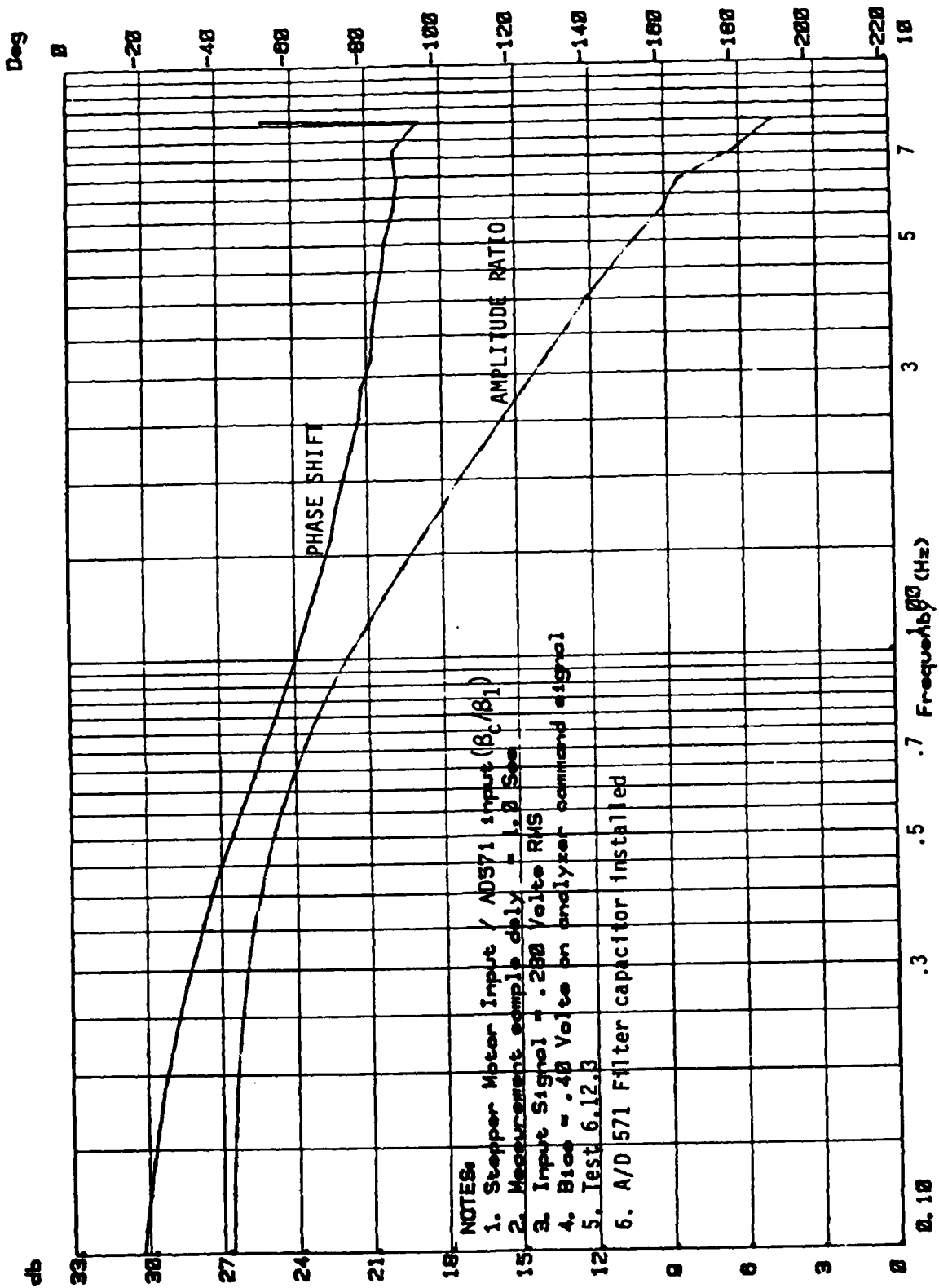


Figure 69 Frequency response of digital circuitry

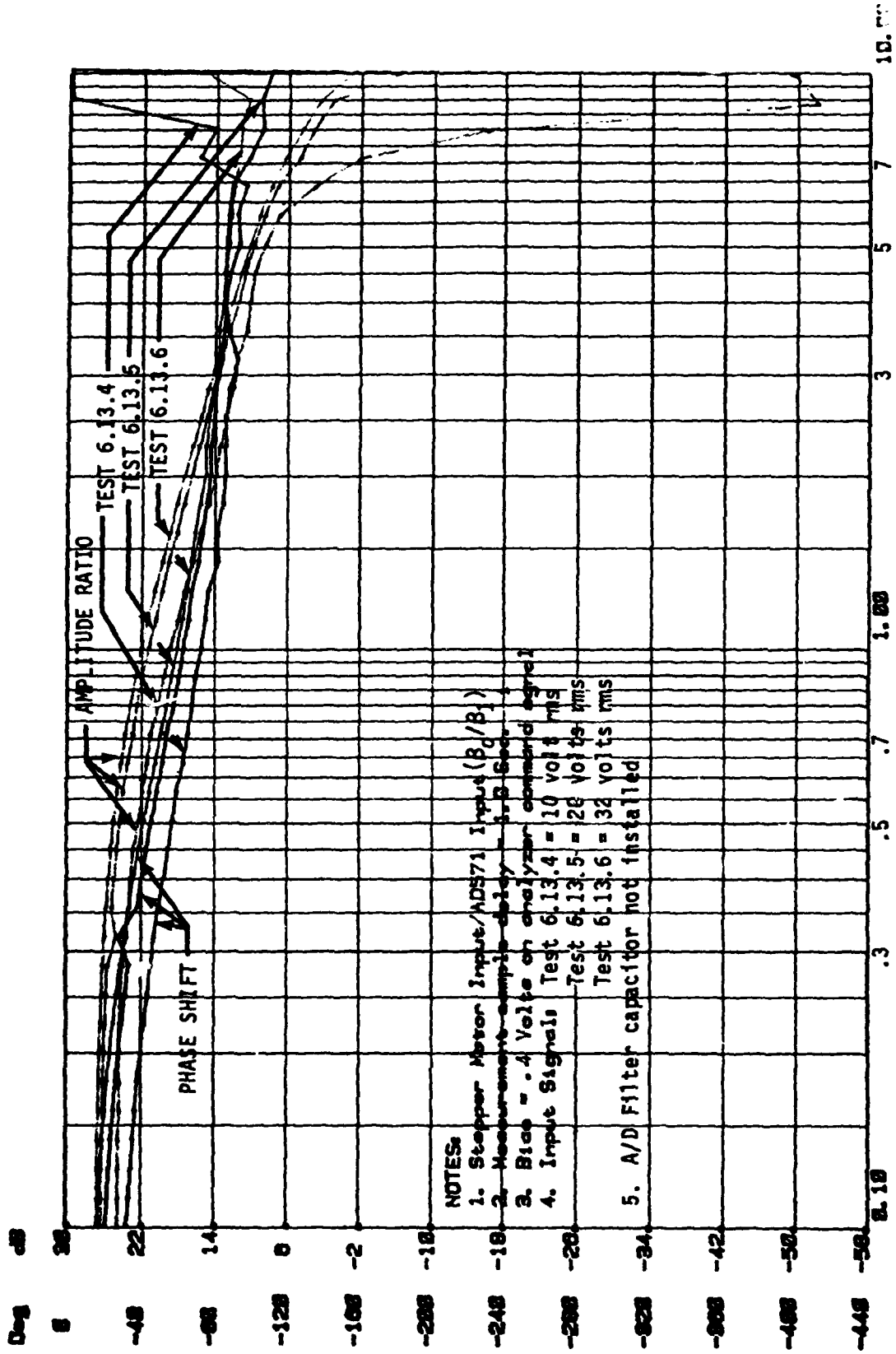


Figure 70 Digital circuitry linearity study

Figures 61, 62 and 63 show the frequency response of the digital electrohydraulic actuator ( $\beta_0/\beta_c$ ); stepper motor, valve, hydraulic motors, and gear box. These data show that this chain of DEHA components has a virtually flat response up to 5 Hz for the voltage levels considered and act approximately as a second-order system having a break frequency greater than 10 Hz.

The frequency response of the various modules of the digital controller were also measured. First, the low-pass filter frequency response data, is shown on Figure 64, were taken.

Second, the frequency response of A/D 571 circuit, microprocessor circuit, and the DEHA ( $\beta_0/\beta_1$ ) were measured; and, the results are shown on Figures 65 through 68. These data were taken prior to fabrication of the test D/A converter, shown Figure 56, which enabled response measurement of the electronics elements alone ( $\beta_c/\beta_1$ ). The data shown on Figure 65 was obtained prior to removing the capacitor from the A/D 571 circuit board discussed above. Test 2 of Figure 65 is directly comparable with Figure 66, Test 1, to observe the influence on frequency response of removing the A/D 571 filter capacitor. Figures 67 and 68 provide comparative data with hydraulic power to both DEHA hydraulic motors and to only one hydraulic motor.

Figures 69 and 70 show the frequency response of the digital controller circuits downstream from the low pass filter ( $\beta_c/\beta_1$ ). Shown on Figure 70 are three measurements of this transfer function at differing command voltage amplitudes. These tests were run to obtain data to evaluate the linearity of the electronic circuits.

### 7.2.3 Durability Tests

The purpose of these tests was to run the DEHA unit under conditions simulating 1,000 flight hours of aircraft operation of the F-16 rudder actuation system. Therefore, a cycling test based upon the endurance design

requirements specified for the F-16 rudder servoactuator in the Reference 6 specification was planned.

In a contact with the General Dynamics Corporation's Fort Worth Division, it was found that those requirements represent the cycling expected over an aircraft life span of 8,000 flight hours. Therefore, the quantities of cycles enumerated in that specification were divided by eight to represent the cycling expected in 1,000 flight hours of operation. The number of cycles and sequence of conditions planned for the DEHA durability test are shown in Table 12.

#### 7.2.3.1 Test Procedure

The durability tests were run in the test setup shown in Figure 71 which was identical to that used for the performance tests (as shown in Figure 52) except for the following modifications:

- a. The load-pressure regulators LPR-1 and LPR-2 were adjusted to act as pressure relief valves.
- b. The load-pressure shutoff valves were used as adjustable orifices to control delivery pressures on the load pump; and, they were identified as load -pressure valves LV-1 and LV-2.
- c. The tubing runs from the load-pressure valves were plumbed to the flow bench return line rather than the pressure line.

During each test phase, hydraulic pressure of 3,000 psi was supplied to both pressure ports of the distributor valve. Load pressure on the load pump and sine-wave input commands to the digital controller were controlled as per Table 11.

It should be noted that, with the hydraulic load circuit used, the durability cycles were not completely representative of the load and velocity relationships normally imposed on an aircraft flight control surface actuator.

TABLE 11 DURABILITY TEST CYCLING SCHEDULE

Phase No.	Load and Deflection	Peak-Load Pressure	Sine-Wave Inputs		Number of Cycles	
			Half-Amplitude	Rate	Planned	Actual
1	± 100%	2,800 psi	512 steps	0.20 Hz	490	501
2	± 80%	2,240 psi	410 steps	0.33 Hz	3,050	3,065
3	± 50%	1,400 psi	256 steps	0.60 Hz	47,525	41,256
4	± 10%	280 psi	51 steps	1.0 Hz	522,500	zero

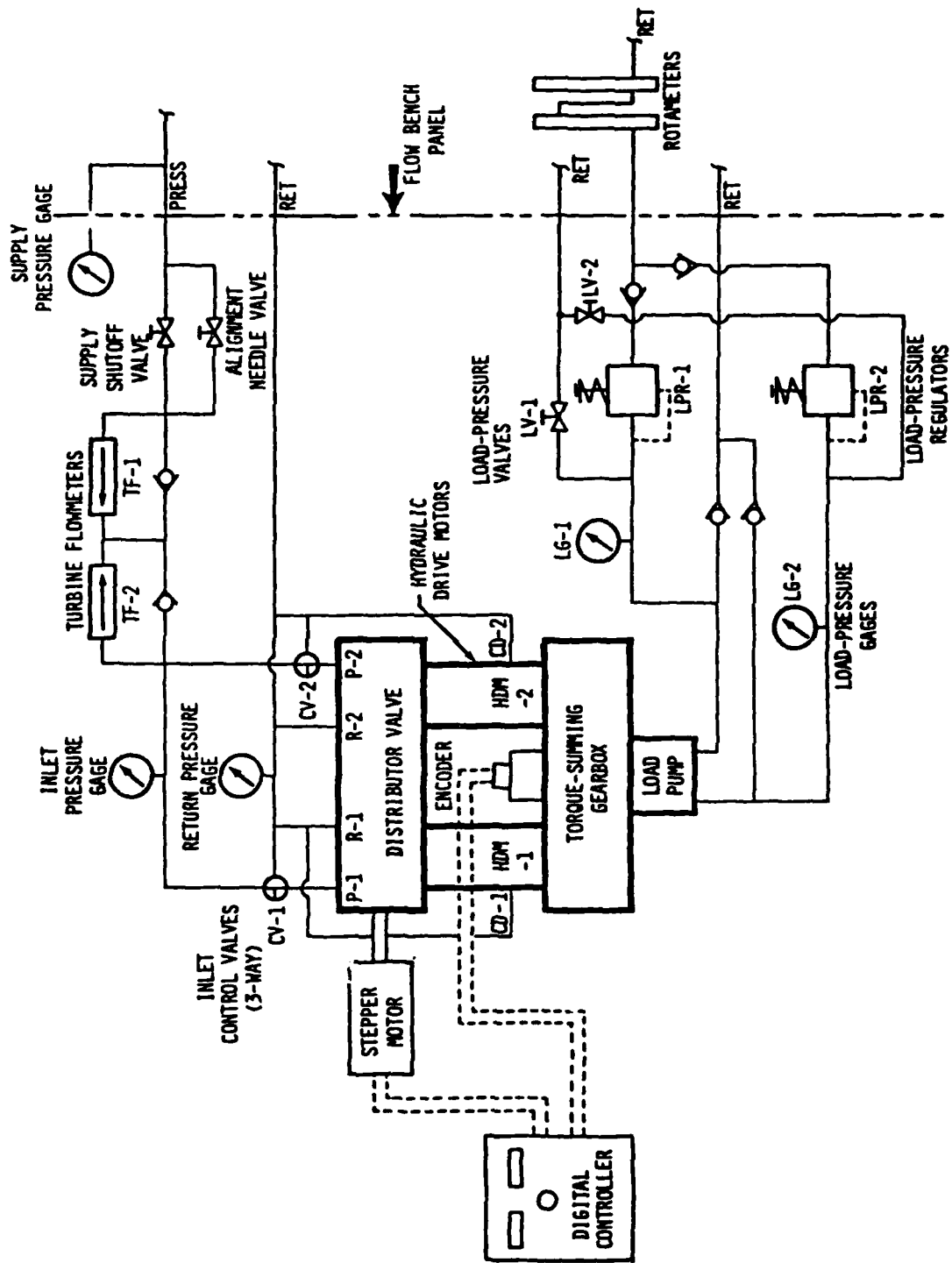


Figure 71 Schematic diagram of the DEHA durability test setup

The test cycles were run with the load phased to output velocity rather than to output positional deflection whereas the loading of an aircraft control surface increases roughly in proportion to the deflection of the surface from a null centered position. The driving motors of an aircraft surface servo thus operate at maximum velocity near the center position of any sinusoidal cycle. However, in the test program, loads were generated by backpressure from the load pump driving flow across an orifice represented by each load pressure valve, making the peak loads occur in phase with the peak output velocity. This was done to avoid the additional expense of fabricating a special loading system for these durability tests. Such a special loading system having the load pressure phased to output deflection would have consisted of a pair of gas loaded accumulators with a controllable hydraulic bleed between their two input lines. Load pump output flow would have been routed to the two accumulator inlets to compress the gas charge of one accumulator at a time.

Although the load and velocity relationships obtained with the test system used were not completely representative of the aircraft condition, they were no less severe. In fact, they were more rigorous from the standpoint of equipment life; and, in that sense, the test was considered a more conservative approach than required.

#### 7.2.3.2 Durability Test Results

Test phases 1 and 2, at 100% load and deflection and at 80% load and deflection respectively, with the number of cycles noted in Table 12, were completed without incident.

For phases 3 and 4, it was decided to automate the cycling so that the test could be run overnight without test personnel in attendance. A Model 2240 Data Logger manufactured by the John Fluke Manufacturing Co. in Seattle, Washington, shown in Figure 72, was used for periodic acquisition and recording of selected data, and for monitoring preset limits on selected data channels. When any of the parameters shown on Table 12 exceeded the noted limits, the Data Logger triggered electrical relays to shut down the electric

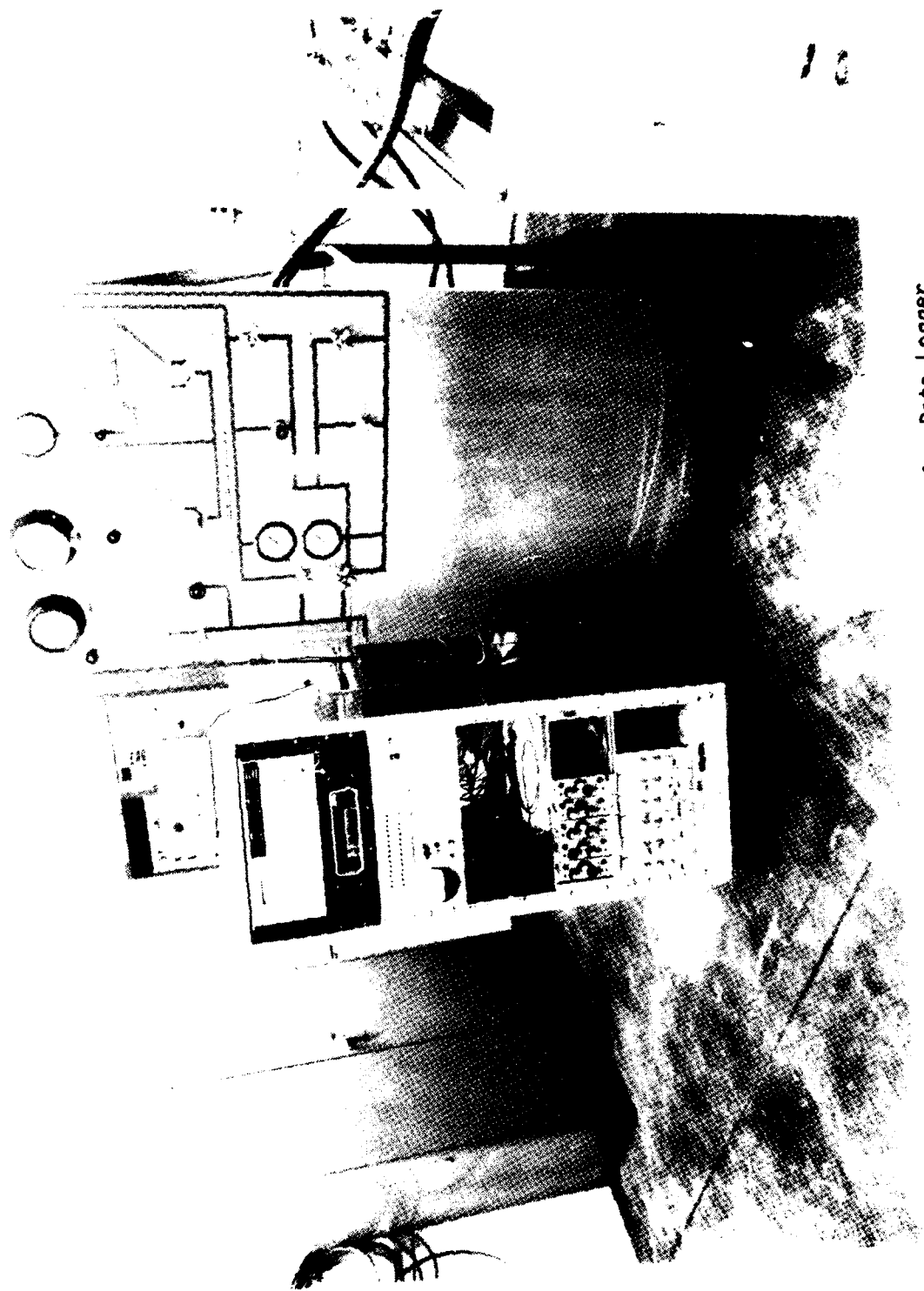


Figure 72 John Fluke Manufacturing Co. Data Logger

TABLE 13 TEST PARAMETER LIMITS FOR AUTOMATIC SHUTDOWN OF THE DURABILITY TEST

Failure Mode	Parameter	Shutoff Valve
1. Hyd motor (two in actuator)	<ul style="list-style-type: none"> <li>o Cased drain temp</li> <li>o Filter <math>\Delta P</math> increase</li> <li>o Encoder output vs command signal</li> <li>o see leakage failure</li> </ul>	<ul style="list-style-type: none"> <li>o <math>T_1 &gt; 180^\circ\text{F}</math></li> <li>o <math>\Delta P &gt; 8</math> psid</li> <li>o Encodere count @ <math>t_2 \neq</math> count at <math>t_1</math> where <math>t_2 - t_1 \approx 3/\text{freq}</math></li> </ul>
2. Load pump	<ul style="list-style-type: none"> <li>o Case drain temp.</li> <li>o Filter <math>\Delta P</math> increase</li> <li>o see leakage failures</li> </ul>	<ul style="list-style-type: none"> <li>o <math>T_1 &gt; 180^\circ\text{F}</math></li> <li>o <math>\Delta P &gt; 8</math> psid</li> <li>o See Failure Mode No. 6</li> </ul>
3. Gear box (jamming)	<ul style="list-style-type: none"> <li>o Gearbox temp.</li> <li>o Encoder output vs command signal</li> </ul>	<ul style="list-style-type: none"> <li>o <math>T_2 &gt; 180^\circ\text{F}</math></li> <li>o See Failure Mode No. 1</li> </ul>
4. Valve	<ul style="list-style-type: none"> <li>o Encoder output vs command signal</li> <li>o See leakage failures</li> </ul>	<ul style="list-style-type: none"> <li>o See Failure Mode No. 1</li> <li>o See Failure Mode No. 6</li> </ul>
5. Lube oil system	<ul style="list-style-type: none"> <li>o Reservoir level</li> </ul>	<ul style="list-style-type: none"> <li>o Level switch set point.</li> </ul>
6. Leakage, supply	<ul style="list-style-type: none"> <li>o Supply pressue (do not measure on rig-vibration)</li> <li>o Reservoir fluid level</li> </ul>	<ul style="list-style-type: none"> <li>o <math>P_1 &lt; 2800</math> psig <math>P_1 &gt; 3250</math></li> <li>o On unit. Set fluid vol 1 gallon above shutoff</li> </ul>
7. Leakage, Return	<ul style="list-style-type: none"> <li>o Valve return press</li> <li>o Reservoir fluid level</li> </ul>	<ul style="list-style-type: none"> <li>o <math>10 \text{ psi} &gt; P_2 &gt; 60</math> psig</li> <li>o On unit, See F.M. No. 6</li> </ul>
8. Reservoir Press, System	<ul style="list-style-type: none"> <li>o Reservoir pressure</li> </ul>	<ul style="list-style-type: none"> <li>o On hyd units</li> </ul>
9. Load Press Reg's (two)	<ul style="list-style-type: none"> <li>o Load pressure</li> </ul>	<ul style="list-style-type: none"> <li>o <math>P_3</math> or <math>P_4 &gt; 150\% P_{\text{load}}</math> (<math>P_{\text{load}}</math> is a test variable.)</li> </ul>

motor driving the hydraulic power supply pump, the reservoir pressurization source, the shutoff valve in the pressure supply line to the DEHA, and the electric-motor-driven gearbox lube pump.

During the automated cycling in Phase 3, several nuisance failures occurred. These included failures in some of the 1/4-inch steel tubes in the hydraulic test circuit, and a failure of one of the 3/8-inch plastic hoses in the gearbox lube system. These were repaired and testing continued until leakage occurred in the DEHA rotary valve housing after 41,256 cycles of the planned 47,525 Phase-3 cycles had been completed.

Upon close examination, it was found that the leakage occurred from a crack formed in the rotary valve housing between test ports No. 1 and No. 3 on the System No. 2 end of the manifold, (the end farthest from the valve shaft extension). A pressure test was made which indicated that this crack did not penetrate the housing wall to the surface of the valve sleeve. For this test, a rubber plug was inserted under each of the fittings used to plug the System No. 2 test ports. These plugs effectively stopped the high-pressure leakage from the cracked area and thus verified that the crack did not penetrate the housing wall into the sleeve surface.

Subsequently, the housing was subjected to ultrasonic inspection which indicated that the crack actually laid primarily in a plane parallel to the surface where it broke out, approximately 0.20 inches below the surface, rather than normal to that surface. This explains why the crack did not penetrate into the bore holding the valve sleeve. Upon finding this, it was recommended that a Loctite sealant be applied in the cracked area and that the crack interfaces be drawn together with three special bolts screwed into the adjacent test gage ports Nos. 1, 3, and 6. Other possibilities considered were:

a. Welding the cracked surface.

Bendix had considered both electron-beam and laser-beam welding, but concluded that the chances for a successful weldment were small.

- b. Installing the slide and sleeve assembly in another valve housing. Bendix had a second housing which could be used. However, it was considered that there is a high probability that the shrink-fitted valve sleeve would either be excessively damaged during extraction from the cracked housing or that its residual stresses would cause an unacceptable curvature in its bore.

Therefore, a Loctite sealant was applied in the cracked area, and the crack interface was drawn together with the three special bolts screwed into the adjacent test ports. In addition, a rubber plug was installed below the bolt in each of those ports; and, in a subsequent pressure test, the unit was found leak free.

Durability testing was terminated at that point to preserve what life was left in the valve housing. Further operation of the unit was used to refine performance data taken earlier and to correct a phase error between the hydraulic motors which had been introduced by improper assembly of the motors on the output gearbox. See Section 6.5. In less than two hours of additional running time ranging from 500 to 3,000 stepper pulses per second, three more housing cracks appeared each having the same general character of the first crack. Cracking occurred in a plane within 20 degrees of the surface plane of the housing block. One end of each crack appeared to start or terminate on the root of the thread in one cylinder test port and to extend far enough to break through the block surface plane causing a high-pressure leak from that particular motor cylinder clearance volume. When testing was finally discontinued, three cracks had occurred in the area of the No. 2 motor test ports with one crack in the No. 1 motor test port area. The total number of operating cycles completed are shown in Table 11.

The presence of high residual stresses in the valve block surface area was verified by comparative measurement across the block cross section near its midsection (across the sleeve axis) and across the same section near the corners of the block. This measurement indicated that the sleeve shrink fit had caused an approximate 0.006-inch diametrial bulge across the flats of the block. This bulge seemed to explain why the block was sensitive to cracking in this area. However, the very rapid onset of further cracking in

the same general area suggested that a further mechanism of repeated stress cycling was responsible as well.

Block stresses induced in the area of the cracks are normally quite low when static supply pressure of 3,000 psi is applied to any combination of motor cylinders in any normal sequence. The cyclic stresses believed to be responsible for the rapid crack formation can be explained as a result of high-frequency operation of the unit at low loads which produce near null phase conditions on the motor valve combination. Under these conditions, the flow from the motor cylinder whose piston is rising toward the cylinder head is momentarily blocked by the rotary valve action when the valve switches that cylinder from supply to return source pressures. This fluid lock condition can cause a very high spike of pressure above the level of the 3,000 psi supply to occur in each motor cylinder at the instant of pressure switching. This theory of cyclic stresses contributing to crack formation in the valve block is supported further by the nature of the measured performance curves of Figure 54. The upward spread of these power demand curves with input pulse rate indicates a source of motor drag torque related to motor velocity which defies explanation by most other theories which do not suppose a transient cylinder pressure rise at the pressure switching point. A discussion of possible design steps to effect a reduction of this pressure spiking phenomenon is included in Section 8.2 which covers ways of improving DEHA power reversibility and is directed at improvements of the operating power efficiency of the demonstrated DEHA unit.

## VIII. POST-TEST EVALUATION

### 8.1 PERFORMANCE EVALUATION

The flow-demand performance curves in Figure 54 show the extreme importance of reducing speed related losses, including flow losses, to an absolute minimum in order to realize the full potential benefits of a power reversible system. Intercepts of the actuator flow demand curves on the zero-load pressure axis indicate the degree to which the DEHA motor phase, and therefore the system power loss is increased by increasing speed. Points on the zero-load pressure axis are shown to illustrate the effect of eliminating the rate related drag of the load pump unit from the system. With the drag effect of the load pump eliminated from this display, the upward spread of the actuator flow curves with output rate is still disturbing since this spread indicates that the resulting system will have much less power recovery than had been intended. If all sources of velocity-dependent drag on the DEHA motors and their associated hydraulic lines could be eliminated, the zero-load intercepts of the curves in Figure 54 should represent load flows proportional to the input pulse rate.

Motoring tests of the DEHA system were run using the load pump to turn the system with the rotary valve held at various fixed positions. This type of testing was used to indicate the relative magnitude of the various drag producing factors which caused these load flow curves to spread upward with input velocity.

Of these factors, the combined friction loss of both DEHA motors with the effect of steady-state line flow losses was roughly equal in magnitude to the load pump losses indicated by the three reference points on the zero-load axis of Figure 54. The rest of this unexplained actuator phase shift with speed is thought to be explained by transient "wire drawing" of flow across the active metering lands of the rotary valve. This "wire drawing" effect occurs at the time of switching of each cylinder pressure between the load and return pressure states.

No attempt has been made to isolate and break down the sources of motor velocity related drag. The general direction of measures to improve the motor friction and churning losses have been discussed in Section 6.3.1. Steady-state flow losses across the valve metering orifices measured at Bendix during acceptance testing were on the order of 250 psi at the rated flow of 9 gpm. This steady state flow induced pressure differential is a minor factor in the aforementioned upward spread of the performance curves. The major factor in this spread is believed to be the, so called, "wire drawing" at the valve metering orifices which limit the rate of pressure buildup or decay in the individual cylinders.

In any rotary valve commutation cycle, any particular motor cylinder will be repeatedly switched between pressure and return flow sources. During this switching transition interval, either a high transient cylinder pressure or a momentary cavitation of that cylinder may occur. It is most important that, upon switching, the cylinder pressure should rise or drop rapidly in the sense of the desired pressure change. The exact instant of switching is less important than the rate of the pressure change induced by the switching input. "Wire drawing" of valve flow during the transient switching interval will cause cylinder pressure excursions above the supply pressure and will reduce the rate of pressure change in the desired switching direction.

The following methods can be used to reduce the effect of "wire drawing" flow resistance in rotary commutating valves.

- a. The stepping increment of the electrical stepping motor driving the valve should be equal to the least-bit increment desired from the rotary valve. The use of three 1.25-degree stepper increments to generate a single 3.75-degree least-bit valve step in the present DEPA unit design is ill advised because of the "wire drawing" which occurs while the valve rotor hesitates at the conclusion of the 1.25-degree step following the cylinder switching point. The use of a stepping motor with a 3.75-degree single-step output would have resulted in a considerable improvement in the valve metering-area rate at the switching point. However, no such stepping motor was available when the component selections were made.

- b. The number of valve phases could be increased from four to six to allow the use of the existing stepping motor in a full-step 2.5-degree stepping mode. This design doubles the valve metering orifice area opened at the completion of a single electrical step which switches pressure on a given motor cylinder when compared with the existing DEHA design.
- c. The valve metering-area rate could be improved by increasing the number of parallel metering ports opened at each of the switching points of a valve rotation. This represents a return to the original form of the DEHA valve in which all cylinder ports appeared in each metering phase segment of the sleeve circumference. This design doubles the metering area rate from that of a valve built on the alternating phase metering pattern of the present valve unit. This feature must be weighed against the other effects of an increase of the number of phases used in a 360-degree valve rotation since such features increase the density of the circumferential porting; and, if carried to extremes, they will cause restriction of the feed passages in the sleeve which serve the valve metering orifices.
- d. All simple rotary valve designs, not employing secondary relay valves, should use the longest metering orifice slots which can be practically designed into the valve envelope.
- e. Individual, secondary-relay-type fast-acting poppet switching valves could be provided at each motor cylinder. This would reduce the size of both the stepping motor and of the rotary valve needed for a particular hydraulic motor drive. Such a relay valve, as described in Figure 73, is a rather complex scheme to reduce valve flow-induced velocity losses. A fast-acting double poppet valve system is used to provide the fast opening of pressure and return source pressure demanded by the motor cylinders. The rotary valve need only be large enough to manipulate the hydraulic power necessary to throw the shuttle relay devices. The shuttle, described above, serves as an overpressure and anticavitation valve to limit cylinder pressure as well as acting as a power relay. Hydraulic power required to drive a set of 12 such valves would be at least partially compensated by the reduced leakage of the smaller diameter rotary valve now required to merely trigger the system of shuttle relay

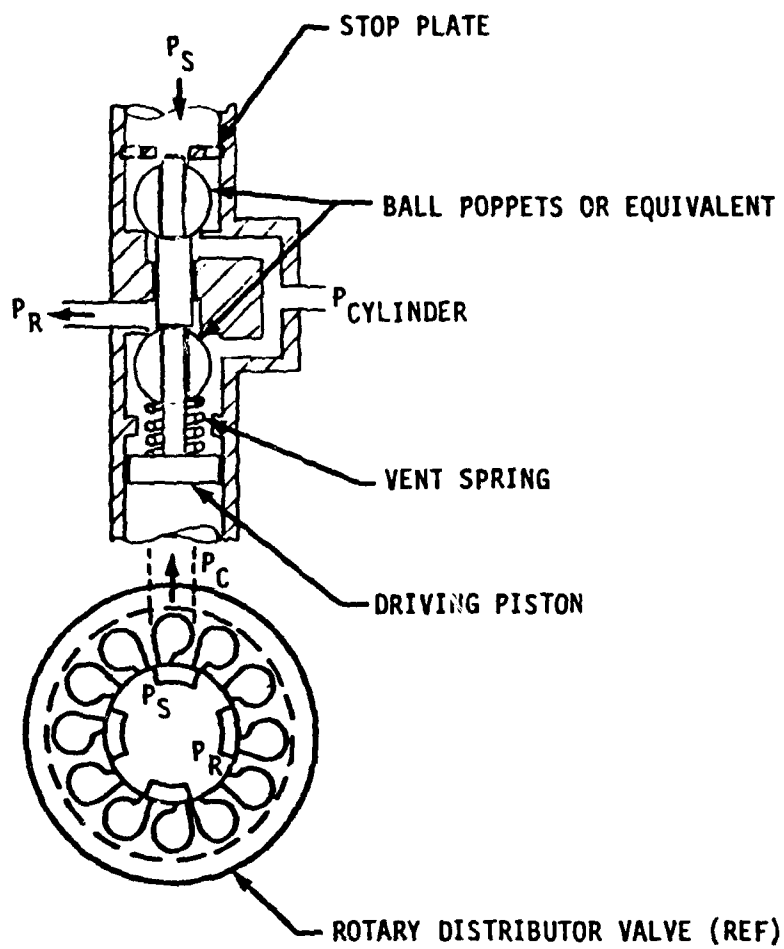


Figure 73 Shuttle-relay valve with dual relief-valve function



poppets. Valves which are functionally similar to the illustrated sketch are currently in use for missile fin control and are marketed by the AiResearch Division of the Carrett Corp.

- f. Overpressure and anticavitation relief valves may be provided for each motor cylinder. In theory, if "wire drawing" of flow exists at the valve switching points, a very high transient pressure should occur in each cylinder as it is switched from pressure to return. No attempt was made to measure cylinder transient pressures to detect abnormal cyclic pressure spikes. However, the repeated appearance of surface cracks in the housing area around the cylinder test ports suggests that such pressure spikes may have been present. This theory suggests a possible solution to the problem of motor phase shift with speed induced by "wire drawing" of valve switching flows. This solution consists of a pair of check relief valves installed on each motor cylinder head-space and connected to relieve cylinder overpressure to the supply line and to vent the cylinder to return at the onset of cavitation.

Such relief valves, as shown in Figure 74, may easily make a worthwhile contribution to the ability of DEHA type units to operate as power reversible systems even after maximum use of quick opening valve design techniques already discussed have been fully exploited.

If any attempt is made in the future to operate the DEHA unit up to its rated speed of 6,000 pulses per second, a high-response-type crystal pressure transducer should be connected to one of the remaining cylinder test ports which is not yet showing a surface crack failure. A minimum line volume should be added with this transducer connection. Observation of the cylinder pressure wave as motor speed is increased should verify or refute the above theory of the importance of "wire drawing" losses from the valve switching transient restriction of flow.

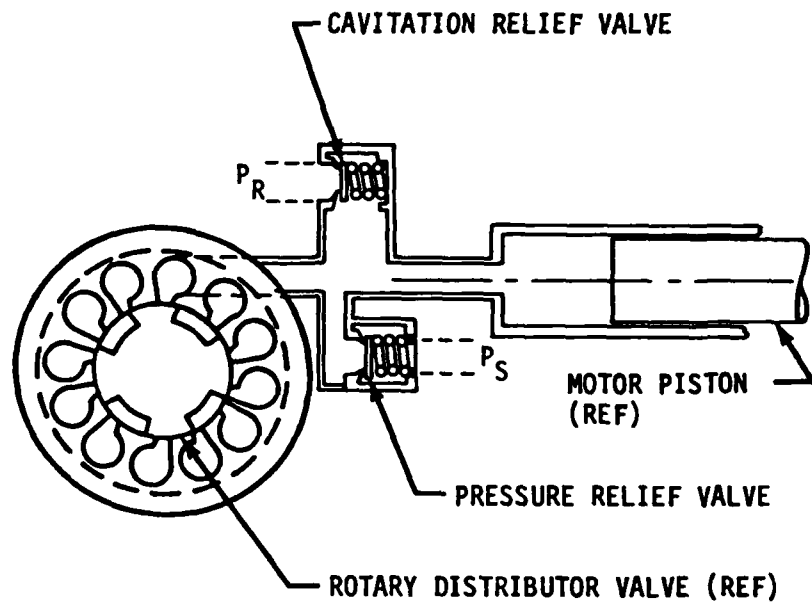


Figure 74 Typical installation of check-relief valves

## 8.2 DESIGN EVALUATION

### 8.2.1 General Design Considerations

The performance curves in Figure 54 show that, to a large degree, power adaptable performance of the DEHA test unit has been achieved. These test results have also demonstrated that power recoverable performance of such units is possible. However, to exploit the potential benefits of power recovery, some design innovation of the valving scheme is required to allow more rapid switching of motor cylinder pressures. This is necessary to minimize the motor phase buildup with speed which is indicated by the upward spread of the curves in Figure 54.

An optimum valve design would be one which, by compromise, produces a satisfactory combination of the following factors: Minimum internal leakage, minimum internal pressure losses related to steady or average flow, maximum rate of cylinder pressure change, in the desired sense, at the pressure switching point, and a minimum increment of cylinder clearance volume added to the motor by the valve connecting passages.

Test results have indicated that the present valve design is less than optimum in several respects. It is believed that cylinder pressure spikes occur during the pressure switching transients. This indicates that the desired pressure rate produced by the valve action is inadequate to overcome the parasitic pressure rate induced by the piston motion pumping flow across the restricted metering orifice of the valve.

The pressure rate switching capability of the valve can be improved by a shift from a four-phase valve to a six-phase valve. This allows a single 2.5-degree step to be used to replace the present three 1.25-degree half steps which represent a least bit with the current valve. This change of valve phase count would increase the metering area rate by roughly a factor of three. A further factor of two could be obtained by doubling the length of the valve metering slots. A second factor of two would result from a doubling of the metering port circumferential density of the current valve so that each

valve phase segment contains each of the six cylinder ports. This last change, although possible, may not be feasible due to the complexity of the resulting longitudinal passageway system within the body of the valve sleeve.

### 8.2.2 Specific Design Details

The heavy shrink fit used to seal the valve sleeve in the housing tends to make both the sleeve and its housing into non-replacable items in the valve assembly. This drawback was apparent when cracks started to appear in the valve housing during the durability test. Straightness and uniform diameter are very difficult to insure over the length of the long bore in the housing in which the sleeve is fitted. This heavy shrink fit between sleeve and housing may have been a primary cause of the repeated instances of surface cracking in the housing area of the cylinder test ports. These cracks started to appear after the unit had been operated for only a part of the planned durability test. The shrink fit between sleeve and housing was also apparently non uniform over the length of the sleeve. Leaks of high pressure oil occurred from the ends of the sleeve-body interface whenever the thermal expansion of the valve body relaxed the fit of the outermost lands of the sleeve in the valve housing. This leakage became significant at temperatures above 160F measured in the valve return flow and caused testing to be limited to avoid higher oil temperatures.

An improved valve design which would correct the above deficiencies might incorporate some of the following features:

- a. Longitudinal passages within the sleeve body might be totally eliminated by the metering scheme illustrated in Figure 35.
- b. Annular manifolds for collection of valve metering port flows could be formed internal to the sleeve body instead of being made as annular grooves in the outer cylindrical surface of the sleeve. With such internal manifolding, the sleeve could be slip fit or lightly pressed into

the valve body by using materials of like coefficient of thermal expansion for sleeve and valve body. Pressure and return supply flows would be sealed at the sleeve-to-body interface by annular O-rings while cylinder feed passages would cross this interface at the intersection of tubular passages terminating at the spool-to-sleeve metal-to-metal interface. A six-phase valve design would be used to replace the present four-phase design to take advantage of the ability of the Sigma stepping motor to step in 2.5-degree full-step increments.

- c. Another design deficiency of the DEHA unit as demonstrated involves the lack of an error limit stop between valve and hydraulic motor output. The current DEHA unit as it would be applied to an aircraft control surface drive cannot be safely stalled. When such a simple electrohydraulic stepper unit is stalled it tends to lose control of its output load much in the manner of a stalled synchronous electric motor. This problem can be circumvented by the provision of a mechanical-error angle-limiting stop between the rotary valve and the hydraulic motor output. Such a stop mechanism would limit the valve phase error to  $\pm 90$  degrees. The monitor feedback encoder could then be connected either to the valve rotor or to the motor output as is done with the demonstration system. The present location of the valve rotational axis at right angles to the motor output axis does not lend itself to the easy implementation of such an error stop. Mounting of the rotary valve with its axis parallel to the motor output axis facilitates the placement of such an error-limiting stop mechanism but creates another problem in terms of the increased cylinder clearance volume necessary to interconnect the valve with the motor cylinders.
- d. Consideration of the use of an error limit stop between rotary valve and hydraulic motor suggests the possibility of another type of error limit device for use with the electrical stepping motor driving electronics. Once the error limit stop described in (c) above is implemented, the monitor feedback encoder function may be served by an encoder either on the electric stepper output or on the hydraulic motor output where it is presently installed. Assuming the encoder mounted to sense stepper (valve) position, a continuous monitor of stepper electrical phase angle

is available. This phase signal now sensed can be limited to  $\pm 90$  electrical degrees by simply delaying the input pulse train whenever this  $90^\circ$  criterion is exceeded. Such a circuit would provide a near ideal ramping function for the electrical stepping motor without paying the penalty of degraded frequency response which was noted from the use of first order signal filtering at the stepper input with the system as tested.

## IX. CONCLUSIONS

The hydraulic-motor incremental-digital (stepper) actuation system assembled on this program offers a number of advantages over other digital actuation concepts considered. Although such incremental schemes are characteristically closer in function to analog devices than to digital devices, they can provide the fine position resolution required for primary flight control surface actuation systems. All of the parallel-digital actuation schemes considered require too many hydraulic valves.

Other incremental systems can be arranged to provide two of the three advantages which are above those originally anticipated, i.e., elimination of hardover transients due to open-circuit failure of a feedback element, and a reduction in the steady-state quiescent leakage flow associated with electrohydraulic servovalves. However, of all the incremental schemes considered, only the selected system has the potential for adapting to the load torque in a manner to reduce hydraulic power and flow demands under low loads and for returning flow to the hydraulic system under aiding loads.

Despite a number of deficiencies, the test results demonstrate that significant reductions in the flow and power normally required with a hydraulic-motor actuation system (with conventional motors and proportional valves) can be obtained. With the distributor valve modifications outlined herein, even greater reductions in demand flow under resisting loads, and increased flow recovery under aiding loads, should be realized. These and other changes, including the addition of pressure relief valves to limit transient pressure spikes, and the avoidance of high shrink-fit stresses in the valve housing, should also improve its durability.

The test results also demonstrate that, if electric stepper motors are to be used as primary elements in future control systems, additional development of their driving electronics is required. A principal merit of an incremental system lies in its ability to operate "open loop" with good positional fidelity. However, the incremental stepper element can only achieve this positional fidelity by producing a fast, positive, and well-damped response to individual single-step commands. Existing electric

stepper motor controllers, including the one used in this program, have inadequate or poorly controlled damping of single steps and are intolerant of any deviation from a smoothly changing input pulse rate. Likewise, acceleration of such motors must not disrupt the smooth character of the input pulse train. A possible solution to this problem might be in the use of an encoder coupled to the stepper shaft to provide a phase-limiting feedback around the stepper motor as outlined in 8.2.2.d. This could be used in conjunction with an error limit stop between the valve and hydraulic motor output which is required to prevent loss of control synchronization in the event that the unit is stalled by an overload.

However, before such efforts are undertaken, the potential use of high performance hydraulic motor actuation systems should be reviewed and all factors examined. For one, the possibility that a motor-driven power-hinge system can jam due the failure of a single element must be considered before they are used for essential applications such as primary flight control. Torque-summing motor arrangements (which are the easiest way to provide power source redundancy) are subject to jamming due to a seizure failure of any single motor or a jamming failure of a gearbox unless they can be declutched. However, none of the torque-summed systems provide a means for continued operation following a jam in the output gearing.

Velocity-summing arrangements of two independent motors with outputs mixed on a final differential gear set at the surface hinge point could be considered. A pressure-released brake at each motor, to provide a reaction point in the event of a hydraulic system pressure failure, would allow the active motor to continue to supply torque through the differential to the surface and also in the event of a jam in the other motor or its gearbox.

However, the arrangement of velocity-summing power hinges would be difficult. For instance, if a velocity-summed system is used to actuate a trailing-edge surface, and it is desired that the hydraulic motors be located at one end of the hinge line submerged in the fuselage, two separate motor output shafts running parallel to the hinge line would be required. One of the two hydraulic-motor drive units and output shaft would be mounted ahead of the rear spar of the wing or fin and the other behind the spar. This leaves

little room for either aerodynamic balance area or counterweights ahead of the surface hinge, and causes a structural weight penalty by introducing cutouts in the spar web. The alternative would be to install one motor at each end of the hinge line. In either case, the differential gearing must be at the final output stage and be designed to carry the full aerodynamic load.

Justification for further development of the selected DEHA concept may depend on its acceptability for other applications such as the actuation of secondary flight controls or utility functions. Hydraulic-motor-driven power-hinge systems have been used for actuating wing flaps, wing fold mechanisms, and weapon bay doors on a number of aircraft. Hydraulic motors are also used for gun drives, radar antenna drives, emergency generator drives, and other continuous rotation functions. Of all of these applications, probably the only ones which could provide hydraulic systems benefits from the load-adaptive characteristic of the selected DEHA concept are the fast-acting leading edge flap systems. Since the flow demands for leading-edge flap actuation have become one of the major hydraulic loads on recent aircraft, and since these surfaces have widely variable load curves, flow reductions from a DEHA motor system could be worthwhile. However, there is little need for digital control of such flap systems; and, there are simpler ways, such as the use of variable-displacement motors, to reduce hydraulic flow demands.

The program was of value in that it provided a comprehensive comparison of candidate actuation schemes for a specific application and an actual demonstration of the load-adaptive feature of the selected concept. However, there are other load-adaptive control schemes which can be applied either to hydraulic ram type servoactuators or to motor-driven actuation systems which may have a better prospect of acceptance.

## REFERENCES

1. SAE Paper 760940, Hydraulics for a Hot Performer, The F-16 Fluid Power System, by W.O. Lee, General Dynamics, Fort Worth Division, October 1976.
2. Hydraulics & Pneumatics magazine article, Electrohydraulic Digital Controls for Machine Tools, by G. Diessel, September 1973.
3. Hydraulics & Pneumatics magazine article, Guide to Performance and Specifications of EHSMs, Part 1: Stepping Motor Definitions for Hydraulic Engineers, by Joseph E. Dahmen, March 1972.
4. Hydraulics & Pneumatics magazine article, Guide to Performance and Specifications of EHSMs, Part 2: Survey of Manufacturers: Charts and Curves of What's Available, by Edwin Jacobs, Associate Editor, June 1972.
5. AFAPL-TR-77-14, Investigation of Electrohydraulic Pulse Motors for Aircraft Utility Functions, Lockheed-Georgia Company, May 1977.
6. General Dynamics F-16 Specification No. 16ZH001B, Servoactuator Hydraulic Tandem, Electrohydraulically Operated, March 12, 1976.

## APPENDIX A

### POWER ADAPTABILITY AND POWER REVERSIBILITY FEATURES

#### 1. Power Adapability

The feature of power adaptability can be explained by the following logic.

The useful power delivered by a control actuator to an aerodynamic surface can be decribed as a product of surface load and rate. Current valved ram type actuators draw hydraulic power in proportion to their output rate only, and are basically insensitive to variations of surface loading.

The output torque of an axial-piston motor from any single piston varies as a near sinusoidal function as the swash-plate piston-contact pressure angle changes from the piston top and bottom dead-center positions toward the 90-degree displaced position of the swash plate where that piston's torque is maximum. In a free-valve-commutated motor, the relative shaft rotation angle to the centroid of the net piston reaction point varies as the load is applied to the motor starting from a bottom dead-center zero-phase relationship for zero load and going to a maximum torque at a 90-degree phase displacement of the motor shaft with respect to the input piston force vector. Thus, in the absence of friction or flow-velocity related losses, the fluid power drawn by the pistons of such a motor varies from near zero to a maximum as the motor loading causes its swash plate or crank to rotate from the dead-center position toward the 90-degree deflected position. (Note: The phase angles mentioned above are always measured from the bottom dead-center axis of the motor swash plate to the centroid of the pressurized piston group).

A maximum power turn-down ratio with loading can be defined in terms of the ratio between the volumetric displacement of a single piston during each of two equal rotations of the output shaft. In the high-displacement case, the swash plate is assumed to move through an angle which is centered at the 90-degree angle of rotation away from the piston bottom dead center condition. In the minimum-displacement case, the included angle of equal

magnitude is arbitrarily measured from the bottom dead-center position of the motor crank for the particular piston considered. The magnitude of this angle denoted as  $\theta$  is defined as the shaft output angle corresponding to the angular displacement between adjacent motor pistons. In these terms, the power turn-down ratio  $R_p$  can be calculated to be as follows.

CALCULATION OF THE APPROXIMATE EXPRESSION FOR  $R_p$

$$R_p = \frac{2.828 \sqrt{\gamma - (\gamma)^2 / 2}}{(1 - \cos \theta)} \quad \text{where } \gamma = (1 - \cos \frac{\theta}{2})$$

FOR  $\theta = 30^\circ$   $R_p = 3.86$

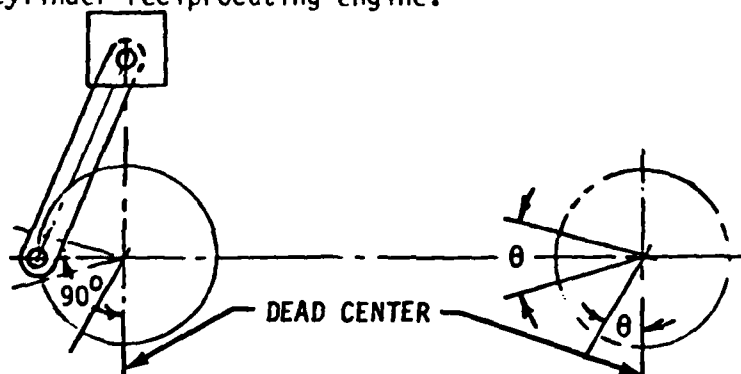
A simpler approximation of the same  $R_p$  term is  $R_p = \left[ \frac{2 \sin \frac{\theta}{2}}{1 - \cos \theta} \right]$

For this approximation --

For  $\theta = 30^\circ$   $R_p = 3.87$

The foregoing ratio is independent of the motor swash-plate inclination angle.

The approximate form of the above expression for  $R_p$  can be explained in simple terms by considering the motion of the connecting rod and the piston of a single-cylinder reciprocating engine.



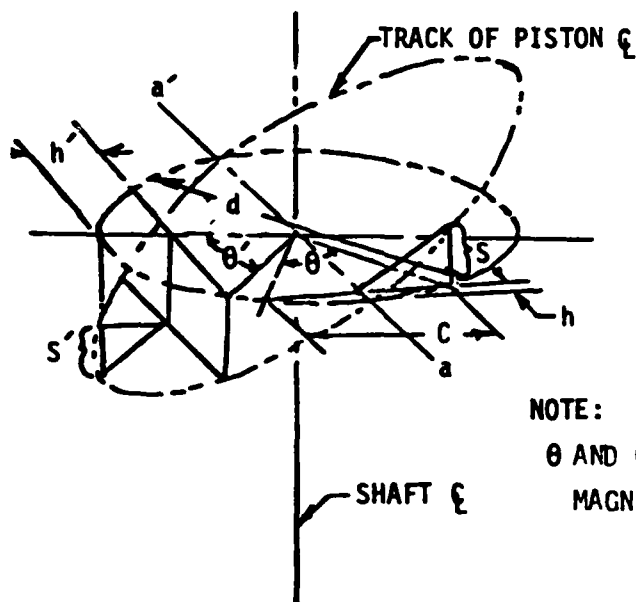
At the 90-degree position of the crank, the piston stroke is approximately  $2R \sin \frac{\theta}{2}$  while the stroke when approaching the dead-center position is nearly  $R(1 - \cos \theta)$ . In each case, we have ignored the angularity of the connecting rod. This assumption improves the approximation when the result is applied to a barrel-type axial-piston hydraulic motor.

The angle  $\theta$  at bottom dead-center was defined to be on one side of the dead-center position in order to avoid the appearance of an infinite turn-down ratio  $P_p$  which would have occurred at zero load with the angle  $\theta$  bisected by the dead-center position radial.

CALCULATION OF TURN DOWN RATIO  $R_p$  FOR AN AXIAL-PISTON MOTOR

Such a calculation requires the determination of incremental piston displacement for two conditions. The ratio of these two displacements taken per unit of output shaft angle for each condition defines the term ( $R_p$ ).

The maximum-displacement condition occurs when the shaft rotation included angle is centered on the position 90-degree from effective crank dead-center. The accompanying minimum-displacement condition occurs with the same shaft included angle measured to one side of the dead-center position.



From plane geometry ----

$$C = 2 \sqrt{h(D-h)}$$

$$h = \frac{d}{2} (1 - \cos \theta)$$

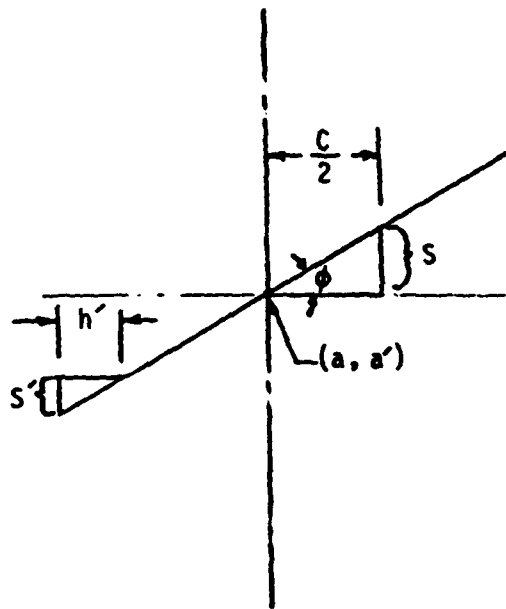
$$C = 2 \sqrt{\frac{d^2}{2} (1 - \cos \theta) - \frac{d^2}{4} (1 - \cos \theta)^2}$$

$$h' = \frac{d}{2} (1 - \cos \theta')$$

NOTE:

$\theta$  AND  $\theta'$  ARE DEFINED TO HAVE EQUAL MAGNITUDE.

Now viewing the above geometric system along the line a, a' in the swash-plate face plane.



During shaft rotation  $\theta$  about the  $90^\circ$  point the piston moves parallel to the shaft a distance  $S$

$$S = \frac{2(d)}{\sqrt{2}} \tan \phi \sqrt{1 - \cos \frac{\theta}{2} - \frac{(1 - \cos \frac{\theta}{2})^2}{2}}$$

During a shaft rotation corresponding to  $\theta'$  about the dead-center point (b), the piston moves through a distance  $S'$ .

$$S' = \frac{d \tan \phi (1 - \cos \theta')}{2}$$

For  $\theta = \theta'$

$$R_p = \frac{S}{S'} = 2.828 \frac{\sqrt{\gamma - (\gamma)^2}}{(1 - \cos \theta)}$$

where  $\gamma = \frac{(1 - \cos \theta)}{2}$

2. Power Reversibility

The basis for the claim of power reversibility in the action of the freely-commutated DEHA motors is explained below.

The angular relationship between valve and motor in the DEHA device is seen to be a function only of motor working load since the valve is not mechanically constrained to rotate with the motor. Thus, when the load causes the motor to lag behind the valve, the motor will drive the load and will draw power roughly in proportion to the valve-to-motor lag angle. Conversely, when an overriding load causes a leading-error angle between motor and valve, the motor will automatically become a pump and will attempt to convert power from the load to the hydraulic system supply pressure line at a rate proportional to the valve-to-motor error angle.

Naturally, any friction drag on the motor or output mechanism or flow related losses within the valve assembly will reduce the motor's ability to advance in phase ahead of the valve controlling it and will thus reduce the degree of power reversibility which can be demonstrated by the unit.

## APPENDIX B

Controller electronics circuits which are not illustrated in Section 5 are collected here in the following figures.

Figure B-1 Digital integrator feedback loop electronics

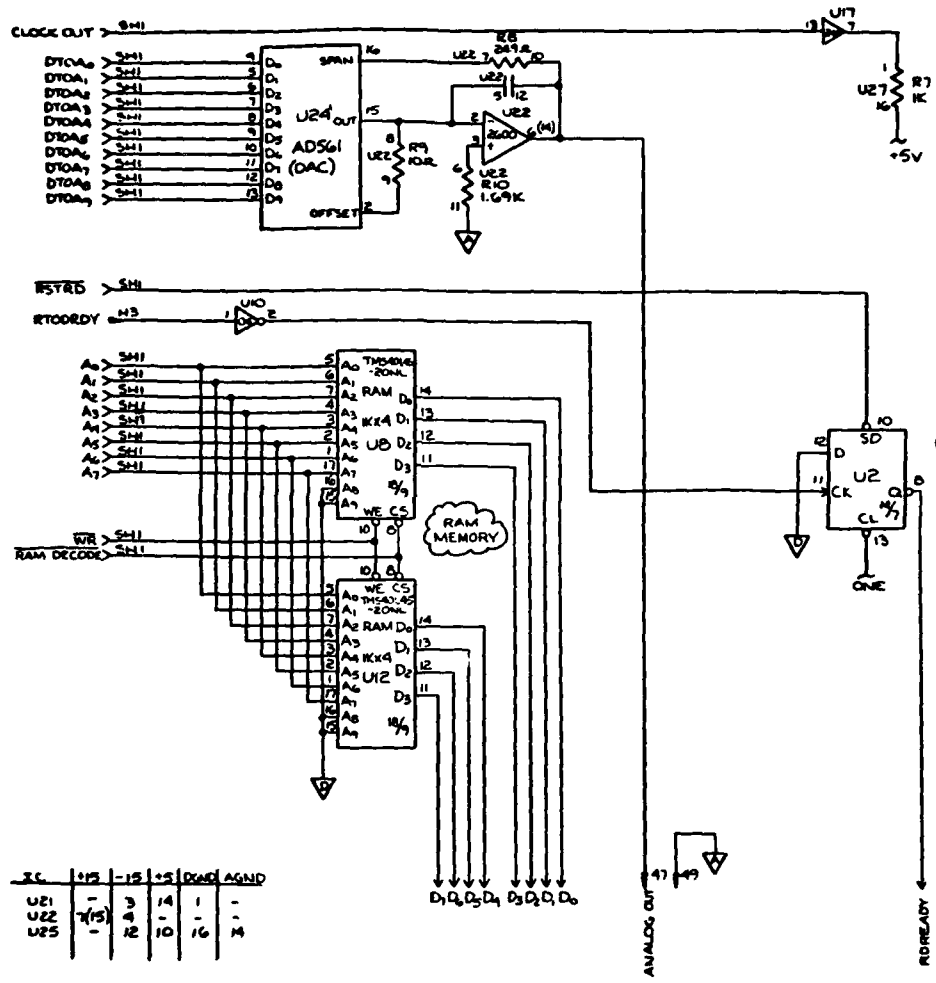
Figure B-2 Display circuits

Figure B-3 Monitor and display circuits









IC	+5	-5	+5	RD	AGND
U21	-	3	14	-	-
U22	7(15)	12	10	16	4
U25	-	-	-	-	-



## GLOSSARY OF TERMS

1. Digital binary word

An array of a fixed number of ordered 1 and 0 bits in which the order and state of listing designates the presence or absence of quantities which are related in magnitude as a binary sequence 1, 2, 4, 8, 16 etc.

2. Digital wordstream

A succession of digital words in which word bit-states may change simultaneously (parallel arrangement) or may change in a serial order (serial arrangement) controlled by a computer clock.

3. Dynavector actuator

This name denotes a fluid vane motor packaged with a concentric epicyclic reduction gear train. This name refers to a product of the Bendix Corporation.

4. Harmonic drive

This is a particular scheme of epicycloidal reduction gearing using a skip-tooth principle and employing a flexible internal gear element. Such gear elements are manufactured by the USM Corporation.

5. Incremental digital control

This expression refers to a digital signal which has been converted to a directional pulse train. This pulse train incorporates only the intelligence derived from the two lowest order bits of the words of a digital wordstream.

6. Monitor feedback

A monitor feedback is a feedback implemented at such a low gain that the dynamic response of a system evidenced by closure of that feedback loop is virtually unaffected.

7. Multistepper

This is a stepping device or motor which is capable of stepping at more than one step amplitude with amplitude selected by command. Such step amplitudes would generally, but not necessarily be related as a binary progression.

8. Power-adaptive control

This term describes the action of an actuation device which adjusts its power consumption in response to changes of load or of output rate.

9. Power-recoverable control

This expression refers to the property of a power-adaptive actuation device in which the power consumption is responsive to both the magnitude and to the directional sign of the work done in interaction with a load.

10. Parallel or absolute digital control

These terms refer to the essential feature of a digital wordstream in which each of the word bit-states are updated simultaneously at equally spaced intervals of time.

11. Wire drawing

This term refers to the high resistance to fluid flow and coincident high local fluid velocities which occur during the process of opening or closing a valve.

LIST OF ABBREVIATIONS, ACRONYMS, AND SYMBOLS

A/D	analog to digital
D/A	digital to analog
BBA	Ducillier, Bendix, Air Equipment (A French Corporation)
DC	direct current
DEHA	digital electrohydraulic actuator
EHSM	electrohydraulic stepping motor
ELSA	electrohydraulic linear stepper actuator
HOBOS	weapon developed by HOBOS program
LED	light-emitting diode
LVDT	linear variable differential transformer
P/N	part number
V/F	voltage to frequency
S1, S2	designates pressure supply system number 1 or 2
C1, C2 etc	designates the number 1 or 2 cylinder of a hydraulic motor
HDM-1, HDM-2	designate hydraulic drive motors 1 and 2
LG-1, LG-2	designate load gages 1 and 2
LPR-1, LPR-2	designate load pressure relief valves 1 and 2
LPSOV	load pressure shutoff valve
P	load pressure
Ps	supply system pressure
Pr	return system pressure
Rp	power turndown ratio
SC	analog command signal
c	digital output signal from microprocessor
out or o	analog transformed encoder signal
l	analog output of low pass second order filter
CW	clockwise
CCW	counterclockwise
CC	cubic centimeter
db	decibels $20 \text{ Log}_{10}$
deg	degrees
F	fahrenheit
ft	foot
gpm	gallons per minute
hr	hour
Hz	cycles per second
in	inch
lb	pound force
min	minute
n	numerical order of a parallel digital word
oz	ounce
PPS	pulse per second
psi	pounds per square inch
psid	pounds per square inch differential
psig	pounds per square inch (gage)
rms	root-mean-square
s	second
sps	steps per second
S	Laplace variable
t	time in seconds
T	temperature in degrees fahrenheit

